Oxidative Carbon-Carbon Bond Formation

A dissertation in partial fulfilment of the requirements for the award of the degree of

Doctor of Philosophy

of the

University of Oxford

Morgan Keenlyside

University College

Hilary Term, 2024

Declaration

This dissertation describes work carried out in the Chemistry Research Laboratory at the University of Oxford between November 2020 and April 2024 under the supervision of Professor Martin D. Smith. The dissertation is a product of my own work and includes no results obtained through collaboration, except where specifically stated in the text.



Morgan Keenlyside

Acknowledgments

I would like to thank Martin Smith for your support and guidance through the trials and difficulties of this DPhil.

Thank you to the Smith research group, past and present - Pearse, Maddie, Zac, Elliot, Ben, Edvinas, Chai, Callan, Xiaofei, and everyone else - for your advice, friendship, and for irrevocably changing my taste in music.

Thank you to Ben, Harry, and Mia for making Denmark Street a place I loved living, despite the lockdowns and the slugs.

Thank you to my friends, those still in Oxford and further afield, for your support and encouragement - even when I wasn't responding to your messages.

A special thank you to Becca. I probably wouldn't have got past the title without you, and I certainly wouldn't have made it to the end. Love.

Thank you to my family, who put up with me living at home and eating your food for the last four months (and the rest of my life). Thank you for the love and support, it got me to Oxford and all the way back.

Abbreviations

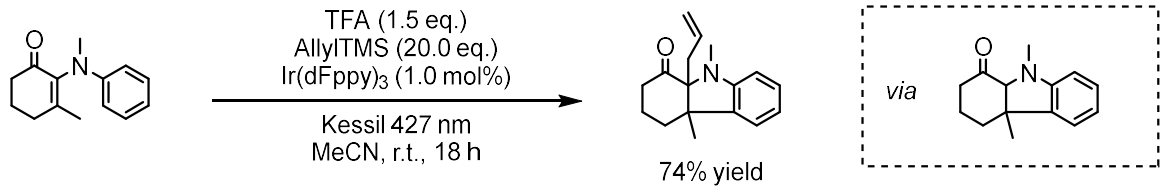
°C	degrees celsius
ν	frequency
(*Z*)	zusammen
[O]	oxidant
Ac	acetyl
allylTMS	allyltrimethylsilane
aq.	aqueous
Ar	aryl group, generic
AT	atom transfer
b.p.	boiling point
BINOL	1,1'-bi-2-naphthol
Bn	benzyl
Boc	tert-butoxycarbonyl
Bu	butyl
C(sp^3)	sp^3-hybridised carbon
CDI	carbonyldiimidazole
CMD	concerted metallation-deprotonation
conc.	concentrated
CPA	chiral phosphoric acid
CSA	camphorsulfonic acid
d	doublet
d.r.	diastereomeric ratio
DCE	1,2-dichloroethane
DDQ	2,3-dichloro-5,6-dicyano-1,4-benzoquinone
DIAD	diisopropyl azodicarboxylate
DIBAL	diisobutylaluminium hydride
DIPEA	N,N-diisopropylethylamine
DKR	dynamic kinetic resolution
DMAP	4-(dimethylamino)pyridine
DMDS	dimethyl disulfide
DMF	N,N-dimethylformamide
DMSO	dimethylsulfoxide
DTBP	di-tert-butyl peroxide
e	electron
e.r.	enantiomeric ratio
endo	endocyclic
eq.	equivalents
equiv.	equivalents
ESI	electron spray ionisation
ESR	electron spin resonance
Et	ethyl
exo	exocyclic
FTIR	fourier transform infrared
g	gram

h	hour
h	Planck constant
HAT	hydrogen-atom transfer
HFIP	1,1,1,3,3,3-hexafluoro-2-propanol
HPLC	high-performance liquid chromatography
HRMS	high-resolution mass spectrometry
Hz	Hertz
^{i}Pr	isopropyl
Ir(dFppy3)	tris[3,5-difluoro-2-(2-pyridinyl)phenyl]iridium(III)
ISC	intersystem crossing
IUPAC	international union of pure and applied chemistry
J	coupling constant
k	rate constant
kJ	kilojoules
L	litre(s)
LDA	lithium diisopropylamide
LED	light emitting diode
LRMS	low-resolution mass spectrometry
M	molar
m	meta
m	multiplet
m.p.	melting point
Me	methyl
min	minute(s)
mL	millilitre
mm	millimetre
mmol	millimoles
mol	moles
NBS	N-bromosuccinimide
^{n}Bu	normal butyl
NCS	N-chlorosuccinimde
nm	nanometre
NMR	nuclear magnetic resonance
o	ortho
p	para
Ph	phenyl
PIDA	(diacetoxyiodo)benzene
ppm	parts per million
Pr	propyl
PyBOX	pyridine-bis(oxazoline)
q	quartet
R, R', etc.	substituent (generic)
r.t.	room temperature
RPC	radical-polar crossover
s	singlet
SCE	standard calomel electrode

SET	single electron transfer
t	time
t	triplet
TBPB	tert-butyl peroxybenzoate
^{t}Bu	tert-butyl
TEMPO	2,2,6,6-tetramethylpiperidinyloxy
TET	triplet energy transfer
TFA	trifluoroacetic acid
TFE	2,2,2-trifluoroethanol
THF	tetrahydrofuran
TLC	thin-layer chromatography
tosMIC	para-toluenesulfonyl isocyanide
trig	trigonal
Ts	para-toluenesulfonyl
UV	ultraviolet
V	volts
w/w	weight-percent concentration
X	halogen or other substituent
λ	wavelength
μ	micro-
τ_R	retention time

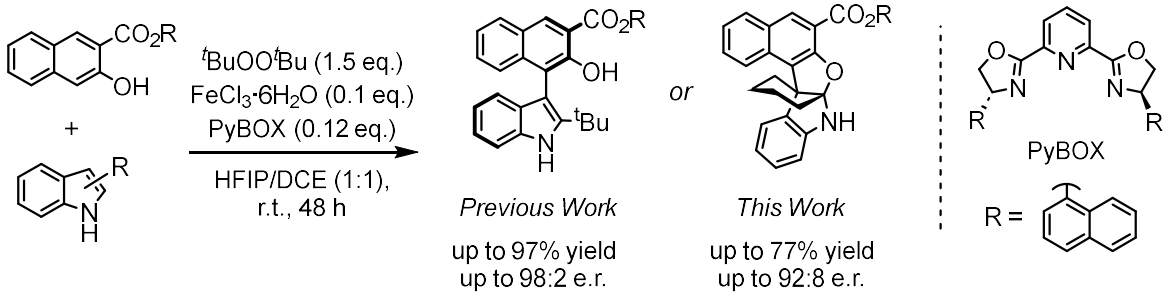
Abstract

Oxidative bond formation is a powerful technique for the efficient and atom-economic construction of carbon-carbon bonds. This thesis explores two systems that harness this reactivity to generate densely functionalised products. Initially, we describe an oxidative allylation discovered during a visible light eliminative photocyclisation. Investigation into the reaction mechanism determined that the cyclisation and oxidative allylation are two independent steps. However, the reaction is extremely substrate and nucleophile dependant, with limited tolerance for modification.



Scheme i. Tandem visible light photocyclisation/oxidative allylation

The expansion of an oxidative cross-coupling between C-2 substituted indoles and 2-naphthols developed by the group is described, in which the synthesis of atropisomeric heterobiaryls had been achieved chemo- and enantioselectively with the use of a $FeCl_3$/PyBOX ligand system. The reaction mechanism is determined: single electron oxidation of the naphtholic partner to the Fe(III)-bound naphthoxy radical. This is followed by a nucleophilic attack by the indole, geometrically controlled by the asymmetric environment created by the ligand. During this investigation, the off-cycle oxidation of an indole to the radical cation and its cyclisation to an unexpected 6,5,6-tricyclic chlorinated product is observed. Modification of the substitution pattern of the indolic partner in the cross-coupling allows for the synthesis of cyclised naphthofuro[2,3-b]indolines *via* the same methodology. This is achieved in a racemic fashion for a selection of 2-naphthols and 3- and 2,3-substituted indoles. Reintroduction of the PyBOX ligand leads to the successful induction of enantioselectivity into the coupling, producing the products in up to 77% yield and 92:8 e.r.



Scheme ii. Oxidative cross-coupling of indoles and naphthols in the synthesis of heterobiaryls and naphthofuroindolines

Contents

Section 1

Chapter 1: Introduction to Oxidation

1.1 Oxidation in Organic Reactions 1
1.2 Methods for Oxidation 2
1.2.1 Electron transfer 2
1.2.2 Atom transfer 4
1.2.3 Reductive Elimination 6
1.3 Oxidative Carbon-Carbon Bond Formation 7
1.4 Strategies for Oxidative Carbon-Carbon Bond Formation 9
1.4.1 One-pot Two Electron Oxidative Functional Group Interconversion/Nucleophilic Trapping 9
1.4.2 Radical Generation and Trapping 10
1.4.3 Coupling Between Nucleophiles 11
1.4.4 Activation of Carbon-Hydrogen Bonds 13
1.5 Project Aims 16

Section 2

Chapter 2: Oxidative Photocyclisation

2.1 Photocyclisation 17
2.2 Classifications of 6-π systems 18
2.3 Accessing Heteroaromatic Products *via* Photocyclization 19
2.4 Visible Light Photocyclisation 21
2.4.1 Non-Eliminative Cyclisations 21
2.4.2 Eliminative Visible Light Photocyclisation 23
2.5 Radical-Polar Crossover 24
2.6 Observed Oxidative Cyclisation 25
2.7 Confirmation of Reactivity 27
2.8 Exploration of the Reaction System 30
2.9 Observing Reaction Progression 33
2.10 Oxidation Interrogation 37
2.11 Mechanistic proposal 40
2.12 Mechanism Validation 43

Chapter 3: Substrate Scope

2.13 Variation of the Reagents 46
2.13.1 Variation of the Acid Component 46
2.13.2 Variation of the Nucleophile 47
2.13.3 Inclusion of Additives 49
2.14 Substrate Synthesis 50
2.15 Substrate Scope 53
2.16 Conclusion 56

Section 3

Chapter 4: Atropisomeric Biaryl Synthesis

3.1 Introduction to Atropisomerism 57
3.2 Atroposelective Synthesis of Heterobiaryls 59
3.2.1 Modification of symmetric biaryls 59
3.2.2 Centre-to-Axial Chirality Transfer 60
3.2.3 Atroposelective Ring Construction 61
3.2.4 Direct Coupling of Aryl Components 62
3.3 Continuation of the Cross-Coupling Reaction 65
3.4 Mechanism Investigation 67
3.5 Mechanistic Proposal 71

Chapter 5: Indole Radical Cation Cyclisation

3.6 Introduction to the Indole Radical Cation 74
3.7 Indole Cyclisation Mechanism Proposal 79
3.8 Substrate Variation 82
3.8.1 Linear Alkenes 82
3.8.2 Branched Alkenes 84
3.8.3 Radical Traps at the C-3 Position 85
3.9 Cyclisation Optimisation 87
3.10 Conclusion 93
3.11 Introduction to Benzofuroindolines 95

Chapter 6: Synthesis of Naphthofuroindolines

3.12 Introduction to Naphthofuroindolines 100
3.13 Exploration of the Racemic Reaction 102
3.14 Mechanistic Proposal 109
3.15 Racemic Couplings with Naphthoates. 111

3.16 Enantioselective Cross-Coupling 113
3.17 Optimisation of the Enantioselective Reaction 117

Section 4

4.1 Conclusions 121
4.2 Future Work 123

Section 5

5.1 General Information 125
5.2 Characterisation of Compounds 132
5.2.1 Photochemistry (Section 2) 132
5.2.2 Iron-Catalysed Oxidation (Section 3) 144
Appendix A 184
References 190

Section 1

Chapter 1: Introduction to Oxidation

1.1 Oxidation in Organic Reactions

The transfer of electrons from one molecule to another forms the underpinning of a considerable proportion of chemical transformations. Oxidation, initially understood solely in the context of reactions with molecular oxygen, is now more generally defined as the loss of electrons from a compound. This describes one half of a transfer and is accompanied by a concomitant reduction of an electron acceptor.

In order to quantify this process, oxidation state nomenclature assigns a number to every atom in a compound, based on how oxidised or reduced it is compared with the neutral element. Carbon, with the ability to form four covalent bonds, can exist in a wide range of oxidation states. Bonds to elements more electronegative than carbon (such as oxygen and nitrogen) increase the oxidation state of the carbon centre, whereas bonds to less electronegative elements (most commonly hydrogen, but this also includes metals) decrease it – carbon-carbon bonds have no effect on the oxidation state.

The reactivity of organic molecules is dictated by the functional groups present in the molecule. In general, functionalisation goes hand-in-hand with oxidation – saturated hydrocarbons are extremely unreactive, and the majority of functional groups are defined by the presence of bonds to atoms more electronegative than hydrogen (including carbon in the case of alkene and alkyne groups) (Figure 1.1).

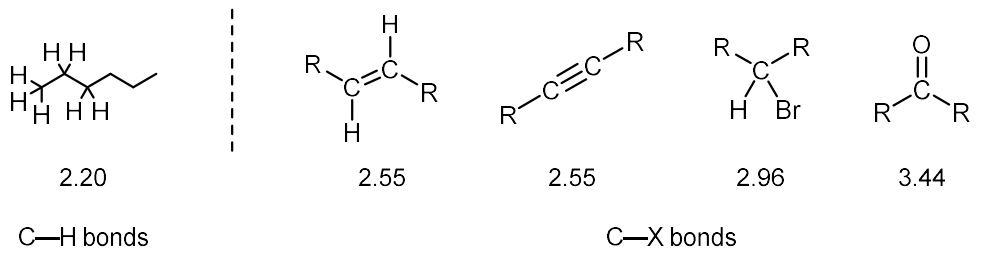


Figure 1.1. A comparison of a saturated hydrocarbon with some common functional groups, with the electronegativities of the relevant elements bonded to the carbon centre given below.

Many transformations involve no net change in the total oxidation state of the carbons in a reaction. This is the case for simple reactions like functional group interconversion at the same oxidation level, and for more complex reactions such as those between electrophiles and nucleophiles, where the oxidations and reductions of the starting materials are equivalent.

Other transformations may lead to a change in total oxidation state of the substrates, allowing for access to a wider range of available reactivity. This is achieved by external oxidants removing electrons from, or reductants adding electrons to, the system of interest.

The oxidation of less functionalised substrates to more functionalised ones is massively important for synthesis. Increasing the functionalisation of a carbon scaffold provides additional scope for reactivity when compared with the simple saturated hydrocarbon analogue.

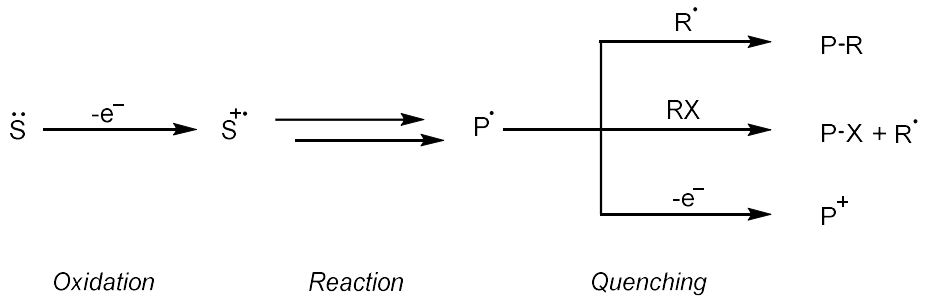
This is also true of biosynthetic routes found in nature. Oxidation of intermediates to more oxidised material is vital for the installation of key functional groups necessary for biological activity, and is controlled by a wide range of oxidative enzymes.

1.2 Methods for Oxidation

All methods for effecting oxidation rely on a reagents ability to permanently remove electrons from the substrate. This is generally achieved in two ways: *via* electron transfer (ET) or atom transfer (AT).[1,2]

1.2.1 Electron transfer

Electron transfer is the transfer of a single electron from the substrate to the oxidant, through one of a number of methodologies.[3] Upon removal of an electron, a radical species is generated. This can then exhibit typical radical reactivity, before returning to a closed-shell state through standard radical quenching methods (such as radical-radical combination or atom abstraction) or *via* a second one-electron oxidation event (Scheme 1.1).



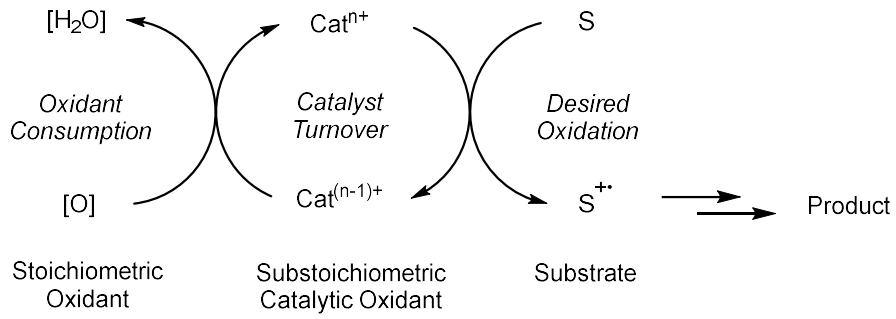
Scheme 1.1. An example of typical progression of an ET oxidation

Conceptually, the simplest ET event is the heterogeneous electron transfer seen in electrochemistry. This involves the use of an electrode and an applied voltage to directly remove electrons from the molecule of interest, and thus effect oxidation. Initially utilised in the field of inorganic chemistry as far back as the 19th century, it has more recently become a fast-growing research area of synthetic organic chemistry.[4] Perfect atom economy and the incredibly fine control over the strength of the oxidative environment make it an ideal approach to oxidation, but its current scope and usability is limited due to the field being in its infancy.[4]

Another electron transfer methodology is the use of chemical reagents, often oxidised metal compounds. Electron transfer from organic molecules to a metal centre occurs through either an inner or outer sphere mechanism (depending on the organic compound and metal complex in question), resulting in an oxidised substrate and reduced metal centre[2]. Thus, use of a stoichiometric amount of metal oxidant leads to product formation. An example of an ET oxidant is cerium ammonium nitrate.[5]

It is also possible to achieve such ET reactions catalytically, with an active oxidising agent present in sub-stoichiometric amounts. A co-oxidant is used to re-oxidise and turn the catalyst over (Scheme 1.2).

One such example is oxidative photoredox chemistry. In this, irradiation of a photocatalyst leads to photoexcitation. The activated photocatalyst has an elevated oxidation potential, which promotes the single electron oxidation of otherwise inaccessible substrates.[6]



Scheme 1.2. An example of typical catalytic cycle of a catalytic ET oxidation

ET relies on the existence of easily accessible electrons in the substrate, limiting the generally applicability. Chemoselectivity can also be an issue, as it can be difficult to control which components of a reaction are oxidised and, for larger molecules, which site is oxidised.

Non-catalytic approaches require stoichiometric quantities of the metal oxidant – something typically avoided in synthesis due to environmental and financial concerns, especially if more convoluted complexes are necessary for selectivity and reactivity.

1.2.2 Atom transfer

Atom transfer oxidation describes the method of oxidation achieved by the transfer of atoms between the oxidant and the substrate, in particular heteroatoms to the substrate or hydride and hydrogen atoms from it.[1]

A common approach is the use of a reactive and highly oxidised additive that can react with the substrate to produce a lower energy, reduced by-product and supply the necessary heteroatom. In fact, this is the mode of action that describes reactions of molecular oxygen. Molecular oxygen is an ideal oxidising agent, as it is freely available and produces only water as a by-product. Of course, directing the reactivity of oxygen is a challenge; modern efforts to utilize this reactivity in a controlled manner have led to the development of other species that exploit the chemistry of higher-than-usual oxygen oxidation states, such as peracids, peroxides, and ozone (Figure 1.2).[7]

Other oxygen transfer reagents have oxide bonded to highly oxidised centres, which are reduced in the oxygen transfer step. This includes many metal complexes (such as chromium and manganese oxides), hypervalent halogens, and highly oxidised nitrogen species such as nitric acid (Figure 1.2).[8–11]

Heteroatoms other than oxygen can also be transferred to effect oxidation. These reagents often rely on weak heteroatom-heteroatom bonds and higher than usual oxidation states, leading to electrophilic sources of traditionally nucleophilic elements. In most cases, the atom itself is reduced in the transfer, as in diatomic halogens like bromine or electrophilic sources of nitrogen like oxaziridines (Figure 1.2).[12,13]

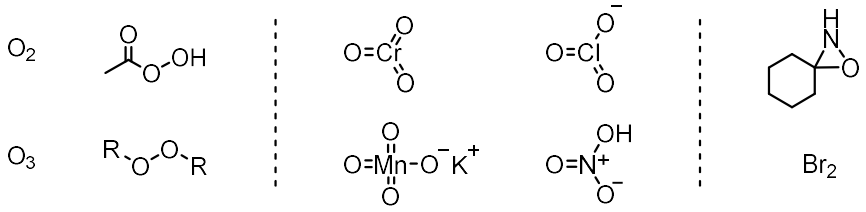
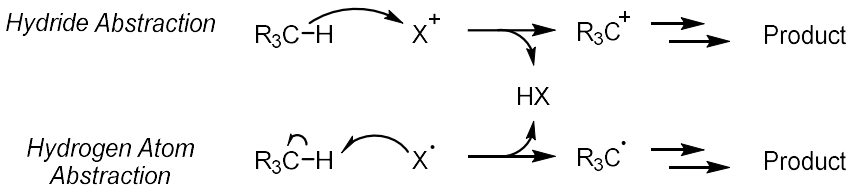


Figure 1.2. Examples of AT oxidation reagents

These reactions tend to be fairly simple and are mostly capable only of installing heteroatoms. Each reagent is also typically only able to able to promote a specific type of reactivity, and it can be difficult to control the oxidative power of a given system. The generation of stoichiometric quantities of reduced by-product leads to poor atom economy.

Hydrogen and hydride abstraction is less common than heteroatom transfer, but still used synthetically.[14,15] Removal of a hydride generates a cationic intermediate, that can either be quenched by a nucleophile or by elimination of a neighbouring proton (Scheme 1.3). Hydride abstraction agents include stabilised carbocations, such as trityl salts.[14] Hydrogen atom abstraction occurs in a similar fashion, but represents a one-electron oxidation and thus requires a radical termination step. These reactions rely on the substrates being proficient hydride or hydrogen donors and can suffer from regio- or chemoselectivity issues when multiple hydrogens are accessible. The atom economy of these

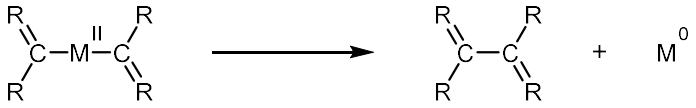
transformations tends to be low, as the mass of the hydride or hydrogen abstraction agent consumed will be many magnitudes larger than that of the hydrogen it removes.



Scheme 1.3. Comparison of the mode of action of Hydride and Hydrogen Atom abstraction methodologies.

1.2.3 Reductive Elimination

Many oxidative transition-metal-catalysed couplings are more complex than the binary of ET or AT. The method of oxidation employed in these is reductive elimination from the metal centre, so-called because the metal centre is reduced (Scheme 1.4). Reductive elimination is an oxidative process that describes the forming of a carbon-carbon bond between two metal-bound carbon species as the excess bonding electrons are transferred to the metal centre.[16] As such, this does not involve an atom transfer event, but is not strictly an electron transfer either.



Scheme 1.4. Reductive elimination showing reduction of the metal centre and oxidative formation of the carbon-carbon bond

A sub-stoichiometric quantity of a transition-metal catalyst is used to promote the desired reaction, and a stoichiometric amount of terminal oxidant allows the catalyst to turn over. The turn-over oxidation can be achieved with ET or AT.

The variety of the reactions achieved with the methodology is staggering, as it allows for many transformations not accessible by other systems. This includes oxidation of non-nucleophilic aryl carbons and direct carbon-carbon couplings – both hugely important in synthesis.[16]

It also avoids an issue associated with previously mentioned non-catalytic methods; the use of a catalytic rather than stoichiometric reagent allows for far more elaborate oxidants to be used as the reactivity-controlling species. Low catalyst loading offsets the expense of the more complex compounds and thus allows for finer tuning of selectivity than is available with bulk oxidants.

1.3 Oxidative Carbon-Carbon Bond Formation

These approaches can be utilised in oxidative catalytic carbon-carbon bond formations. Carbon-carbon bond formation is understandably of great importance to the synthetic chemist, as it necessary for the construction of carbon scaffolds. There is a huge body of work discussing the importance of, and approaches to, carbon-carbon bond formation, including many with a particular focus on oxidative methods.[17–19]

There are three approaches to carbon-carbon bond formation: neutral, reductive, and oxidative.

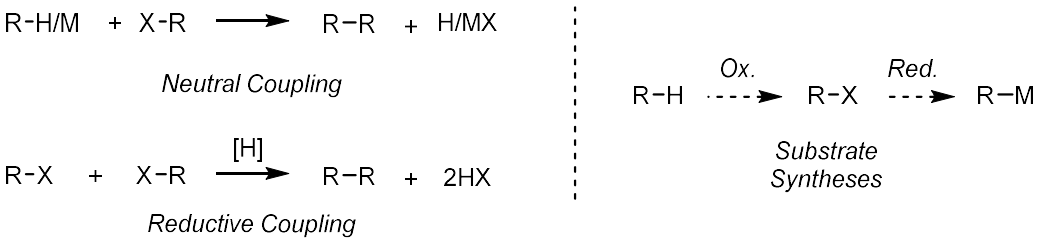
Neutral carbon-carbon bond formation is an incredibly widespread and well-explored reaction manifold, often occurring between an electrophilic and nucleophilic centre (Scheme 1.5).[20,21] The simplest neutral carbon-carbon bond formation reaction is nucleophilic substitution with a carbon nucleophile, but more complex reactions such as transition-metal-catalysed cross-couplings are also incredibly common in organic synthesis – in fact, the neutral carbon-carbon cross-coupling Suzuki reaction is the one of the most utilised reactions in drug manufacture.[22]

Neutral reactions benefit from clearly defined chemo- and regioselectivity; the match in polarity between the two functional groups limits production of undesired homocoupled products, and the functionalisation acts as a handle to control exactly where the carbon-carbon bond is formed.

However, this pre-functionalisation comes at a cost. Generation of electrophiles is often oxidative in nature, and it introduces additional steps into a synthetic route (when low step counts are preferred). This can also be the case for many nucleophiles, as the starting materials for many organometallic compounds are halogenated compounds. Use of these leaving groups in the coupling reaction

generates a stoichiometric amount of ionic side-product, which leads to low atom economy and environmental concerns about the waste created during the multiple steps.

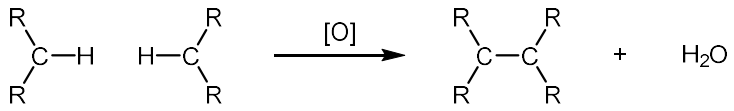
Reductive bond formation is less commonly employed and is achieved by the combination of two electrophilic partners, such as carbonyl species and aryl halides (Scheme 1.5).[23,24] However, access to these is again often oxidative in nature (although it avoids the need for organometallic components) and so imposes additional steps on the synthetic route.



Scheme 1.5. Neutral and reductive carbon-carbon bond formation, demonstrating the need for prefunctionalisation.

Oxidative carbon-carbon bond formation attempts to address these issues of pre-functionalisation.

The ideal disconnection of a carbon-carbon bond is the dehydrogenative bond formation between two unfunctionalized carbons (Scheme 1.6).



Scheme 1.6. The ideal oxidative carbon-carbon bond formation. The by-product is water, the reduced form of the theoretical oxidant

This conversion of two carbon-hydrogen bonds to a carbon-carbon bond is inherently oxidative and represents the ideal coupling reaction. It removes the need for any pre-functionalisation of the substrates and has almost perfect atom economy (as the only waste product is water).

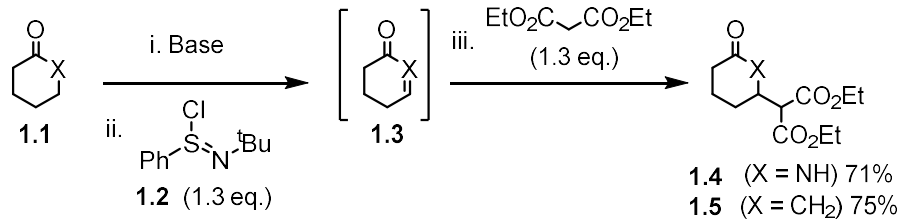
Obviously, such a simple reaction is purely theoretical, and completely infeasible *in vitro*. But by targeting this reactivity, a number of efficient and elegant methodologies have been devised that embody the benefits.

1.4 Strategies for Oxidative Carbon-Carbon Bond Formation

In order to oxidatively form a carbon-carbon bond, the bond must replace two carbon-hydrogen or -metal bonds, as the oxidation state must increase – it must replace bonds to elements less electronegative than carbon.

1.4.1 One-pot Two Electron Oxidative Functional Group Interconversion/Nucleophilic Trapping

Some of the easiest carbon-hydrogen bonds to replace are those of already functionalised carbons. Oxidation of these functionalised carbons to more reactive species allows for *in situ* trapping with a carbon-centred nucleophile. This approach is functionally identical to the previously described non-carbon-carbon bond-forming oxidations with the inclusion of a nucleophilic additive. The reactive intermediates can be generated in a wide variety of ways. The one-pot oxidative variants of Mannich and Michael additions developed by Ishibashi and coworkers are examples of this reactivity (Scheme 1.7).[25,26] In these, common electrophiles used in neutral reactions (imines and α,β-unsaturated ketones) are generated oxidatively by sulfinimidoyl chloride from their saturated precursors **1.2** and trapped by ethyl malonate.



Scheme 1.7. One-pot oxidation and Mannich/Michael addition of malonates. Base used was *n*-butyllithium (1.3 eq.) with X= NH and NaH (1.15 eq.) with X = CH_2 (an additional 1.3 eq. of NaH was added with the malonate in this reaction). Reaction was performed in THF at -78 °C with 30 minutes of stirring between each stage.

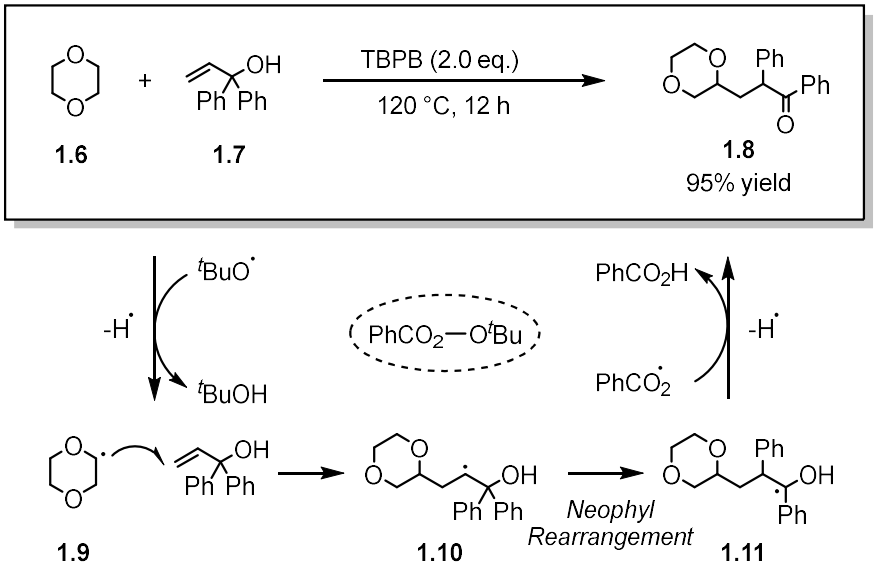
This approach is reliant on having a nucleophile/electrophile framework. Thus, it is limited to starting materials that can be oxidised to reactive intermediates and to nucleophiles that can tolerate the conditions. If achieved, the electronic match will allow for complete selectivity over the homocoupling reaction. However, given the two-step system, there are often atom economy problems, especially if the oxidation step is simply the installation of a leaving group.

1.4.2 Radical Generation and Trapping

In a similar vein to the two-electron processes described above, there are also one-electron methods for cascade oxidation/trapping processes.[19]

In these cases, oxidative generation of a carbon-centred radical (often by hydrogen atom abstraction or SET) initiates reactivity. This radical may then undergo a transformation to another radical species, such as addition to a π system or isomerisation. The reaction is terminated either by trapping with another radical species, or a second oxidation step followed by nucleophilic trapping of the cation.

This reactivity can be seen in the oxidative alkylation/rearrangement cascade reported by Ji and coworkers (Scheme 1.8).[27] In this, an oxygen-centred radical generated by thermal homolysis of TBPB abstracts a hydrogen from dioxane (**1.6**) to generate α-oxyradical **1.9** in the oxidative initiation step. This radical undergoes a series of neutral reactions (addition to an alkene followed by a rearrangement) to generate the final radical **1.11**. A second hydrogen abstraction yields the desired oxidised product **1.8**.



Scheme 1.8. Oxidative radical alkylation of **1.7** with **1.6** achieved by two hydrogen atom abstractions. **1.6** was employed as the solvent.

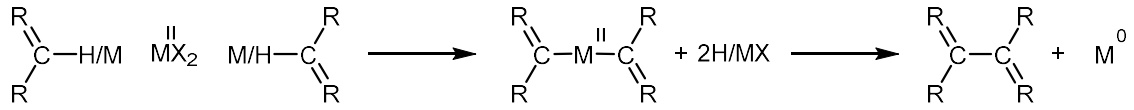
The parallels between this radical approach and the aforementioned ionic methodology are continued in the drawbacks of the approach. Specific functional groups in position on the carbon centre (such as

ethers or amines) are necessary for efficient and controlled generation of the radical intermediate.[19] This allows for complete control over the regiochemistry, but also limits the generality of the reaction or requires installation of the functional group. Unwanted radical-radical combination leads to unintended side-products, as the electronic control can be less pronounced.

1.4.3 Coupling Between Nucleophiles

A wide-spread approach to oxidative carbon-carbon bond formation is the combination of two carbon-centred nucleophiles.[28] It inverts the traditional electronics of these nucleophiles, and so gives access to reactivity and combinations of starting materials that would otherwise be challenging.

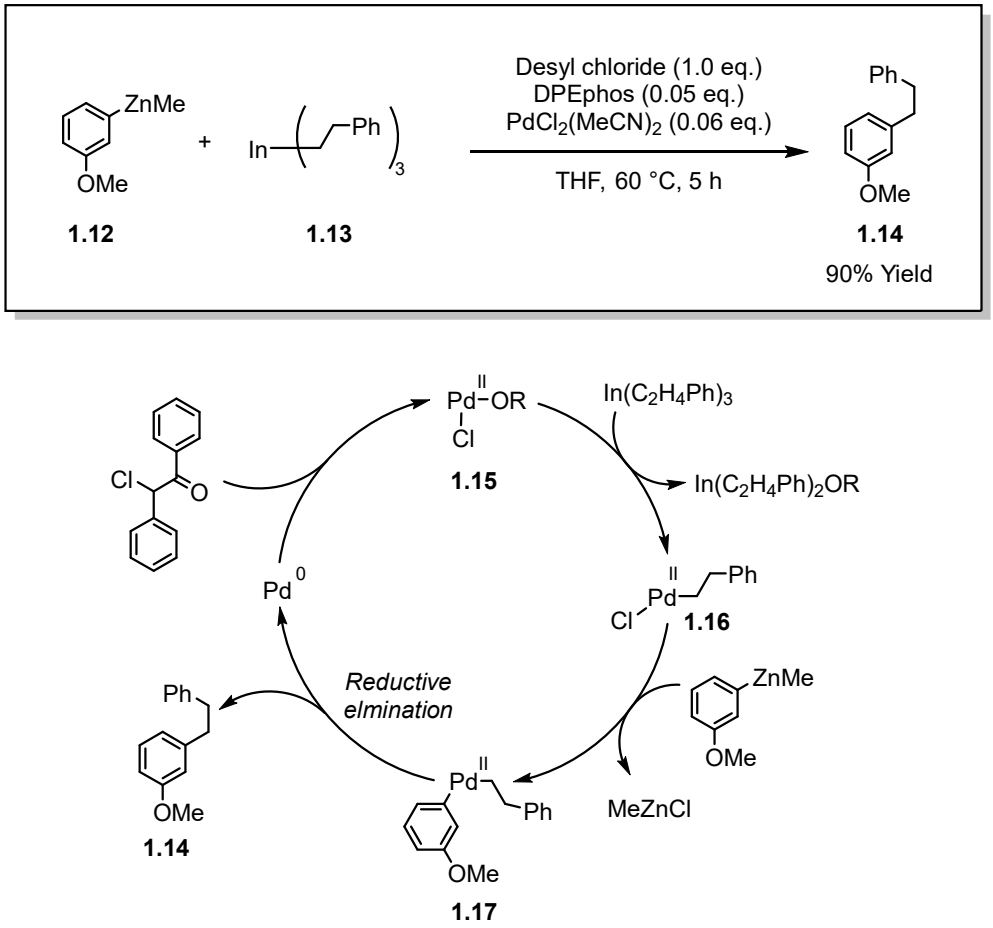
This is often achieved by the use of a transition metal catalyst, and relies on the oxidative pathway supplied by a reductive elimination from the metal centre after electronically neutral complexation of the two nucleophilic components (Scheme 1.9).[29]



Scheme 1.9. Oxidative coupling of two nucleophilic components.

Organometallic carbon nucleophiles are ubiquitous in neutral cross-couplings when paired with an electrophilic partner, they can also be utilised in oxidative cross-couplings. Transmetallation of both partners with a cationic transition metal species leads to the disubstituted intermediate able to reductively eliminate.

For example, Lei and coworkers developed a cross-coupling between arylzinc (**1.12**) and trialkylindium (**1.13**) nucleophiles, catalysed by palladium (Scheme 1.10).[30] Transmetallation of the alkyl (**1.13**) and aryl (**1.12**) components onto the palladium centre (**1.15**) allowed for a reductive elimination to the product **1.14** and resulted in the reduced palladium^0. This was recycled by oxidation with desyl chloride *via* oxidative insertion into the carbon-chlorine bond and migration to the oxygen, furnishing **1.15** and completing the cycle.



Scheme 1.10. Oxidative coupling of two organometallic components. The reaction conditions were as stated with **1.12** (1.1 eq.) and **1.13** (1.2 eq.)

Use of this methodology is fairly limited, as it has some significant downsides. The prefunctionalisation of the substrates negates many of the benefits of an oxidative coupling (such as synthetic simplicity) while still struggling with the chemoselectivity of hetero- vs homocoupling.

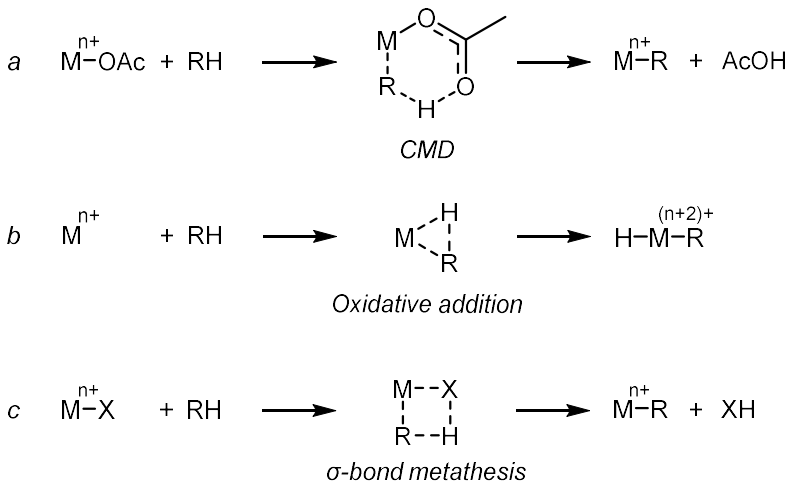
This prefunctionalisation led to significant metal salt waste production - the given example produced a stoichiometric quantity of both indium and zinc waste, as well as small quantity of palladium.

Like many transition-metal-catalysed cross-couplings, it is often necessary for one or both of the coupling partners to be aryl and vinyl species, with C(sp^3) centres being a particular challenge.

1.4.4 Activation of Carbon-Hydrogen Bonds

C—H activation (or the use of hydrocarbons as nucleophiles) is an offshoot of the previous approach. By replacing one or both of the organometallics with the hydrogenated substrate, a reaction much closer to the "ideal dehydrogenative coupling" is achieved. However, successful utilisation of a carbon-hydrogen bond as a nucleophile in a coupling requires cleaving the often strong bond, which can be extremely challenging with non-acidic and non-nucleophilic centres.[31] Despite this, it is a popular field of research, and interest is only increasing.[28,32,33]

Activation of these sites is achieved by a number of mechanisms (Scheme 1.11).[34] The route that has received the most attention is concerted metallation/deprotonation (or CMD) (Scheme 1.11a). The cooperative action of a basic additive (almost always an acetate) and a transition metal in a cyclic transition state leads to synchronised deprotonation of the hydrocarbon centre and complexation to the transition metal. Less common mechanisms involve direct oxidative addition of the metal to a C—H or σ-bond metathesis (Scheme 1.11b and c).

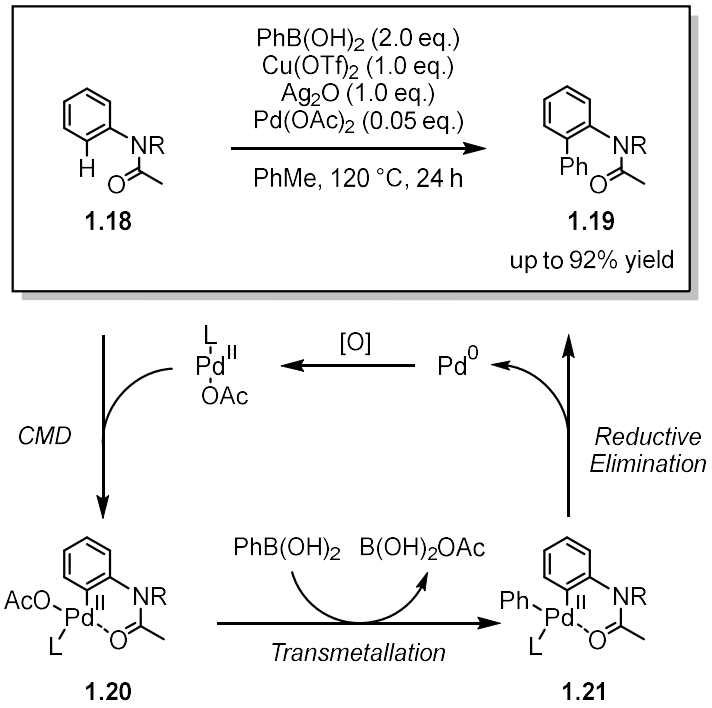


Scheme 1.11. Mechanisms for the activation of carbon-hydrogen bonds by transition metal complexes

Once the reaction is initiated by a C—H bond activation and the carbon-metal bond is formed, the cross-coupling proceeds just like any other neutral cross-coupling after an oxidative addition. Often, the transition metal complex acquires a second carbanion ligand, followed by reductive elimination to the oxidised product. This can originate from transmetallation with an organometallic additive or a second C—H activation.

An example of this reactivity can be seen in the report by Shi and coworkers of an oxidative Suzuki–Miyaura coupling (Scheme 1.12).[35] Acetate-enabled CMD forms the palladacycle **1.20**. Transmetallation with the boronic acid affords the **1.21**, followed by reductive elimination to **1.19** in high yield. The palladium is reoxidised by copper(I) triflate, completing the catalytic cycle. Inclusion of silver(I) oxide was necessary to prevent homocoupling.

The regiochemistry of the C—H activation is controlled by the chelation of the palladium to the pendant amide group, directing it to the desired carbon-hydrogen bond.



Scheme 1.12. An oxidative Suzuki-Miyaura reaction between N-arylacetamide **1.18** and phenylboronic acids.

Other approaches to carbon-carbon bonding from the intermediate organometallic, such as a Heck-type reactions, are also possible.[36]

C—H activation has an obvious benefit –the need for prefunctionalisation of the coupling partners is removed. By utilising the ubiquitous carbon-hydrogen bond, the additional steps to synthesise the traditional intermediates can be avoided.

However, there are a number of complicating factors. C—H bonds are strong, and so activating them to react can be difficult; many C—H activations rely on specific aryl substituents to promote reactivity. Selectivity can also be an issue. Homocoupling competes with the desired cross-coupling, and regioselectivity can be an issue when multiple C—H centres are accessible *via* activation.[32] To avoid this, use of directing groups (appended structures geometrically near the site of interest, typically nucleophilic in nature in order to chelate the transition metal centre) can amplify the reactivity of the C—H activation agent and direct the reactivity to the desired centre.[31] Installation of these functional groups often adds additional steps to the synthetic route, and can require removal after the fact.

1.5 Project Aims

In this DPhil work, we aim to develop oxidative methods for the construction of complex scaffolds *via* carbon-carbon bond formation. To achieve this, we explore two reaction systems developed by the group (a photocyclisation with visible light and an iron catalysed oxidative cross-coupling), with particular focus on novel reactivity uncovered serendipitously during the investigations.

Section 2

The first project is an exploration of an anomalous oxidative allylation observed during a visible light mediated triplet-energy-transfer (TET) 6-π cyclisation reaction.

Chapter 2: Oxidative Photocyclisation

2.1 Photocyclisation

Certain conjugated 6-electron π systems are able to undergo cyclization reactions, which are powerful approaches to carbon-carbon bond-formation that can be applied to the synthesis of many cyclic compounds.[37]

This transformation can be achieved in two ways: in a concerted pericyclic reaction or in a stepwise fashion.[38]

The concerted reaction occurs through a process known as electrocyclisation, in a "cyclic electronic shift" in which orbital overlap and symmetry dictate reactivity and the stereochemical outcome.[39] These can be initiated either with thermal energy (in which case the cyclisation is disrotatory) or photochemically (where the cyclisation is conrotatory, due to an inversion of symmetry from the electron promotion).



Scheme 2.1. Electrocyclisation reactions

Stepwise reactions are less clearly defined. The term describes reactions that produce the same products as electrocyclisations but proceed by a number of discrete steps, each with their own transition state and energy barriers. One well-utilised stepwise approach to the cyclisation of 6-π conjugated systems is the photochemical excitation to a diradical species, which reacts in a classical stepwise radical approach to the product.

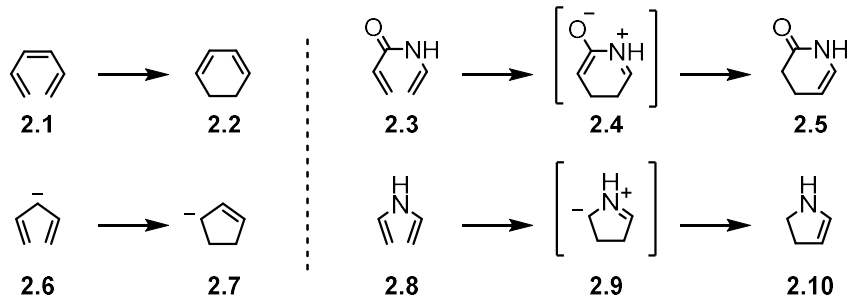
Both of the described approaches to photochemical cyclisation (pericyclic and stepwise) are referred to by the umbrella term of "photocyclisation". Often, the mechanism of a photocyclisation is difficult to validate without exhaustive study, and so the term is used without mechanistic clarification for light-driven cyclisations unless the nature of the transformation is relevant.

2.2 Classifications of 6-π systems

6-π photocyclisations can be understood by analogy to two simple hydrocarbon frameworks: hexatriene for 6-membered ring formation or the pentadienyl anion for 5-membered (Scheme 2.2).

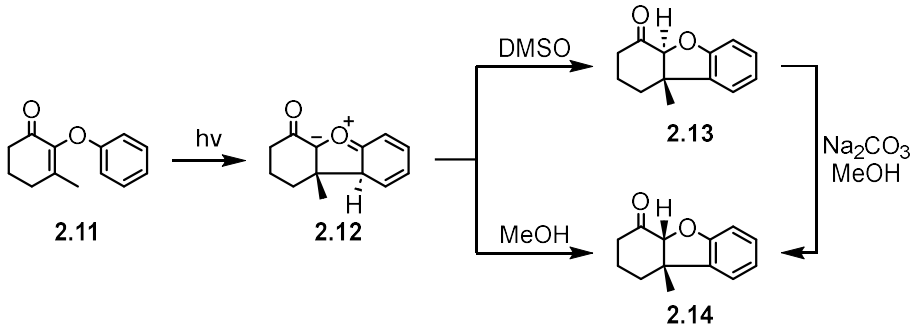
Inclusion of heteroatoms into these structures can be isoelectronic, and these cases they can cyclise *via* the same cyclisation patterns as the hydrocarbon frameworks. However, the changes in electronic structure lead to different stable endpoints of the reactions. Hydrocarbon substrates produce neutral compounds as the result of the cyclisation (or in the case of **2.6**, an anion). An enamide (**2.3**) as an analogue for **2.1** gives a zwitterionic product which is isoelectronic with the simple diene **2.2**. Dienamines (**2.8**) mimic **2.6**, and also generate a zwitterionic product (**2.9**) isoelectronic to the hydrocarbon cyclisation.

These zwitterions are unstable, and so isomerise further. **2.4** goes on to form the lactam **2.5**, and **2.9** forms the cyclic enamine **2.10**. These apparent tautomerisations can proceed both by the traditional intermolecular protonation and deprotonation events or by an intramolecular hydride shift. The mechanism of a given reaction is dictated by availability of external protons, and the particular molecular scaffold.



Scheme 2.2. Photocyclisations of 6-π systems.

This diversity of mechanism can be observed in the reactions of **2.11** by Schultz and coworkers (Scheme 2.3).[40] As a 6-electron 5-atom system, its photocyclisation is analogous to the pentadienyl anion. After the initial cyclisation, the zwitterionic intermediate is stabilised by the neighbouring carbonyl group. In the aprotic solvent DMSO, the *trans*-fused system is exclusively produced. This is the result of a conrotatory cyclisation to **2.12**, followed by a stereospecific suprafacial 1,4-hydrogen shift to give **2.13**. By changing to a protic solvent (in this case methanol), the selectivity was reversed. The intermediate **2.12** was still produced by the conrotatory cyclisation, but the available protons allowed for a protonation/deprotonation mechanism to afford the lower energy *cis*-fused **2.14**. Interconversion from **2.13** to **2.14** required the addition of base to epimerise the α position.

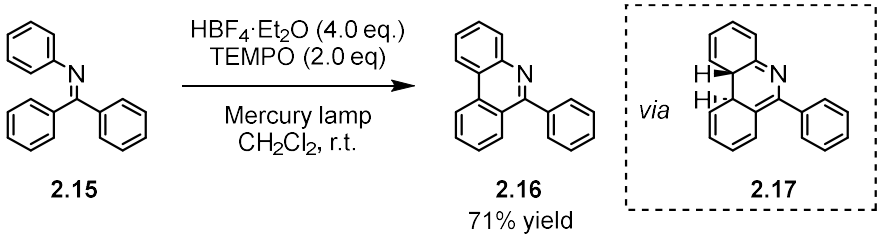


Scheme 2.3. Control of product stereochemical configuration by isomerisation mechanism. Reaction conditions and yields not given.

2.3 Accessing Heteroaromatic Products *via* Photocyclization

Heteroatom-containing photocyclisation reactions give access to dihydro-analogues of aromatic heterocycles (dihydropyridone and dihydropyrrole, respectively, for the examples in Scheme 2.2). It is an isomerisation and results in the conversion of a carbon-carbon pi to sigma bond.

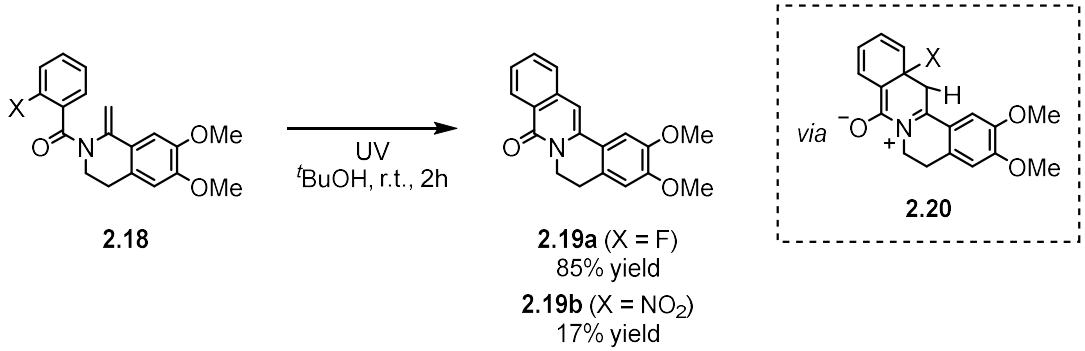
However, access to the aromatic heterocycles is simply a matter of oxidation – by including an external oxidant that can dehydrogenate the products, it is possible to generate the aromatic heterocycles in a single step. For example, Alabugin and coworkers demonstrated the use of TEMPO to produce the oxidised product **2.16** from the cyclisation of **2.15** (Scheme 2.14).[41]



Scheme 2.4. Oxidative cyclisation of **2.15** using TEMPO.

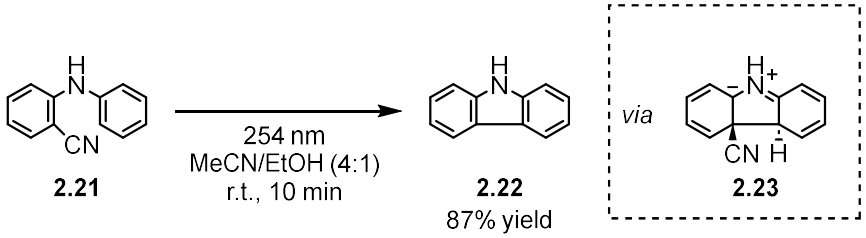
By pre-oxidising the substrate with the inclusion of a leaving group, the photocyclisation can be made to proceed directly to the aromatic product without an external oxidant present.

This can be seen in the modification of the enamide system by Lenz, achieved with success across a range of substituents (Scheme 2.5).[42] In these cases, the eliminative process is proposed to occur *via* cyclisation to the zwitterion **2.20** followed by loss of a proton and the leaving group, rather than the hydrogen shift normally observed. This generates the aromatic pyridone product **2.19**, in yields between 17% for a nitro group and 85% for fluorine.



Scheme 2.5. Eliminative cyclisation of **2.18**.

This reactivity is also observed in dienamine-type cyclisations. Inclusion of a nitrile group in **2.21** led to carbazole production in an 87% yield.[43]

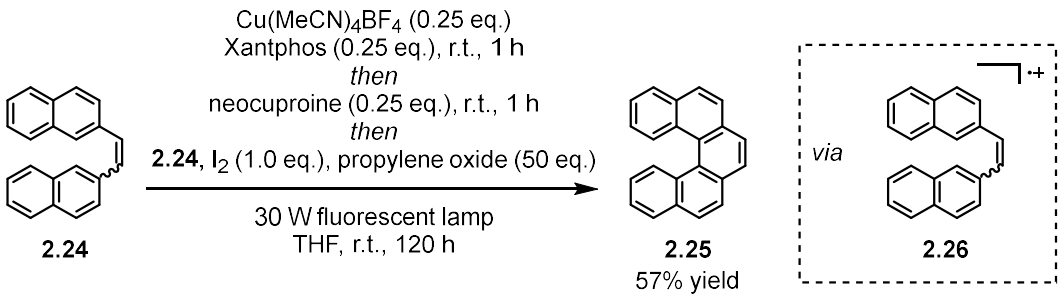


Scheme 2.6. Eliminative cyclisation of **2.21**.

2.4 Visible Light Photocyclisation

2.4.1 Non-Eliminative Cyclisations

A common factor of the photocyclisations discussed thus far was the reliance on UV light as the photon source; it was required in order to reach the excited states necessary for photocyclisation. The use of UV light in organic reactions is valuable as a high energy photon source. However, these harsh conditions can cause undesired side-reactions and decompositions, meaning that many functional groups are not tolerated. This has led to a desire to replace the use of UV light with visible light. One of the earliest examples of the use of a photocatalyst to promote a photocyclisation was by Collins and coworkers in the synthesis of [5]helicene (Scheme 2.7).[44] Ordinarily accessible only with UV irradiation, the *in situ* formation of a copper photoredox catalyst allowed for the use of a white fluorescent lamp in the procedure, giving a yield of 57% (compared to 25% historically achieved with UV light, due to low regioselectivity and overreaction). This was proposed to have been achieved by the single electron oxidation of the stilbene starting material.



Scheme 2.17. Visible-light-mediated oxidative cyclisation of **2.24**

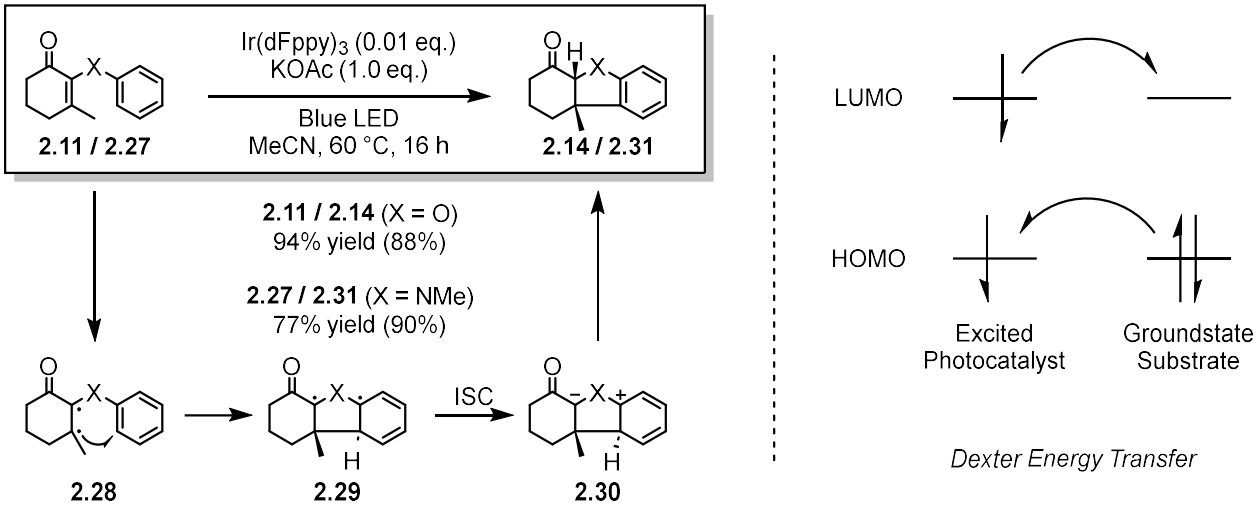
A class of photocatalyst that has seen widespread use in the field of photocyclisation are those based on iridium(III) complexes. These benefit from high absorption of desired visible light wavelengths, and rapid, efficient conversion to long-lived excited states.[45]

For example, the use of an iridium-based photocatalyst by Smith and coworkers allowed for the transferral of the photocyclisation chemistry of **2.11** (described previously in Scheme 2.3) to a visible light-initiated regime (Scheme 2.18).[46] Irradiation of the relevant starting material with blue LEDs in the presence of $Ir(dFppy)_3$ gave **2.14** in a 94% yield, and **2.31** in a 77% yield (comparable to the yields achieved by Schultz and coworkers with UV direct irradiation)[47,48].

This was achieved using triplet energy transfer photosensitization, or TET. This process involves excitation of the iridium catalyst to singlet state, followed by rapid intersystem crossing (ISC) to a long-lived triplet state. Dexter energy transfer (the exchange of the high energy electron for one of low energy and opposite spin) quenches the catalyst and excites the substrate.

Fortunately, the substrates in question have low triplet energies and large reduction potentials. Thus, by selecting iridium photocatalysts with higher triplet energies that were unable to access the necessary redox potentials, the triplet diradical excited state of the enones (**2.28)** could be accessed easily without interference from photoredox pathways. This was achieved by careful tuning of the ligands bound to the iridium(III) centre, a convenient avenue for tuning of the electronic properties of the catalyst. In the case of **2.11** and **2.27**, *fac*-Ir(dFppy)$_3$ was found to be the most effective.

Stepwise cyclisation of the diradical onto the pendant aryl group afforded the cyclised diradical **2.29**, which can undergo intersystem crossing back to the familiar singlet state zwitterion **2.30**. The observed *cis* product is generated either by the known 1,4-hydrogen shift to the *trans* product followed by epimerization, or by independent protonation/deprotonation events.

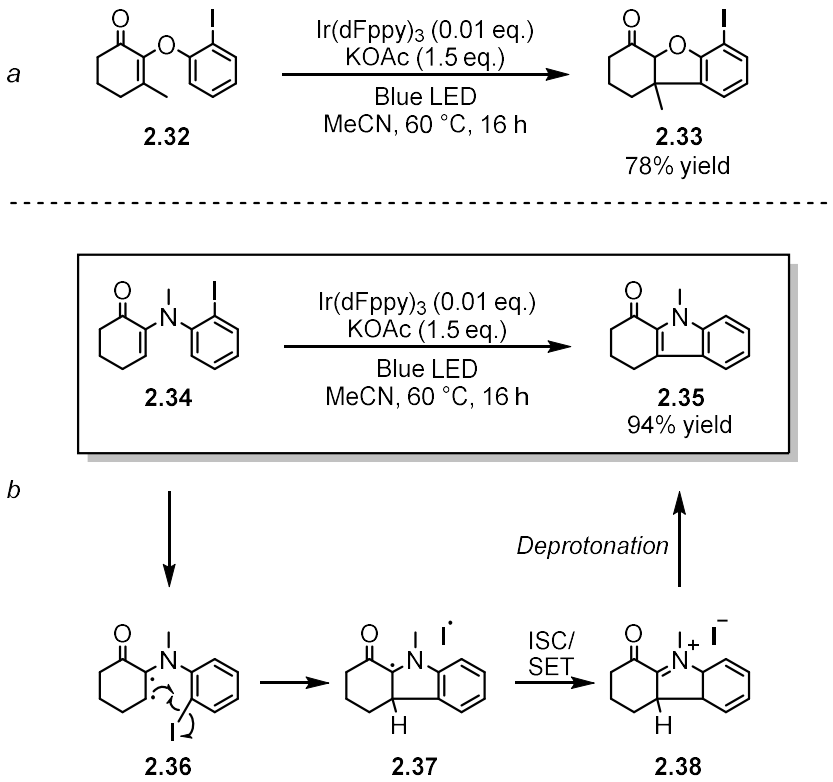


Scheme 2.18. Visible-light-mediated cyclisation of **2.11** and **2.27**. Figures in brackets refer to the literature yields of the equivalent cyclisation with direct UV excitation.

2.4.2 Eliminative Visible Light Photocyclisation

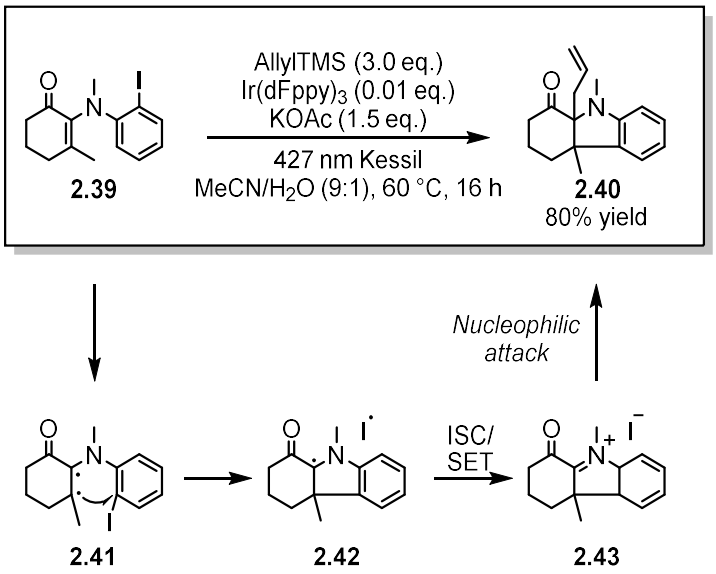
It was found during the scoping of the reaction that **2.32** was tolerant of all ortho substituents and underwent no eliminative cyclisations – **2.33** was produced in a 78% yield (Scheme 2.19a). However, in a subsequent investigation, the reactivity of the **2.34** scaffold (the β-unmethylated version of **2.27**) deviated from the expected pathway.[46] When the *ortho*-iodinate **2.34** was subjected to the photocyclisation conditions, the indole **2.35** was the sole product observed (in a 94% yield), rather than the expected non-eliminative indoline product (Scheme 2.19b).

The mechanism of this was shown to be different from the eliminative photocyclisations discussed previously. Rather than photocyclisation followed by elimination, the reaction proceeds through the excited diradical triplet **2.36** and an *ipso*-substitution of the aryl iodide (**2.37**). The iodine/**2.37** radical pair undergoes an ISC/SET event to the iminium **2.38**. With the proton at the β position, a simple imine/enamine tautomerisation provided the rearomatised indole product **2.35**.



Scheme 2.19. Visible-light-mediated cyclisation of **2.32** and eliminative cyclisation of **2.34**.

However, by returning to the **2.27** scaffold with a β-methyl blocking group, this rearomatisation is prevented, and the iminium **2.43** can be isolated (often as the hemiacetal) or trapped with a range of nucleophiles. (Scheme 2.20)

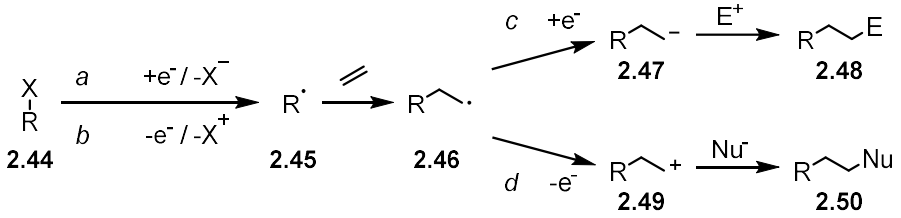


Scheme 2.20. Visible-light-mediated eliminative cyclisation and trapping of **2.39**.

2.5 Radical-Polar Crossover

This is an example of a radical-polar crossover reaction (RPC); a reaction in which an initial one-electron (radical) process transitions into a two-electron (polar) process, often by means of a single electron oxidation or reduction of a radical intermediate.

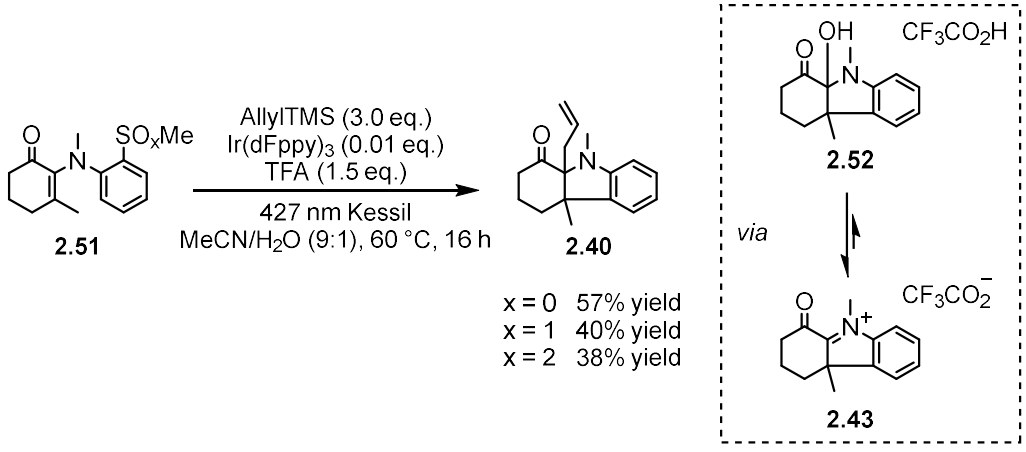
RPC reactivity is a very powerful tool, that allows a transformation to benefit from radical and ionic behaviour. An often-utilised approach in photoredox chemistry is the generation of a radical (such as **2.45)** by an initial SET event (*a* or *b*), that is then trapped by a π system.[49] A second SET (*c* or *d*) converts the resulting combined radical **2.46** into an ion, trapped by the appropriate reagent. Each SET can be either oxidative or reductive. The total RPC reaction is often reductive (a and c) or neutral (*a*/*d* or *b*/*c*) in nature, and the oxidative route (*b* and *d*) is less common.[50 51]



Scheme 2.21. Common routes available for the radical/polar crossover reaction of a photoredox/alkene trap system.

RPC's implementation in TET (rather than photoredox chemistry) is less well-explored, making the reactivity discovered by Smith and coworkers unusual.

In further studies, it was found that as well as iodides, methyl sulphides, sulphoxides, and sulphones were able to act as the necessary redox shuttles to support the radical-polar crossover (Scheme 2.22). The nucleophilic trapping of the iminium **2.43** when generated from sulphurous substrates was initially low yielding, due to competitive formation of the hemiaminal side-product **2.52**. This formed reversibly by the trapping of the iminium with adventitious water. The solution found was inclusion of TFA, to promote the elimination of water and the formation of the iminium trifluoroacetate salt **2.43**. This was successful in promoting the desired reactivity.

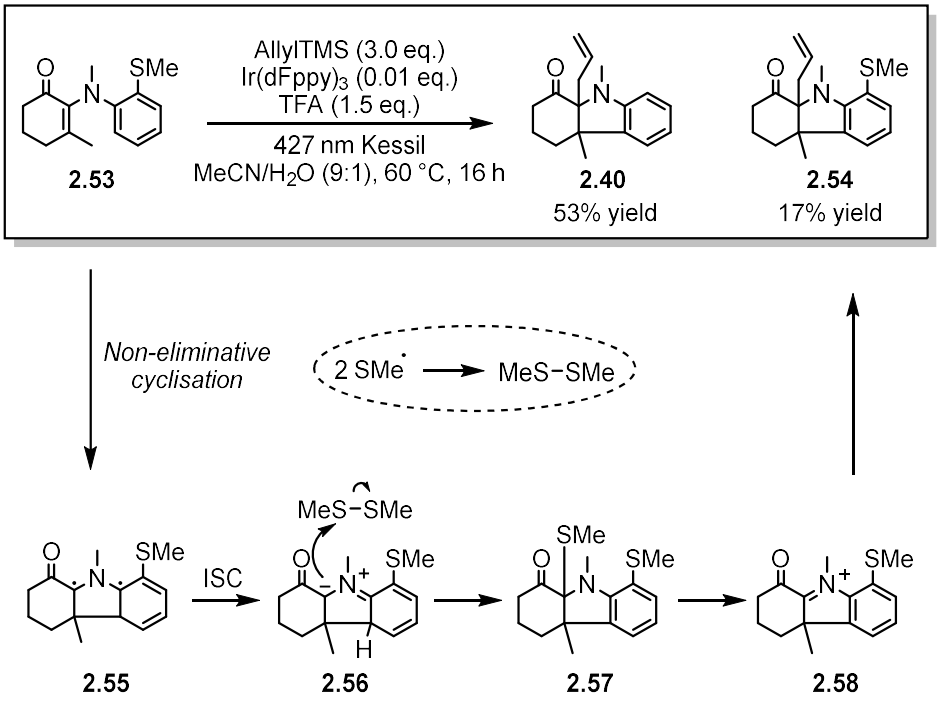


Scheme 2.22. Eliminative cyclisation of with sulphur-containing leaving groups. Yields determined by quantitative ^{1}H NMR

2.6 Observed Oxidative Cyclisation

However, the inclusion of TFA also lead to the recovery of the side-product **2.54**, a formally oxidised, non-eliminative trapping product (Scheme 2.23).

There was no explanation for this within the reaction landscape of the RPC photocyclisation, and so an alternative route was proposed. The hypothesis was that methyl sulphide radicals produced in the standard eliminative reaction dimerised to produce dimethyl disulphide (DMDS). This intercepted the zwitterionic intermediate of the non-eliminative pathway (**2.56**) and acted as a two-electron AT oxidant to produce the thioaminal **2.57**. The methyl sulphide substituent on the aryl group of **2.54** had no part in the reaction and was only relevant in order to generate DMDS *via* production of **2.40**.



Scheme 2.23. Non-eliminative oxidative cyclisation of **2.53**, suggested to occur by interception of **2.56** by DMDS. Yields determined by quantitative ^{1}H NMR.

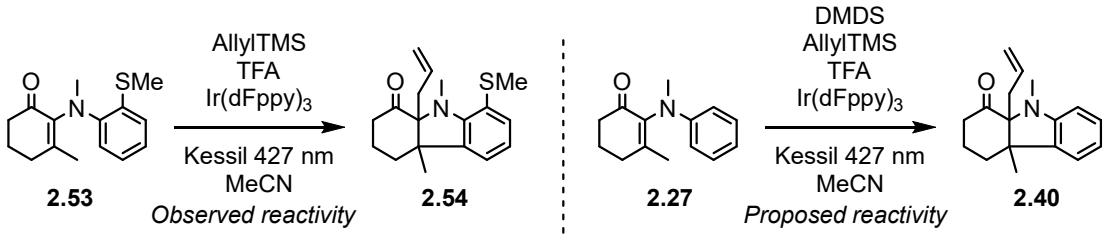
Although low yielding, this transformation demonstrated a number of unusual reactivities. It was an example of an oxidative photocyclisation. These are fairly common, as photocyclisation products are often very amenable to oxidation in order to aromatise. However, the production of a reactive intermediate (in this case, the iminium) as the oxidised product rather than the stable aromatic is less well-known. The oxidative step is also an interruption to the photocyclisation cascade, rather than a discrete second telescoped reaction. This type of reactivity is not novel (reductive applications for this reactivity are known) but it certainly is remarkable.[52]

It was also an example of a net-oxidative and TET-induced RPC reaction. These two factors result in an electronically neutral radical generation and an oxidative trapping, rather than the more familiar procedure of the oxidations taking place during radical step, followed by a neutral quenching.

Ultimately, it is a reaction that develops a large amount of complexity in a single step, forming two carbon-carbon sigma bonds and one quaternary centre. Achieving this oxidatively opens the doors for a wide range of off-the-shelf nucleophilic traps (as was possible with the iodine-elimination reaction) without the need to prefunctionalise the enaminone – a process that complicates the substrate synthesis, requiring *de novo* construction of the cyclic enone.

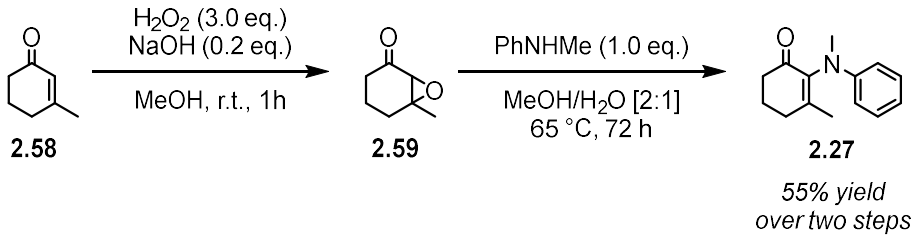
2.7 Confirmation of Reactivity

The most logical starting point for continuing the investigation was to confirm the proposed mechanism of the oxidation. If it was accurate, then addition of excess dimethyl disulphide (DMDS) to a reaction mixture containing the unfunctionalised (**2.27**) rather than thiolated (**2.53**) substrate would still lead to formation of the allylated trapping product **2.40**.



Scheme 2.24. Oxidation products were observed in the reaction of **2.53**. It was proposed that addition of DMDS to a similar, unthiolated substrate **2.27** could induce the same oxidation reaction.

Fortunately, the synthetic route to hexenone **2.27** is well-known and facile (Scheme 2.25). Commercially available 3-methylcyclohexenone **2.58** reacts with hydrogen peroxide and sodium hydroxide in a nucleophilic epoxidation. The epoxide can then be opened with N-methylaniline and the created β-hydroxyketone dehydrated in one step to reform the hexenone moiety in a 55% yield over the two steps. Low nucleophilicity of the methylaniline limits the efficiency the coupling step but given the availability of the starting materials this was not a serious concern.



Scheme 2.25. Synthesis of **2.27**. The epoxidation of **2.58** is followed by ring-opening with N-methylaniline.

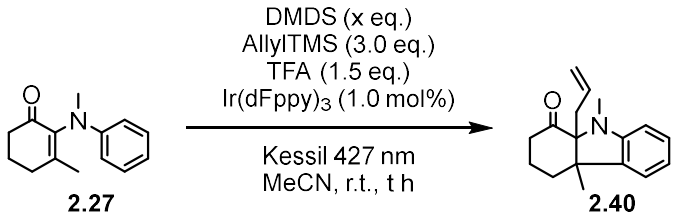
With access to the substrate, we were able to test the hypothesis. Exact repetition of the initial trapping reaction's condition with the addition of an excess (5.4 equivalents) of DMDS lead to an encouraging early hit: the allylated product **2.40** was found in a 45% yield (Table 2.1, Entry 1).

With this apparent confirmation of the proposed reactivity, we set out to explore the scope of the reactivity. The mechanism of the theorised DMDS oxidation only requires a single equivalent for full conversion to the oxidised product, so the amount of the DMDS included was reduced. Reactivity was conserved at both 3.0 and 1.0 equivalents (Entries 2-3, 50% and 61% yield respectively).

The recovery of significant amounts of **2.27** prompted an increase in reaction time; after 42 hours the yield was increased slightly to 60%, but all **2.27** was consumed (entry 4)

The allylated product was still found in a 57% yield with only 0.5 equivalents of DMDS despite the hypothesised stoichiometry (Entry 5). Even more surprisingly, control experiments with no DMDS also consistently gave 52-62% yields over several repeats (Entry 6).

We noticed a decrease in the recovery of **2.27** as the equivalents of DMDS decreased, without any accompanying increase in yield. Although not necessary for the oxidation, it apparently had an effect on the rate of degradation of the starting material.



Entry	x / eq.	t / h	Conversion / %	Yield / %
1	5.4	18	66	45[a]
2	5.4	42	100	60
3	3.0	18	61	50
4	1.0	18	83	61
5	0.5	18	88	57
6	0	18	100	52-62

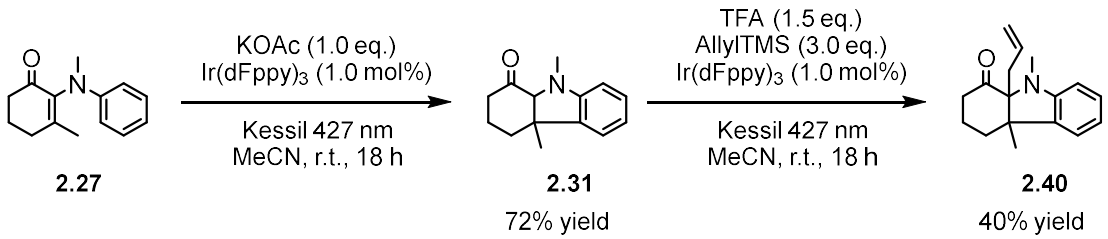
Table 2.1. Conversions and yields were measured by quantitative ^{1}H NMR spectroscopy against dimethyl terephthalate (0.04 eq.) unless otherwise stated. [a] Isolated yield

The discovery that the oxidation was not due to DMDS interference in the cyclisation raised a number of questions: how did the oxidation occur, and what was the oxidant?

We started with the first question; whether the allylation took place during the initial excitation and cyclisation of the hexenone substrate, or if the standard cyclisation happens first and is followed by a discrete oxidation step. To probe this, the cyclised compound **2.31** was synthesised using the original non-eliminative photocyclization method, as it would be the intermediate in the second case (Scheme 2.26).[53] This compound is thought to be photochemically inactive under the current conditions, as the enone chromophore is absent and thus there is no easily accessible triplet state for the iridium sensitiser to induce.

The pre-cyclised but un-allylated product was then subjected to the oxidation conditions, and the allylated product was produced in a 40% yield – confirming that the allylation can occur as a second separate reaction with the cyclised substrate. Despite this low yield, the starting material was fully

consumed and no other species could be identified in the crude reaction mixture. It was thus presumed that the mass loss was due to decomposition of a key species during the reaction. It is possible that interception of the sensitised triplet diradical formed in the cyclisation may also contribute to the product formation, but the anomalous oxidation of **2.31** was of more interest and was possible to analyse in isolation.



Scheme 2.26. Synthesis of **2.31** was achieved with the known photocyclisation. Subjection of **2.31** to lead to the oxidised product **2.40.**

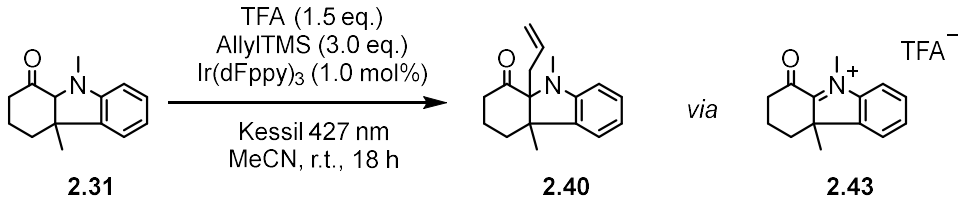
Thus, our understanding of this tandem cyclisation/oxidative allylation was that the known TET-mediated cyclisation occurred, forming **2.31**, followed by an as-yet unidentified oxidation process which generated **2.40**. In an effort to focus on the novel oxidation step and avoid any effects stemming from the efficiency of the cyclisation, the rest of the investigation was performed on the pre-cyclised substrate.

2.8 Exploration of the Reaction System

With no immediate explanation for the origin of the oxidation, other components were removed in turn to probe their effect on the reaction. (Table 2.2). The presence of the TFA was found to be the most important factor, as there was no observed allylation when absent (Entry 1). The iridium photocatalyst and irradiation with visible light both had a substantial effect on the yield (15% and 5% without, respectively), but production of **2.40** was still observed in their absence (Entries 2-3).

One initial theory for the source of the anomalous oxidation was that the allyltrimethylsilane (allylTMS) was not only acting as a nucleophilic trap, but also contributing to the reaction as a stoichiometric oxidant. The superstoichiometric loading of 3.0 equivalents would allow for its consumption in both roles without limiting availability. It was proposed that protonation to the silicon-stabilised β-

carbocation would provide the opportunity for electron transfer oxidation from **2.31** to the cation, reducing an equivalent of allylTMS and effecting a single-electron oxidation of the substrate. However, when the allylTMS was removed from the reaction, reactivity was still observed (Entry 4). Absence of the allylTMS necessarily prevented allylation, but **2.31** was still fully consumed. NMR analysis of the crude reaction mixture showed a side-product that was tentatively identified as the iminium **2.43**. This was a likely candidate for the electrophilic species that accepted the allyl group from the allylTMS, as it had been previously identified as the electrophile capable of trapping allylTMS in the eliminative radical-polar crossover reactions based on this framework. In addition, observation of a mixture of allylTMS and TFA in acetonitrile by both ^{1}H and ^{19}F NMR showed no noticeable reactivity, both in the dark and after irradiation - if protonation were the source of oxidation, then this would likely not be the case. These findings suggest that the oxidation event was independent of the allylTMS, which served only as an innocent nucleophilic trap.



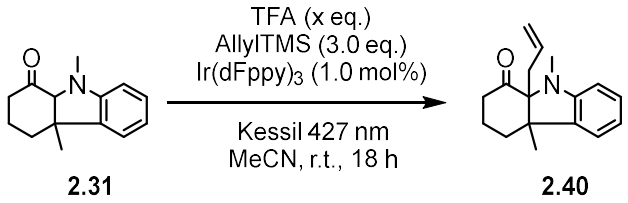
Entry	Component Removed	Conversion / %	Yield / %
1	TFA	57	0
2	$Ir(dFppy)_3$	55	15
3	Kessil 427 nm	60	5
4	AllylTMS	100	-[a]

Table 2.2. Conversions and yields were measured by quantitative ^{1}H NMR spectroscopy against dimethyl terephthalate (0.04 eq.). [a] Allylated product was not observed in the absence of the allylating agent. Instead, an intermediate consistent with the iminium **2.43** was observed

Having identified the TFA as a key component of the system, we decided that it was the place to start in order to optimise the yield of the reaction and probe the mechanism (Table 2.3).

Increasing from 1.5 to 3.0 equivalents had no major change on the yield (Entry 1), suggesting that either TFA quantity has little impact on product formation or that the decrease in pH of excess TFA decomposes one or more of the components.

However, dropping to sub-stoichiometric quantities of TFA also led to decreased yields (Entries 3-4). From observing such a marked decline, we believe that at these decreased concentrations the TFA became a limiting reagent. As the yields appeared to tend towards 50% when calculated relative to the moles of TFA (as if it were becoming the limiting reagent), a preliminary hypothesis was that two equivalents of TFA are required for full conversion.



2.31 **2.40**

Entry	x / eq.	Conversion / %	Yield / %
1	3.0	100	47
2	1.5	100	40
3	0.5	100	25
4	0.1	35	5

Table 2.3. Conversions and yields were measured by quantitative ^{1}H NMR spectroscopy against dimethyl terephthalate (0.04 eq.).

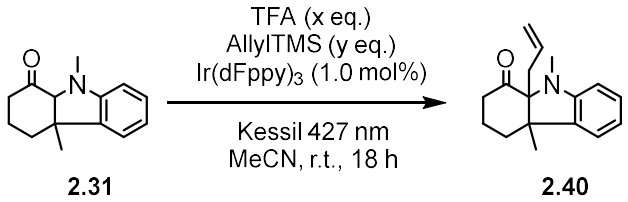
Variation of the amount of allylTMS was also a simple avenue to explore (Table 2.4, Entries 1-2). Doubling the equivalents to 6.0 gave a moderate increase to 59% yield and increasing further to large excess of 20.0 equivalents led to the highest yields so far, at 74%.

AllylTMS was not believed to contribute to the oxidative step, so the substantial uptick in yield is likely not due to more efficient oxidation – rather, to more efficient trapping of the oxidation product. The

excess allylTMS serves to increase the rate at which this trapping takes place, out-competing potential side reactions of the reactive iminium intermediate **2.43**.

Such a large improvement was very promising, but such excessive quantities of allylTMS were not desirable. We proposed that increasing both the TFA and allylTMS could increase the rate of oxidation, but also trap **2.43** more effectively and therefore avoiding the increased decomposition.

However, twofold increase in both led only to a disappointing 46% yield (Entry 3). In fact, increasing TFA to 2.0 or even 3.0 equivalents with the previously superlative 20.0 equivalents of allylTMS showed a slight decrease in yield relative to 1.5 equivalents (Entries 4-5).



2.31 **2.40**

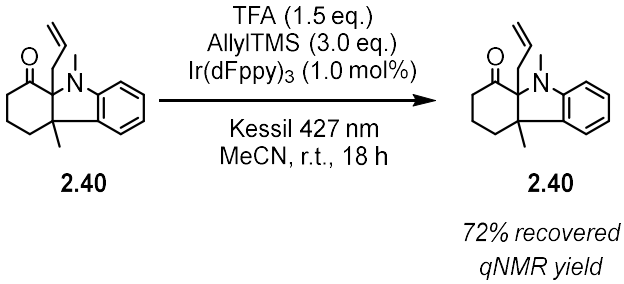
Entry	TFA / eq.	AllylTMS / eq.	Conversion / %	Yield / %
1	1.5	6.0	100	59
2	1.5	20.0	100	74
3	3.0	6.0	100	46
4[a]	2.0	20.0	100	71
5[a]	3.0	20.0	100	72

Table 2.4. Conversions and yields were measured by quantitative ^{1}H NMR spectroscopy against dimethyl terephthalate (0.04eq.). [a] Reactions were performed on the uncyclized starting material **2.27** rather than **2.31**.

2.9 Observing Reaction Progression

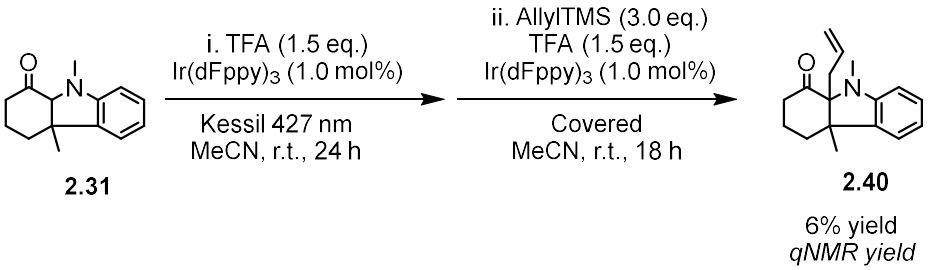
Reactions with an excess of both TFA and allylTMS showed a consistent yield of around 75%, which appeared to be an upper bound on reactivity. In order to increase the yield further, it was necessary to understand what was causing the reaction to stall.

One cause of this apparent upper limit on yield could have been instability of the product **2.40** under the reaction conditions, where the reaction proceeded with high conversion but the product decomposed over time. To test this, a sample of **2.40** was resubmitted to the reaction conditions and monitored *via* quantitative ^{1}H NMR (Scheme 2.27). After 18 hours, only 72% of the sample remained – confirming the instability of the product under the reaction conditions. The agreement between this result and the highest yields achieved in the reaction suggest that at high allylTMS loadings, the decomposition of **2.40** is a major source of material loss.



Scheme 2.27. Monitoring of the decomposition of **2.40** under the reaction conditions with ^{1}H quantitative NMR.

To assess the stability of the iminium intermediate **2.43**, the reaction was again performed without allylTMS. After 24 hours, allylTMS was added and the mixture left to stir in the dark for another 18 hours. If the iminium were stable over the reaction timeframe, then a temporal separation between its generation under irradiation and its trapping with allylTMS would have minimal impact on the yield. In fact, despite full consumption of the starting material, only a 6% yield was observed. This confirmed that the intermediate generated by the reaction independent of allylTMS was unstable under the reaction conditions, suggesting a possible source of material loss. This explained why increased allylTMS loading had such a marked effect on the yield as the greater concentration lead to more rapid trapping.



Scheme 2.28. Observation of the decomposition of **2.31** under the reaction conditions, by pre-generating the iminium before trapping in the dark.

^{1}H NMR monitoring was used to probe the reaction progression directly. By utilising a J Young NMR tube, we hoped we would be able to identify any reactive or air sensitive intermediates that could not survive the standard workup (**Figure 2.1**). However, no species other than **2.31** and **2.40** (seen at t = 0 h and t = 18 h respectively) could be identified in the reaction mixture. A small, complex multiplet in the aromatic region (t = 18 h, 7.65 – 7.40 ppm) were the only other aromatic protons detected, but no structural information could be extracted – they presumably belonged the decomposition product or products. The starting material was fully consumed as expected.

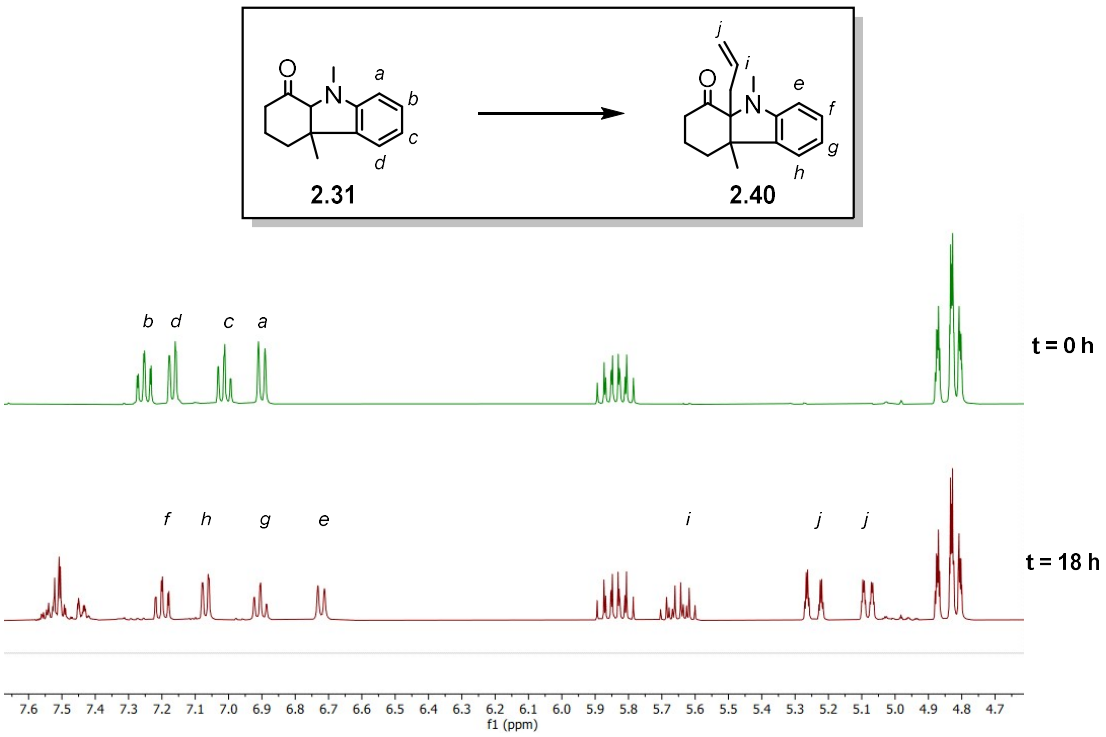


Figure 2.1. Comparison of the ^{1}H NMR spectra of the starting materials (top, t = 0 h) and crude reaction mixture (bottom, t = 18 h) in d^{3}-acetonitrile. An unassigned downfield multiplet was observed in the product mixture at t = 18 h.

To investigate the relative rates of product formation and starting material consumption, we observed the reaction progress over time (Figure 2.2) The standard reaction was again performed in a J Young NMR tube, where it was irradiated in one-hour increments, between which an NMR spectrum was acquired. Given the low yield of the reaction performed in the dark (Table 2.2, Entry 3), it was assumed that the reaction progression would be effectively paused during the acquisitions. After only an hour of irradiation, 29% of **2.31** had been converted, although there was only a 15% yield of **2.40**. Therefore, 14% of the material was unaccounted for. Similar progression was seen over the second hour, where the yield increased by 20% while another 17% of the material was lost. After hour three, the increase in **2.40** had begun to level off, with a total yield of 42% (only 7% more than t = 2), and by 18 hours the yield was 57% with no starting material remaining – implying a material loss of 43%.

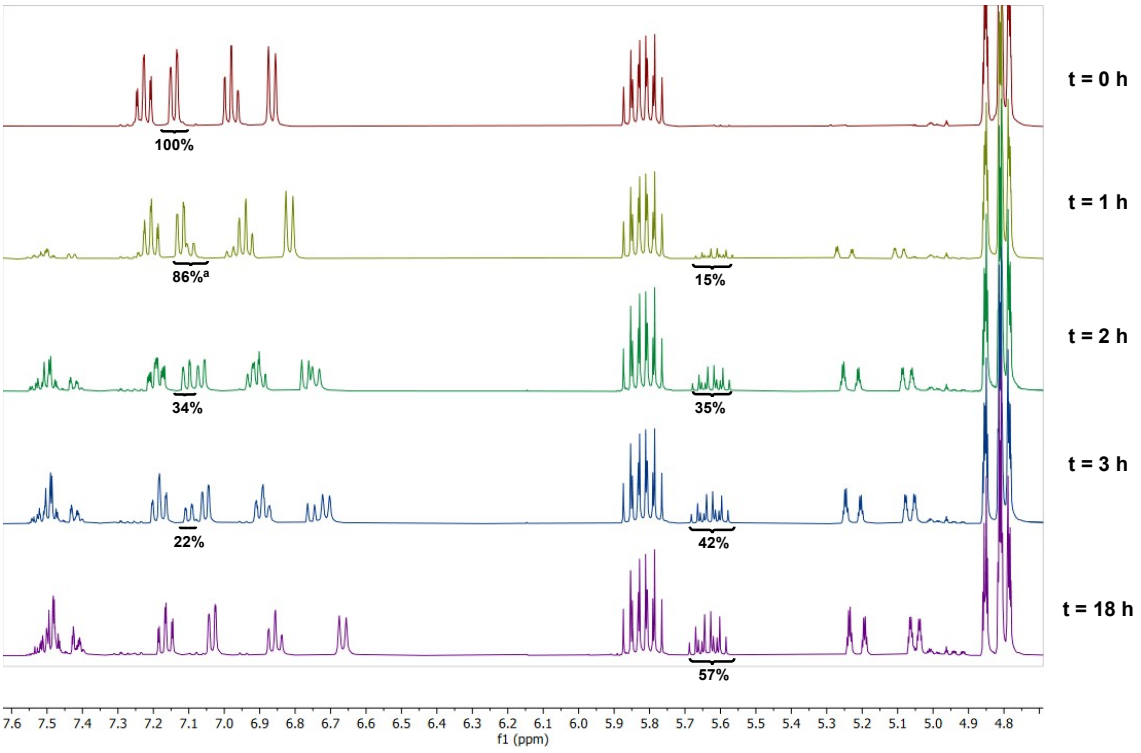


Figure 2.2. Comparison of the ^{1}H NMR spectra of the allylation of **2.31** over time. The reaction was performed in a Youngs NMR tube in d^{3}-acetonitrile, with NMR spectrum acquisition between 1 h periods of irradiation. Material loss was estimated as yield of **2.40** subtracted from the conversion of **2.31**. This gave values of 0%, 14%, 31%, 36%, 43% for t = 0, 1, 2, 3, 18 hours respectively. [a] no isolated **2.31** peaks could be found, so a cumulative peak of **2.31** and **2.40** was measured and the quantity of **2.31** approximated by subtraction.

This experiment had two important takeaways. Firstly, this confirms that the loss of yield over the course of the reaction is not solely due to decomposition of **2.40**. Over 70% was recovered after 18

hours in the previous decomposition investigation, giving a rough estimate for the rate of decomposition. This is incompatible with the observations after the first hour – wherein there was an almost 1:1 ratio between product formation and decomposition. This rate of decomposition would equate to a recovery of **2.40** of 52% after just 1 hour, far lower than the 70% observed after 18 h in reality. Thus, there must be an additional decomposition pathway(s).

Secondly, the initial oxidation step is slow. A large portion of **2.31** was still present even after three hours, showing that oxidation to the iminium had not occurred. Therefore, regardless of how efficient the trapping step can be rendered, the reaction time would be limited by the rate of oxidation. Given that **2.40** is unstable in the reaction conditions, having a long reaction time would also cause the yield to suffer. Therefore, achieving a high-yielding transformation with the current reaction system is unlikely.

2.10 Oxidation Interrogation

At this point, it was unclear which species in the reaction mixture were capable of oxidising the material, or indeed what the ultimate fate of the electrons was (i.e. the identity of the terminal oxidant).

On the surface, there would seem to be a likely candidate for each: the iridium photocatalyst as the reagent enabling the oxidation, and atmospheric oxygen as the eventual electron sink.

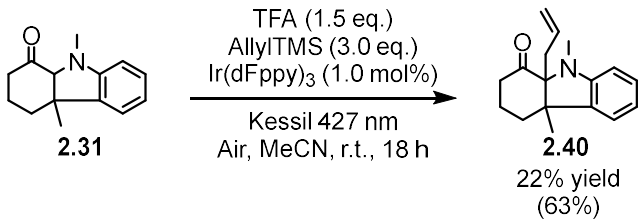
Iridium photocatalysts are very proficient photo-redox catalysts as well as TET.[6] Despite $Ir(dFppy)_3$ being initially chosen to avoid redox chemistry with ether linked substrates and to solely act as a TET sensitiser, it was possible that it was capable of oxidising **2.31**.

To test this, we measured the oxidation and reduction potentials of parts of the system using square wave voltammetry. The literature value for the oxidation potential of the Ir(III)*/Ir(II) couple for $Ir(dFppy)_3$ is +0.39V vs SCE.[54] The measured oxidation potential of **2.31** was +0.78 V vs SCE, likely corresponding to the loss of a nitrogen lone pair electron. **2.31** in the presence of TFA showed an even

higher +0.89 vs SCE, as protonation of the neutral species lead to increased electron affinity. This showed that oxidation of **2.31** is outside of the range of $Ir(dFppy)_3$.

In terms of the terminal oxidant, the initial suspect was atmospheric oxygen. Although the reaction was performed under an argon atmosphere and was subject to a thorough freeze-pump-thaw degassing routine, we were unable to discount the possibility that adventitious oxygen was the cause. When skipping the degassing step and performing the reaction under air, we observed a significant drop in yield to just 22% and recovered 63% of the starting material (in contrast to the anaerobic reaction, in which no starting material remained) (Scheme 2.29).

This suggested that oxygen contamination is not responsible for oxidation – as did the relative consistency in yield across repeats, utilising both freeze-pump-thaw and sparging techniques.



Scheme 2.29. Oxidative allylation in the presence of air. The figure in bracket refers to **2.31** recovered. Yield and recovery were measured by quantitative ^1H NMR spectroscopy against dimethyl terephthalate (0.04eq.).

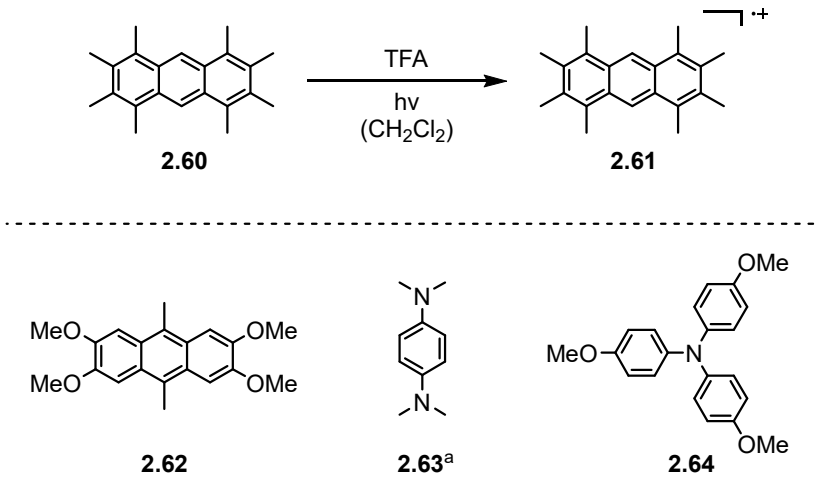
With both conventional suspects discounted, attention turned to other options. In fact, the only remaining uninterrogated component of the reaction is TFA. Although an unusual suggestion for an oxidant, it is not without precedent.

There are a few examples in the literature where TFA has been identified as a one-electron oxidant, especially when under irradiation with light. [55–58]

The encouragingly titled report "Why is Trifluoroacetic acid such an effective one-electron oxidant?" by Radner and Eberson contains an example of this (Scheme 2.30).[59] During the TFA-mediated synthesis of **2.60**, they noticed the production of the radical cation **2.61** by single electron oxidation even after rigorous degassing to remove oxygen (the oxidation potential of **2.60** was measured at 0.86

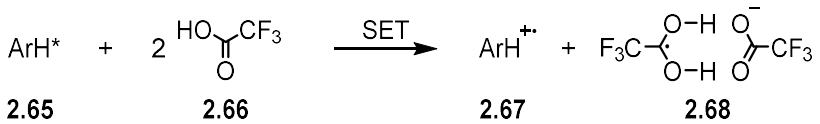
V vs SCE). They reasonably ascribed this oxidation to TFA, given the lack of another compound in the sample. Continuing to probe this reactivity, they showed that it was applicable to a range of other anthracenyl compounds, such as **2.62**. They noted that when the sample of **2.62** was kept in the dark, very little radical cation production was seen – but when exposed to diffuse daylight or a 300W "sun lamp" the rate was significantly increased. The explanation given for this reactivity was that the excitation of the aromatic species to a higher energy singlet state facilitated electron transfer to TFA.

The reactivity was not limited to anthracenes, and **2.63** and **2.64** both exhibited oxidation to their radical cations.



Scheme 2.30 Observed single electron oxidation of aromatic compounds when dissolved in neat TFA or with CH_2Cl_2.
[a] The radical cation was observed only in dilute solution with CH_2Cl_2, due to excessive protonation preventing oxidation.

They also suggested a structure for the reduction product of the TFA: **2.68**. A dimeric complex with a second TFA molecule stabilising the radical formed.



Scheme 2.31. Proposed stabilisation of the TFA radical anion

Although certainly an example of TFA oxidation, this is quite dissimilar to the oxidative allylation observed with **2.31** in the presence of TFA.

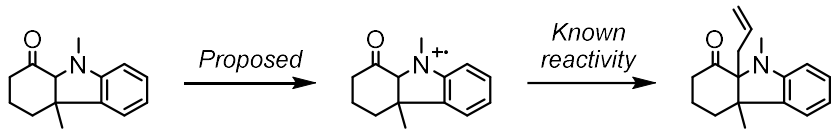
It is possible that the iridium photocatalysts plays some role in the activation of the TFA or substrate, given the significantly lower yields observed when it was removed and the irradiation was maintained, but there is no clear mechanism for that process.

However, with no alternative hypothesis for the oxidation, this was our working explanation.

2.11 Mechanistic proposal

With an understanding of how the allylation occurs and the identity of the oxidant, we had enough data to consider proposing a mechanism.

Single electron oxidation of the aniline nitrogen lone pair of **2.31** by a TFA-facilitated oxidation creates the amine radical cation **2.69** and a presumed single electron reduction product of TFA. This represents one half of the total two-electron oxidation.



Scheme 2.32 Proposed single electron oxidation of **2.31** on the route to **2.40**

Amine radical cations such as **2.69** are a well-explored class of reactive intermediate, especially in the discipline of photochemistry, and are a synthetically valuable route to α-functionalised amines such as **2.40**.[60] This can be achieved by two convergent mechanisms (Scheme 2.33).

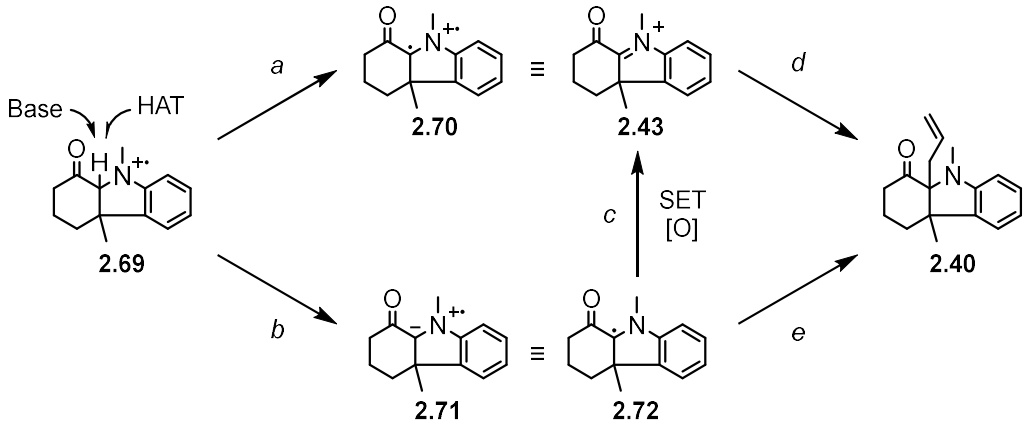
Hydrogen atom abstraction of the α-hydrogen (route *a*) leads directly to **2.43**, which can then be trapped by a nucleophile – but requires a species proficient in HAT to actually occur. The iminium formed can be trapped with nucleophilic allylTMS (route *d*). Given the unknown fate of the TFA reduction product, it's impossible to rule that out as a source of an HAT agent, but it's also not a very compelling proposition.

The other route to α-functionalisation is deprotonation of the α-hydrogen (route *b*) to form the neutral radical **2.72**. Protons α to amine radical cations are known to be more acidic than those in the neutral

counterparts, although this effect is less pronounced with arylamines.[61,62] The presence of the ketone group in **2.69** will also significantly contribute to the acidity of the position, promoting this route.

Two fates of this radical can be envisaged. Direct trapping of the allylTMS by the radical (route *e*) would arrive directly at **2.40** with the loss of a silyl radical. This addition of radicals to allylTMS is known, although α-amino radicals are nucleophilic and tend to be trapped with electrophilic Michael acceptors.[60,63,64]

α-Amino radicals are also highly reducing.[60] Oxidation of the radical produces the iminium **2.43** (route *c*), which – like in the HAT route or the original eliminative cyclisation – can be trapped by a nucleophile (route *d*). Given this reaction already relies on a single electron oxidation to start, proposing a second one is no greater leap despite the unconventional means of oxidation, especially considering the ease of oxidation of **2.72**.

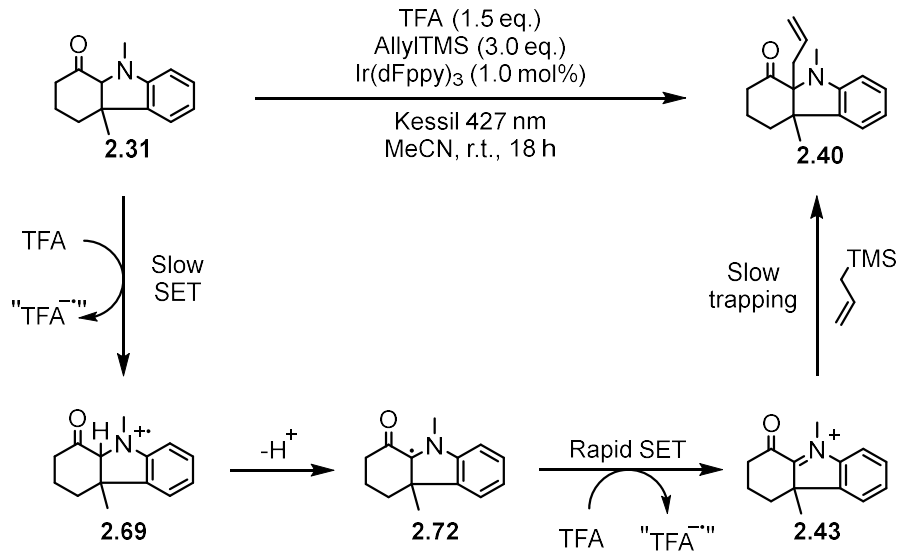


Scheme 2.33. Available pathways from radical cation **2.69** to **2.40**.

The deprotonation/oxidation pathway (route *b*-*c*-*d*) seemed like the most likely candidate for the mechanism of the oxidative allylation (Scheme 2.34).

Single electron oxidation of **2.31** to the radical cation **2.69** by an equivalent of TFA occurs slowly. Deprotonation of **2.72** by any slightly basic reaction component (such as trifluoroacetate, **2.31**, or the reduction product of TFA) leads to **2.72**. This reducing radical is more rapidly oxidised by a second

molecule of TFA, producing the iminium **2.43** and completing the oxidative process. The iminium is unstable and will eventually decompose unless trapped by the nucleophile allylTMS in a slow, inefficient trapping reaction.



Scheme 2.34. Mechanism for the oxidative allylation

There are a number of results from the mechanistic investigation that support this theory.

The observation of an intermediate identified as the iminium **2.43** lends significant validity to the model, as the radical attack pathway (Scheme 2.33 route *e*) does not go through the intermediate.

The dual single electron oxidation by TFA is also consistent. TFA was the component definitively required for oxidation. As a single-electron oxidant, two equivalents would be needed for full conversion, and this stoichiometry is seen in the variations where TFA is limiting. At low loadings of TFA, the yields were half of the equivalents of the TFA. At high allylTMS loadings, yields reached a maximum of approximately 75%, again half the equivalents of TFA used.

Assuming that the TFA were the oxidant, it would provide an explanation for the increased decomposition and loss of material observed in experiments with larger TFA quantities, as the oxidation rate increases without concomitant increased trapping of the unstable iminium.

2.12 Mechanism Validation

We investigated a number of the implications of this reactivity in order to validate this proposed mechanism.

The most pressing question was, of course, whether TFA was capable of oxidising **2.31**. Measuring the reduction potential of TFA by square wave voltammetry gave a value for the TFA/$TFA^{-\bullet}$ couple of -0.49 V vs SCE. This showed that TFA in the ground-state is unable to oxidise **2.31**, as expected. Given the importance of irradiation and $Ir(dFppy)_3$ to the reactivity, it was always unlikely that the mechanism for this oxidation was simple electron transfer in the ground state, and thus this measured reduction potential did not necessarily inform on the validity of TFA involvement in the oxidation.

As the terminal oxidant in the mechanism, stoichiometric quantities of TFA would be reduced. This would presumably be detectable *via* tracking the formation of a second fluorinated species by ^{19}F NMR. Repeating the procedure of the previous ^{1}H NMR tracking study would give an understanding of the progression of this over time (Figure 2.3). However, only a single fluorine peak was observed, although it slightly shifts downfield as the reaction progresses.

This most likely indicates that TFA does not react and is not substantially changed under the oxidative conditions, counter to the proposal that it is reduced.

It is possible that intermolecular exchange between a reduction product and neutral TFA (*via* a structure like the one proposed by Radner and Eberson, Scheme 2.31, **2.68**) could happen at speeds greater than the NMR timescale, and so lead to a single averaged peak. This would most likely result in greater change in the chemical shift, however.

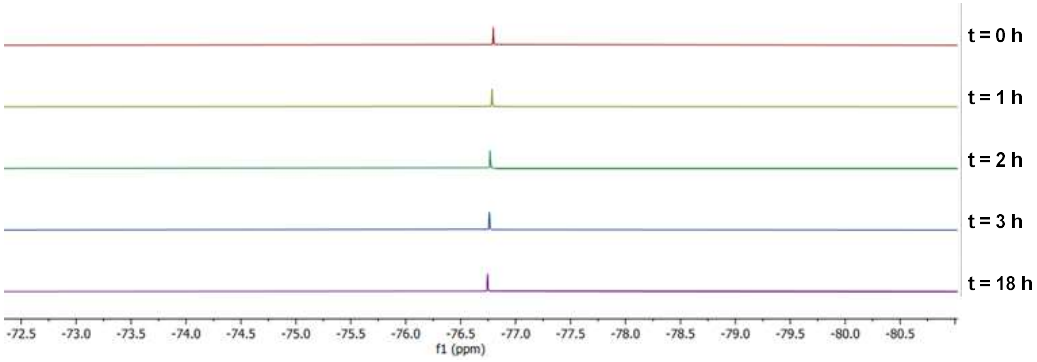


Figure 2.3. Comparison of the ^{19}F NMR spectra of the allylation of **2.31** over time. The reaction was performed in a Youngs NMR tube in d^3-acetonitrile and the same procedure as Figure 2.2, with NMR spectrum acquisition between 1 h periods of irradiation.

It was decided to use electron spin resonance spectroscopy (ESR) to attempt to find direct evidence for the single electron oxidation. This was done in collaboration with Dr. William Myers at the University of Oxford CAESR institution. Any open-shell species would be detectable, and the postulated radical intermediates would be evidence for a one-electron pathway.

A control sample of **2.31**, allylTMS, and $Ir(dFppy)_3$ dissolved in acetonitrile was made up and irradiated with 427 nm blue light while in the spectrometer. As expected, no signal was seen, indicating no radicals were present in the non-acidic reaction. TFA was then added to an identical sample, which was irradiated and measured in the same way. This ESR trace also showed no radical formation, contrary to expectations. This indicates that even in the presence of TFA, no single electron oxidation occurs.

This does not conclusively disprove the proposed mechanism, as any generated radical species may simply have too short a half-life to be detected, but it is far from the conclusive confirmation for which we had hoped.

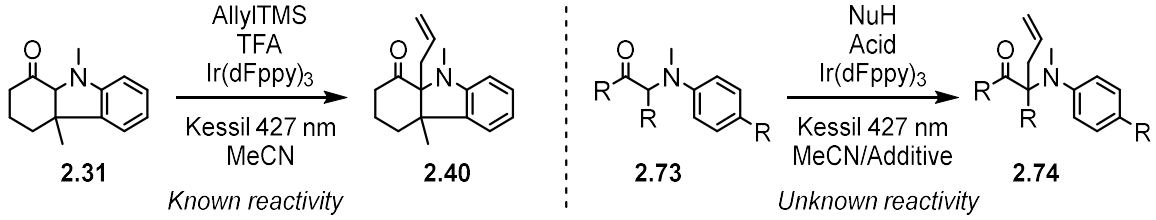
Further work on this area was possible. Attempting to induce the desired reactivity with alternative approaches to oxidation (such as electrochemistry or chemical oxidants) would indicate the feasibility of the oxidation, as well as a better understanding of the chemistry necessary to effect it.

However, given the time and resources that had already been put into this area, the decision to postpone further investigation of the mechanism of the transformations of **2.31** was made, in order to gain novel insights into the more general application of the reaction.

Chapter 3: Substrate Scope

2.13 Variation of the Reagents

All of the data collected so far was about the reactivity of a specific system. In order expand our understanding of the reaction as a whole, it was necessary to explore the wider scope (Scheme 2.35). It would be more efficient to explore the larger reaction space than focusing solely on the known reaction as insights from varying the components would feed back into our understanding of the reactivity.



Scheme 2.35. Description of the known reaction and the various areas where variation can be introduced

2.13.1 Variation of the Acid Component

Given the importance of the TFA to reactivity in the original system, it seemed to be an efficient starting point. We tested a variety of acids across a range of pKas (Table 2.5), as it was anticipated that less acidic conditions may lead to less material loss from decomposition.

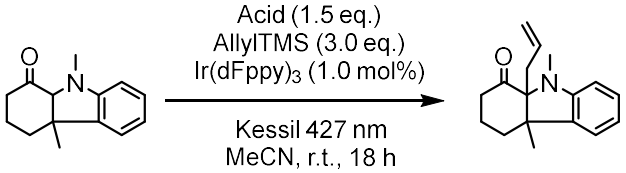
Low pKa acids such as tosic and camphorsulfonic acid (CSA) were tolerated well (Entries 2-3), with no significant deviation from TFA. Aqueous hydroiodic acid (Entry 4), however, gave no **2.40**. This may be due to the significant structural differences between it and the carboxylic and sulphonic acids, but it's also likely that the addition of water was an issue. There was also a concern that the freeze-pump-thaw degassing procedure removed the hydrogen iodide gas from the reaction mixture.

Attempts to track the fate of CSA in the reaction using ^{1}H NMR showed no other camphor derivatives generated.

Higher pH solutions were not as well tolerated. Acetic acid (Entry 5), despite its superficial structural similarities, was unable to accomplish the oxidation – potentially either due to its low acidity or the lack of fluorination changing its affinity for accepting an electron.

Triethylamine hydrochloride (Entry 6) was also unsuccessful, again most likely due to even lower acidity. Using a base instead of acid (Entry 7) led to no product formation.

The necessity for strong acids suggests protonation of the substrate or an intermediate is an important factor dictating reactivity. It is possible that the reactive species is not **2.31**, but rather the protonated or enolized form.



2.31 **2.40**

Entry	Acid	pKa in MeCN	Conversion / %	Yield / %
1	TFA	12.6[65]	100	40
2	CSA	Unknown	80	41
3	Tosic acid	8.5[66]	100	37
4	HI (aq.)	2.8[66]	60	0
5	Acetic acid	23.5[66]	-[a]	0
6	NEt_3·HCl	18.8[67]	60	0
7[b]	KOAc	-	53	0

Table 2.5. Conversions and yields were measured by quantitative ^{1}H NMR spectroscopy against dimethyl terephthalate (0.04 eq.). [a] Conversion could not be quantified due to noise in the NMR spectrum but could be determined to be less than 100% [b] This reaction was performed on **2.27** (the uncyclized substrate). The conversion figure refers to the amount of the cyclised **2.31** recovered – no **2.27** was recovered.

2.13.2 Variation of the Nucleophile

The eliminative radical-polar crossover experiments that initiated this work were able to utilise many different nucleophile traps for the iminium generated. Despite different methods of generation, the

intermediate generated by both is very similar – only differing by the counterion (iodide vs trifluoroacetate).

Previous success with TosMIC, N-methylindole and furan was not replicated in the oxidation reaction, as none of these were trapped (Figure 2.4, Entries 1 to 3). This may be a result of lack of stability in the acidic conditions of the TFA solution. The trifluoroacetate counterion may also lend the iminium greater stability than the iodide.

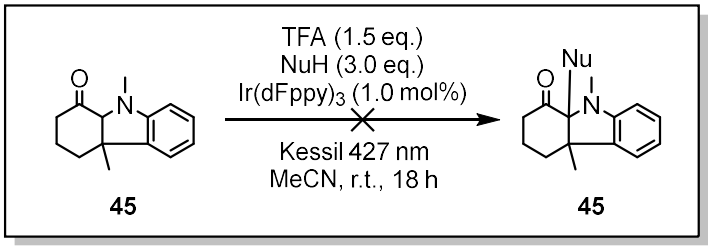
The focus returned to allylsilanes; a class of nucleophiles that is definitely productive in the oxidative system (Entries 4 to 6).

A replacement that was more nucleophilic than allylTMS was desired, as the inefficiency of the trapping appeared to have a significant impact on the yield of **2.40**. 2-methylallylsilane (Entry 4) was chosen, due to the additional stability afforded to the carbocationic intermediate (formed upon attack onto the iminium) by the methyl group, leading to higher nucleophilicity.[21]

Surprisingly the was no trace of the trapping product at all. This may have been due to an increased affinity for protonation by the TFA (and thus formation of a tertiary, silicon-stabilised carbocation).

Dr Lockhart ran a trial of the original eliminative cyclisation (which does not include an acidic additive) utilising it in order to investigate this dramatic change in reactivity. 2-Methylallylsilane was again unreactive under the conditions, indicating that the difficulty can be attributed to the silane rather than to the oxidation conditions. The surprising behaviour thus may arise from increased bulk on the silane, hindering the attack into a crowded site, rather than protonation.

Influencing the electronic characteristic of the silane by varying the silicon substituent while maintaining the small allyl group was equally unsuccessful (Entries 5 and 6). Neither trimethoxy- nor trichloroallylsilane were trapped.



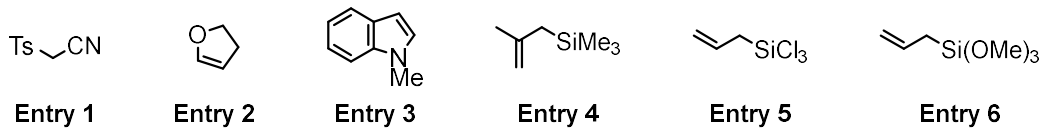
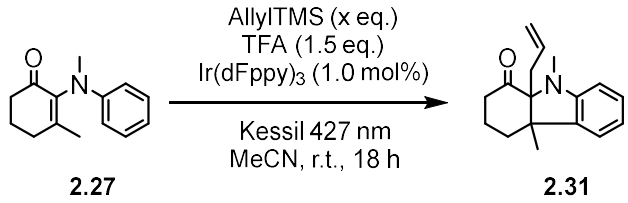


Figure 2.4. The unsuccessful nucleophiles used in attempted scope. None yielded any trapped product.

As no other tolerated nucleophiles were found, focus moved onto other areas.

2.13.3 Inclusion of Additives

A brief collection of additives was investigated (Table 2.6). Reintroduction of DMDS was trialled (Entry 1), as the initial findings showed significantly more starting material recovery than the later DMDS-free reactions (see Table 2.1). Addition of the DMDS to the previous forcing conditions gave a slight drop in yield, from 74% (the yield without DMDS) to 67%. Inclusion of water (Entry 2) or HFIP (Entry 3) in the solvent mixture only served to inhibit reactivity – the aqueous reaction returned only starting material, and addition of HFIP had a significantly lower 23% yield and 44% starting material recovered.



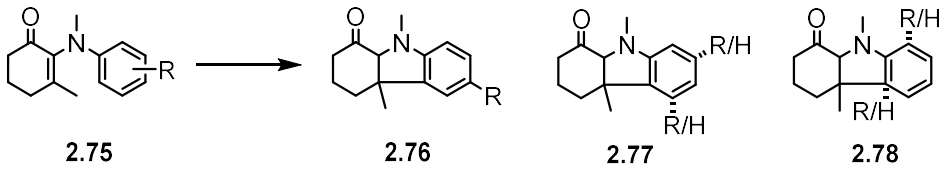
Entry	Additive	AllylTMS / eq.	Conversion / %	Yield / %
1	DMDS (1.0 eq.)	20.0	100	67
2	H_2O (10% v/v)	3.0	37	0
3	HFIP (10% v/v)	3.0	56	23

Table 2.6. [a] Conversions and yields were measured by quantitative ^{1}H NMR spectroscopy against dimethyl terephthalate (0.04 eq.)

2.14 Substrate Synthesis

After an exhaustive range of variations on the original reaction and a large time investment, the only improvement over the original methodology that was found was the use of a large excess of alllylTMS. Content that we had reached the upper limit on this reactivity, we decided to take what we had learnt and apply it to a small substrate scope, with the hope that results would then feed back into our understanding of the reaction mechanism.

The easiest modifications of the substrate were *via* functionalisation of the aryl ring (Scheme 2.36), as it allows for divergent syntheses from epoxide **2.58** with a variety of N-methylanilines. These kinds of changes were well tolerated in both the standard and eliminative 6π cyclisations.[46,53] Changing the electronic properties of the aniline would also provide insight into the reaction mechanism of the oxidation, as the accessibility of nitrogen lone pair of the aniline is potentially reactivity-defining. Thus, we aimed to introduce a diverse range of substituents to the aniline. The scope focused on various *para*-substituted anilines to avoid complications arising from the regioselectivity of the cyclisation (Scheme 2.36).



Scheme 2.36. *Para*-functionalisation of **2.27** leads to a single regioisomer

However, synthesis of these materials was more difficult than anticipated, stemming from the inefficiency of the epoxide opening (Figure 2.5). The yields with N-methylaniline were previously disappointing, and the inclusion of most electron-withdrawing substituents reduced the nucleophilicity enough that the reaction was unproductive (**2.83** to **2.85**). Only 4-chloroaniline (**2.81**) was able to open the epoxide, although in poor yield. The more nucleophilic 4-methoxy-N-methylaniline was more productive (**2.82**). Tetrahydroquinoline (**2.85**), despite the increased electron density, was unable to attack the epoxide, likely due to increased steric bulk around the nitrogen.

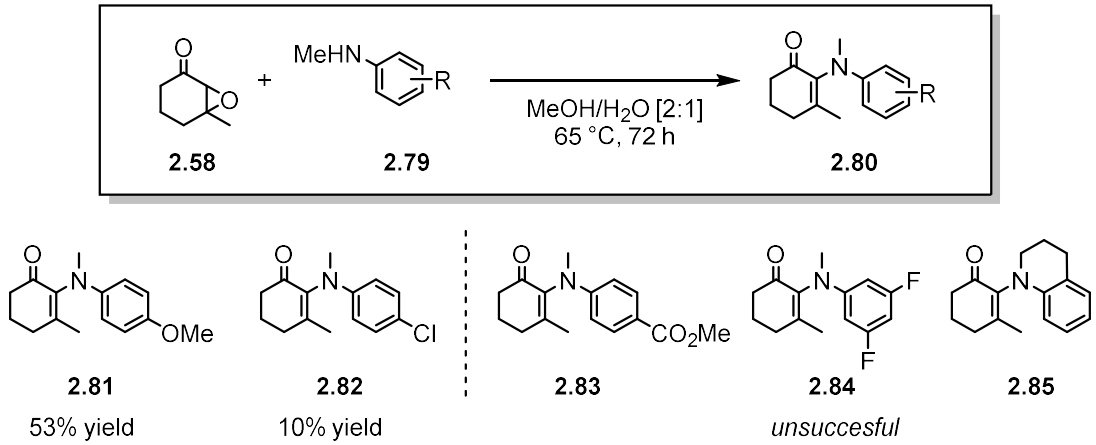


Figure 2.5. Results of the coupling reaction with modified N-methylanilines. Reaction conditions as stated, with **2.58** (1.0 eq.) and **2.79** (1.0 eq.)

Limitations imposed by the availability of N-methylanilines and the inefficiency of the coupling prompted a change of tactics, towards functionalisation of the aniline ring of **2.27**. Modification of the unsubstituted substrate *via* electrophilic aromatic substitution was able to furnish additional electron-poor analogues of **2.80** (Figure 2.7). Bromination and iodination using the relevant N-halosuccinimide were productive. Attempts at Menke nitration and Vilsmeier–Haack formylation resulted in the undesired hydrolysis of the central C—N bond.

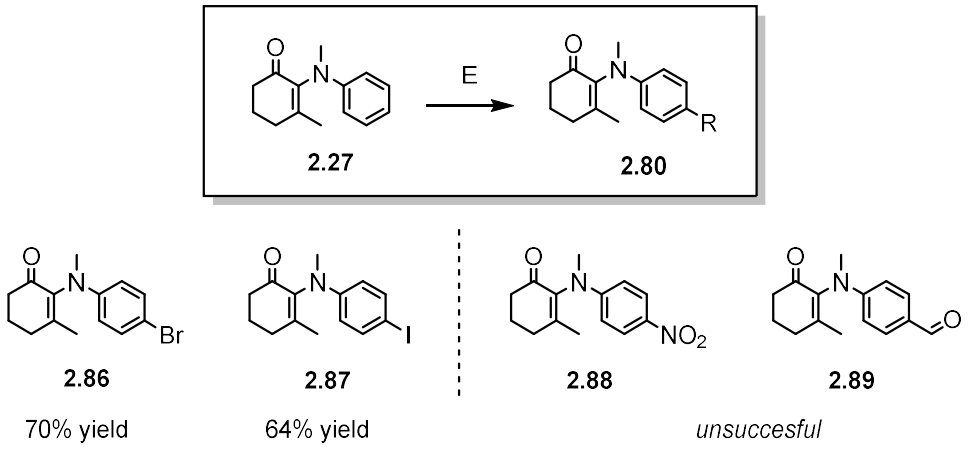


Figure 2.7. Results of the electrophilic aromatic substitutions of **2.27**. Reaction conditions: **2.86** and **2.87**: **2.27** (1.0 eq.), NXS (1.05 eq.), MeCN, r.t., 2 h. **2.88**: **2.27** (1.0 eq.), $Cu(NO_3)_2 \cdot H_2O$ (1.0 eq.), $NaHCO_3$, Ac_2O/AcOH (1:1), r.t., 1 h **2.89**: **2.27** (1.0 eq.), $POCl_3$ (1.2 eq.), DMF (2 eq.), 65 °C, 17 h.

We then attempted to modify the brominated substrate **2.86** using various transition-metal-catalysed cross-couplings (Figure 2.8) The synthesis of electron-rich anilines *via* Suzuki (**2.90**) and Buchwald-Hartwig (**2.91** and **2.92**) cross-couplings gave no coupled products. Other approaches to electron-poor

anilines were tried with a coupling with a lithiated enol ether (**2.93**) and a cobalt-catalysed reductive carboxylation (**2.94**). Unfortunately, neither of these cross-couplings were successful.

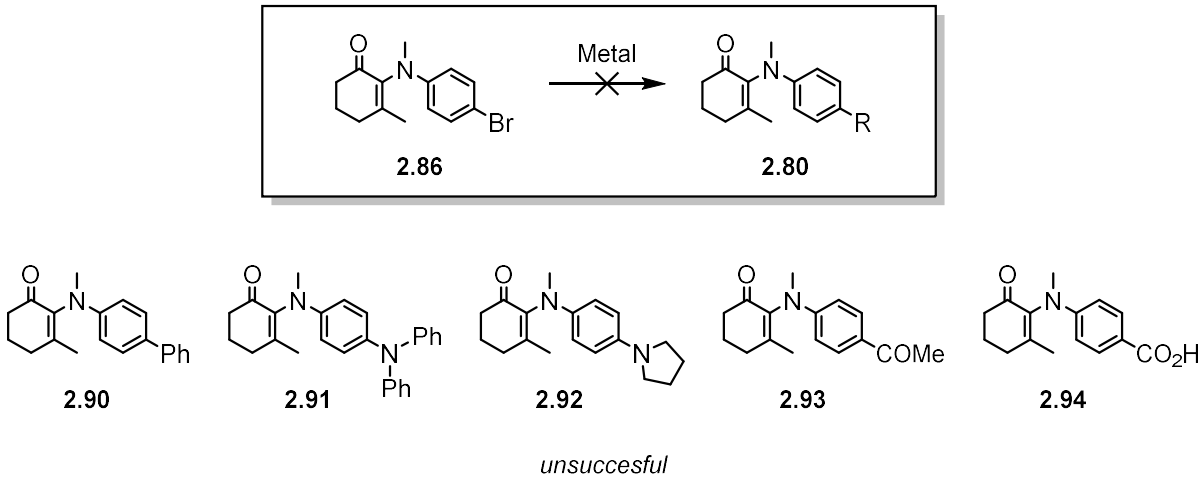


Figure 2.8. Unsuccessful transition-metal-catalysed couplings of **2.86**. Reaction conditions: **2.90**: **2.86** (1.0 eq.), phenylboronic acid (1.1 eq.), Na_2CO_3 (2.0 eq.), $Pd(dppf)Cl_2$ (0.05 eq.), H_2O/dioxane (1:1), 100 °C, 18 h. **2.91**: **2.86** (1.0 eq.), diphenylamine (1.0 eq.), NaO^tBu (1.5 eq.), $Pd(OAc)_2$ (0.02 eq.), $P(^tBu)_3{\cdot}HBF4$ (0.06 eq.), benzene, 90 °C, 18 h. **2.92**: **2.86** (1.0 eq.), pyrrolidine (1.5 eq.), Cs_2CO_3 (1.6 eq.), Pd_2dba_3 (0.05 eq.), XPhos (0.15 eq.), dioxane, 80 °C, 24 h. **2.93**: ethyl vinyl ether (1.5 eq.), *n*-BuLi (1.5 eq.), THF, -78 °C, 30 min *then* **2.86** (1.0 eq.), $Pd_2(dba)_3$ (0.01 eq.), XPhos (0.05 eq.), PhMe, 40 °C, 18 h. **2.94**: **2.86** (1.0 eq.), LiCl (3.0 eq.), Zn dust (2.0 eq.), CoI_2 (0.1 eq.), bipyridine (0.1 eq.), CO_2 atmosphere, MeCN/DMF (10:1), 40 °C, 14 h.

To complement the functionalisation of the aniline moiety, variation of the cyclohexenone-derived substructure was also undertaken.

In order to focus only on the oxidation step and avoid unwanted influence from substrate changes on the cyclisation step, the desired substrates were designed to be analogues of **2.31**, the cyclised intermediate.

These compounds were synthesised *via* nucleophilic substitution of α-bromocarbonyls with N-methylaniline (Figure 2.9). Primary bromides derived from pinacolone (**2.97**) and acetophenone (**2.98**) and secondary bromides from methyl propionate (**2.99**) and propiophenone (**2.100**) were all employed, but the steric bulk and low nucleophilicity of N-methylaniline continued to hinder reactivity.

One-pot Weinreb amidation and reduction of **2.99** to the methylketone **2.101** was attempted but ultimately unproductive.

The cyclohexone derivative **2.104** was a substrate we were interested in due to its structural similarity to **2.31**. However, despite multiple attempts, both bromination and chlorination of **2.102** proved problematic. Other routes to obtain **2.103** are possible (such as other methods of halogenation or by purchasing the materials) but were not explored in this case due to time constraints. This, along with the design of further **2.31** analogues, remains an area for possible further work.

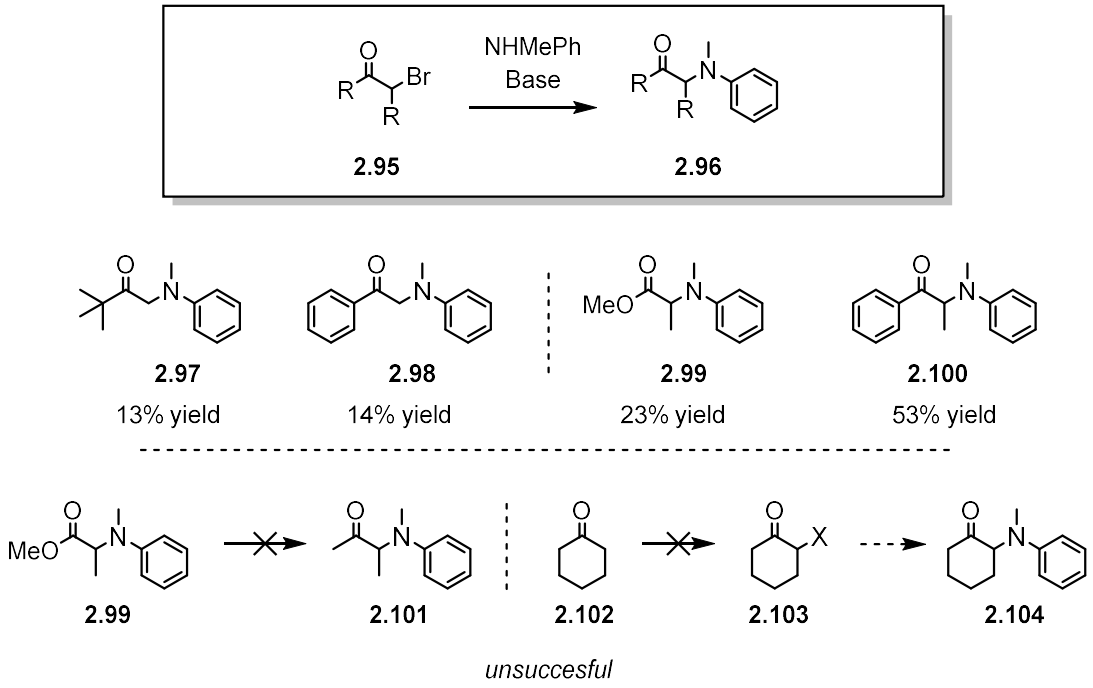


Figure 2.9. Synthesis of a variety of α-N-methylphenylcarbonyl species *via* substitution of the desired α-bromocarbonyl with NHMePh. Reaction conditions: **2.98**, **2.99** and **2.100:** α-bromoketone (1.25 eq.), N-methylaniline (1.0 eq.), Na_2CO_3, MeOH, 75 °C, 3.5 h. **2.97**: α-bromoketone (1.2 eq.), N-methylaniline (1.0 eq.), DIPEA (0.1 eq.), NaI (1.2 eq.), MeCN, 40 °C, 24 h. **2.101**: **2.99** (1.0 eq.), MeONHMe (1.25 eq.), MeMgBr (6.5 eq.), THF, -5 °C, 5 h. **2.103**: **2.102** (1.0 eq.), NXS (1.2 eq.), DCM, 30 °C, 18 h. *or* **2.102** (1.0 eq.), Br_2 (1.0 eq.), H_2O, 10 °C, 1.5 h.

2.15 Substrate Scope

We turned to evaluation of performance of the substrates in the oxidative allylation (Figure 2.10).

The *para*-functionalised aniline substrates were examined with the original conditions i.e. only three equivalents of allylTMS. This was so that the relative efficiencies of the trappings could be more clearly observed, allowing for insight into the affects of functionalisation on the reactivity.

para-Functionalisation of the aniline was generally well-tolerated. The iodide (**2.109**) was the lowest yielding at 21%, and only identified in the NMR spectrum of the crude reaction mixture as the product

protodeiodinated to **2.40** during isolation. A 10% yield of **2.40** was additionally observed in the crude reaction mixture, demonstrating the iodide's lability under the reaction condition. The chloro- (**2.107**) and bromo- (**2.108**) derivatives were stable. 4-chlorinated **2.82** showed similar reactivity to the unfunctionalized substrate, producing **2.107** in a slightly lower yield. The 4-bromoaniline **2.86** was the highest yielding modified substrate, out-performing even the unfunctionalised substrate at a 61% yield. This result was surprising, and the reason for the higher yield was unclear. Reduced electron density caused by the withdrawing effect of the bromine would seem to impede the oxidation.

The 4-methoxyaniline (**2.106**) had a slightly lower yield (34%) than the unfunctionalised substrate **2.27**, which gave a yield of 40%. However, a significant amount of starting material was recovered, in contrast to the full consumption of **2.27**. This starting material recovery suggests a lower rate of oxidation of the starting material compared with **2.27**, contrary to what would be expected by increased electron density of the aniline, which intuitively would make the electrons more accessible to the oxidant.

Although a lower absolute yield than **2.27**, when calculated based on recovered starting material, the yield of **2.106** was 47%. This indicated that a higher proportion of the oxidised material went on to be trapped at the iminium step than with in the reaction of **2.27**. The increased efficiency of the trapping can be ascribed to stabilisation of the reactive iminium intermediate, increasing its lifespan and reducing decomposition from undesired side reactions.

Efforts to change the substrate more dramatically were less successful. N-phenylpyrrolidine, as a simple tertiary aniline, isolates the proposed site of reactivity in **2.31**, a proton α to an arylamine. However, no allylated product (**2.114**) was observed, and 79% of the starting material was recovered.

Inclusion of the carbonyl group β to the amine was thus considered necessary. Ester-containing alanine-derivate **2.112** was similarly inactive, with 71% of the starting material remaining unreacted.

Pinacolone **2.110** was also unproductive, but with only 20% starting material recovery. This indicated that the aminoketone was reactive under the conditions, unlike previous substrates, although it did not follow the same reaction path as **2.31**.

Arylketones **2.111** and **2.113** both produced very small amounts of what appeared to be allylated product by ^{1}H NMR of the crude reaction mixture, but isolation and purification proved intractable.

It was clear that despite the apparent similarities between the novel substrates and **2.31**, there was a significant gulf in productivity between them. The substrates were missing the key to the reactivity, and it was unknown what that was. The understood mechanism for the transformation could not explain these apparent inconsistencies.

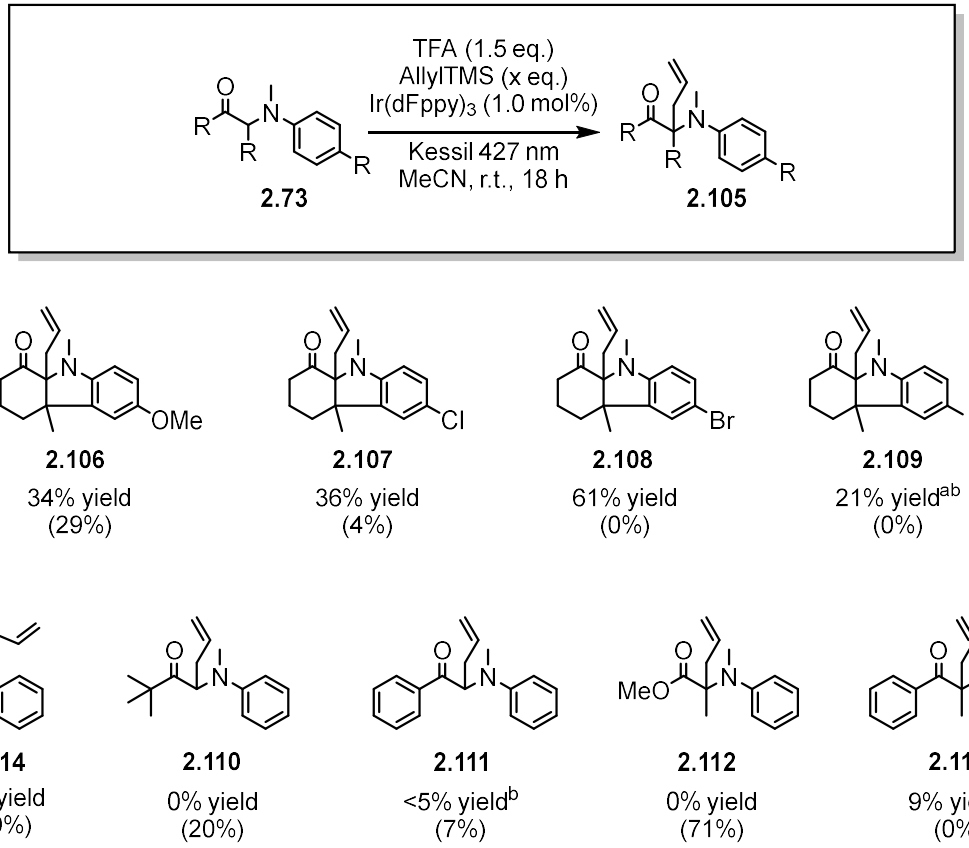


Figure 2.10. Scope of the oxidative allylation, with variation the aniline and cyclohexanone fragments. Figures in brackets indicate the yield of recovered starting material measured by quantitative 1H NMR spectroscopy against dimethyl terephthalate (0.04 eq.) [a] A 10% yield of the protodeiodinated product **2.40** was also observed by quantitative ^{1}H NMR. [b] Tentative yields were measured by quantitative ^{1}H NMR spectroscopy against dimethyl terephthalate (0.04 eq.) and the material was not isolated for characterisation

2.16 Conclusion

The observed tandem photocyclisation/oxidation/trapping observed for **2.31** was an interesting and novel reaction. Initial investigation lead to a plausible mechanistic proposition but we were unable to determine its validity with further study. Despite significant efforts, we were unable to expand this reactivity to any other systems and our understanding of the reaction mechanism could not account for this failure.

Further elaboration of the substrate scaffold (especially in regard to the variations performed in Figure 2.9) may yield an avenue towards generality of the reaction, but t was decided that the project had not shown sufficient progress to justify its continuation, and so these questions will go unanswered.

Section 3

This project is based on an atroposelective oxidative cross-coupling of indoles and naphthols, and exploration of novel reactivities discovered during the investigation.

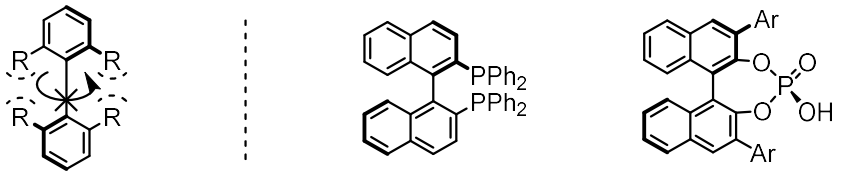
Chapter 4: Atropisomeric Biaryl Synthesis

3.1 Introduction to Atropisomerism

Atropisomerism describes chirality that derives from restricted rotation around a single bond, rather than from the fixed geometry of a point or points. Atropisomerism is common in biaryl systems featuring a single bond between two aromatic rings (such as **3.1**), where the restriction arises from sterically bulky substituents on the ortho positions of the aromatic rings preventing rotation past each other.

The degree of atropisomerism displayed by a molecule can be described by the barrier to rotation: the energy necessary to overcome the restriction of the rotation caused by steric interactions. The calculation of this energy barrier also provides a half-life, indicating the enantiostability of a given atropisomeric compound over time. From these concepts come a number of definitions of atropisomerism. Ōki defined it as when a compound has rate of interconversion between its conformers such that the half-life is greater than 1000 seconds.[68] LaPlante instead organised atropisomers into three classes (in the context of pharmaceutical development): Class 1, in which the barrier is low (less than 84 kJ/mol) and the rotation is rapid i.e. less than a minute; Class 2, when the barrier is moderate (between 84 and 117 kJ/mol) and the half-life is in the hour to month range; and Class 3 (or stable atropisomers), when the barrier is greater than 117 kJ/mol and the half-life is thus longer than 6 months.[69] Class 1 compounds can be considered to be racemic for most applications, whereas the atropisomerism of Class 2 and 3 compounds will have effects on their chemistry. The interconversion of Class 2 compounds prevents isolation of a single enantiomer and limits their utility, but stable Class 3 atropisomeric biaryls have many uses in medicinal and synthetic chemistry.

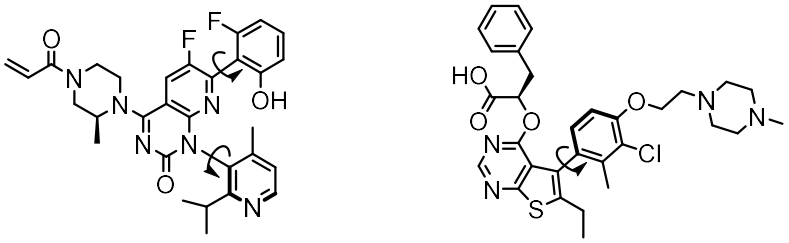
Compounds based on the binaphthyl architecture are well-known for their roles in enantioselective reactivity, acting as ligands for transition metals (such as BINAP (**3.2**)) or as chiral proton sources (**3.3**).[70,71]



3.1 3.2 3.3

Figure 3.1. Atropisomerism in a biaryl scaffold

Given the preponderance of aromaticity in drug design, atropisomerism appears in many pharmaceutical candidates (see figure 3.2 for two examples of stable atropisomeric biaryl bioactive compounds).[72–75] By controlling atropisomerism, it is possible to avoid inactive or even dangerous undesired enantiomers of atropisomeric drugs. In fact, it is even possible to harness atropisomerism as a target in drug design to increase efficacy, as it affords access to novel attachment vectors away from the 2D plane and thus represents one approach to escaping from the "flatland" of aromatic compounds.[76,77]

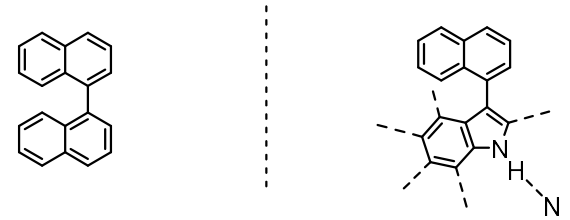


Sotorasib *MCL-1 Inhibitor*

Figure 3.2. Bioactive compounds that exhibit atropisomerism, with arrows highlighting the bonds around which rotation is hindered.

Notably, many of the atropisomerism-generating structures in these drugs are not carbocyclic, but heterocyclic. Heterobiaryls describe this class of biaryls, in which one or both of the aromatic rings is heteroaromatic.

A heterobiaryl of particular interest to this project is the 3-arylindole system (Fig 3.3, **3.5**). Although the motif is present in a number of bioactive compounds, their synthesis is less well-researched than carbocyclic biaryls.[78–81] The changes in electronics and geometry allow their chemistry to deviate from that of the binaphthyl system (**3.4**) in important ways. Inclusion of a heteroatom modulates the electronic properties of the rings, allowing for greater variation in the library of atropisomeric ligands. By incorporating indole specifically, it introduces hydrogen-bonding sites, potentially offering alternate sites for binding to substrates. The geometry of 5-membered rings differs from that of a benzene ring, providing variation in bonding angles and barriers to rotation.



3.4
Bi-naphthyl

3.5
3-arylindole

Fig 3.3. Heterobiaryls, such as 3-arylindole, give access to different bonding vectors to benzene-based scaffolds while also introducing hydrogen bond acceptors and/or donors.

3.2 Atroposelective Synthesis of Heterobiaryls

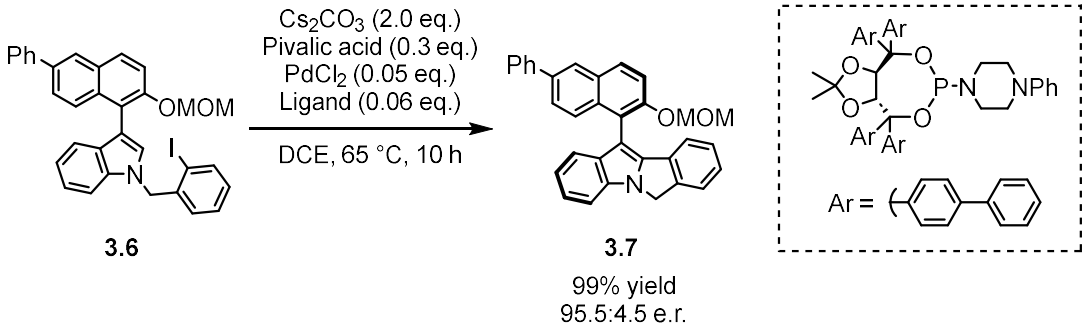
To this end, a range of approaches have been taken in the atroposelective synthesis of heterobiaryls, and of 3-arylindoles specifically.[82] These can be broadly broken down into four types: modification of symmetric biaryls; centre-to-axial chirality transfer; *de novo* ring construction; and direct coupling of aryl components.

3.2.1 Modification of symmetric biaryls

Atroposelective modification of a symmetric biaryl can be achieved in two ways, depending on the nature of the starting biaryl.

If the biaryl rapidly interconverts between conformers, then an atroposelective reaction that restricts rotation of the product can lead to a dynamic kinetic resolution (DKR), as demonstrated by Gu and

coworkers (Scheme 3.1).[83] By selectively cyclising only one conformer, they were able to generate the conformationally locked **3.7** in a 99% yield and 92:8 er.



Scheme 3.1. Dynamic kinetic resolution of **3.6**

Alternatively, if the symmetric biaryl is conformationally locked but plane symmetric (as in *meso* compounds), desymmetrisation reactions that confer chirality by regioselective modification can be utilised. There are no examples of this chemistry with 3-arylindoles, but it bears noting as an approach that has been utilised with other heterobiaryls.[82]

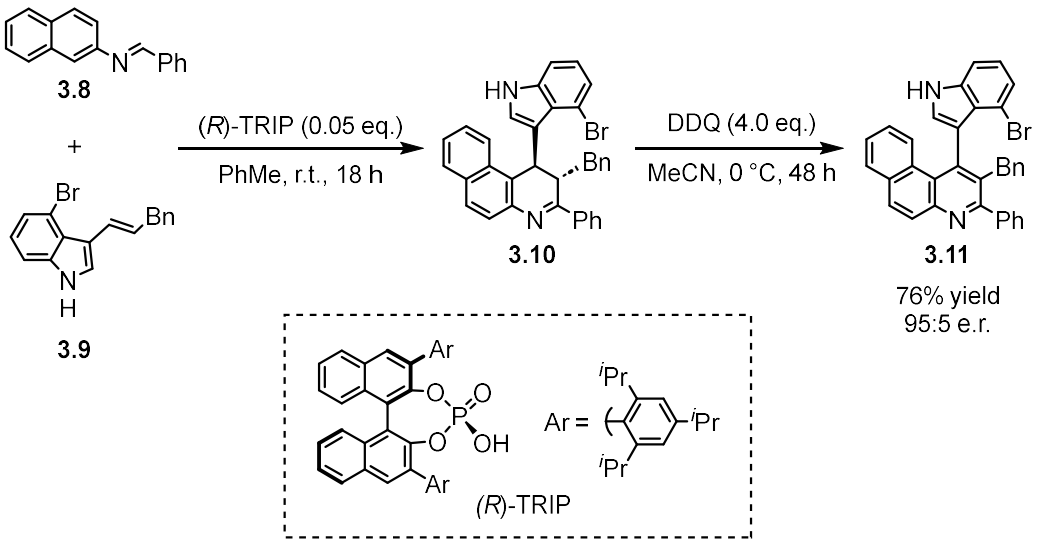
Both of these approaches are very step inefficient, as the biaryl must be pre-formed prior to the modification. They are also very substrate-dependant: DKR relies on the ability to affect the barrier to rotation of the biaryl with a simple modification in order to trap the prefer conformer, and desymmetrisation necessitates a *meso* starting material, limiting the applicability of the methodology.

3.2.2 Centre-to-Axial Chirality Transfer

Centre-to-axial chirality transfer is also a multistep process. Initially a precursor to the biaryl is synthesised stereoselectively, in which one or both of the atoms participating in the central key bond is C(sp^3) hybridised. A second, stereospecific step takes place that aromatises the rings, where the stereochemistry around the bond is dictated by the geometry of the chiral centres. In this way, the chirality is said to have been transferred from the stereocentre(s) to the axis.

This approach is fairly uncommon as it relies on high stereocontrol in two separate steps, which can be difficult to achieve. One example of this methodology in the synthesis of 3-arylindoles was reported by Corti and coworkers. (Scheme 3.2).[84] A chiral-phosphoric-acid-catalysed cyclisation of **3.8** onto **3.9**

afforded the indoline **3.10** in high e.r.. A subsequent DDQ-mediated oxidation afforded 3-arylindole **3.11** in high yield and maintained the high e.r..



Scheme 3.2. Chiral-to-axial chirality transfer in the synthesis of **3.11** *via* **3.10**. The synthesis of **3.10**: The reaction conditions were as described with **3.8** (1.0 eq.) and **3.9** (1.5 eq.).

The concept of chiral-to-axial chirality transfer is a powerful mechanism for inducing a desired enantiomer in an atropisomeric product. Aspects of the transformation often appear in other approaches, typically in the transitions from point-chiral unstable intermediates to axially-chiral products.

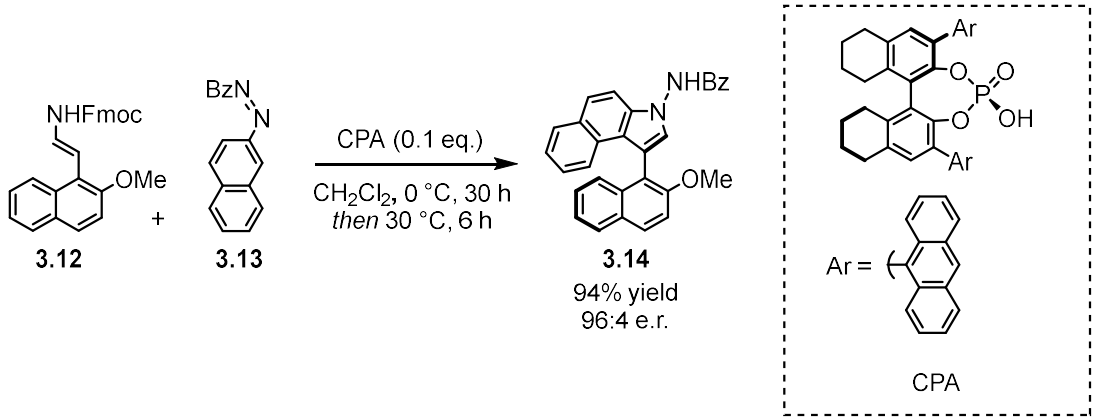
3.2.3 Atroposelective Ring Construction

Due to the desire to minimise step count in a synthesis, single-step construction of the biaryl in an atroposelective way is often preferred. One approach is the *de novo* synthesis of one of the aromatic rings in an enantioselective manner. This approach is especially interesting for heterobiaryls, as the construction of aromatic heterocycles is a field that is well established.[85,86]

However, aromatic heterocycles are typically achiral (as they are flat and have a mirror plane), and thus little of this work has been done on their synthesis enantio- (and atropo-) selectively.

Still, construction of an indole ring atroposelectively has been used by a number of groups. Zhou and coworkers utilised a chiral phosphoric acid to direct an indole ring construction (Scheme 3.3).[87] The

cyclisation is followed directly by an elimination that produces the aromatic 3-naphthylindole **3.14** in a single step.

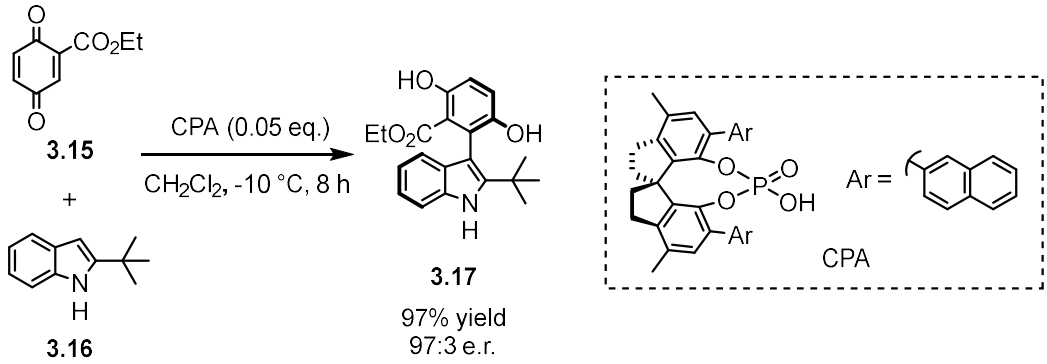


Scheme 3.3. *De novo* synthesis of **3.14**. The reaction conditions were as described with **3.12** (1.2 eq.) and **3.13** (1.0 eq.).

3.2.4 Direct Coupling of Aryl Components

Perhaps the most elementary disconnection for the synthesis of biaryl compounds is direct, atroposelective formation of the central bond. Aryl-aryl bond formation is an incredibly well-trodden area of chemistry, often achieved with transition-metal-catalysed cross-couplings, and it is no surprise that this methodology has been widely used in the synthesis of heterobiaryls.[88]

For the 3-arylindole scaffold, many routes employ the inherent nucleophilicity of the C-3 position of indole. By combining an indole with an electrophile, a carbon-carbon bond is formed without the need for a transition metal catalyst. Examples of electrophiles used include azo-arenes, and quinones as shown in Scheme 3.4.[89,90]



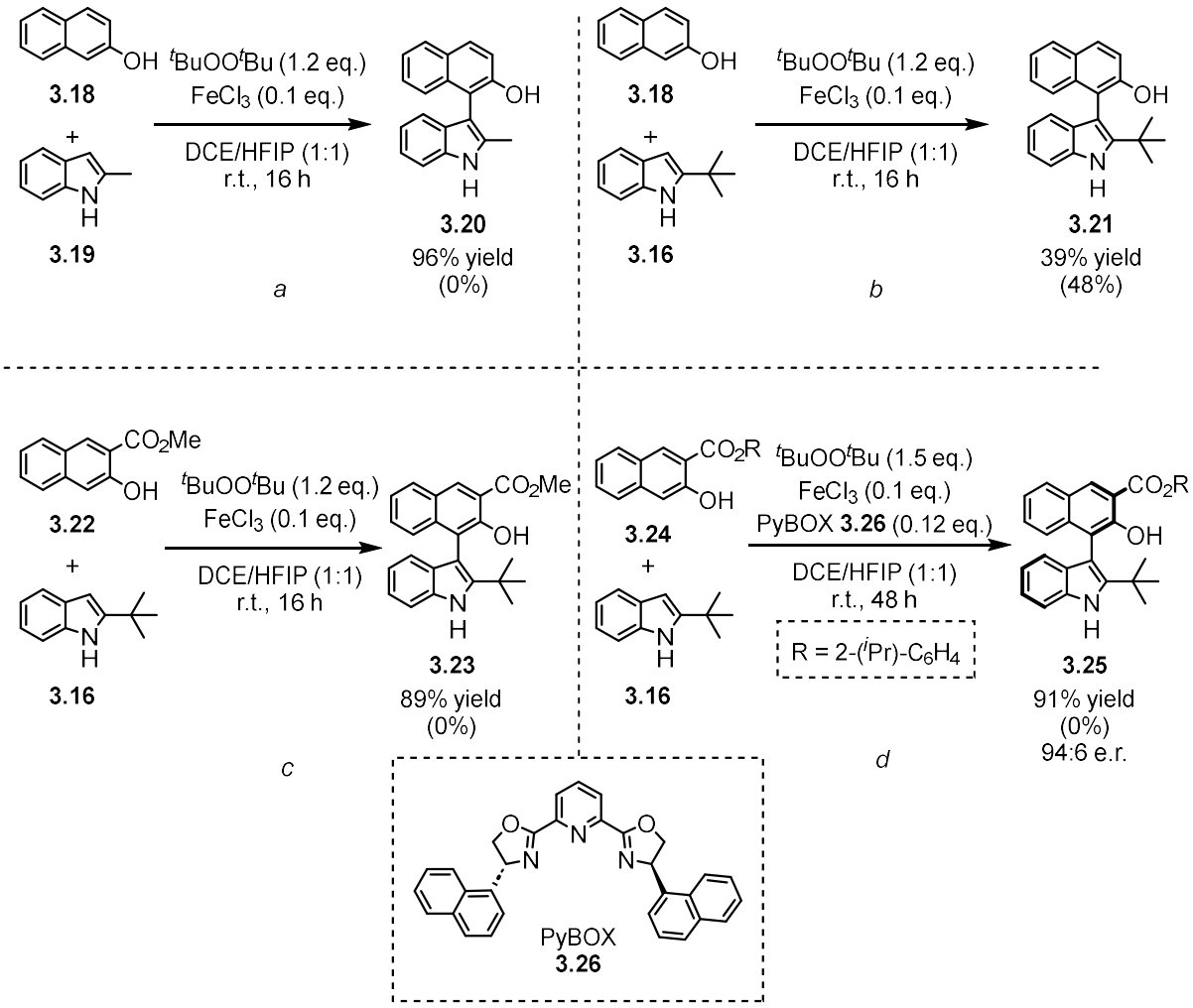
Scheme 3.4. Nucleophilic coupling of **3.15** and **3.16**. The reaction conditions were as described with **3.15** (1.0 eq.) and **3.16** (1.2 eq.).

However, there were no examples of the oxidative equivalent to this atroposelective cross-coupling of indoles at the C-3 position. As discussed previously, oxidative cross-couplings have a number of benefits over traditional neutral couplings: they avoid the need for prefunctionalisation of the coupling partners; and are able to directly couple two nucleophilic species in a single step (see Section 1.3).

To utilise this reactivity in the synthesis of 3-arylindoles, Smith and coworkers developed a high yielding and chemoselective cross-coupling between 2-naphthol (**3.18**) and 2-methyl indole (**3.19**) catalysed by iron chloride and di-tert-butylperoxide (DTBP) as the co-oxidant (Scheme 3.5a).[91] However, efforts to increase the bulk on the indole C-2 position to increase the barrier to rotation of the biaryl led to competitive BINOL formation (Scheme 3.5b). They were also unable to induce any enantioselectivity in the coupling.

Switching to a 2-hydroxy-3-naphthoate (**3.22**) as the coupling partner solved both of these problems (Scheme 3.5c). Introduction of the ester group reduced the nucleophilicity and electron density of the naphthol aromatic system, reducing the favourability of naphthol homocoupling.

The ester group also allowed for the introduction of enantioselectivity. By including a PyBOX ligand (**3.26**), the coupling was able to be achieved in 91% yield and 94:6 e.r. (Scheme 3.5d).



Scheme 3.5. Development of the iron-catalysed oxidative cross-coupling of 3-substsituted indoles and 2-naphthols. Figures in brackets refer to the yield of the BINOL-type side-products. The reaction conditions were as described with naphthols (1.0 eq.) and indoles (1.5 eq.).

With a successful cross-coupling in hand, this reactivity was successfully applied to a wide range of naphthoate and indole substrates (Figure 3.4).[92]

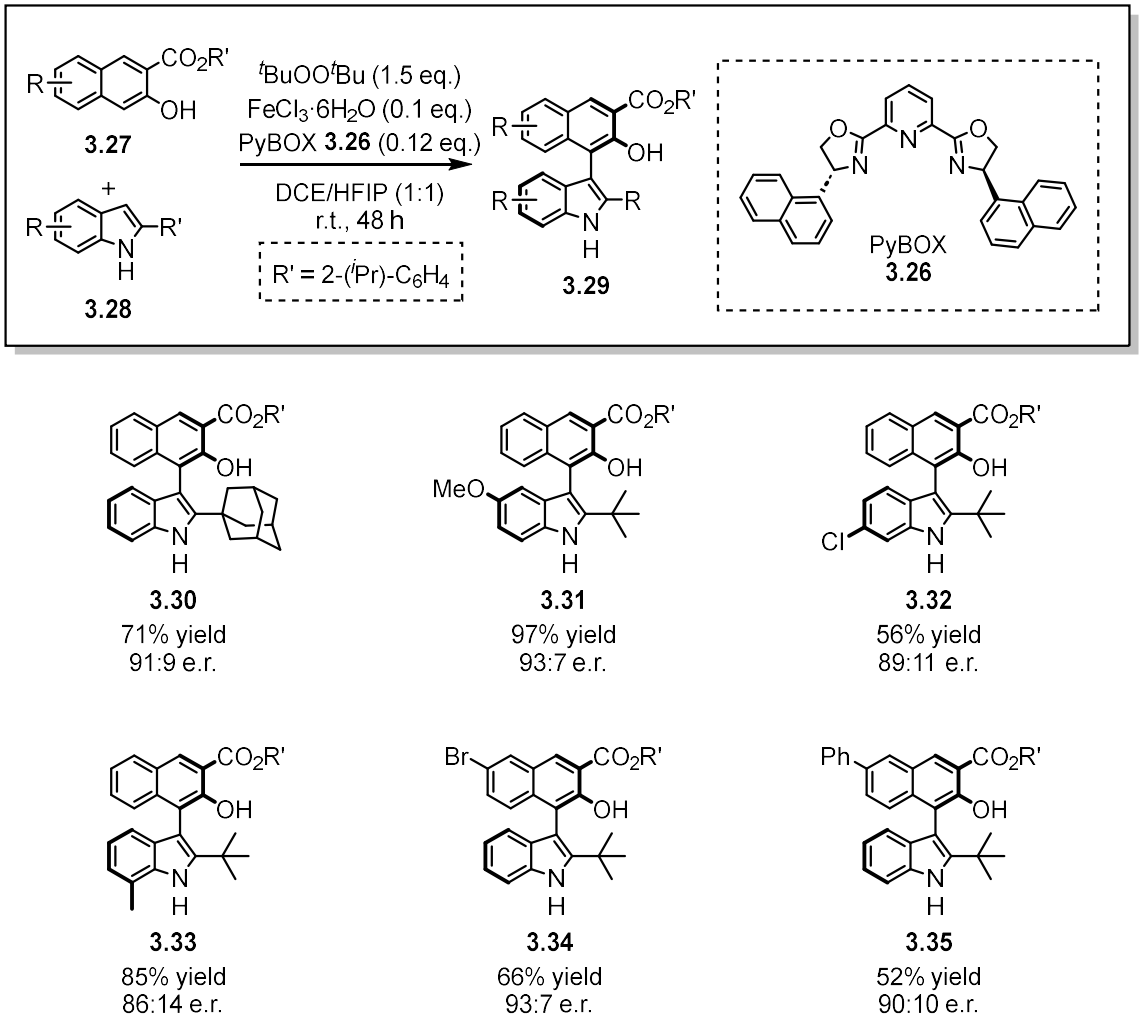
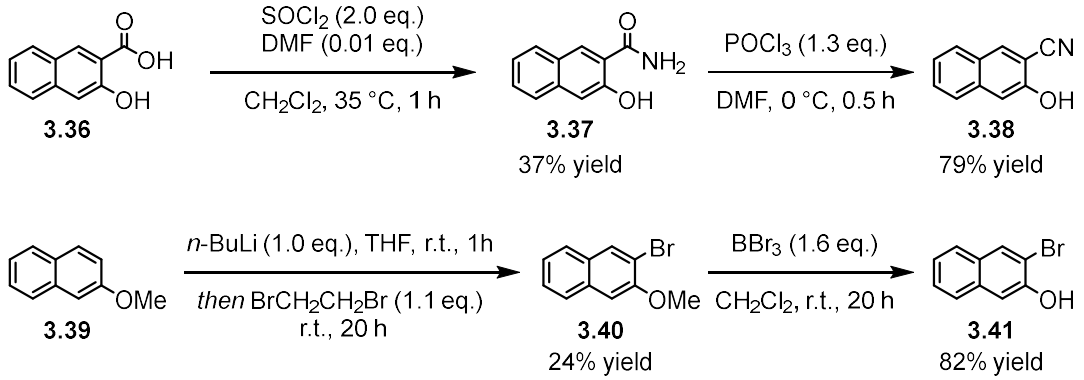


Fig 3.4. Representative collection from the published scope of the cross-coupling, showing the tolerated variations and well-conserved structures. The reaction conditions were as described with naphthols (1.0 eq.) and indoles (1.5 eq.).

3.3 Continuation of the Cross-Coupling Reaction

Given the importance of the ester group in **3.24** to the chemo- and stereoselectivity of the reaction, it is no surprise that it was well-conserved in the explorations of the reactivity. Thus, no work was done to evaluate the effectiveness of other directing groups that may be capable of binding the iron centre. The first step for our continuation of the project was to expand on this area of the previously made scope. We chose three withdrawing groups capable of chelation to the iron centre – terminal amide, nitrile and bromide (**3.37**, **3.38**, and **3.41**) (Scheme 3.6).

Synthesis of the three naphthols of interest was easily accomplished. **3.37** was synthesised by amidation of **3.36** *via* the acyl chloride. **3.38** could then be made by dehydration of **3.37**. **3.41** was made in two steps – bromination *via* deprotonation of **3.39**, followed by demethylation.



Scheme 3.6. Synthesis of 3-substituted 2-hydroxynaphthalenes **3.37**, **3.38**, and **3.41.**

With the substrates in hand, they were subjected to the reaction conditions chosen in the original investigation for a cross-coupling with **3.16** (Figure 3.5). **3.37** showed no cross-coupling or homocoupling – only starting materials were recovered. **3.38** underwent a very small amount of cross-coupling and produced the resultant biaryl **3.45** in low e.r.. **3.41** was the most successful at mimicking the reactivity of the naphthoate substrates, with a similar yield (92% compared with 91% for **3.24**) but with lower enantioselectivity (85:15 versus 94:6). None of the naphthols showed any homocoupling.

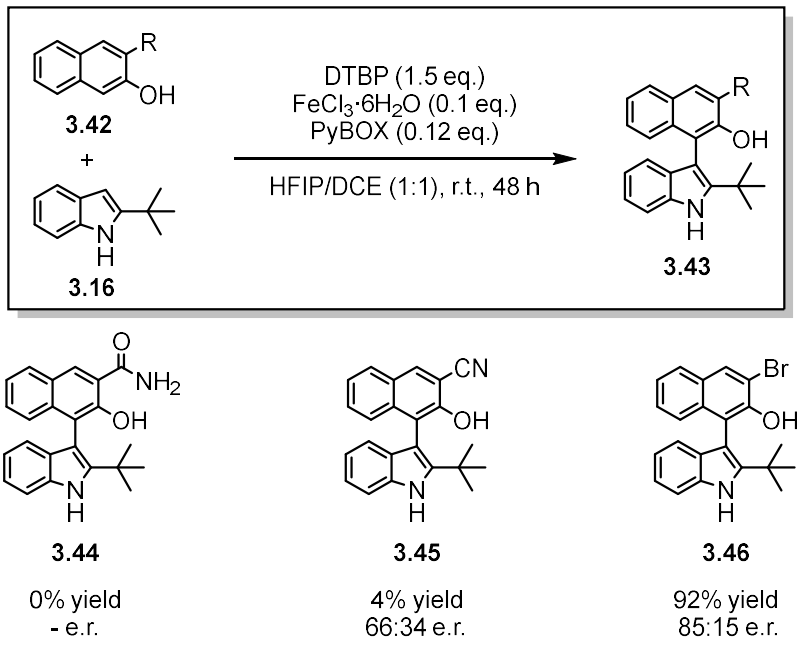


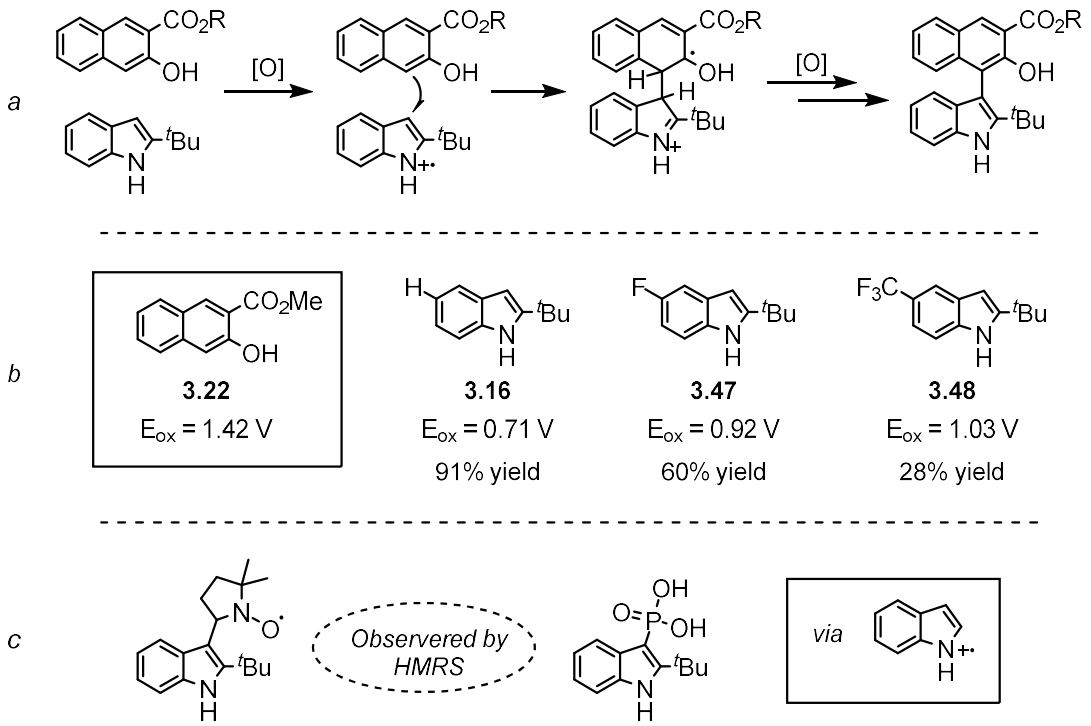
Figure 3.5. Iron-catalysed coupling of 3-functionalised 2-hydroxynaphthalenes with **3.16**. The reaction conditions are as stated, with naphthols (1.0 eq.) and **3.16** (1.5 eq.). e.r.s determined by chiral HPLC.

The reduced performance of these substrates compared to the naphthoate confirmed the necessity of the ester group for optimal yields and stereocontrol. Bromide, as the most tolerated, can approximate the binding of the ester group, but is less tightly bound to the iron and so controlled the enantioselectivity less effectively. The linear geometry of the nitrile makes the bidentate binding much less favourable, hence the marginal enantioselectivity. It was also more deactivating than the ester group and reduced the electron density of the naphthol more, thus lowering reactivity.[93] The primary amide's inability to undergo the reaction is perhaps unsurprising, given how different its reactivity is to the relatively inert ester.

3.4 Mechanism Investigation

Focus then moved to further investigation of the naphthoate reaction, with the aim of conclusively determining the mechanism. Previously, the Smith group had come to the consensus that the indole coupling partner is initially oxidised by the iron catalyst, and then trapped by nucleophilic attack from the naphthol (Scheme 3.7a).[91]

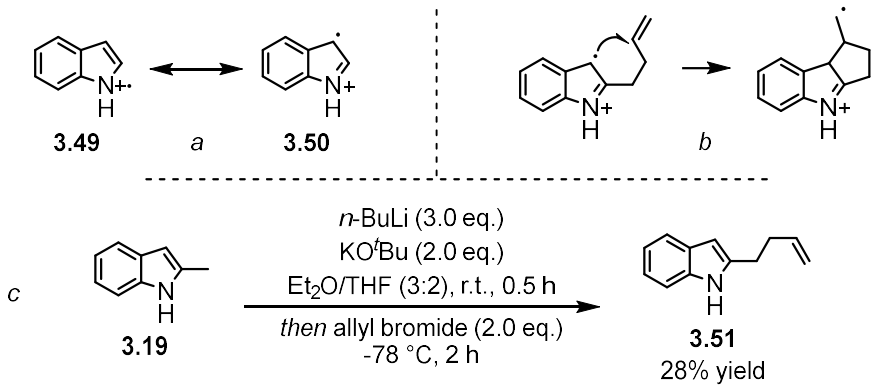
The evidence for this claim came from a number of sources (Scheme 3.7b and c). Comparing the oxidation potentials of indole **3.16** and naphthol **3.22** shows that the oxidation of **3.16** is significantly more accessible. Additionally, the oxidation potentials across a range of 5-substituted indoles showed increased cross-coupling yield with more electron-dense indoles. Radical trapping reactions with 5,5-dimethyl-1-pyrroline N-oxide and triethyl phosphite (Scheme 3.7c) found only evidence of indole radical formation, and no trapping products deriving from naphthol radicals. ESR experiments observed a very low concentration of an iron-bound indole radical and no naphthol-derived radicals across a range of set-ups.



Scheme 3.7. Initial investigation into the mechanism of the oxidative coupling. a) Proposed mechanism showing indole oxidation as starting point. b) Measured oxidation potentials of the naphthoate and a range of indoles c) Observed trapping products of the indole radical cation. No trapping products were seen with the naphthoate.

All of these pointed towards a reaction controlled by the rate of oxidation of the indole, followed by facile trapping of the resultant radical with naphthol.

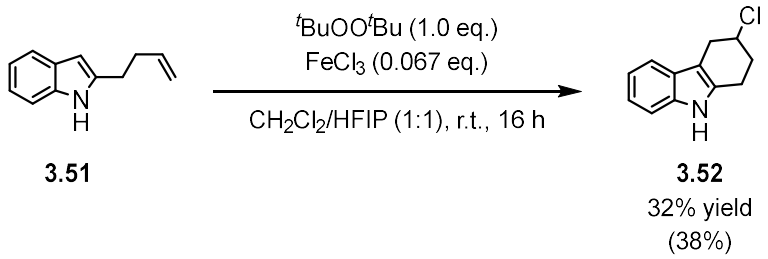
However, none of the experiments directly probed the role of the indole radical in the cross-coupling reaction – they simply showed that it is formed. To do this, synthesis of an intramolecular radical trap (**3.51**) was undertaken. Upon oxidation of an indole, the radical is most likely delocalised across the nitrogen and the C-3 position in resonance forms **3.49** and **3.50**. To directly measure the amount of indole oxidation, an alkenyl group was appended to an indole in the correct position for a rapid 5-*exo*-*trig* cyclisation of the radical from either position. As the trap is intramolecular, it should outcompete the intermolecular cross-coupling, confirming whether the indole oxidation is part of the reaction pathway or simply an unproductive side-reaction. Allylation with allyl bromide of 2-methylindole **3.19** (deprotonated by the *in-situ* formation of Schlosser's base from *n*-butyllithium and potassium *tert*-butoxide) afforded the indole of interest in a low but useable yield (Scheme 3.8c, 28%).



Scheme 3.8. Development of an intramolecular radical trap **3.51**. a) two resonance forms of the indole radical cation, demonstrating the location of the radical character b) the proposed trapping reaction c) synthesis of the indole containing an intramolecular radical trap (**3.51**)

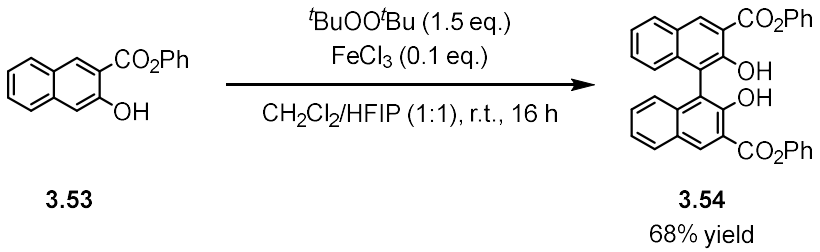
The first step in this approach to mechanistic determination was to observe the reactivity of **3.51** under the reaction conditions (Scheme 3.9). The stoichiometry of this reaction as written is unintuitive. The established cross-coupling notation is standardised against 1.0 equivalent of naphthoate and 1.5 equivalents of indole. As such, the molar ratios between reagents in the individual oxidation of **3.51** have been conserved, but they are now reported relative to the indole.

Subjecting **3.51** to the oxidative conditions did indeed lead to significant cyclisation of the radical onto the pendant alkenyl group, generating a 32% yield of **3.52**. The nature of this cyclised product, however, was unexpected. Rather than a 5-*exo*-*trig* product, it gave a product that would be expected of the 6-*endo*-*trig* cyclisation. The resultant radical had also been trapped by an apparent chlorine radical, despite no dedicated chlorine source being present in the reaction. Other than this product, the only other species recovered was a moderate quantity of the starting indole **3.51** (38%). The rest of the material had presumably decomposed – a fate common for the indoles used in this reaction, hence the excess in the standard preparation.



Scheme 3.9. Intramolecular trapping reaction of **3.51** under the oxidative coupling conditions. The figure in brackets refers to the yield of recovered starting material **3.51.**

From previous work, it was known that subjecting the naphthoate **3.53** to identical conditions would produce the BINOL derivative **3.54** in 68% yield (Scheme 3.10).[92]



3.53 **3.54**
68% yield

Scheme 3.10. Homocoupling of **3.53** under the oxidative coupling conditions

Confident in our understanding of the behaviour of both coupling partners under the oxidative conditions individually, we turned to the competition experiment (Scheme 3.11). When both were included in the reaction, the major product was the heterocoupled biaryl **3.55**. The indole intramolecular cyclisation product was observed in a less than 5% yield, and no naphthoate-derived BINOL was seen (10% of the unreacted naphthoate was recovered).

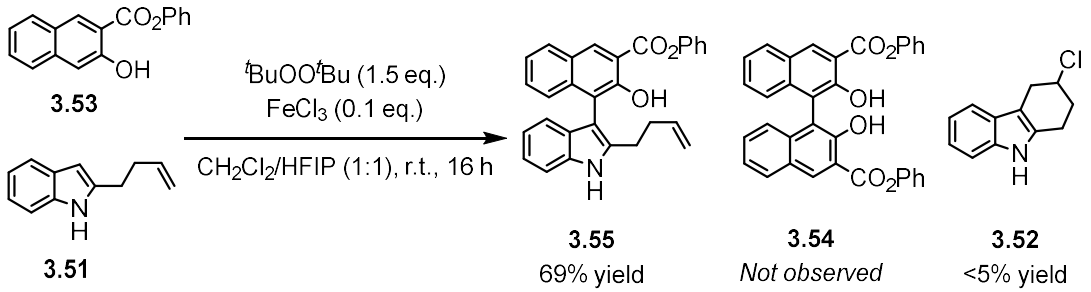
No alternative cross-coupling products – ones that would result from a trapping of the cyclised-indole **3.52** or an intermediate radical by the naphthoate **3.53** – were observed.

This was a significant departure from previous mechanistic probes, as it strongly indicated that the indole oxidation is not in fact a productive part of the reaction pathway.

If significant amounts of indole were oxidised, we would expect to see a large quantity of the resultant cyclisation – the intramolecular radical trapping should be rapid and outcompete intermolecular nucleophilic attack by the naphthol. However, what we observed was minimal indole cyclisation, and therefore minimal indole oxidation took place.

However, there was still a good yield of the cross-coupled product **3.55**, from the reaction between the indole **3.51** (rather than a cyclisation product) and naphthoate **3.53**. In order for this product to be formed, there must have been an oxidative cross-coupling and thus an initial oxidation event. Given

the evidence against indole oxidation, it was reasoned that the naphthoate oxidation is the initiation step in the reaction.



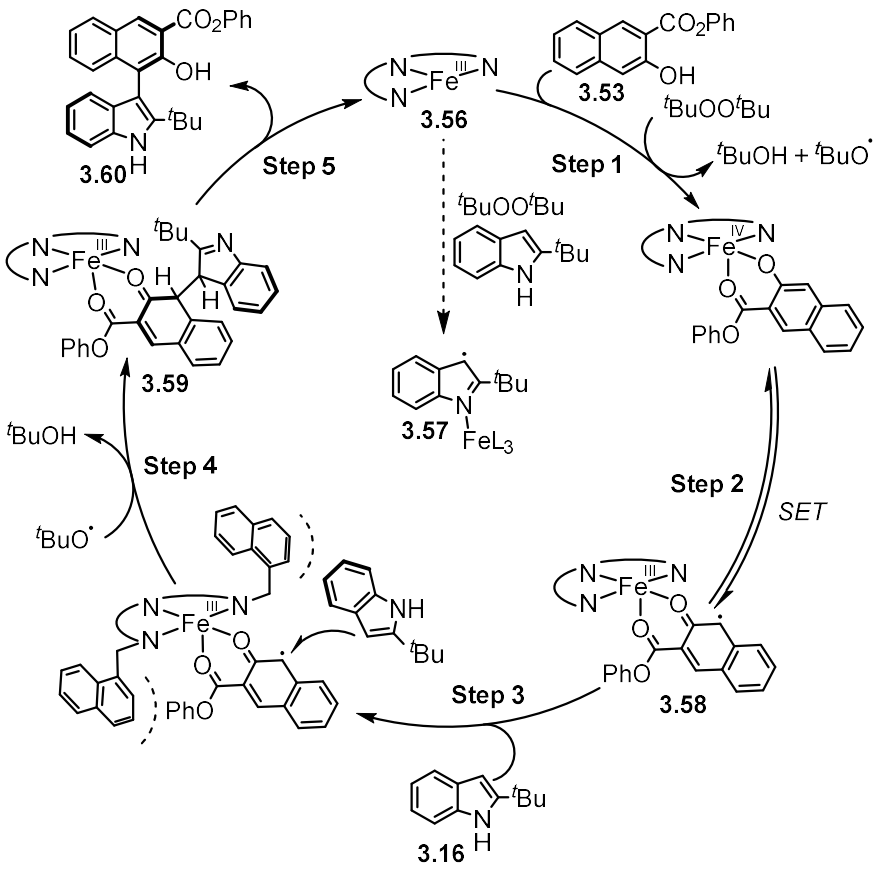
Scheme 3.11. Competition experiment between intramolecular radical trapping and intermolecular coupling. The reaction conditions are as stated, with **3.53** (1.0 eq.) and **3.51** (1.5 eq.). 10% of **3.53** was recovered, and no **3.51** was.

3.5 Mechanistic Proposal

With this in mind, we devised an alternate mechanistic proposal (Scheme 3.12). The outline of the reaction is similar to the previously proposed mechanism, but with the roles of the coupling partners reversed. It begins with strong bidentate binding of the iron-ligand complex to the naphthoate **3.53**. Oxidation of Fe(III) to Fe(IV) by DTBP sets up for a single electron oxidation of the naphthoate (Step 2). The radical **3.58** is then subject to nucleophilic attack by the indole, forming the key carbon-carbon bond. Hydrogen atom abstraction by a tertbutoxy radical (Step 4) completes the two-electron oxidation, and tautomerisation of the resulting closed-shell compound **3.59** affords the heterobiaryl product **3.60**.

The stereochemical outcome is dictated by the geometry of the indole attack (Step 3), which is controlled by the chiral environment around PyBOX-iron-naphthoxy-radical complex, held rigid by the multidentate binding of both ligands. Transfer of the chirality from point (**3.59**) to axial (**3.60**) occurs in the tautomerisation step (Step 5).

Indole oxidation is still possible but is a nonproductive pathway. Formation of a small amount of indole radical occurs, but stabilisation from binding to the iron centre renders it persistent – leading to the population implied by the radical trapping products and observed by ESR.



Scheme 3.12. Proposed mechanism of the iron-catalysed cross-coupling of **3.53** and **3.16**.

A number of other previous results originally used to support the indole oxidation route can be also justified by this framework.

The effect of substitution of the indole on cross-coupling yields (Scheme 3.7b) is explained by the changing electron density affecting the nucleophilicity of the indole, rather than the oxidation potential. This impacts the efficiency of the nucleophilic coupling with the naphthoxy radical.

The significant switch in chemoselectivity observed in the transition from naphthol to naphthoate substrates can also be rationalized. BINOL-type products (as were seen in the reactivity described in Scheme 3.5b) were produced when the naphthoxy radical **3.58** was trapped by a second naphthol molecule in a nucleophilic attack, outcompeting the indole attack. This reactivity became dominant as the steric bulk on the indole increased, decreasing its nucleophilicity. With the introduction of electron-withdrawing ester group causing a decrease in nucleophilicity of the naphtholic coupling

partner, the indole returned to being the more effective nucleophile and only the cross-coupled product was formed (Scheme 3.5c).

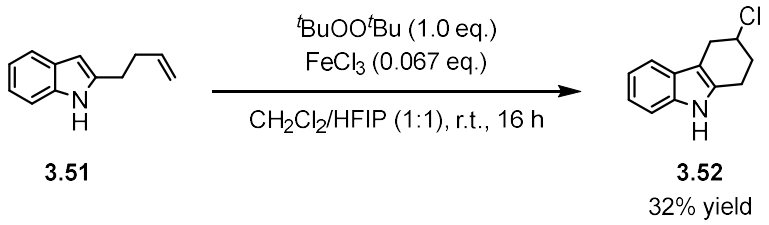
The only evidence that does not support this mechanism is the measured oxidation potentials. Indole **3.16**, with an oxidation potential of 0.71 V, is much more easily oxidised than the naphthols and naphthoates. However, this only takes thermodynamic considerations into account. Fe(III) forms strong complexes with phenols and is well-known to oxidise phenolic ligands.[94] It is likely that, despite indole oxidation being energetically more accessible, the kinetic effects of tight iron-naphthoate binding and effective ligand-to-metal charge-transfer leads to preferential oxidation of the naphthol components. The sequestering of the iron catalyst explains the decrease in yield of the cyclised **3.52** upon the inclusion of naphthoate **3.53**, as the iron was no longer accessible to catalyse the side-reaction.

With the investigation into the mechanism concluded, we turned our attention onto other possibilities with the reaction system.

Chapter 5: Indole Radical Cation Cyclisation

3.6 Introduction to the Indole Radical Cation

Although the main aim of this project was the investigation of the oxidative cross-coupling, the surprising cyclisation reaction found during the competition experiments was also of real interest (Scheme 3.13).



3.51 **3.52** 32% yield

Scheme 3.13 Oxidative cyclisation of **3.51**, catalysed by $FeCl_3$

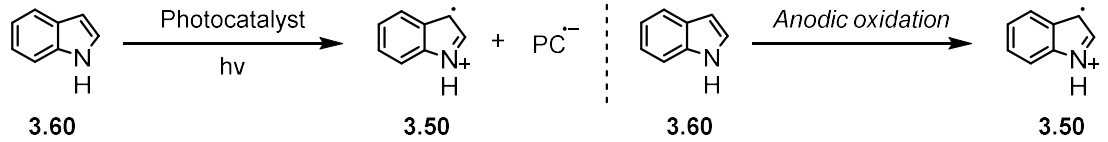
Single electron oxidation of indoles to the indole radical cation is a well-known reaction.[95]

The oxidation of tryptophan's indole-containing sidechain within enzymes is known to promote a diverse set of biological transformations and facilitate rapid electron transport. This has led to great interest in gaining a better understanding of the behaviour and reactivity of the radical cation.[96,97]

Synthetically, the indole radical cation has been harnessed as an avenue to reactivities unobtainable from the closed-shell neutral indole. Diverse methods for the functionalisation of indole are vital, owing to the prevalence of the moiety across natural products and bioactive compounds.[98,99] The reactivity of indoles is dominated by nucleophilicity, especially at the C-3 position. Oxidation fundamentally changes this behaviour, leading to a range of electrophilic and radical reactivities.

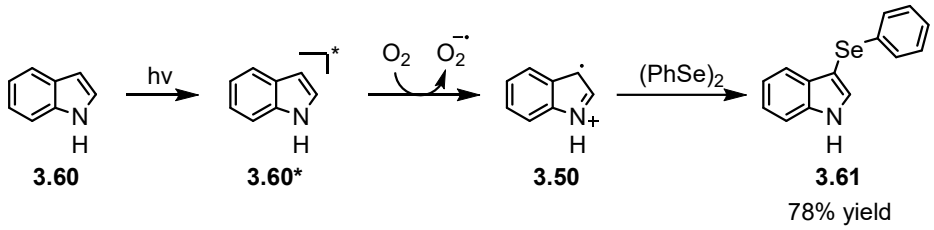
To this end, synthetic access to the radical cation is of great interest and has been achieved for a number of purposes. However, the range of practical approaches to its generation is fairly narrow. The two common approaches are electron transfer *via* electrochemical or photochemical means, as may be expected for a single electron oxidation (Scheme 3.14). [95,100]

Electrochemical approaches use anodic oxidation to generate the radical cation. Photochemical approaches use a photoredox catalyst that is strongly oxidising when excited to remove the electron. The catalyst is regenerated by a stoichiometric external oxidant or by reduction of the substrate in a closed cycle.



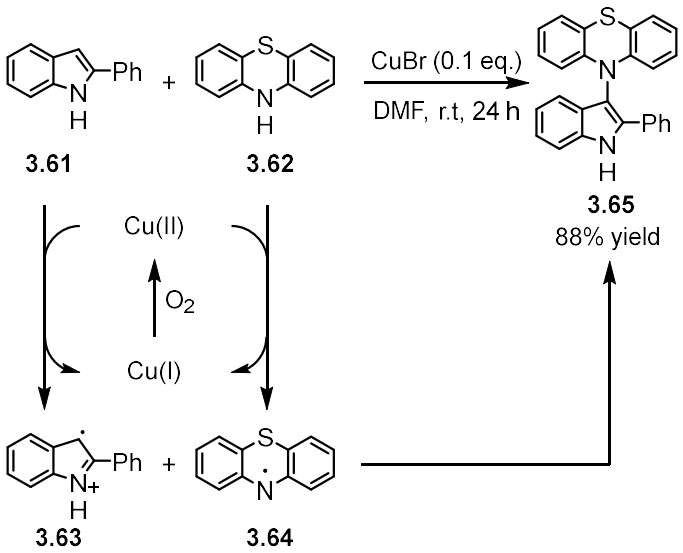
Scheme 3.14. Oxidation of indole by photoredox and electrochemistry – the two most common approaches.

There is also one example of direct excitation of the indole with visible light, reported by Kumar and coworkers. The oxidation occurs by electron transfer from the excited indole **3.60*** to atmospheric oxygen, in a variation on the traditional photoredox formula.[101]



Scheme 3.15. Synthesis of **3.61** *via* direct excitation of indole and the radical cation. Reaction conditions: **3.60** (2.0 eq.), $(PhSe)_2$ (1.0 eq.), sunlight, acetone, r.t., 6 h.

Less common is the generation of **3.50** by a traditional oxidant. One rare example is the oxidation of an indole by a Cu(II)/Cu(I) system reported by Liu and coworkers (Scheme 3.16).[102] Single electron transfer from **3.61** produces **3.63**, which combines with a similarly generated radical (**3.64**). The reaction turns over by utilising atmospheric oxygen to recycle the copper catalyst.



Scheme 3.16. Synthesis of **3.65** *via* single electron oxidation of **3.61** and **3.62**, followed by radical-radical combination. The reaction conditions were as stated with **3.61** (2.0 eq.) and **3.62** (1.0 eq.)

Computational investigation into the structure of the indole radical cation indicated that it is best understood by its resonance form **3.50**.[103] This positions the radical character on the C-3 position and the cation character on C-2.

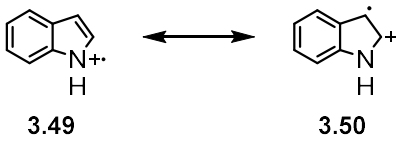
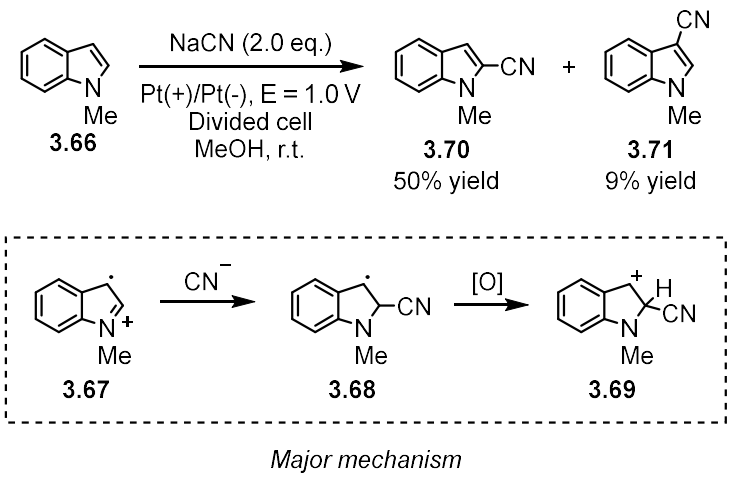


Figure 3.6. Major resonance forms of the indole radical cation.

The ramifications of this are observed in the reactions of **3.50** derivatives, as regioselectivity is markedly different depending on the mode of reaction.

Reactions with nucleophiles tend to happen at the C-2 position (Scheme 3.17). For example, Yoshida showed that electrochemically generated **3.67** reacted with cyanide anions to form the 2-cyano radical species **3.68**.[104] The radical species then underwent a second oxidation to the cation **3.69** and deprotonated to rearomatise. This reaction showed a preference for cyanation at the C-2 position, although a moderate amount of the undesired isomer was also formed.

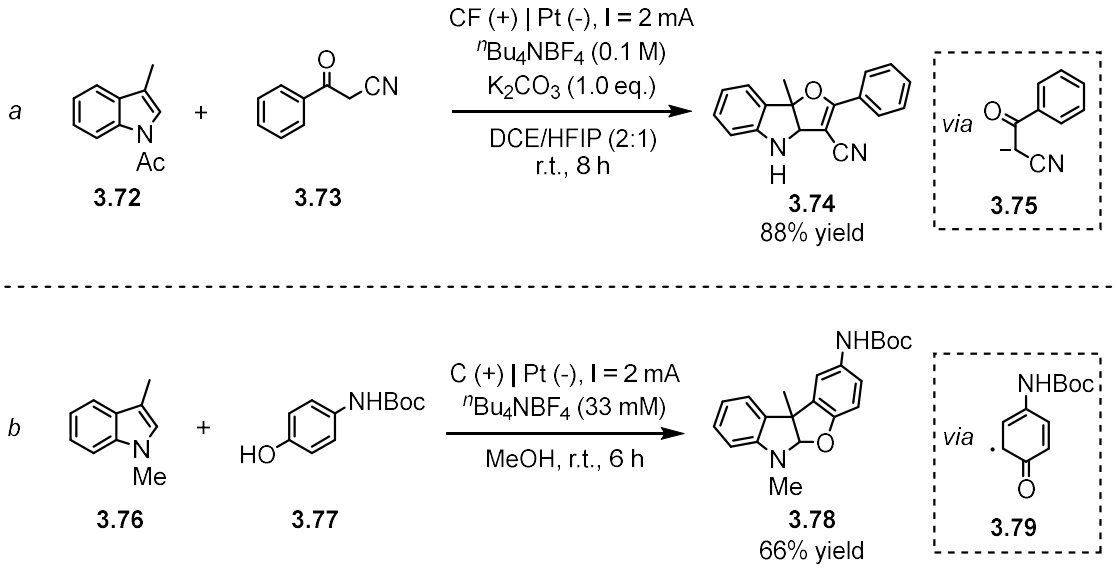


Scheme 3.17. Electrochemical cyanation of **3.66**

This reactivity is also observed in more complex reactions, such as the annulation between benzoylacetonitrile and an electrochemically-generated indole radical cation (Scheme 3.18a).[103] The enolate **3.75** (formed by the deprotonation of **3.73**) attacked the radical cation solely at the C-2 position, and a second oxidation and cyclisation of the ketone produced furo[3,2-b]indoline **3.74** in an 88% yield.

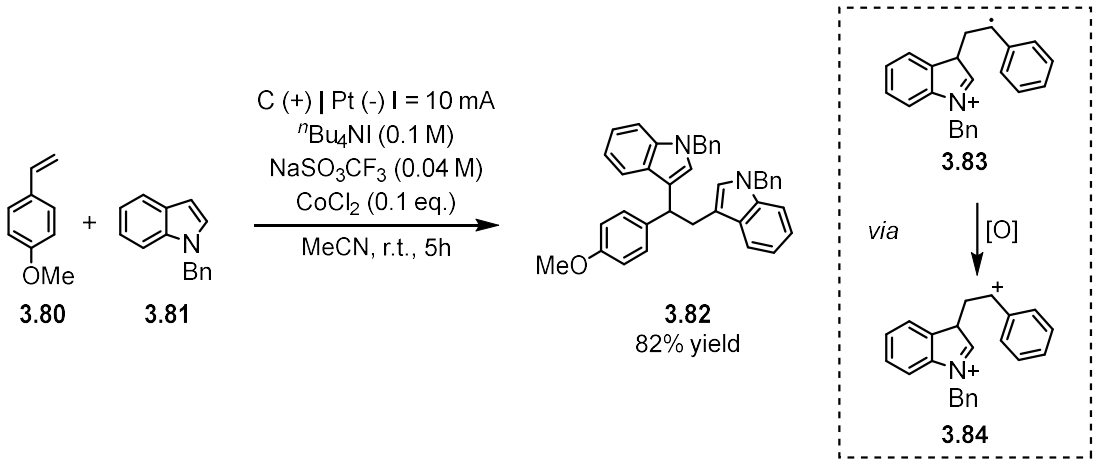
Radical reactions, conversely, happen at the C-3 position (Scheme 3.18b). Oxidation of **3.76** generated the radical **3.79** which instead reacted with the radical cation at the C-3 position to give the benzofuro[2,3-b]indoline **3.78** after the phenolic hydroxyl group cyclised onto the C-2 position.

This example neatly shows how the regiochemistry of reactions with the radical cation can be controlled by the mode of reactivity.



Scheme 3.18. Electrochemical generation of indole radical cations, followed by combination with a) an enolate or b) a radical **3.79**. Reaction conditions: a: The reaction conditions were as described with **3.72** (1.0 eq.) and **3.73** (1.5 eq.). b: The reaction conditions were as described with **3.76** (2.0 eq.) and **3.77** (1.0 eq.).

As well as radical-radical combinations, this selectivity also extends to other typical radical reactions. Li and coworkers reported the trapping of an indole radical cation by an addition into an alkene (Scheme 3.19).[105] Electrochemical generation of the radical cation in the presence of **3.80** led to the radical attack from the C-3 position and the formation of benzyl radical **3.83**. A second oxidation afforded the benzyl cation **3.84**, which was trapped by a second equivalent of neutral **3.81** acting as nucleophile. This transition from radical to ionic chemistry is an example of a radical polar crossover.

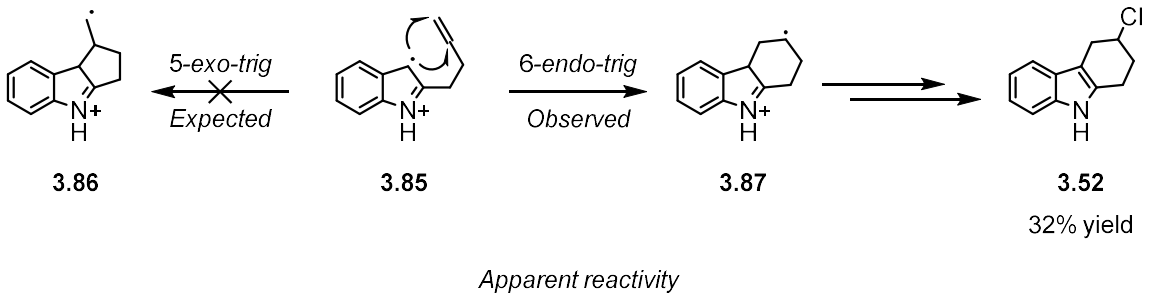


Scheme 3.19. Trapping of indole radical cation of **3.81** by styrene **3.80**, followed by a nucleophilic trapping of a second **3.81**. The reaction conditions were as described with **3.80** (1.0 eq.) and **3.81** (3.0 eq.).

With this in mind, we endeavoured to explore the novel intramolecular trapping of a chemically generated indole radical cation.

3.7 Indole Cyclisation Mechanism Proposal

Although the radical cation **3.85** cyclised onto the alkenyl trap as expected, the product it formed was surprising (**3.52**).



Scheme 3.20. Apparent reactivity of **3.85**. Reaction conditions: **3.51** (1.0 eq.), ^{t}BuOO^{t}Bu (1.0 eq.), $FeCl_3$ (0.067 eq.), CH_2Cl_2/HFIP (1:1), r.t., 16 h

The substrate had been designed with the intention of facilitating a facile 5-*exo-trig* radical cyclisation, a reaction that is known to proceed rapidly. However, a 5-*exo-trig* would lead to a 6,5,5-tricyclic core with a pendant methylene radical (**3.86**); no prediction had been made for the eventual fate of the radical, but it was assumed it would be trapped by another component of the reaction mixture to produce a 6,5,5-tricylic product.

The observed product was in fact a 6,5,6 tricycle – a tetrahydrocarbazole (**3.52**). The identity of this unexpected product was confirmed by NMR and mass spectrometry. Cyclisation was confirmed by the absence of the C-3 proton in the ^{1}H NMR spectrum. The ^{1}H and ^{13}C NMR spectra identified the four aliphatic environments of the saturated ring, with two protons in both benzylic environments. The higher shifted environment (and thus likely α to a heteroatom) has only a single proton and is coupled to two CH_2 centres. Mass spectrometry showed a component with the mass of **3.52** that exhibited the expected chlorine isotopic abundance (a 3:1 ratio between two species separated by two atomic mass units) from ^{35}Cl and ^{37}Cl, and the analogous alcohol was not observed. No evidence of an HFIP-derived product (in particular the septet from the central proton in ^{1}H NMR) was observed.

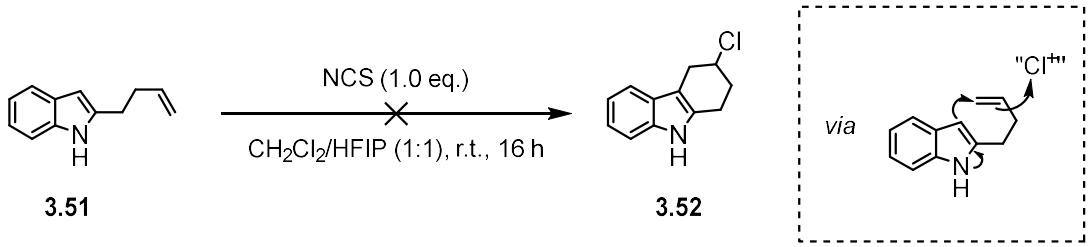
The obvious pathway for the formation of this product was the 6-*endo-trig* cyclisation to a secondary radical (**3.87**). However, as outlined by Baldwin's rules for cyclisations, 6-*endo-trig* cyclisation in radicals is significantly disfavoured, and the 5-*exo-trig* should be overwhelmingly preferred in cases without specific geometric biases.[106] Both attacks are geometrically feasible in the substrate, so an inherent preference for 6-*endo-trig* is unlikely.

A cationic rather than radical 6-*endo-trig* would not be subject to these restrictions, but a route for the initiation of a cationic pathway is less clearcut.

Generation of a cationic rather than radical cationic intermediate would likely occur by iron(III) chloride acting as a Lewis acid. The formation of a cationic intermediate by this pathway could occur at either the indole or the pendant alkene – both locations for cation formation would allow for a cyclisation to the observed product.

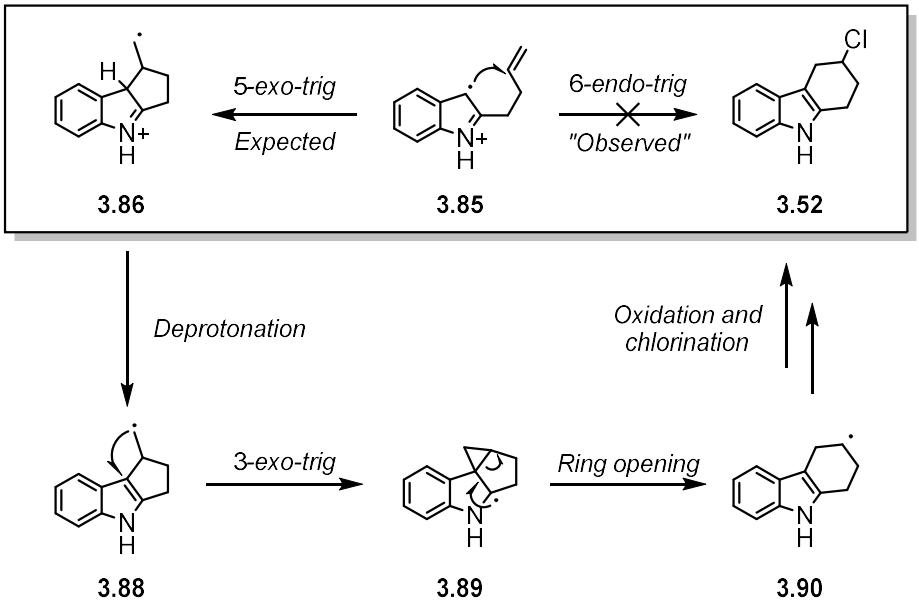
However, this reactivity was discovered in the context of single electron oxidation, and previous probes of this system have observed products consistent with the radical cation formation (specifically the radical trapping reactions performed by Dr Surgenor, shown in Scheme **3.7**). Given then the observed reactivity of indoles under these conditions, a distinct mechanistic pathway for this oxidative cyclisation was deemed unlikely.

The chlorine trapped in the product may suggest an alternative cationic mechanism. The generation of a cationic source of chlorine in the reaction mixture would allow for a cationic cyclisation cascade (Scheme 3.21). However, use of N-chlorosuccinimide (NCS) as a cationic chlorine source did not lead to **3.52**, and so it's unlikely that this cationic pathway was the cause of the cyclisation.



Scheme 3.21. Potential cationic pathway for the 6-*endo-trig* cyclisation

The final possibility, then, is that the reaction does indeed proceed through the 5-*exo-trig* radical cyclisation initially, but then undergoes additional steps to reach the product (Scheme 3.22). The intermediate **3.86**, formed after the cyclisation, was an unstabilised primary radical and thus unlikely to persist long enough to be trapped intermolecularly. Instead, after a rapid deprotonation and rearomatisation of the indole to afford **3.88**, the methylene radical attacked the indole double bond in a 3-*exo-trig* cyclisation. The subsequent cyclopropane **3.89** was opened by the radical to give the ring-expanded secondary radical **3.90**, amounting to a neophyl rearrangement of **3.88**. With no further rearrangements possible and increased stability due to the increased substitution, the secondary radical persisted. An attempt to trap this radical with TEMPO to confirm this was unsuccessful; the only materials recovered were the starting material and an unidentified uncyclized derivative of **3.51** with the alkenyl trap intact.



Scheme 3.22. Proposed mechanism for the formation of **3.52** from the radical cation **3.86** *via* a neophyl rearrangement.

The steps between **3.90** and the chlorinated product **3.52** are harder to surmise. Two possibilities were that **3.90** abstracted a chlorine radical, or that **3.90** was oxidised a second time to a cationic species and trapped a chloride ion.

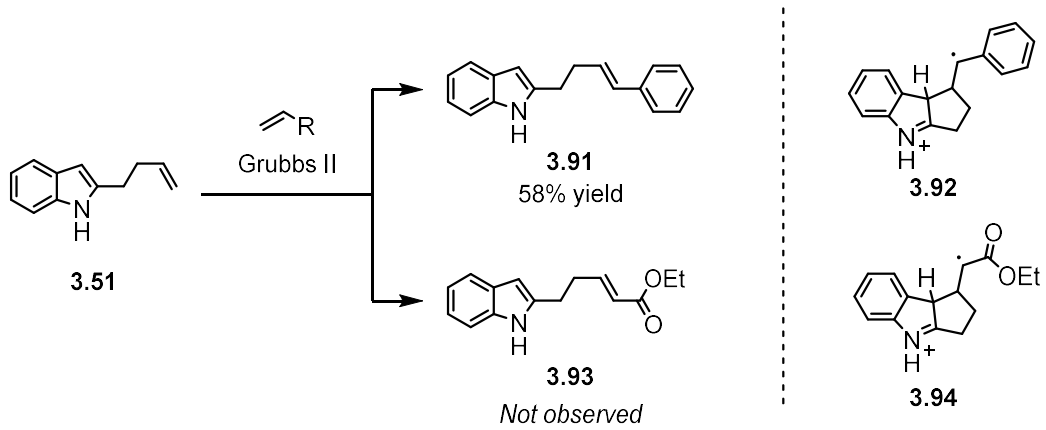
The potential source of a chloride ion is obvious ($FeCl_3$) - but a source of a chlorine radical less so. It would either originate from the $FeCl_3$ or the CH_2Cl_2, as they were the only two chlorinated materials in the reaction mixture.

3.8 Substrate Variation

With a theorised reaction mechanism, it was possible to design a number of substrates that could undergo this transformation. By adding substituents to the alkene, we hoped to alter the stability of the radical intermediates (**3.85**, **3.86** and **3.90**) in order to increase the efficiency of the cyclisation.

3.8.1 Linear Alkenes

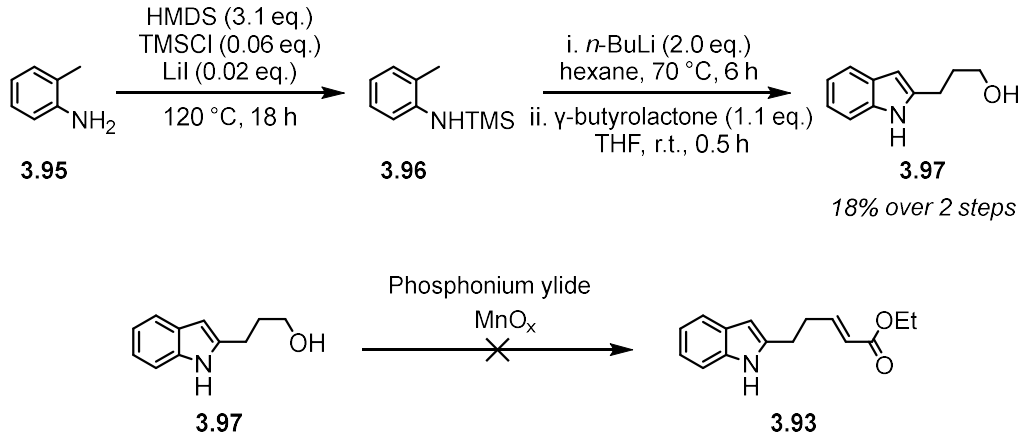
The first substrates devised (**3.91** and **3.93**) were intended to stabilise the radical product of the 5-*exo-trig* cyclisation (**3.85**). The π systems of the phenyl and ester groups appended to the terminal position of the alkenyl trap would allow for resonance stabilisation of the previously unstabilised primary radical (**3.92** and **3.94**). Initial routes to these employed Grubb's second-generation catalyst to affect a cross-metathesis. This transformation was achieved in a moderate yield for **3.91** (58% yield) but was unsuccessful when the methodology was applied to the synthesis of **3.93**. Further exploration of applicable catalysts (in particular Hoveyda-Grubbs II) may have led to success with this route – however, financial concerns instead encouraged a change of approach to **3.93**.



Scheme 3.23. Synthesis of modified radical traps, intended to stabilise the radical formed in the initial 5-*exo-trig* attack. Reaction conditions: Synthesis of **3.91**: **3.51** (1.0 eq), *trans*-stilbene (4.0 eq.), Grubbs II (0.04 eq.), CH_2Cl_2, 40 °C, 18 h. Attempted synthesis of **3.93** : **3.51** (1.0 eq.), ethyl acrylate (10 eq.), Grubbs II (0.04 eq.), CH_2Cl_2, r.t., 18 h.

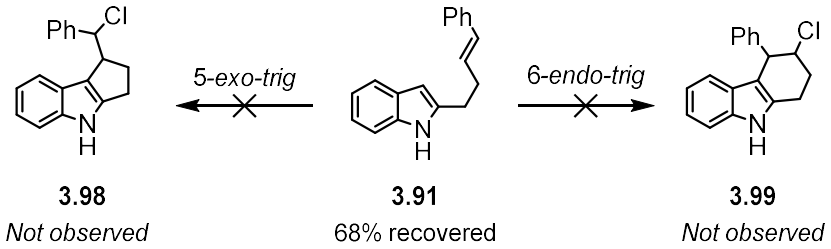
An alternate route to the ester was devised, by replacing the olefin metathesis with a Wittig olefination. However, access to the aldehyde intermediate was limited, so synthesis of the primary alcohol precursor **3.97** was undertaken by construction of the indole heterocycle (Scheme 3.24).

Silylation of **3.95** was successful and the cyclisation to **3.96** was achieved without issue. In an effort to avoid the isolation of the potentially unstable aldehyde, one pot oxidation/Wittig olefinations with both MnO_2 and $BaMnO_4$ were attempted. They gave only trace amounts of **3.93** and proved unable to supply the material needed for trial.



Scheme 3.24. Synthetic route to **3.93**. Reaction conditions of the one-pot oxidation/olefinations: a) **3.97** (1.0 eq.), (carbethoxymethylene)triphenylphosphorane (1.2 eq.), MnO_2 (10 eq.), PhMe, 110 °C, 18 h. b) **3.97** (1.0 eq.), triphenylphosphine (1.2 eq.), ethyl bromoacetate (1.2 eq.), $BaMnO_4$ (1.2 eq.), MeCN, 80 °C, 24 h

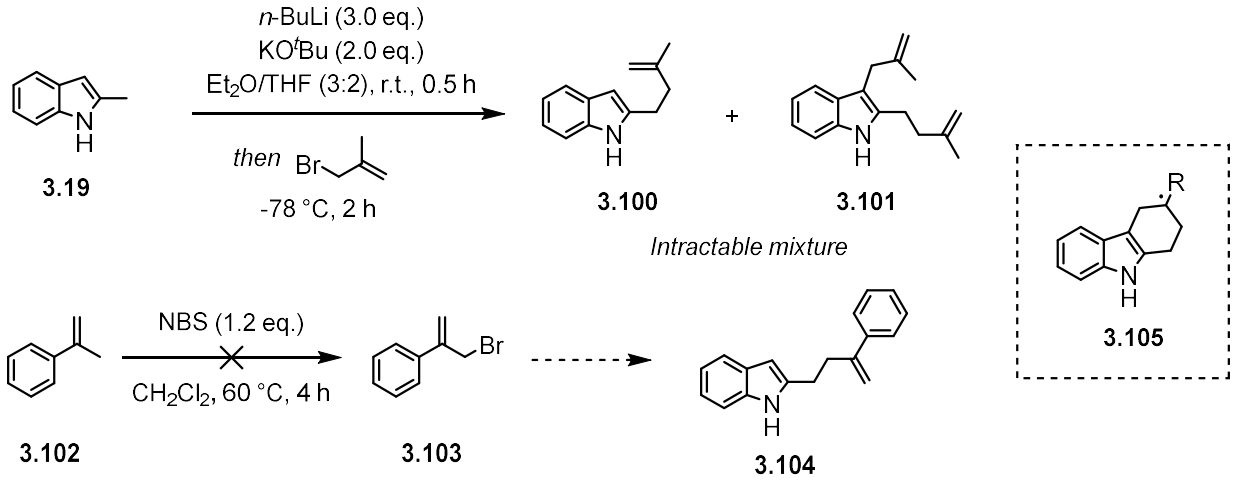
3.91 was subjected to the oxidising conditions. The expected product was either the phenylated 6,5,6 tricycle **3.99** analogous to **3.52**, or potentially a 6,5,5 tricycle **3.98** derived from the 5-*exo*-*trig* cyclisation product with no further rearrangement. However, no cyclisation products were found in the crude reaction mixture and the starting material was recovered in a 68% yield. It was unclear why additional stabilisation of the theorised radical intermediate would completely remove all reactivity. It is unlikely that the steric bulk of the phenyl group addition would have had an impact on the cyclisation, as it was a significant distance from the site of attack.



Scheme 3.25. Behaviour of the modified intramolecular trap **3.91** under the oxidative conditions. Reaction conditions: **3.91** (1.0 eq.), ^{t}BuOO^{t}Bu (1.0 eq.), $FeCl_3$ (0.067 eq.), CH_2Cl_2/HFIP (1:1), r.t., 16 h

3.8.2 Branched Alkenes

We then turned our attention to the synthesis of branched terminal alkenes, in an attempt to stabilise the secondary radicals that would be formed after the proposed neophyl rearrangement (**3.105**). These were to be accessed by replacing allyl bromide in the synthesis of **3.51** with branched allyl bromides derived from isobutene (to produce **3.100**) and α-methylstyrene (to produce **3.104**). Despite a number of attempts at the allylation to **3.100**, the product was inseparable from the diallylated side product **3.101**. **3.103** was not commercially available and so it was necessary to synthesise it. However, bromination of **3.102** proved uncooperative and was abandoned, as no reaction was observed with NBS. Given the difficulties in acquiring the branched alkenes, this substrate class was abandoned.



Scheme 3.26. Attempted syntheses of **3.100** and **3.104**, branched alkenes that would produce the stabilised radicals **3.101** and **3.105** respectively.

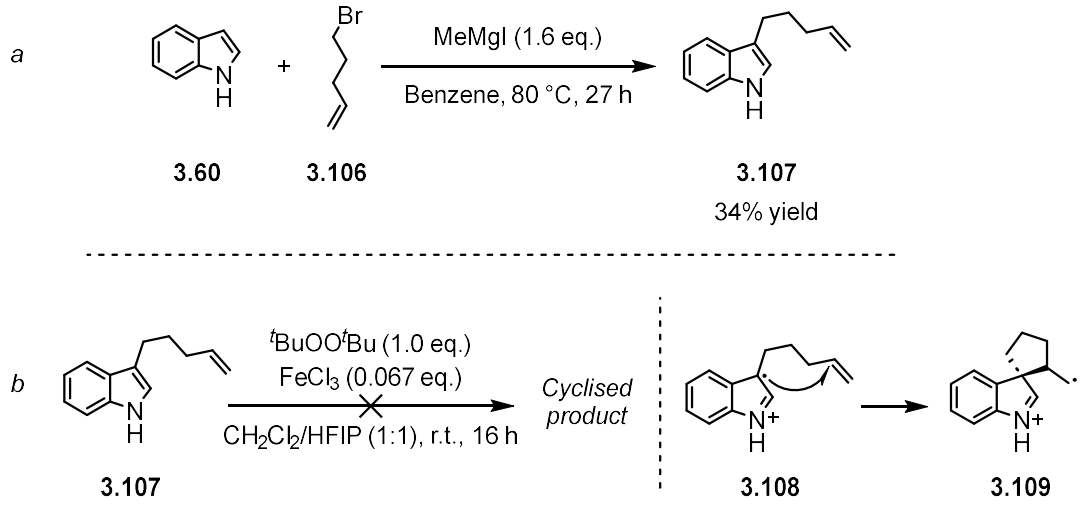
3.8.3 Radical Traps at the C-3 Position

With little success in modulation of the original terminal alkene trap appended to the C-2 position, we turned towards other structures that would also function as intramolecular radical traps – in particular ones attached at the C-3 position, in order to impart greater stability to the initial indole radical cation.

The first attempt stuck closely to the previous methodology, with a tethered terminal alkene set up for a 5-*exo-trig* cyclisation from the C-3 centred radical (Scheme 3.27). However, the tether attachment at the C-3 position would now lead to the formation of a 5,5-spiro radical **3.109** that, due to the quaternary centre at the C-3 position, would not be able to rearomatise. This would allow for specific insights into the efficiency of the oxidation and cyclisation without the compounding effects from the neophyl rearrangement.

Synthesis of **3.107** was a simple albeit low-yielding electrophilic aromatic substitution, facilitated by deprotonation of the indole (Scheme 3.27a).

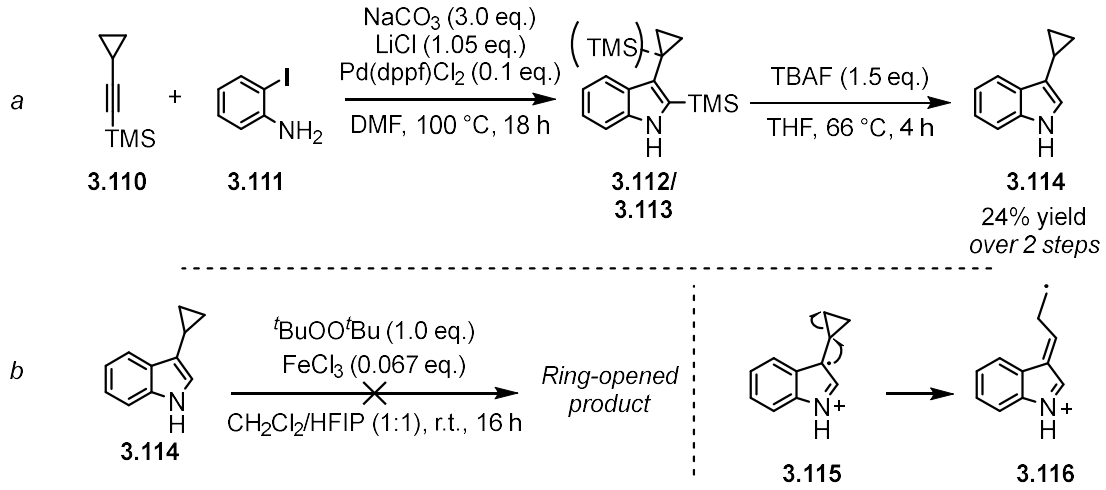
After being subjected to the oxidation conditions, no species other the starting material (37% recovery) could be seen in the crude reaction mixture. The loss of material was due to reactivity under the reaction conditions, but without a product to identify, no conclusions could be drawn.



Scheme 3.27. C-3-tethered alkenyl intramolecular radical trap. a) The reaction conditions are as stated, with **3.60** (1.5 eq.) and **3.106** (1.0 eq.). b) Results of oxidation of **3.107** showing no cyclisation products, intended to have occurred through a 5-*exo-trig* cyclisation to the 5,5-spiro radical **3.109**.

The second alternative substrate relied on a different radical clock to the previous reactions. Rather than the cyclisation of the radical onto an alkenyl group, it reacts *via* the cyclopropylcarbinyl ring opening reaction (Scheme 3.28b). The formation of the initial C-3 centred radical cation **3.115** should be intercepted by a rapid opening of an adjacent cyclopropyl ring to **3.116**. This reaction was likely to be subject to the same termination complications as the olefin cyclisation, as the ring-opening product **3.116** is again a primary radical with no prescribed next step, but it would provide a different perspective on the oxidation and termination steps.

Synthesis of this substrate was more involved (Scheme 3.28a). Installation of the cyclopropyl group necessitated construction of the indole ring rather than a simple functionalisation. Silylation of cyclopropylacetylene (to **3.110**) allowed for a palladium-catalysed Heck-type vinylation/intramolecular amination cascade leading to **3.112** (and the disilylated product **3.113**). The resultant mixture proved resistant to desilylation and required two passes with TBAF, but ultimately produced **3.114** in a 24% yield over 2 steps (relative to **3.111**). When the radical probe **3.114** was subjected to the oxidation conditions, no products could be found. The crude reaction mixture was exclusively starting material, although only 33% was recovered. This, again, did not give any additional insights into the reaction mechanism.



Scheme 3.28. C-3-tethered cyclopropyl intramolecular radical trap. a) The reaction conditions are as stated, with **3.110** (1.1 eq.) and **3.111** (1.0 eq.). The sample of **3.112/3.113** was subjected to the given desilylation conditions twice before isolation of **3.114** b) Results of oxidation of **3.114** showing no ring-opening products, intended to have occurred through a cyclopropylcarbinyl ring opening.

3.9 Cyclisation Optimisation

We returned to the previous productive substrate, **3.51**.

As interesting as the reaction of the original C-2 tether **3.51** was, the 32% yield was too low for it to be synthetically useful. The recovery of unreacted starting material suggested that greater yields may be achieved by increasing the efficiency of the reaction. We identified two key steps of the reaction that were likely responsible for the low yields: the iron-catalysed oxidation and the terminating chlorination.

To gain insight into the reaction, the progression was monitored over time (Figure 3.7). This was achieved by taking aliquots from the reaction and passing the samples through a silica plug in order to remove the iron catalyst. The samples were then analysed by quantitative ^{1}H NMR. From visual analysis, it appeared that the results at t = 3 were anomalous and were not included in the analysis. However, the data point is presented for completeness.

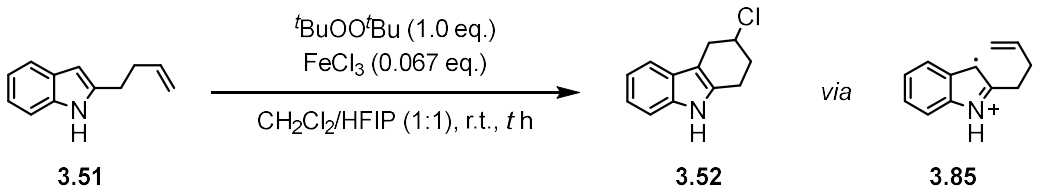
The first thing this study demonstrated was that the reaction proceeded slowly. This had been inferred from the low yields and consistent presence of starting material in the crude reaction mixtures of 18-hour reactions, but those results could also have been seen in a reaction that occurred by rapid but incomplete conversion.

The slow accumulation of product observed in the monitored reaction showed that the limited conversion was due to slow initiation of the oxidation cascade, indicating a need for more forcing conditions or longer reaction time.

The second finding was that the loss of material proceeded at a comparable rate to product formation. After 7 hours, nearly 50% of the starting material had been converted into unknown and undesired side-products. This loss of material may have resulted from undesired reactivity of the radical cation **3.85** or any of the subsequent intermediates, or from instability of the product in the reaction conditions. It was unknown which of these was more impactful, although given the low yield and high

conversion early in the progression (9% and 29% respectively) it seemed likely it was not solely a stability issue.

The combination of these two factors (slow production and rapid decomposition) meant that simply reducing reaction time to limit decomposition would not work. Instead, it was necessary to slow the decomposition and increase the efficiency of the transformation itself. To this end, variation of the reaction conditions and components was undertaken to better understand their roles in both of these factors.



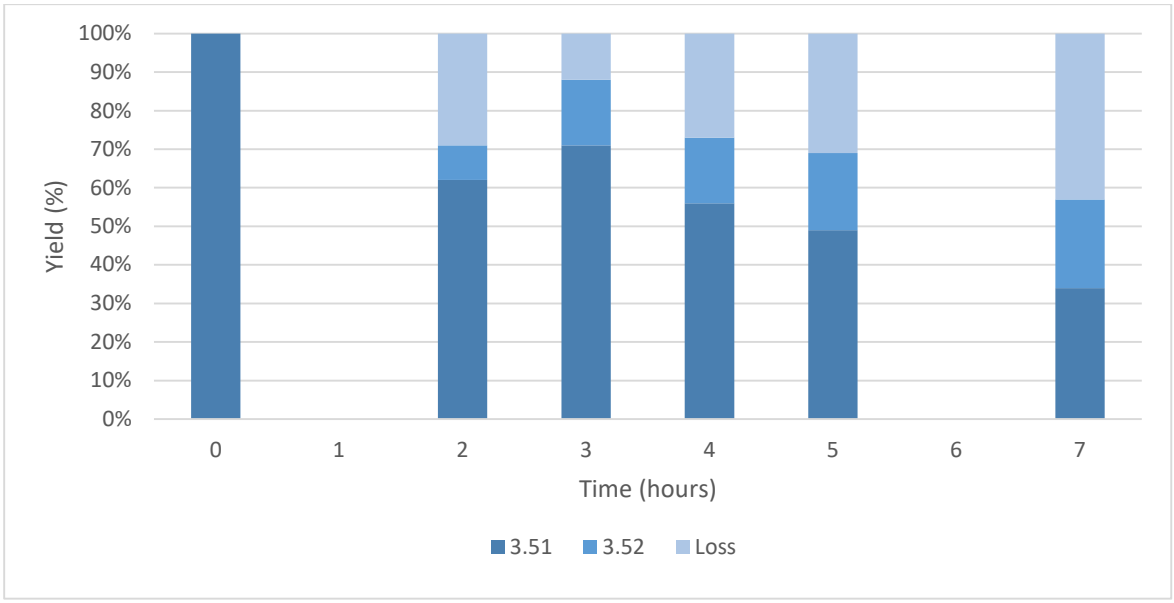


Figure 3.7. Time-monitoring study of the oxidative cyclisation of **3.51**. 0.1 mL aliquots were taken at *t* = 0, 2, 3, 4, 5, and 7 h. Conversions and yields were measured by quantitative ^{1}H NMR spectroscopy against trimethoxybenzene (0.74 eq.).

Given the obvious role the iron catalyst played in the oxidation (the likely cause of both reactivity and decomposition) and the potential role it played as the chloride source, it seemed prudent to focus on it as an avenue to improve the reaction.

Thus, a screen of catalyst loadings was undertaken (Table 3.1).

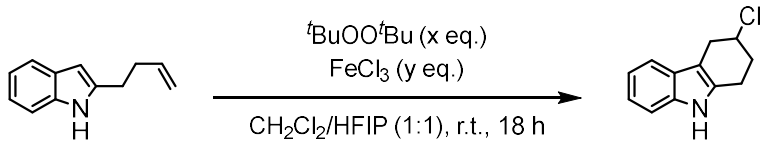
As expected, removal of the iron catalyst led to no product formation, and the starting material was recovered unchanged (Entry 1). Halving the catalyst loading to 3.3% (Entry 2) gave an incredibly reduced yield of 5%, consistent with a slower product formation caused by less catalyst. It also spoke to the role of iron-catalysed oxidation in the decomposition, as the starting material was recovered in a significantly higher quantity (61%).

Doubling the catalyst loading to 13.3% (Entry 4) did lead to a higher conversion of 76%, but the yield was unfortunately lower than the standard reaction (Entry 3). More of the material decomposed under the reaction conditions, with only 24% starting material recovered, confirming the iron's role in the side-reactions causing loss of yield. This was reenforced by an even higher catalyst loading of 26.7% (Entry 5) leading to similar yield and almost no starting material recovery (5%).

Even further, 100% catalyst loading led to an intractable mixture, from which no species could be identified – neither **3.51** nor **3.52** were observed in the crude reaction mixture (Entry 6).

However, maintaining this loading without the DTBP (the co-oxidant) was better tolerated (Entry 7). By restricting the turnover of the iron catalyst and using it as a stoichiometric oxidant, a yield of 15% was achieved. This showed the Fe(III)/Fe(II) couple was also capable of promoting the reaction, as was the case when a similar experiment was run with naphthol homocoupling by the group at the inception of the cross-coupling.[91] Given the lower yield for the Fe(III)/Fe(II) system, it's likely that in the presence of DTBP the reaction proceeds *via* Fe(IV).

This screen confirmed that the original catalyst loading was the best option – the lower loadings led to slower reactivity and thus lower yield, and the higher than original loadings lead to more decomposition and thus also lower yield.

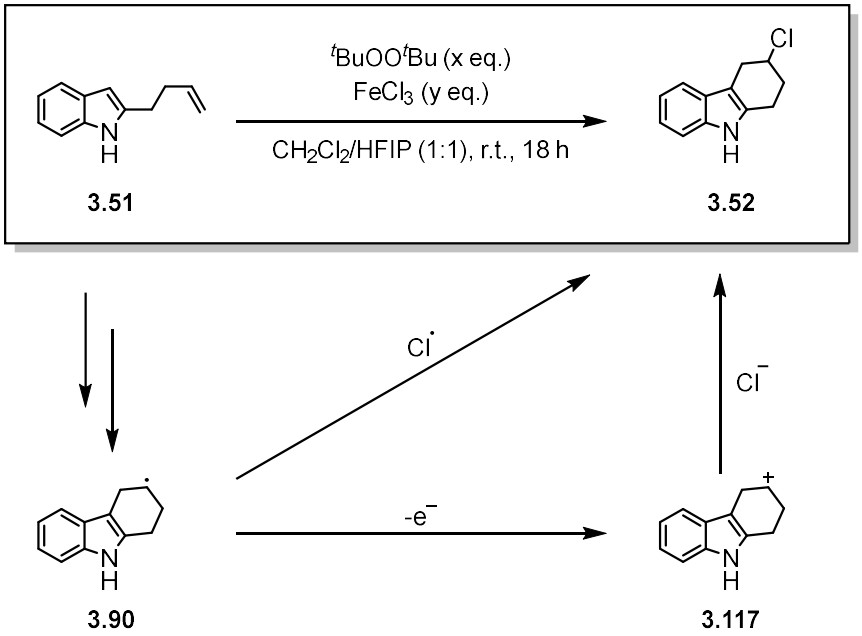


3.51 3.52

Entry	$FeCl_3$ / mol%	DTBP / eq.	Conversion / %	Yield / %
1	0	1.0	3	-
2	3.3	1.0	39	5
3	6.7	1.0	62	32[a]
4	13.3	1.0	76	21
5	26.7	1.0	95	21
6	100.0	1.0	100	-
7	100.0	0	60	15

Table 3.1. Results of varying the equivalents of $FeCl_3$ in the reaction. Entry 3 is data from a previous experiment (Scheme 3.9) included as a reference. Conversions and yields were measured by quantitative ^1H NMR spectroscopy against trimethoxybenzene (0.074 eq.) unless otherwise stated. [a] Isolated yield

Our understanding of the termination step of this reaction was limited, and it was unknown whether the chlorination was a one- or two-electron process i.e. whether it occurred by chloride radical abstraction or by oxidation to the cation and nucleophilic attack of a chloride anion (Scheme 3.29).



Scheme 3.29. Possible routes from **3.90** to **3.51**

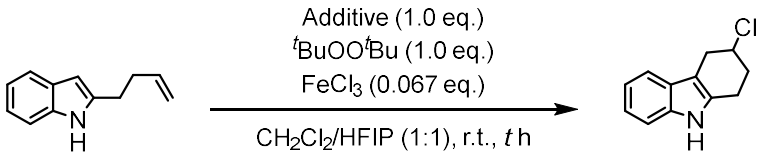
Therefore, both types of additive were trialled in the hopes that increasing the efficiency of the trapping would have led to increased yields and less material lost (Table 3.2).

The addition of two different external chloride sources (Entry 1 and Entry 2) led to almost identical outcomes: a large drop in yield and a slight increase in starting material recovery. Entry 2 was repeated with a longer reaction time, as the increase in starting material recovery suggested the rate of reaction had decreased. However, even a three-fold increase only had a marginal effect on the yield. The negative impact on the yield caused by the ionic additives implied a quenching of reactivity, considering the plateau reached in the extended trial.

Tetrahalomethanes were chosen as chlorine radical sources, as their structural similarity to dichloromethane was reasoned to prevent any unwanted interference in the reaction other than in the desired trapping step. They would also be better halogen donors than dichloromethane, due to the increased stability of the resultant trihalomethyl radicals.

Tetrachloromethane (Entry 4) caused a decrease in both the yield and recovered starting material. Bromotrichloromethane (Entry 5) led to similar yield of the chlorinated product **3.52** as Entry 4, and

lower quantity of **3.51** recovered. However, the reaction was far less clean than Entry 4, and the NMR spectrum of the crude reaction mixture had a number of peaks consistent with a trace (less than 5%) amount of the brominated analogue of **3.52**. Although this could not be isolated, it would suggest that it was possible for **3.90**, the intermediate cyclohexyl radical, to abstract halogens as the termination of the reaction. But without any further confirmation, this was not able to be conclusively proved.



3.51 **3.52**

Entry	Additive	Time / h	Conversion / %	Yield / %
1	NH_4Cl	18	54	12
2	LiCl	18	54	10
3	LiCl	72	58	14
4	CCl_4	18	68	14
5	$CBrCl_3$	18	97	18[a]

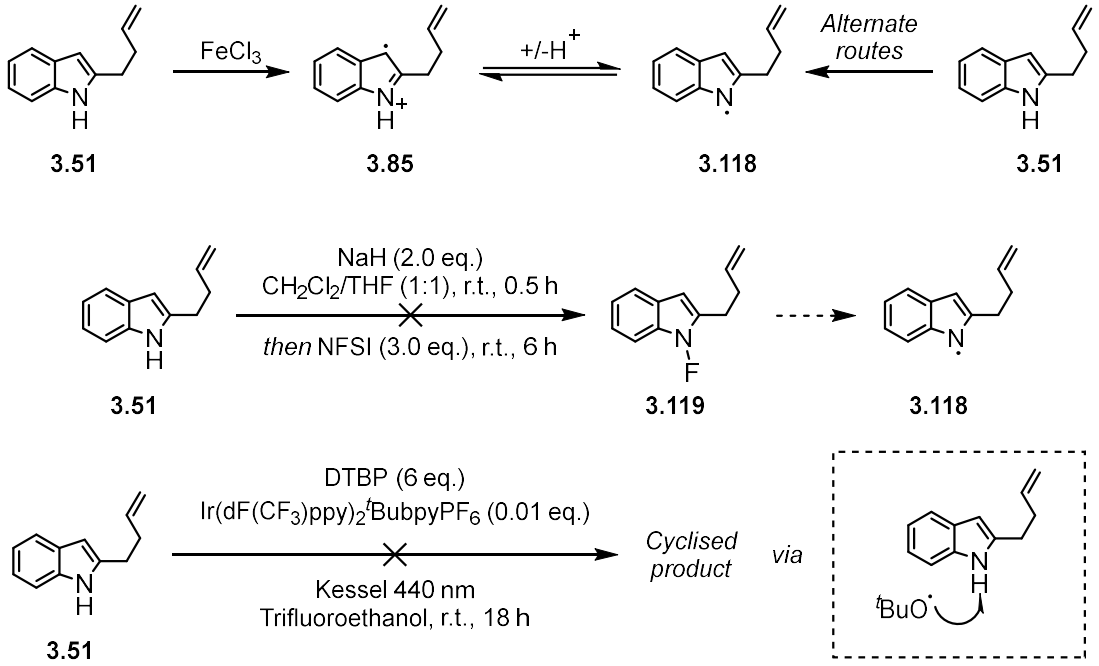
Table 3.2. Inclusion of various chloride sources in the oxidative cyclisation. Conversions and yields were measured by quantitative ^{1}H NMR spectroscopy against trimethoxybenzene (0.074 eq.). [a] A trace amount of what appeared to be the brominated product was also observed.

We decided to try alternative approaches to form an indole radical in order to better understand the cyclisation, with the aim to study the termination step in the absence of $FeCl_3$ (Scheme 3.30). Both methods seek to form the N-centred radical **3.118** rather than the radical cation **3.85** proposed for the iron-catalysed reaction. This was not seen as an issue, as **3.118** is simply the protonated form of **3.85** so interconversion to the active form should be facile in a mechanism that already relies on proton exchange.

The first approach was *via* a homolysis of a nitrogen-halogen bond. By fluorinating the indole and then breaking the N—F bond in a Hofmann-Löffler-Freytag-type reaction, it was envisaged that the resultant

indole radical would undergo an identical cyclisation-rearrangement cascade to the iron-generated radical. Unfortunately, attempts to synthesise **3.119** were unsuccessful.

The second approach was to promote tert-butoxyl radical formation from the DTBP already present in the reaction mixture, with the idea that it may abstract the indole nitrogen proton.[107] The DTBP would be excited by triplet energy transfer from an excited iridium photocatalyst, as reported by Stahl and coworkers.[108] Only starting material was recovered from this reaction, showing that this was not an effective method of generating the desired indole radical.



Scheme 3.30 Alternative approaches to N-centred radical generation to access the unprotonated neutral radical **3.118**.

3.10 Conclusion

At this point, it was decided that we had sufficiently explored the reactivity of the indole radical cation generation. We had been unable to increase the yield above that of the starting result, despite variation of many of the parameters. The reaction showed little generality, with no other substrates demonstrating production of the cyclised product and no ability to vary the termination (chlorination) step.

If interest in this reactivity were renewed, there are a small collection of possible avenues to continue.

The most important next step would be to understand and control the final trapping step – by finding a source chlorine or other group that can trap the reactive intermediate rapidly, it would be possible to avoid material loss and to diversify the products formed.

Modification of the indole itself rather than the alkenyl trap may also lead to higher yields, by tuning the electronics of the oxidation and the stability of the resulting radical cation.

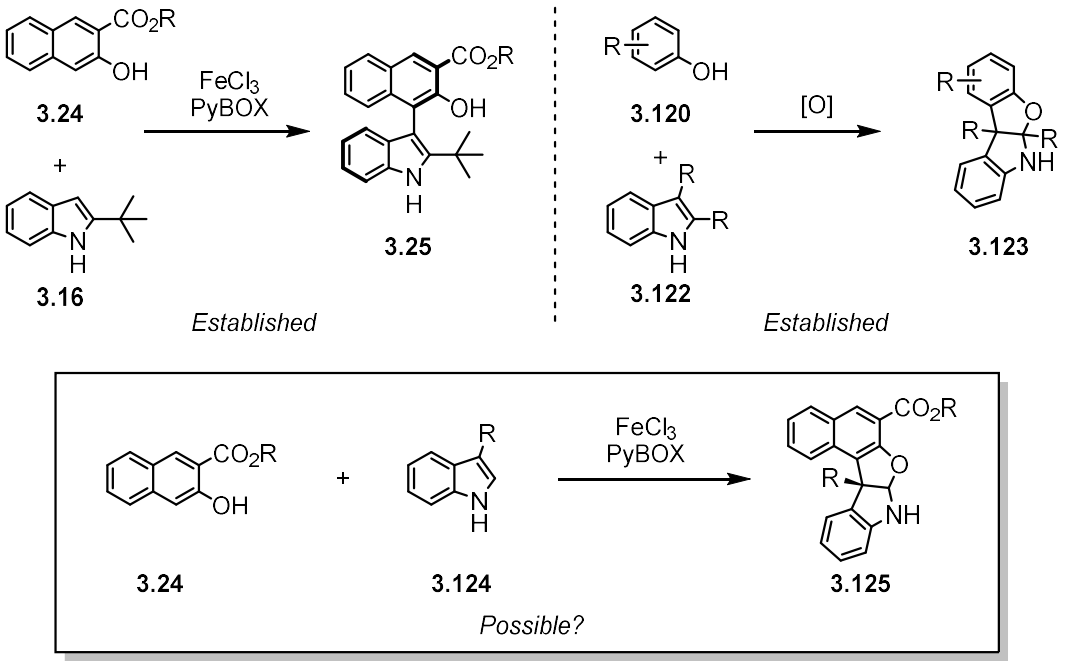
Exploration of other iron sources could also lead to increasing the efficiency of the oxidation as well as affecting the final trapping step. Iron(III) chloride was used only because it was able to facilitate the cross coupling this reaction derived from, but others may well be capable of oxidising indoles that were ineffective for the oxidation of naphthols.

Chapter 6: Synthesis of Naphthofuroindolines

3.11 Introduction to Benzofuroindolines

Having concluded the investigation into the indole oxidation, our attention returned to the cross-coupling reaction. The understood mechanism for the coupling (Scheme 3.12) raised the possibility that, as well as the biaryl formation, other products may be accessible with the methodology. In particular, naphthofuro[2,3-b]indolines (**3.125**).

The original development of the iron-catalysed oxidative system was grounded in reported syntheses of benzofuroindoline systems. There is a large body of research into the oxidative reactions of indoles and phenols, and they are well-known to result in the cyclised (**3.123**) rather than biaryl (**3.25**) product. The switch in reactivity was achieved by modification of the indole substitution pattern to position sterically bulky groups at the C-2 position to favour the biaryl. It was reasoned that this selectivity could be reversed by reverting this change of substitution pattern. This would supply the naphthofuroindoline rather than 3-naphthylindole product and allow for the possibility of their synthesis enantioselectively with the novel ligand system developed.



Scheme 3.31. Proposal for the enantioselective synthesis of naphthofuro[2,3-b]indolines (**3.125**) using the oxidative cross-coupling system developed for biaryl coupling

These naphthofuroindoline products would be examples of a wider class of molecule: benzofuroindolines (Figure 3.8). More specifically, **3.125** is an example of a benzofuro[2,3-b]indoline, the basic structure of which is seen in **3.126**, and will hereafter be referred to simply as benzofuroindolines unless otherwise stated. The synthesis of benzofuroindolines has been described by a number of groups, in large part driven by work towards a selection of natural product targets such as Diazonamide A and Azonazine.[109,110]

Many approaches mimic the route taken to the structure in nature – an oxidative coupling between an indole and a phenol.[111] Reactions following this route can also give rise to the [3,2-b] fused ring system **3.127** (Figure 3.8).[112]

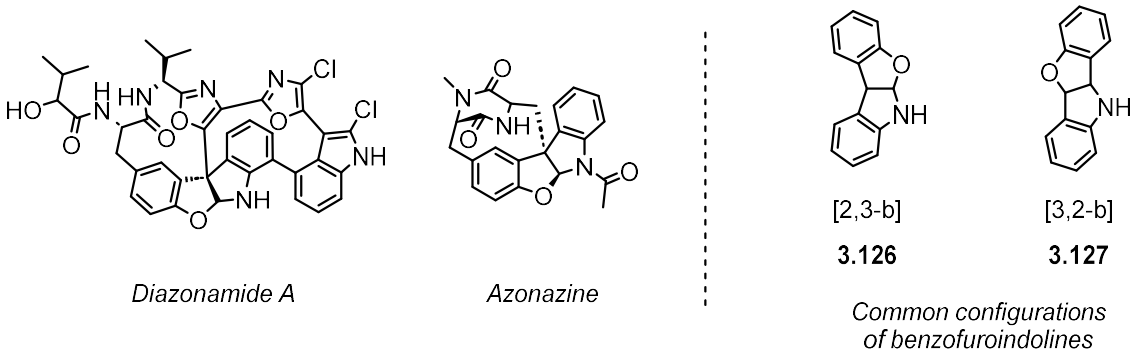
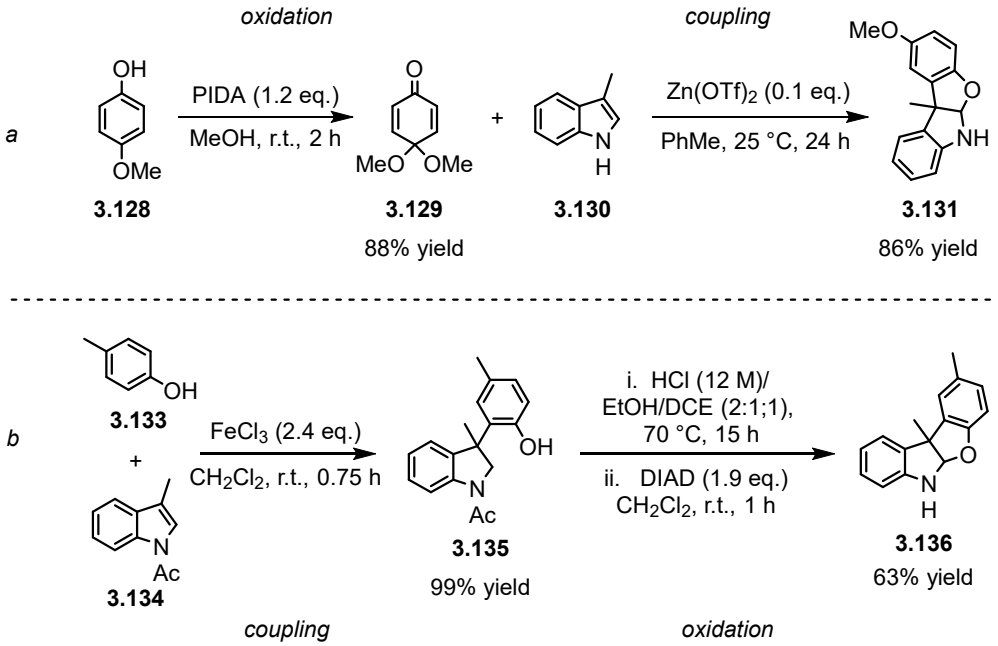


Figure 3.8. Benzofuroindolines as a scaffold

This oxidative coupling can easily be achieved in multistep processes. By separating the oxidation and the coupling into two discrete steps, the reaction is easier to predict and control.

Initial oxidation of the phenol to quinones allowed Zhang and coworkers to synthesise a range of 2-alkoxybenzofuroindolines in a neutral nucleophilic attack (Scheme 3.32a).[113] The order of the oxidation and coupling steps may be reversed, as in the route described by Vincent and coworkers (Scheme 3.32b).[114] A Friedel-Crafts-type attack of phenol **3.133** onto an iron-bound N-acetylindole **3.134** affords the C-3 quaternary indoline **3.135** in 99% yield. Bidentate iron binding to the N-acetyl group and the C-2 position in the indole enabled the umpolung chemistry observed. Hydrolysis of the acetyl

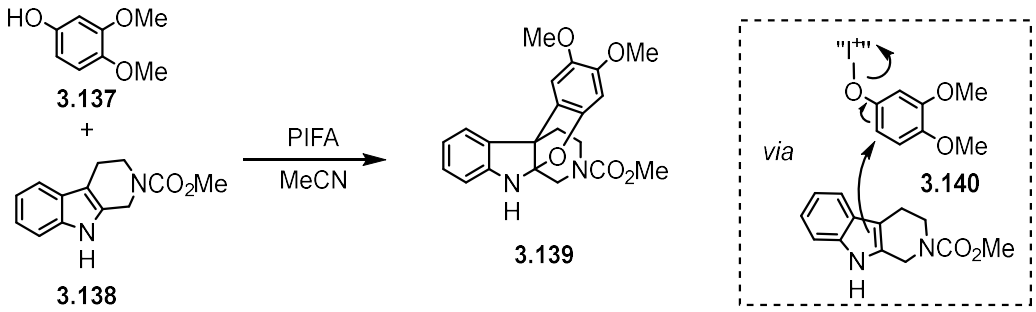
protecting group followed by oxidation of the indoline to an imine with DIAD enabled the cyclisation of the phenol hydroxyl group, affording the desired benzofuroindoline in a 63% yield.



Scheme 3.32. Two step oxidation/coupling routes to benzofuroindolines. Reaction conditions: a: The reaction conditions were as described with **3.130** (1.0 eq.) and **3.129** (1.5 eq.). b: The reaction conditions were as described with **3.133** (2.2 eq.) and **3.134** (1.0 eq.).

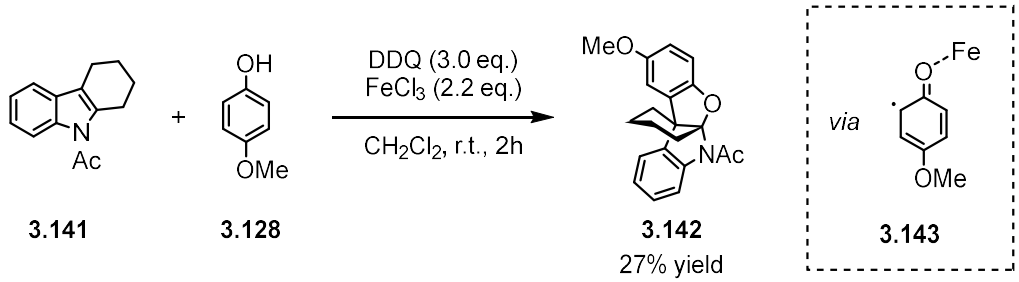
A more direct route to the structure is the combination of indoles and phenols in one-step oxidative cross-couplings. This is typically achieved by the oxidation of a phenol, followed by a nucleophilic attack by the indole. A diverse selection of oxidation conditions has been reported.

The earliest methods developed utilised hypervalent iodine as the oxidant (Scheme 3.33).[115] Rather than quinone formation, this formed an O-iodinated species **3.140** from which the hypervalent iodine can act as a leaving group. This reversed the reactivity of the phenol from a C-2 nucleophile to a C-2 electrophile.



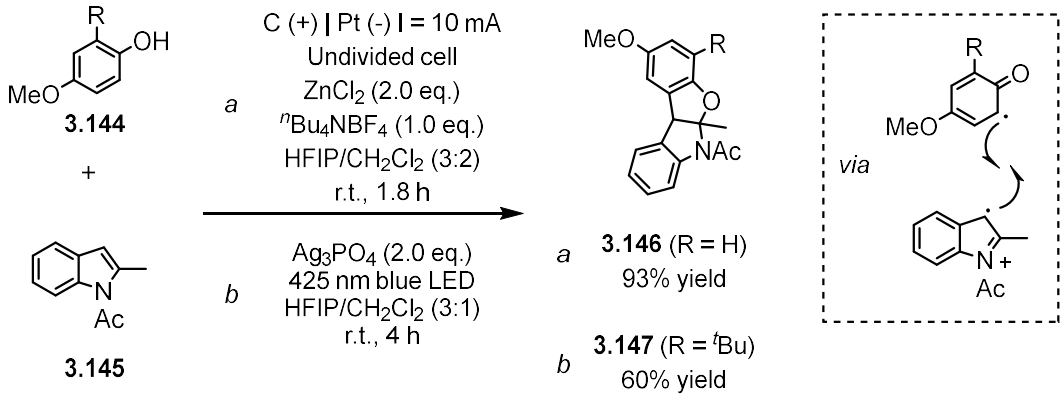
Scheme 3.33. Oxidation of phenolic hydroxy group allows for indole attack and cyclisation to **3.139**. Reaction conditions not given.

Another route is the use of transition metal oxidants. Vincent and coworkers showed that an iron catalyst with a stoichiometric oxidant can effect a single electron oxidation of the phenol coupling partner, leading to the iron-stabilised radical species **3.143**.[116] The use of an N-acetyl protecting group on the indoles led to a strong preference for the [3,2-b] isomer (Figure 3.8, **3.127**) in most substrates, but a handful of benzofuro[2,3-b]indolines were produced.



Scheme 3.34. Oxidative synthesis of **3.142** from **3.141** and **3.128**, catalysed by $FeCl_3$. The reaction conditions were as stated with **3.128** (1.0 eq.) and **3.141** (3.2 eq.)

Lei and coworkers demonstrated an electrochemical approach to the coupling (Scheme 3.35a).[117] It was proposed that this occurred by oxidation of both **3.144** and **3.145** at the anode of the cell, followed by radical-radical combination and cyclisation into the iminium. A photochemical oxidation with visible light was described by Wang and coworkers with a similar mode of action (Scheme 3.35b).[118] Irradiation of silver phosphate nanoparticles led to the formation of electron/hole pairs on the surface. The holes were highly oxidising and able to remove electrons from both the phenol and indole species. The radicals generated reacted in a manner similar to those in the electrochemical approach.

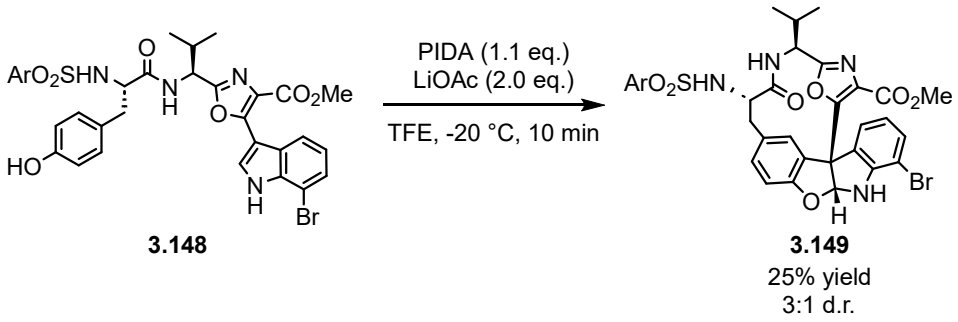


Scheme 3.35. Single electron oxidation of the indole and phenol component, followed by radical-radical combination. a) The reaction conditions were as stated with **3.144** (1.0 eq.) and **3.145** (1.5 eq.) b) The reaction conditions were as stated with **3.144** (1.0 eq.) and **3.145** (2.0 eq.)

In both cases, production of the benzofuro[2,3-b]indolines was limited to 2- and 2,3-substituted indoles; 2-H indoles instead formed the [3,2-b] structure. As previously discussed in Section 3.6, the radical character of indole radical cations is situated mostly at the C-3 position. However, the regioselectivity this imparts is not absolute, and so indoles with more steric bulk at the C-3 position will react at C-2 instead.

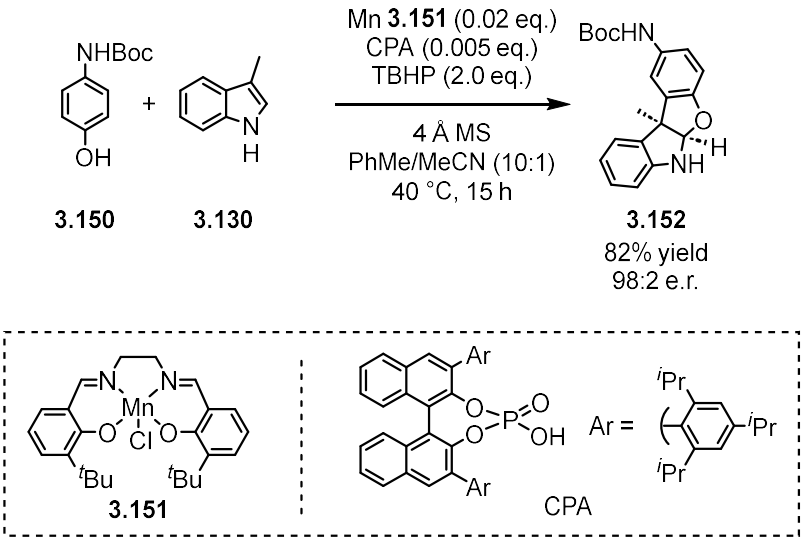
Despite this wide selection of routes, there are only two reports of one-step stereoselective oxidative syntheses of benzofuroindolines.

One of the oldest accounts of oxidative benzofuroindoline coupling is from Harran and coworkers, in an enantioselective synthesis of (−)-Diazonamide A (Scheme 3.36).[109] It made use of a symmetric hypervalent iodine oxidant to perform the oxidative coupling, and the asymmetric environment derived instead from the chiral starting material. Therefore, although it preferentially formed one enantiomer of the benzofuroindoline core, it is better understood as a diastereoselective reaction. It was also only moderately selective, with a d.r. of approximately 3:1.



Scheme 3.36. Diastereoselective intramolecular coupling of **3.148** in the synthesis of (−)-Diazonamide A.

The only enantioselective oxidative synthesis of benzofuroindolines was performed by Zhong and coworkers (Scheme 3.37).[119] This was achieved by the one pot cascade of oxidation of an N-Boc-4-aminophenol to the quinone monoimine by a manganese/*t*-butyl peroxide system, followed by an enantioselective nucleophilic attack of the indole controlled by a chiral phosphoric acid.



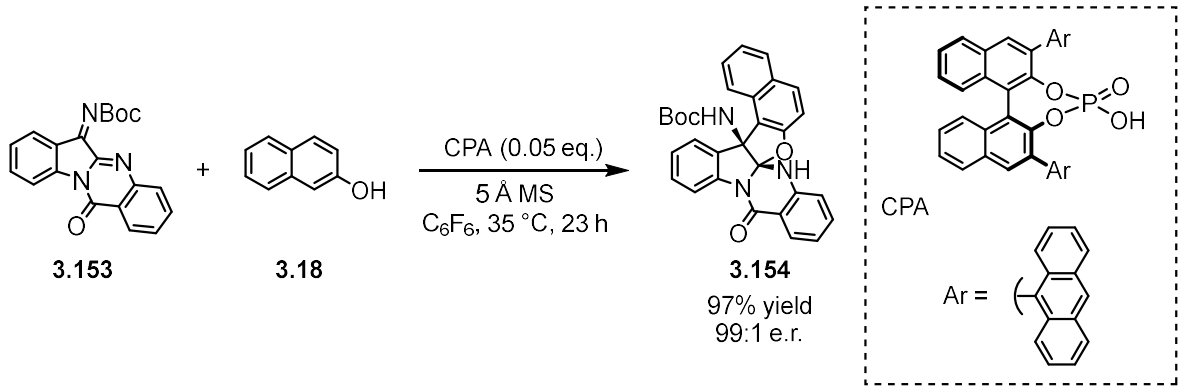
Scheme 3.37. Enantioselective synthesis of **3.152** *via* an oxidation/coupling cascade. The reaction conditions are as stated with **3.150** (1.0 eq.) and **3.130** (2.0 eq.)

Enantioselective quinone/indole couplings such as these are well-known, but this remains the sole example where the oxidation to the quinone and the coupling happen in tandem.[120] There are no examples of a one-step enantioselective oxidative coupling between indoles and phenols.

3.12 Introduction to Naphthofuroindolines

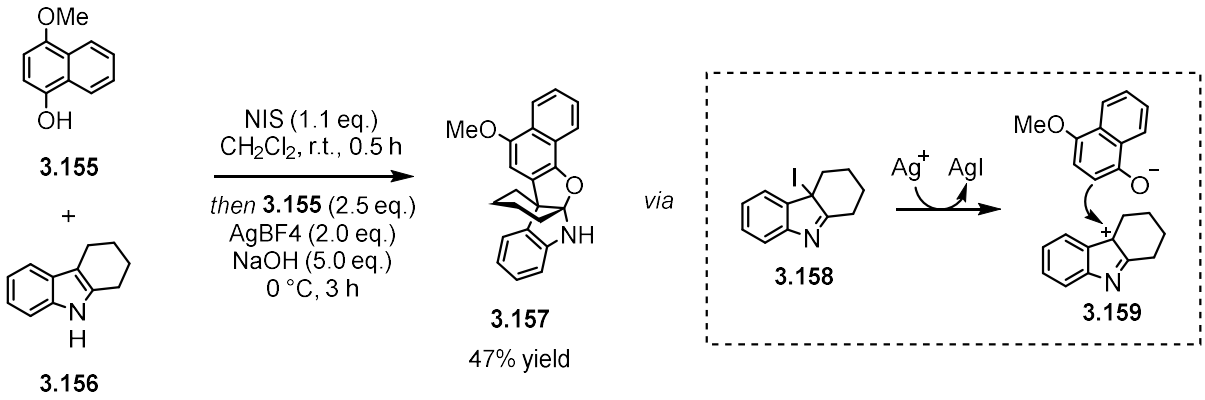
As a subset of benzofuroindolines, naphthofuroindolines are less well explored. In fact, there are only two previous examples of the synthesis of naphthofuro[2,3-b]indolines.

Yuan and coworkers developed an approach with the intention of generating diverse tryptanthrin derivatives (Scheme 3.38), with the naphthofuroindoline motif an incidental product of the reagents chosen. [121] The transformation relied on the oxidised nature of the tryptanthrin (**3.153**) scaffold to facilitate a nucleophilic attack by 2-naphthol **3.18**, followed by the attack of the hydroxyl group into an imine exocyclic to the "indole" of interest. This was a very high yielding reaction and impressively enantioselective, but was wholly substrate-specific.



Scheme 3.38. Neutral coupling of tryptanthrin (**3.153**) and 2-naphthols (**3.18**). The reaction conditions are as stated with **3.153** (1.0 eq.) and **3.18** (1.2 eq.)

The other example is a single entry in the scope of an oxidative coupling of a phenols and indoles in the synthesis of a benzofuroindolines, also by Vincent and coworkers (Scheme 3.39).[111] The reaction was another example of a one-pot oxidation/coupling cascade. In it, the indole was oxidised to **3.158** and the iodide abstracted by a silver salt to produce the cationic **3.159**. Attack by **3.155** formed the carbon-carbon bond. Unfortunately, the reactivity was limited to *para*-methoxy phenols (and thus 1-napthol) and was fairly low yielding, in part due to the uncontrolled reactivity of **3.159** producing a suite of side-products.



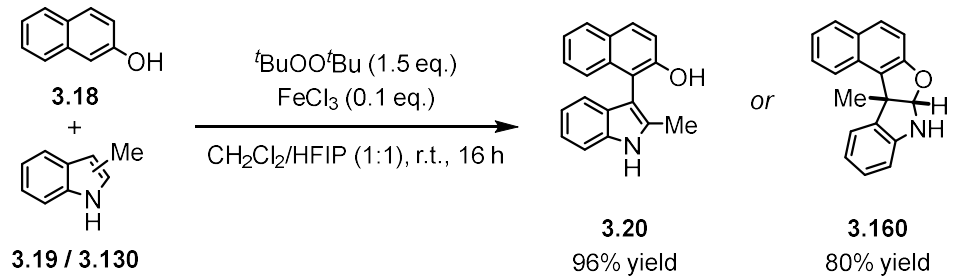
Scheme 3.39. Oxidative coupling of **3.155** and **3.156.** The reaction conditions are as stated with **3.155** (2.5 eq.) and **3.156** (1.0 eq.)

As it stood, there were no general approaches to the synthesis of naphthofuro[2,3-b]indolines. A widely applicable oxidative methodology to the naphthofuro[2,3-b]indoline core in line with the one found for the biaryl cross-coupling would be unique in that regard.

The prospect of utilising the known iron-catalysed biaryl cross-coupling to give access to an enantioselective oxidative coupling of indoles and 2-naphthols to naphthofuroindolines, as a representative of benzofuroindolines more generally, would signify an advance on two related fronts.

3.13 Exploration of the Racemic Reaction

As suspected, a simple change of substitution pattern on the indole radically changed the final product of the cross-coupling (Scheme 3.40). By performing the simplest version of the known cross-coupling reaction (2-naphthol **3.18** and anhydrous iron(III) chloride) and switching to 3-methylindole (**3.130**), the relevant *cis*-fused naphthofuroindoline **3.160** was produced in an 80% yield with no BINOL formation.



Scheme 3.40. Iron-catalysed cross-couplings of naphthol and methylindoles demonstrating the variation in product with a minor substitution change. The reactions conditions are as stated with **3.18** (1.0 eq.) and **3.19/3.130** (1.5 eq.)

Variation of both coupling partners was important in order to understand the roles both of these played in the reactivity. Indole variation focused on the substituent at the C-3 position, as the proximity of the C-3 substituent to the key bond formed in the cross-coupling meant that its variation would likely have a significant impact of the reaction. It would also lead to a more diverse set of products with a variety of groups adjacent to the central quaternary centre – a challenging proposition. Naphthol variation, meanwhile, mainly consisted of more distant modifications with the intent to modulate the electronic properties, as this type of variety was well-tolerated in the biaryl cross-coupling. Attempts to deviate from simple 2-naphthols as the phenolic coupling partner were also envisaged.

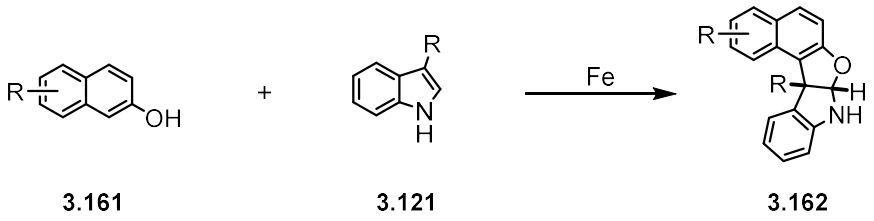
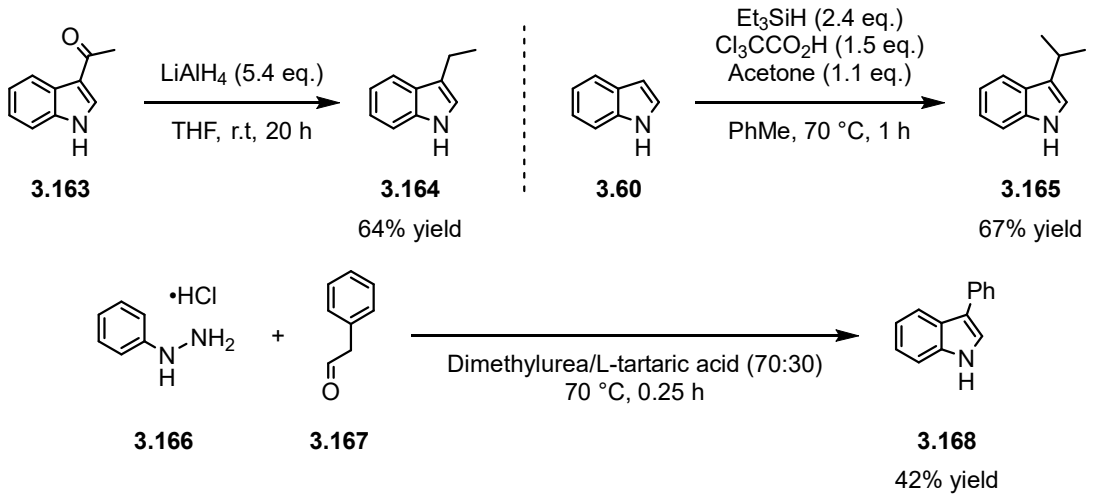


Figure 3.41. Avenues of variation planned for the substrates

A wide range of 3-substituted indoles were available commercially and, as the synthesis of indoles is a well-trodden area of chemistry, access to the few that were not was simple (Scheme 3.42). Reduction of **3.163** gave 3-ethylindole (**3.164**) in a 64% yield, and reductive alkylation of indole with acetone gave **3.60** in 67% yield. **3.168** was accessed by a Fischer indole synthesis in a 42% yield.



Scheme 3.42. Synthesis of 3-substituted indoles. Synthesis of **3.168**: Reaction conditions as described with **3.166** (1.0 eq.) and **3.167** (1.0 eq.).

A diverse group of 3- and 2,3-substituted indoles were subjected to the cross-coupling conditions with 2-naphthol (Figure 3.9).

Simple alkyl groups (**3.171** to **3.175**) were well tolerated. As seen previously (Scheme 3.40), 3-methylindole gave exclusively the cross-coupled product **3.171** in good yield. Increasing the steric bulk to ethyl reduced the yield (**3.172**), and naphthol homocoupling (forming BINOL **3.182**) began to compete with heterocoupling. Increasing the bulk further to isopropyl (**3.173**) brought the yield down further to 27%, and the yield of BINOL increased to the point that it was the major product of the reaction (at 54%). Despite this trend indicating that less hindered indoles were more proficient, 3-H indole did not form the unsubstituted naphthofuroindoline (**3.170**), nor did it revert to the biaryl reactivity – instead, only decomposition products were observed.

2,3-Dimethyl indole (**3.174**), although lower yielding than 3-methyl, was still productive and showed no competitive BINOL formation. Surprisingly, tetrahydrocarbazole (**3.175**) was the most effective coupling partner, despite its apparent larger steric bulk than 2,3-dimethyl. An aryl substituent (**3.176**) was unproductive, with only BINOL found. Sidechains containing heteroatoms were not tolerated (**3.177** to **3.181**). Acetic acid derivative **3.178** was unproductive, as were the ethyl ester (**3.179**) and the nitrile analogue (**3.177**). This was put down to the withdrawing effects of these group reducing the nucleophilicity of the indole, solely leading to the homocoupled BINOL product.

Neither Boc-protected tryptamine (**3.180**) nor melatonin (**3.181**) were tolerated. These did not possess strongly withdrawing groups and so should not have been subject to the deactivation that was observed in **3.177**, **3.178**, and **3.179**. In fact, the methoxy group of the melatonin should enhance the nucleophilicity of the indole. The reason for the failure of these substrates may simply be that the long sidechains and large protecting groups were effective at hindering the nucleophilic attack.

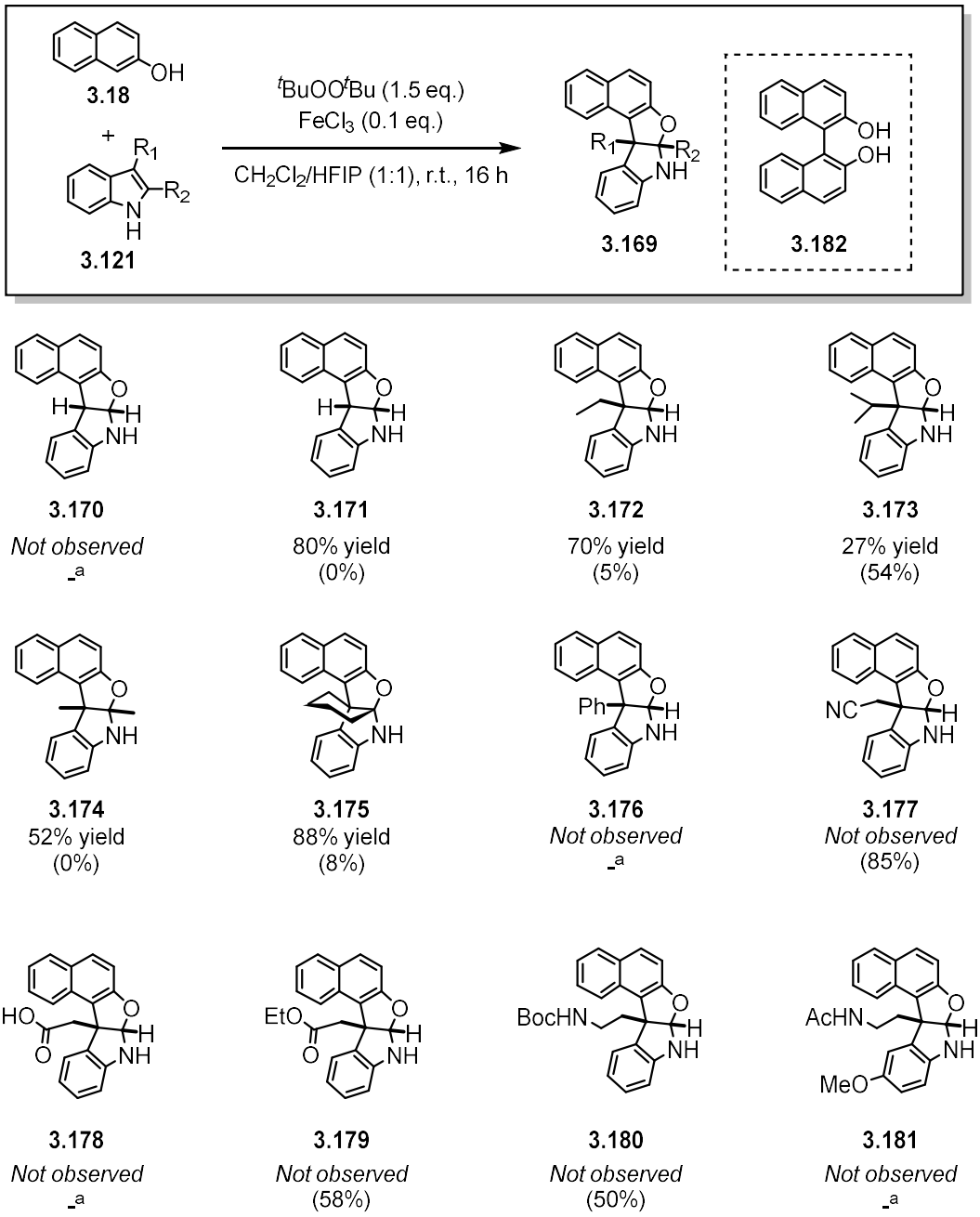
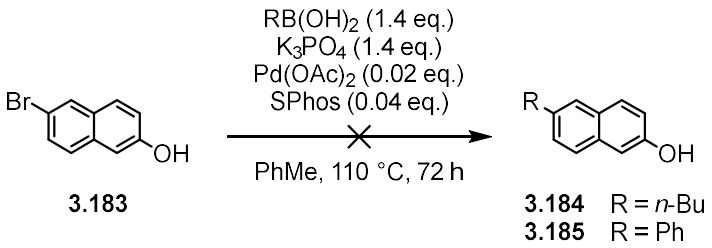


Figure 3.9. Scope of 3-substituted indoles in the oxidative cross-coupling. The reactions conditions are as stated with **3.18** (1.0 eq.) and indoles (1.5 eq.). Figure in brackets refers to the yield of BINOL recovered measured by quantitative ^{1}H NMR spectroscopy against trimethoxybenzene (0.06 eq.). [a] Not determined

Both 6- and 7-functionalised 2-napthols are readily available with a range of functional groups. Two attempts (Scheme 3.43) at modifying **3.183** *via* palladium-catalysed cross-couplings were unsuccessful, and so the scope focused on commercially available substrates.



3.183

3.184 R = *n*-Bu
3.185 R = Ph

Scheme 3.43. Attempted palladium-catalysed cross-couplings of **3.183** to produce alternate 6-substituted 2-naphthols.

Although tetrahydrocarbazole (**3.156**) was the best performing indole in the previous scope, naphthols were evaluated with both it and 3-methylindole (**3.130**) (Figure 3.10). This was because it was unclear what was causing the unintuitively high yields with **3.156**, and the possibility of misrepresenting the more generic reaction with a specific outlier was a concern. **3.130** was chosen, as it was both the simplest substrate and also well-performing.

In fact, tetrahydrocarbazole also had consistently higher yields across the range of naphthols.

6- and 7-bromonnaphthols (**3.191** and **3.192**) were the best partners, with yields of 76% and 61% respectively with **3.156**. Their couplings with methylindole (**3.193** and **3.194**) were less successful, with lower yields of 56% and 17% and moderate BINOL formation (16% and 27%), something which was not seen with the nonbrominated naphthol.

6- and 7- methoxynaphthol were less broadly tolerated. With the 3-methylindole, both produced the heterocoupled product in poor yield. **3.156** again showed more success, although to lesser degree than with the brominated naphthols. **3.193** was produced in a 30% yield, only marginally higher than the methylindole. **3.194** was the only methoxynaphthol product observed in a moderate yield, at 56%. Lower yields of the heterocoupled products with the more nucleophilic methoxynaphthols presumably originated from increased naphthol interception of the naphthoxy radical, leading to competitive

homocoupling. Although no 1,1'-BINOLs could be identified in the reactions with methoxynaphthols, this does not contradict the explanation for low yields. Instead, that is likely due to lower regioselectivity of the homocoupling caused by opposing directing influences from the methoxy and hydroxy groups leading to a mixture of BINOL-type biaryls rather than a single population. This would make 1,1'-BINOLs statistically less likely and individual identification challenging.

6-cyanonaphthols were inactive under the reaction conditions, producing no naphthofuroindolines (**3.190** and **3.195**) or BINOLs. The withdrawing nature of the group likely impeded oxidation of the naphthol, preventing coupling, as was seen with 3-cyanonaphthols in the biaryl coupling (Figure 3.5).

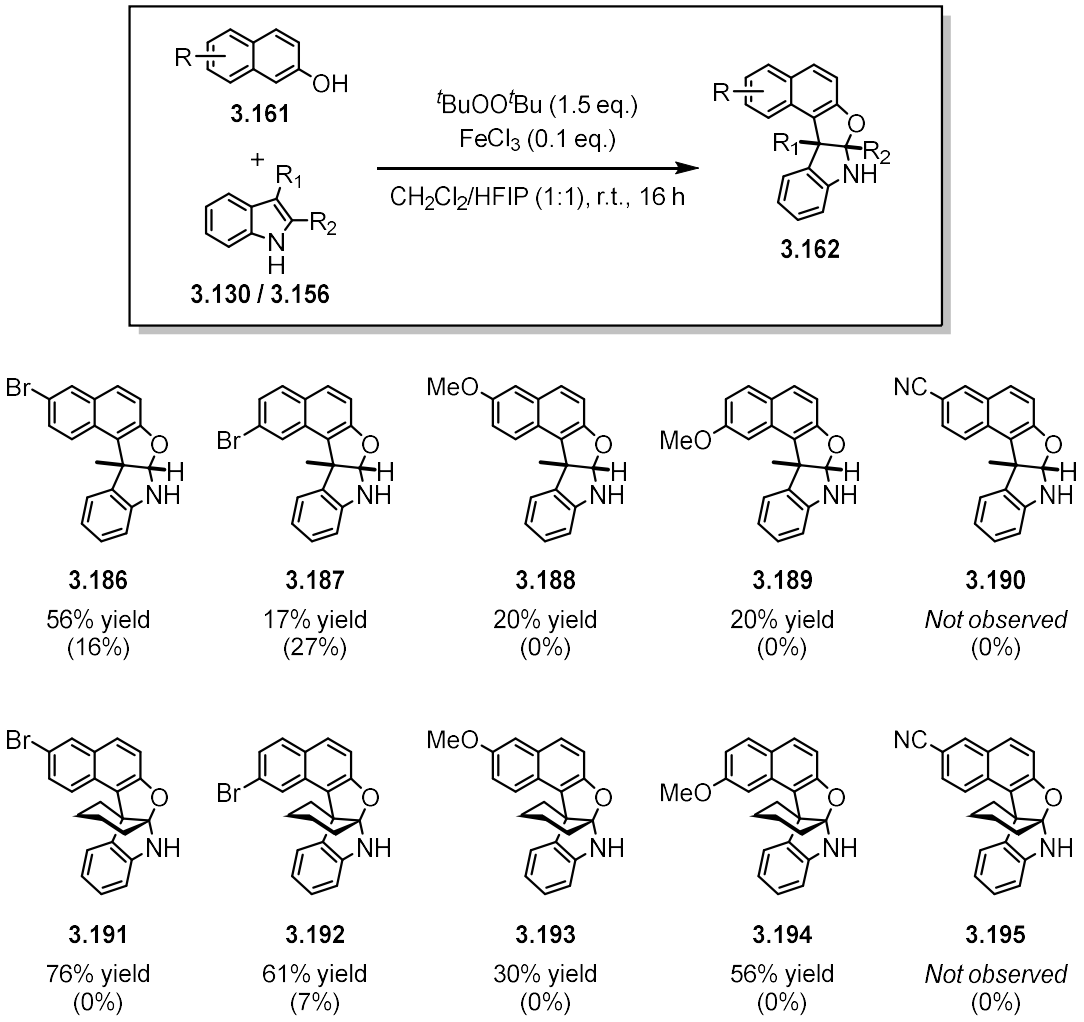


Figure 3.10. Scope of 6- and 7-substituted 2-naphthols in the oxidative cross-coupling. The reactions conditions are as stated with naphthols (1.0 eq.) and indoles (1.5 eq.). Figure in brackets refers to the yield of the relevant 1,1'-BINOL derivative recovered measured by quantitative ^{1}H NMR spectroscopy against trimethoxybenzene (0.06 eq.).

Because the original purpose for the cross-coupling was the synthesis of atropisomeric biaryls, the methodology was optimised for the use of 2-naphthol and its derivatives as the phenolic component, as they provide the geometry necessary to confer restricted rotation around the biaryl bond. However, the naphthofuroindolines synthesised by this route do not rely on restricted rotation, so it would be of interest to attempt the expansion of this new mode of reactivity to phenols. (Figure 3.11)

However, no benzofuroindoline products were observed in any of these cases. The activity of two phenols in the oxidation conditions were tested by deliberate attempts to synthesise the relevant biphenols (**3.204** and **3.205**), but this was also unsuccessful – no coupling products or starting materials were observed, only decomposition of the phenols.

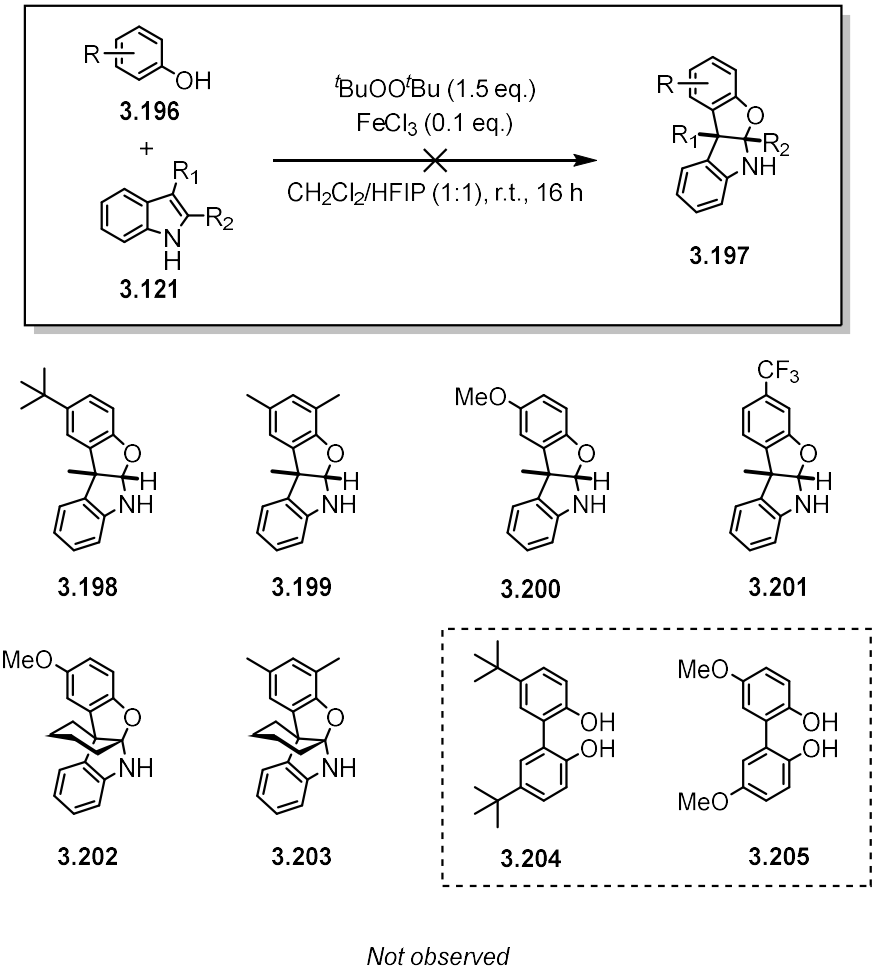


Figure 3.11. Intolerance of phenols in the oxidative cross-coupling. The reactions conditions are as stated with phenols (1.0 eq.) and indoles (1.5 eq.).

3.14 Mechanistic Proposal

These explorations of the coupling demonstrate that the ability of the $FeCl_3$/DTBP system to effectively facilitate the oxidative coupling of 3-indoles and 2-naphthols to synthesise naphthofuroindolines. However, the fact that it is the same oxidative system does not guarantee that this new reactivity proceeds *via* the same mechanism, as was clearly demonstrated by the oxidative indole cyclisations in the previous chapter.

The question of which coupling partner is oxidised and which acts as the nucleophile (or indeed if they are both oxidised) within this manifold was therefore re-addressed.

The oxidation potentials of a selection of tolerated indole substrates were measured with Square Wave voltammetry (Figure 3.12). Although it has become clear that comparing oxidation potentials between the two dissimilar reaction partners to evaluate rate and ease of oxidation can be misleading, it stands to reason that these factors are more strongly correlated in substrates that play the same role in the reaction. The oxidation potentials of the indoles only loosely correlate with the yields of the naphthofuroindoline products. In fact, **3.130** and **3.165** had almost identical oxidation potentials but drastically different yields. Given the difference in steric bulk between a methyl and an isopropyl group, this suggests that steric hinderance around the C-3 position has a larger impact than oxidation potential.

This is consistent with the naphthol-oxidation mechanism proposed for the biaryl coupling. Increased steric bulk of the C-3 position would hinder nucleophilic attack of the indole on the naphthoxy radical leading to decrease yield of the heterocoupled product. This also explains the increase in BINOL side-product observed with the more hindered indoles, as decreased nucleophilicity means that naphthol is competitive in trapping the naphthoxy radical.

The high yield achieved with **3.156** seem to go against this conclusion – the saturated 6-membered ring of **3.156** is certainly larger than the sole methyl group of **3.130**. This can be explained by two

observations. Firstly, the tethering effect of the ring limits available conformations and reduces the effective size when compared to substrates like 3-ethylindole (**3.164)**.

Secondly, the increased substitution of the indole increases the electron density, as seen by the oxidation potentials. **3.156** has an oxidation potential of 0.57 V vs. Ag/AgCl, much lower than that of **3.130** (0.74 V vs. Ag/AgCl). The electrons of **3.156** are far more accessible and less tightly held, and so **3.156** is expected to be more nucleophilic.

With this in mind, the similarity in yield between **3.130** and **3.156** despite the significant disparity in oxidation potentials reaffirms the relative unimportance of oxidation potential in determining yields.

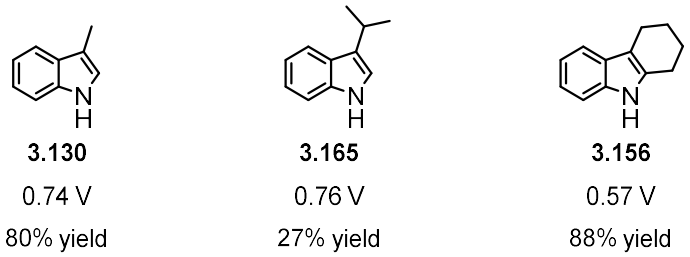
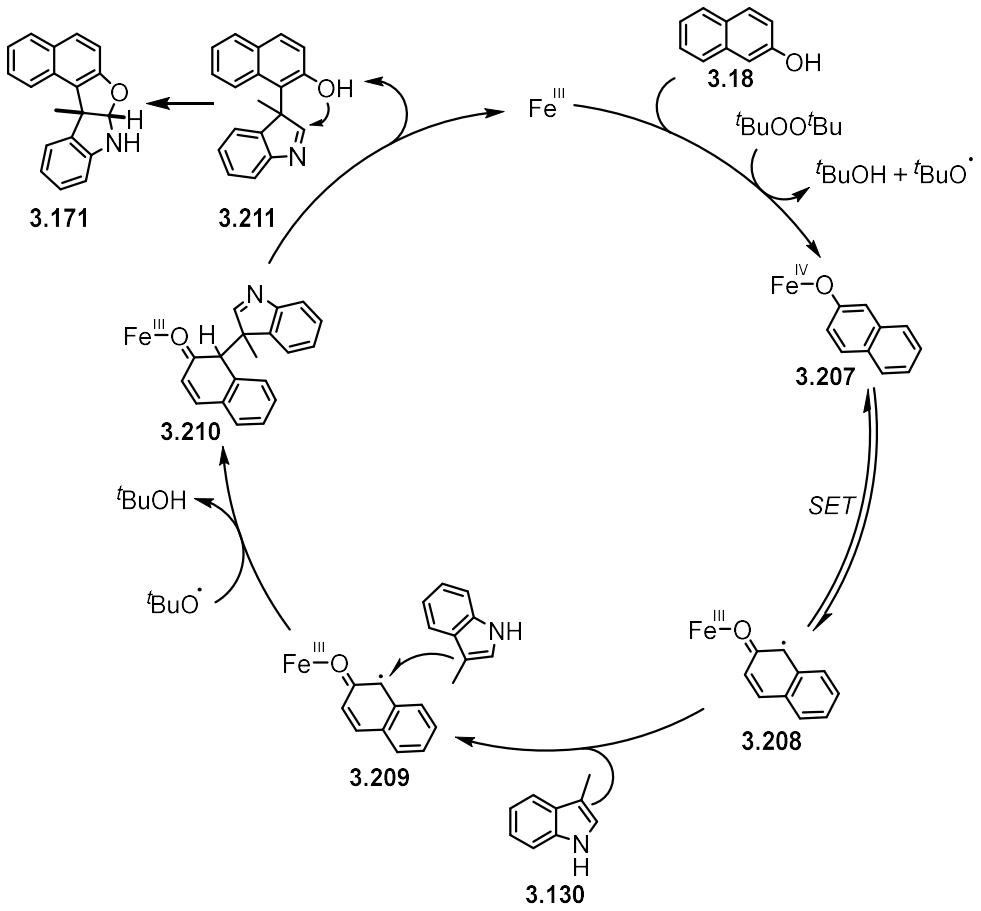


Figure 3.12. Measured oxidation potentials of 3-substituted indoles. The yields refer to the yields of the cross-coupling with 2-naphthol, as described in fig **3.9**

The mechanism, therefore, was determined to be analogous to the proposed mechanism of the biaryl synthesis (Scheme 3.44). Ligation of **3.18** to the iron allowed for rapid SET oxidation to the naphthoxy radical **3.207**. Attack by **3.130** and hydrogen atom abstract by a tertbutoxy radical leads to **3.210**. It is at this point that the mechanisms of the biaryl and naphthofuroindoline syntheses diverge. The substituent at the C-3 position prevents rearomatisation of the indole, meaning that the biaryl axis is not formed. Furthermore, the hydroxy group of the naphthol can cyclise into the imine of **3.211**, forming the pentacyclic structure of the naphthofuroindoline.



Scheme 3.44. Mechanism of the oxidative coupling in the synthesis of naphthofuroindolines from naphthols and 3-substituted indoles.

Unfortunately, as noted in Scheme 3.28, efforts to utilise indoles with intramolecular radical trapping probes positioned on the C-3 position were unsuccessful, and so it was not possible to interrogate this proposition more directly.

3.15 Racemic Couplings with Naphthoates.

The problem of competing BINOL formation that arises from additional steric bulk on the indole was not unique to the naphthofuroindoline synthesis; the same relationship was observed in the development of the biaryl coupling. The solution found was to transition from 2-naphthols to 2-hydroxy-3-naphthoates (such as **3.22**). The inclusion of the withdrawing ester group dramatically decreased the nucleophilicity of the naphthol coupling partner, reducing the rate of homocoupling and returning the reaction to perfect chemoselectivity.

This solution applied to the new reaction, and so many of the indole-naphthol cross-coupling reactions were repeated, replacing **3.18** with **3.22** (Figure 3.13). However, this change dramatically impacted the reactivity, with indoles that were previously productive no longer generating the cross-coupled products. No naphthofuroindoline products were observed for any of the indoles used except **3.156,** to give a trace amount of **3.219** that was observed in the crude reaction mixture.

The reasoning behind this reduction in reactivity was unclear, as the change to **3.22** had significantly increased the yields in the biaryl coupling (Scheme 3.5). It cannot have been due to ineffective oxidation of the naphthoate, and so it must have affected the nucleophilic attack by the indole.

With the change to naphthoates failing to remedy the chemoselectivity issues observed with sterically challenging indoles, it was decided that these were the limit of reactivity possible in the cross-coupling.

This was still a very powerful transformation, given the highly congested nature of the sidechain location in the product (adjacent to a quaternary centre in the centre of the molecule), and the bulk directly inhibiting the key carbon-carbon bond formation.

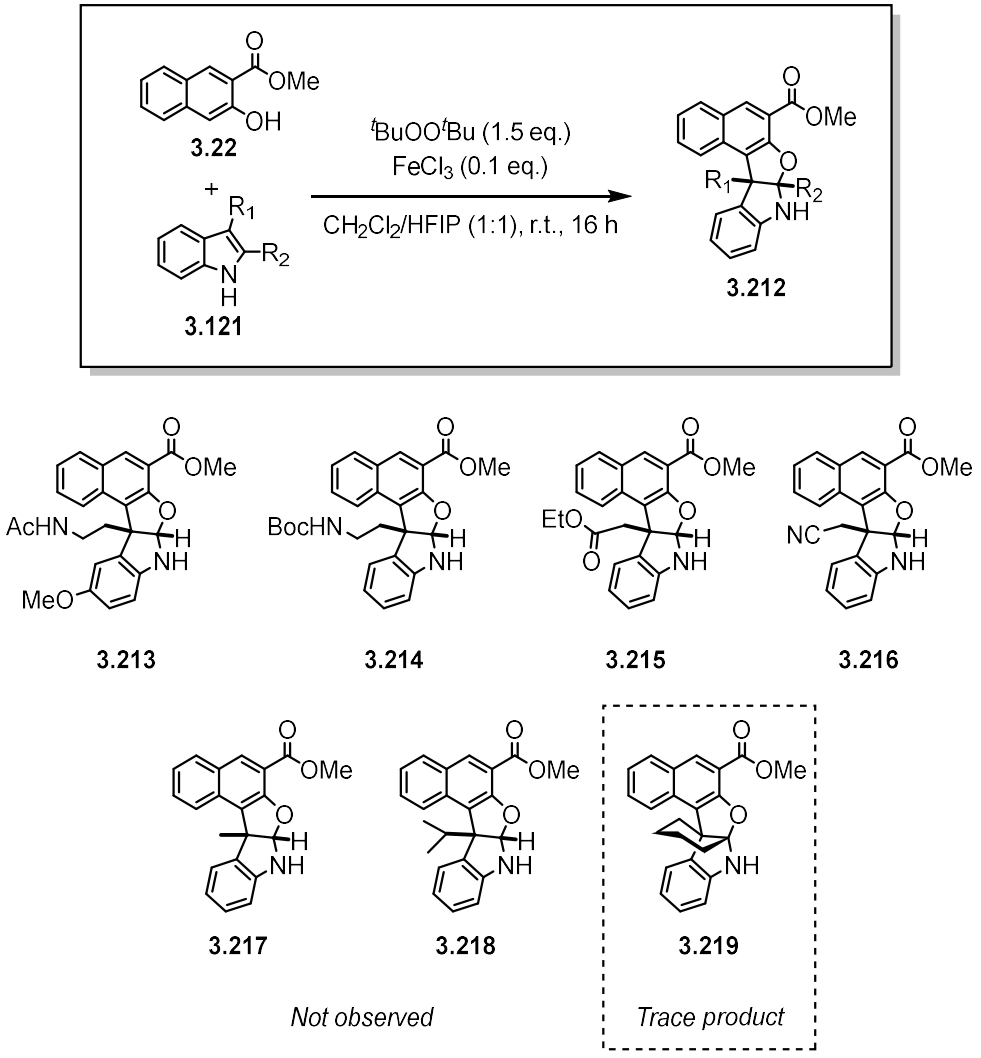


Figure 3.13. Attempts to include an ester group into the naphthoate was not successful.

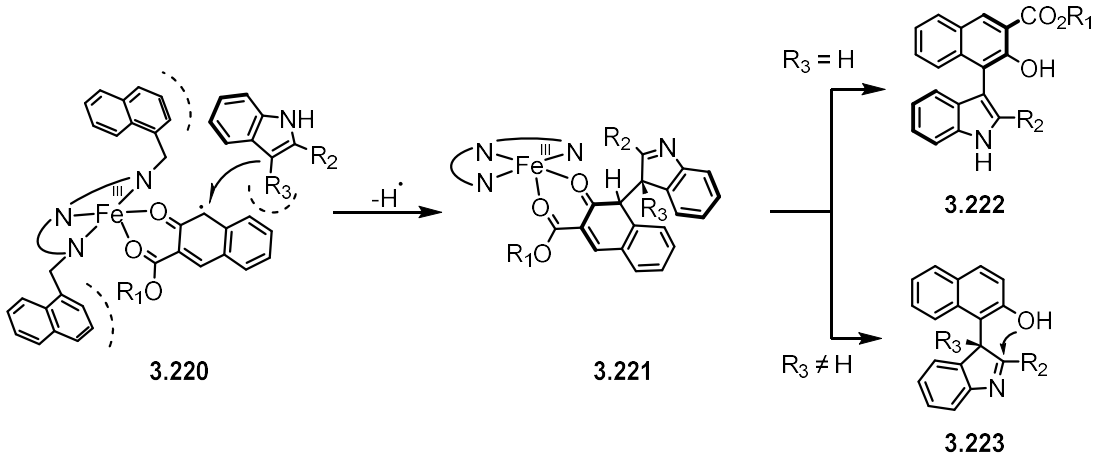
3.16 Enantioselective Cross-Coupling

Focus shifted to combining this methodology for the synthesis of racemic naphthofuroindolines with the known methodology responsible for the stereocontrol in the synthesis of atropisomeric biaryls, in order to induce enantioselectivity in the naphthofuroindoline synthesis. It was thought that the equivalent changes to the reaction system that lead from racemic to enantioselective biaryl formation could lead to enantioselectivity in the naphthofuroindoline case.

As discussed previously (Scheme 3.12), the stereochemistry of the biaryl formed in the cross-coupling is determined by two main factors: the point chirality generated in the indole attack (controlled by the geometry around a rigid ligand-iron-naphthoate complex), and the point-to-axial chirality transfer upon rearomatisation (Scheme 3.45).

The naphthofuroindoline coupling mechanism diverges from the biaryl coupling at the rearomatisation step, after the stereochemistry has been set by the initial attack (**3.220**). The cyclisation step (**3.223**) is stereospecific and has no impact on the quaternary chiral centre at the indole C-3 position. It stands to reason that if the geometry of the attack by the 3-substituted indoles can be controlled in the same way as the 2-substituted indoles then the reaction can be accomplished enantioselectively.

However, the control of the attack is achieved by the conflict between the indole and the PyBOX ligand blocking groups creating a favoured direction and arrangement for the attack. By changing the substitution pattern of the indole and thus the direction the bulky substituent protrudes, it may be that the interactions between 3-substituted indoles and the PyBOX ligand are less well-matched to produce enantioselectivity.



Scheme 3.45. Applicability of the stereoinducing step to the synthesis of naphthofuroindolines.

The differences between the symmetric and asymmetric methodologies are not limited to the inclusion of a PyBOX ligand. To ensure effective complexation with the ligand, the iron source was changed to iron(III) chloride hexahydrate and sonicated for 30 minutes in dichloroethane (replacing dichloromethane). The iron suspension was then pre-stirred with the PyBOX ligand for a further 2 hours, before the coupling partners are added. The reaction time was also doubled to 48 hours.

The presence of the ester group has been shown to have a large impact on the enantioselectivity of the biaryl coupling. However, the work on the racemic reaction showed 3-substituted indoles were

unreactive with naphthoates. Therefore, initial trials of the asymmetric conditions utilised 2-naphthol (**3.18**) as a confirmation of reactivity (Figure 3.14).

Trialling indoles **3.130** and **3.156** under these conditions showed the expected results: successful cross-coupling but no stereocontrol, although the yields were notably lower. **3.171** was produced in a 56% yield, compared with the 80% yield in the symmetric reaction. The use of **3.156** showed an even larger drop-off to a 31% yield of **3.174** (down from 88%). Both samples were more or less racemic: **3.171** had an e.r. of 50:50, while **3.174** had an e.r. of 52:48.

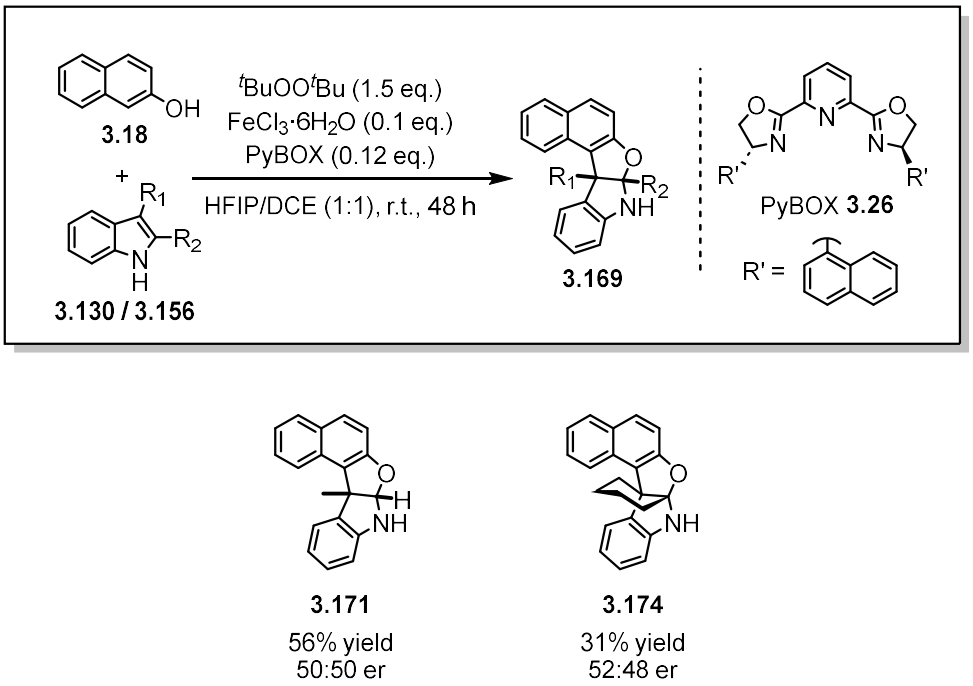


Figure 3.14. Subjection of **3.18** and 3-substituted indoles to the enantioselective conditions, utilising **3.26** as the chiral ligand. The reaction conditions are as described with **3.18** (1.0 eq.) and indoles (1.5 eq.). Yields were measured by quantitative ^{1}H NMR spectroscopy against trimethoxybenzene (0.06 eq.). e.r.s determined by chiral HPLC.

This showed that synthesis of naphthofuroindolines was possible under the enantioselective conditions, but also reinforced the need for the ester directing group in order to achieve enantioselectivity.

The reactions were repeated with a naphthoate coupling partner (Figure 3.15). Despite a lack of reactivity between these reagents in the racemic conditions, inclusion of a ligand facilitated cross-coupling; **3.224** was found in a 54% yield and **3.225** in a 31% yield. Excitingly, the products generated

were no longer racemic, with **3.224** found in an e.r. of 73:27, and **3.225** in an e.r. of 84:16. Such high enantioselectivities before optimisation was a very promising result.

However, this success did not carry over for other indoles. Neither **3.226** nor **3.227** were produced, with the reactions returning only starting materials.

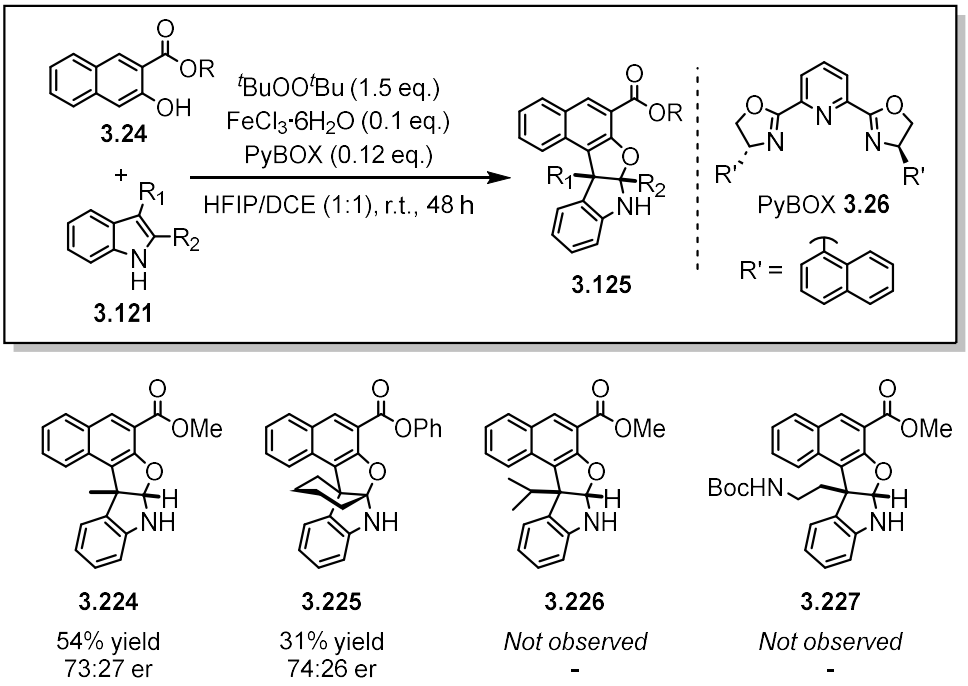


Figure 3.15. Subjection of 2-hydroxy-3-naphthoates and 3-substituted indoles to the enantioselective conditions, utilising **3.26** as the chiral ligand. The reaction conditions are as described with naphthoates (1.0 eq.) and indoles (1.5 eq.). e.r.s determined by chiral HPLC.

Given the drastic change in which phenolic coupling partners were tolerated by the reaction upon the switch to enantioselective conditions, two of the previously unsuccessful phenols were reevaluated (Figure 3.16).

Once again, the phenols did not undergo any coupling reactions, either cross-coupling to form the benzofuroindolines or homocoupling to form the biphenol side-products.

Methyl salicylate was also included in the attempts (**3.230)**, as it shares structurally similarities with the naphthoate substrates (**3.24**). The ortho-ester was proposed to bind to the iron in an analogous fashion to the naphthoates, potentially enabling it to mimic their reactivity. Unfortunately, this was not the case, and no coupling products were observed.

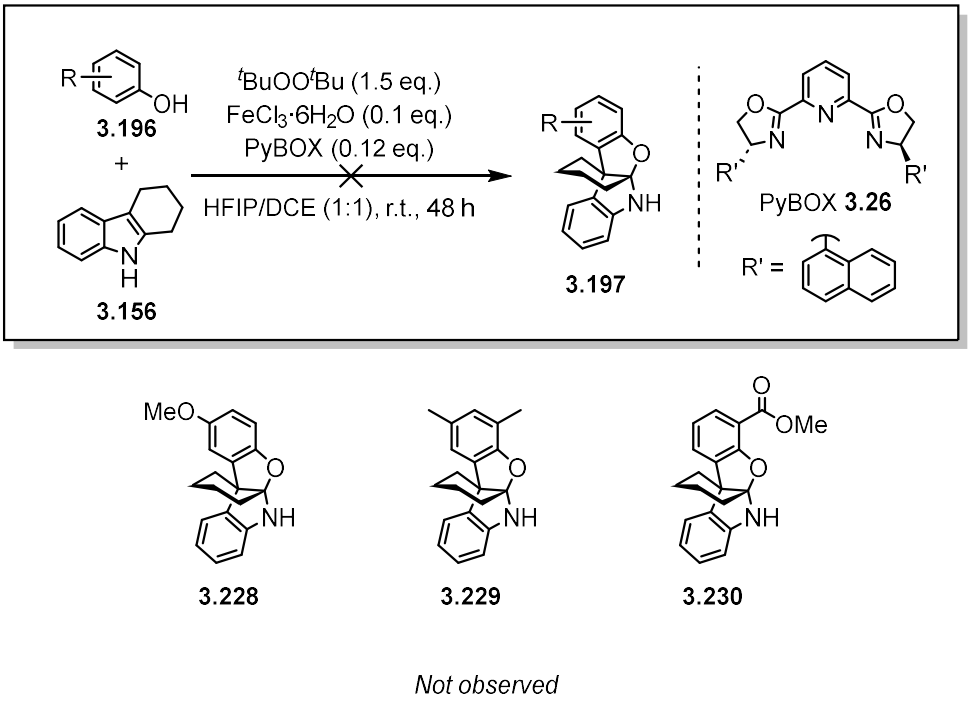


Figure 3.16. Subjection of phenols and **3.156** to the enantioselective conditions, utilising **3.26** as the chiral ligand. The reaction conditions are as described with phenols (1.0 eq.) and **3.156** (1.5 eq.).

3.17 Optimisation of the Enantioselective Reaction

The first approach investigated in an attempt to increase the enantioselectivity was a screen of a selection of PyBOX ligands (Table 3.3). Fortunately, a large number had been synthesised by Dr Surgenor and Dr Liu for the investigation of the biaryl coupling, providing access to a large library.

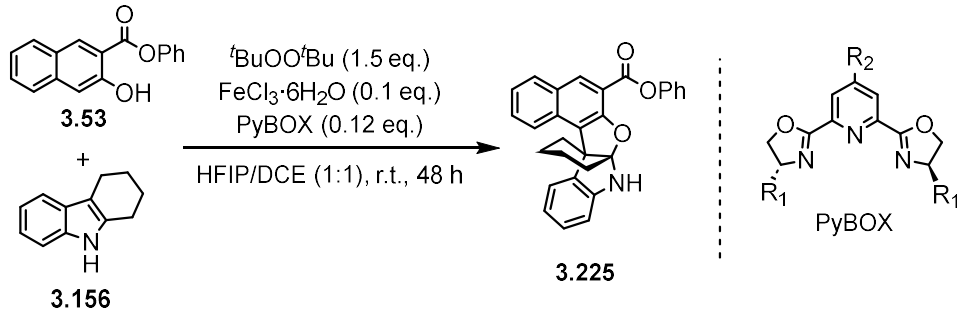
By using the results from the biaryl coupling screen, we were able narrow down our exploration to a selection of diverse ligands that had previously shown good activity in the cross-coupling.

To establish a baseline for comparison, the R_1 = H achiral PyBOX ligand (Entry 1) was also included in the screen, giving a low yield and racemic product.

Variation of R_2 by the inclusion of a methoxy group on the pyridine backbone while maintaining the naphthyl sidechain (Entry 3) led to a significant decrease in yield with minimal e.r. improvement.

Increasing the size of the R_1 polycycle to pyrene (Entry 4) had very little impact on yield or selectivity. However, decreasing the size to the phenyl (Entry 5) was less successful, with a dramatically lower yield of 20%, although the selectivity was maintained.

Adjusting the electronics of the R_1 group was investigated. Fluorination of the phenyl group (Entry 6) was higher yielding but similarly selective to Entry 5. Switching to chlorine (Entry 7) increased the yield further, up to 68% and also increased the selectivity, with an e.r. of 90:10. Even better was a methoxy group (Entry 8), with a yield of 77% and the best e.r. observed of 92:8.



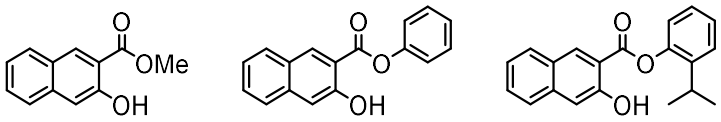
Entry	R_1 =	R_2 =	Yield / %	e.r.
1	H	H	44	50:50
2	2-Naphthalene	H	61	84:16
3	2-Naphthalene	OMe	35	85:15
4	Pyrene	H	61	83:17
5	Ph	H	20	84:16
6	*p*-C_6H_4F	H	39	85:15
7	*p*-C_6H_4Cl	H	68	90:10
8	*p*-C_6H_4OMe	H	77	92:8

Table 3.3. Screening of a library of PyBOX ligands. The reaction conditions are as described with **3.53** (1.0 eq.) and **3.156** (1.5 eq.). e.r.s determined by chiral HPLC. Yields were measured by quantitative ^{1}H NMR spectroscopy against dimethyl terephthalate (0.04 eq.).

With a promising PyBOX ligand candidate in hand, the next step was to further optimise the reaction conditions around it. It was necessary to embark upon a synthesis of the ligand, in order to have enough material to hand. Fortunately, a synthetic route to PyBOX was known from the original synthesis, and a slight alteration provided material for the continuation of the investigation. (For details, see Appendix A).

It was shown in the biaryl cross-coupling investigation that the identity of the ester of the naphthoate had a significant effect on the yield and selectivity – in fact, the best naphthoate substrate found was the 2-isopropylphenyl ester (**3.231**).

All previous reactions involving 2-hydroxy-3-napthoates have utilised the methyl (**3.22**) and phenyl (**3.53**) esters. **3.22** is commercially available, and **3.53** had been synthesised in large quantities previously, and thus supplies were ample.

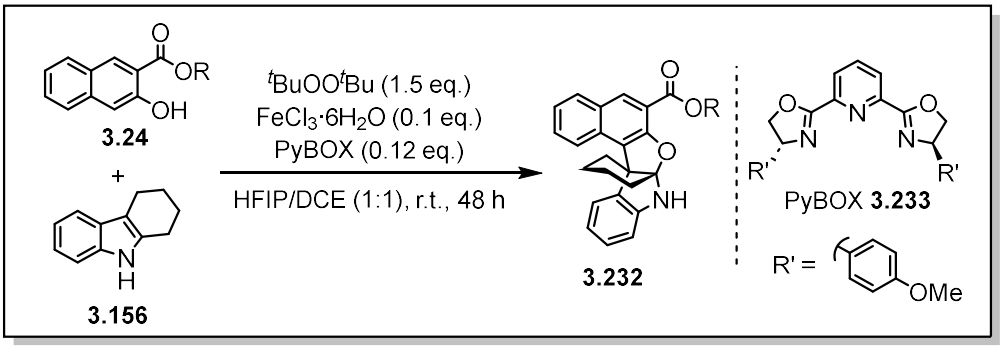


3.22 3.53 3.231

Figure 3.17 . Naphthoates used in the biaryl coupling

With this in mind, we began a screen of a selection of naphthoates from the library synthesised by Dr Surgenor and Dr Liu during the biaryl investigation. (Table 3.4) Entry 1 is the result from the ligand screen included for reference. The methyl ester (Entry 2) gave a yield of 26%, significantly lower than the phenyl. The ethyl ester (Entry 3) gave an even lower 15% yield of the product by quantitative NMR and could not be isolated. Benzyl ester (Entry 4) performed almost as well as the phenyl, with a slight drop in both yield and e.r. The addition of an *ortho* group to the phenyl ester had a strong negative impact on the yield, although the size of that group did not seem to have a consistent effect. Entry 5-7 were found in a 39%, 52%, and 29% yield respectively. The reasoning for the 2-isopropylphenyl ester (Entry 6) being found in the highest yield of the three is unclear. The selectivity of the reaction

decreased as the bulk of the group increased, from an e.r. of 83:17 for Entry 5 down to an e.r. of 76:24 for Entry 7.



Entry	Reference	R =	Yield / %	e.r.
1	**3.225**	Ph	77[a]	92:8
2	**3.234**	Me	26	-[b]
3	**3.235**	Et	15[a]	-[b]
4	**3.236**	Bn	71	87:13
5	**3.237**	2-MeC_6H_4	39	83:17
6	**3.238**	2-$^{i}PrC_6H_4$	52	78:22
7	**3.239**	2-$^{t}BuC_6H_4$	29	76:24

Table 3.4. The reaction conditions are as described with naphthoates (1.0 eq.) and **3.156** (1.5 eq.). e.r.s determined by chiral HPLC. [a] Yield was measured by quantitative ^{1}H NMR spectroscopy against dimethyl terephthalate (0.04 eq.). [b] Not determined

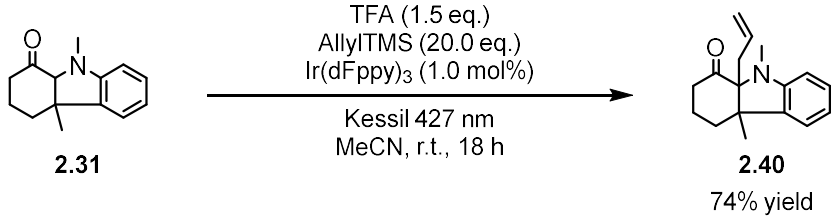
Due to time constraints, no further screenings could be carried out, and the investigation was ended.

Section 4: Conclusions and Future Work

4.1 Conclusions

In Section 1 (Chapter 1), an overview of oxidative methods was discussed, with a focus on the applications of oxidative reactivity in carbon-carbon bond formation. The benefits of oxidative bond formation were outlined, and a small review of common approaches to effecting this reactivity presented.

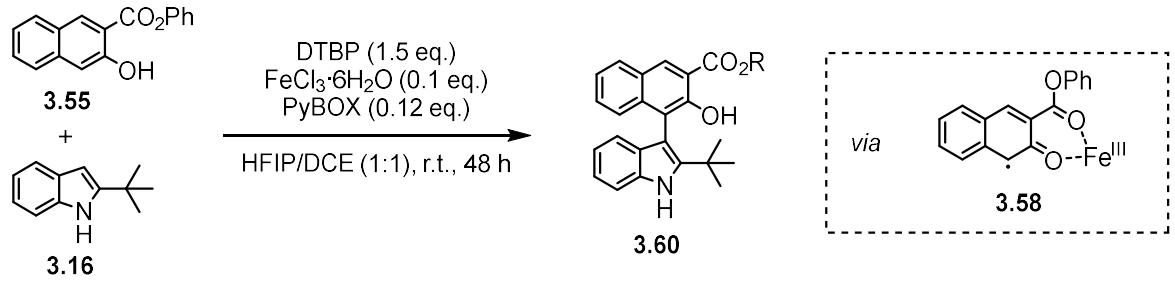
Section 2 (Chapter 2) described the discovery and exploration of a surprising oxidative allylation operating in tandem with a visible light photocyclisation (Scheme 4.1). The reaction proceeded through a single electron oxidation of the aniline substrate, most likely by TFA. Efforts to improve the yield were hampered by decomposition of the product under the reaction conditions and instability of the iminium intermediate, exacerbated by inefficient trapping by the allylTMS. Increasing the equivalents of allylTMS to favour the trapping lead to increased yields, to a maximum of 74%.



Scheme 4.1. Oxidative allylation of **2.31**

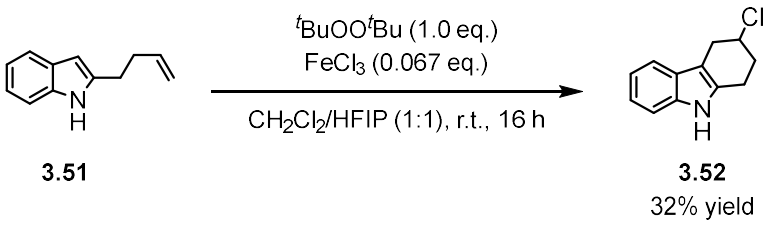
Chapter 3 described the expansion of the reaction system to other reagents and substrates. It was shown that other strong acids were capable of facilitating the oxidation, but no alternative nucleophiles for the final trapping step were found. Modification of the aniline component of the substrate was tolerated, although the syntheses of these substrates proved challenging. Variation of the environment α to the nitrogen (i.e. the site of reaction) was less successful, with no substrates showing meaningful product formation.

Section 3 (Chapter 4) described the continuation of the investigation into an enantioselective iron-catalysed oxidative cross-coupling (Scheme 4.2). Probing the importance of the C-3 substituent in the control of enantioselectivity confirmed that an ester was most suitable. Competition experiments utilising an internal radical trap showed that the coupling proceeds through the oxidation of the naphtholic partner and subsequent attack of the radical by the indole partner.



Scheme 4.2. Oxidative coupling of **3.55** and **3.16** *via* **3.58**

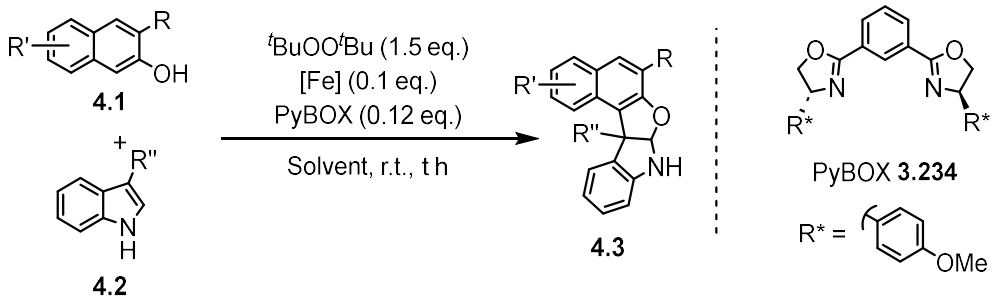
Chapter 5 described the exploration of the reactivity of the internal radical trap used to probe the mechanism of the oxidative cross-coupling (Scheme 4.3). The recovered product was the unexpected chlorinated 6,5,6-tricylic compound **3.52**. Efforts to enhance this reactivity were unsuccessful, and the reaction did not tolerate any modification of the alkenyl trap.



Scheme 4.3 Oxidative cyclisation of **3.51**, catalysed by $FeCl_3$

Chapter 6 described the modification of the biaryl coupling for the synthesis of naphthofuroindolines. The racemic transformation was achieved in moderate yield across a small range of 2-naphthols and 3-substituted indoles. Competitive formation of the BINOL homocouple was observed for the more challenging indole substrates, especially those with sterically bulky substituents. The change to 2-hydroxy-3-naphthoate partners was not tolerated in the simple reaction, but the re-introduction of a PyBOX ligand to the reaction system reinstated reactivity and allowed for the synthesis of the

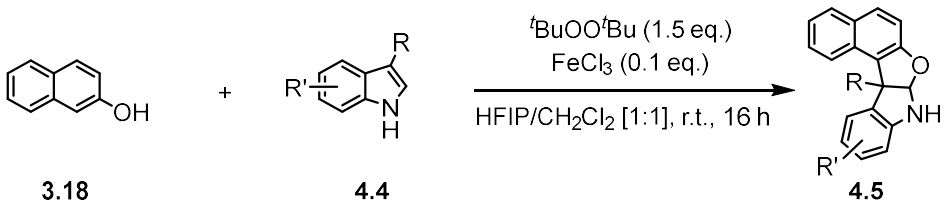
naphthofuroindolines enantioselectively. A screening of alternate PyBOX ligands found the 4-methoxyphenyl variant **3.234** the most effective. The naphthoate esters were evaluated, with the phenyl ester **3.53** the best performing.



Scheme 4.4 Oxidative coupling of naphthols and indoles in the synthesis of naphthofuroindolines

4.2 Future Work

The scope for synthesis of racemic naphthofuroindolines was limited, as many of the indole substituents were not tolerated or showed low activity. It was seen that nucleophilicity of the indole was an important factor in dictating reactivity, and so modifications of the successful 1,2,3,4-tetrahydrocarbazole substrate or efforts to increase the nucleophilicity of the indole with substitution of the carbocyclic backbone may yield improved results (Scheme 4.5).



Scheme 4.5 Modification of alternative sites on the indole component (**4.4**)

Continued optimisation of the enantioselective reaction may lead to a wider tolerance of the indole partner, as well as higher yields and better selectivity. This could be achieved by investigating the reaction components inherited from the biaryl coupling – there may be solvent mixtures, iron sources or co-oxidants that are favoured in this new reactivity, as well as more beneficial reaction conditions. These changes to the oxidising system may lead to expansion of the coupling to phenols, a valuable substrate class that was uncooperative with the original reaction. Further expansion of the indole and

naphthoate libraries may also find additional tolerated substrates, and ones that perform better than the current best examples.

Section 5: Experimental Details

5.1 General Information

Naming and Numbering

Compounds have been named with the use of ChemDraw Professional (Version 22) in accordance to IUPAC naming conventions. The numbering of atoms for the assignment of NMR was done arbitrarily with no relation to the IUPAC number system.

Reagents and Solvents

2-(tert-Butyl)-1H-indole, phenyl 3-hydroxy-2-naphthoate, o-tolyl 3-hydroxy-2-naphthoate, 2-isopropylphenyl 3-hydroxy-2-naphthoate, 2-(tert-butyl)phenyl 3-hydroxy-2-naphthoate, 2,6-bis((R)-4-(naphthalen-1-yl)-4,5-dihydrooxazol-2-yl)pyridine, and $Ir(dFppy)_3$ were sourced from samples synthesised within the group and used without further purification. All other reagents were purchased from major commercial suppliers (Sigma- Aldrich, Merck, Fluorochem, Apollo Scientific, Fischer Scientific, Tokyo Chemical Industry, Acros Organics) and used without further purification. Solvents were used without drying unless otherwise stated, in which case they were obtained from an MBraun SPS-5 solvent purifier. Solvents were used without degassing unless otherwise stated.

Procedures

All reactions were performed under an argon atmosphere unless otherwise stated. Reactions performed under anhydrous conditions (i.e. in a flame-dried vessel with anhydrous solvents) are clearly stated.

Chromatography

Reactions were monitored by thin layer chromatography (TLC) on Supelco TLC Silica gel 60 F_{254} pre-coated (0.2 mm) aluminium plates. Visualisation was achieved with ultraviolet (UV) light

(λmax = 254 nm) and by staining with permanganate or vanillin solutions. Flash column chromatography was performed using Geduran Si 60 (40-63 µm particle size). Chiral HPLC was performed on a Dionex Ultimate 3000 system comprising a Dionex LPG-3400SD pump, WPS-3000SL autosampler, TCC-3000SD column compartment fitted with the appropriate Daicel Chiralpak column (dimensions: 0.46 cm ø x 25 cm) and corresponding guard column (0.4 cm ø × 1 cm), and a DAD-3000 diode array detector. Wavelengths (λ) are reported in nm, retention times (τ_R) in minutes (min), temperatures (T) in °C, and solvent flow rates in mL min^{-1}.

Nuclear Magnetic Resonance

All NMR spectra were acquired at 298 K on Bruker Avance spectrometers. The data are reported as chemical shifts (δ) in part per million (ppm) relative to the residual non-deuterated solvent peak. ^{1}H data are reported as follows: chemical shift (multiplicity, coupling constants, integration, and assignment). Multiplicities are abbreviated as = singlet, d = doublet, t = triplet, q = quartet, m = multiple; coupling constants in Hertz (Hz).^{13}C data are reported as follows: chemical shift (assignment).

High-resolution mass spectrometry

High-resolution mass spectrometry (HRMS) was performed on Bruker MicroTOF or Waters Micromass GCT / BioAccord instruments under electrospray ionisation (ESI).

Melting Points

Melting points (M.P.) were determined using a Reichert melting point apparatus and are uncorrected.

Voltammetry

A PalmSens EmStat3 potentiostat, equipped with a glassy carbon working electrode, Pt wire (0.5 mm diameter) counter electrode and leak-free Ag/AgCl (3.4 M KCl) reference electrode, was

used for redox measurements. Square-wave voltammograms were acquired with a 5 mV step potential, 100 mV modulation amplitude and 5 Hz frequency, and internally referenced to the Fc^{+}/Fc couple; an argon-sparged solution of tetra-*n*-butylammonium hexafluorophosphate in acetonitrile (0.1 M, 5 mL) was used as the supporting electrolyte

Infrared spectroscopy

Fourier transform infrared (FTIR) spectra were recorded as thin films on a Tensor 27 FTIR spectrometer equipped with a diamond attenuated total reflectance (ATR) absorption module. Absorptions are reported in wavenumber (cm^{-1}).

General Procedures

General Procedure A: Symmetric Cross-Coupling

A screw-top vial was charged with $FeCl_3$ (1.6 mg, 0.01 mmol, 0.10 equiv.), the desired naphthol (0.1 mmol, 1.00 equiv.), and the desired indole (0.15 mmol, 1.50 equiv.) under air. A magnetic stir bar was added, and the solids dissolved in [1:1] CH_2Cl_2/HFIP (1 mL). The mixture was stirred for 5 min, and DTBP (27.4 µL, 0.15 mmol, 1.50 equiv.) was added. The reaction was stirred for 16 h at room temperature. After this time, the reaction mixture was filtered through a short silica plug, eluting liberally with CH_2Cl_2 (50 mL). The filtrate was concentrated to dryness and the crude product purified with flash column chromatography [silica gel, see specific compounds for exact conditions].

General Procedure B: Enantioselective Cross-Coupling

A screw-top vial was charged with $FeCl_3 \cdot 6H_2O$ (2.7 mg, 0.01 mmol, 0.100 equiv.) and DCE (0.5 mL) under air. The mixture was sonicated in a water bath for 30 min, until no visible solid remained and a homogeneous yellow solution had formed. A magnetic stir bar and the desired PyBOX ligand (0.012 mmol, 0.12 equiv.) were added, and the mixture stirred for 2 h at room temperature to give an orange solution. HFIP (0.5 mL) was then added and stirring continued for 30 min to afford a brown solution of the iron-ligand complex. The desired naphthol (0.10 mmol, 1.00 equiv.) and indole (0.15 mmol, 1.50 equiv.) were added to the pre-formed solution, forming a dark coloured solution. DTBP (27.4 µL, 0.15 mmol, 1.50 equiv.) was added, and the reaction stirred for 48 h at room temperature. After this time, the reaction mixture was filtered through a short silica plug, eluting liberally with CH_2Cl_2 (50 mL). The filtrate was concentrated to dryness and the crude product purified with flash column chromatography [silica gel, see specific compounds for exact conditions].

General Procedure C: Epoxide Opening with Anilines

A portion of 6-methyl-7-oxabicyclo[4.1.0]heptan-2-one (**2.59**) (1.00 equiv.) and the desired N-methylaniline (1.20 equiv.) were dissolved in [2:1] MeOH/water (0.4 M) and stirred at 70 °C for 72 h. The mixture was then allowed to cool and extracted three times with Et_2O, and the combined organic extracts were washed with brine, dried over Na_2SO_4, filtered, and concentrated *in vacuo*. The crude product purified with flash column chromatography [silica gel, see specific compounds for exact conditions].

General Procedure D: Oxidative Allylation

A flame dried Schlenk flask was charged with the desired substrate (0.10 mmol) and $Ir(dFppy)_3$ (0.8 mg, 0.001 mmol, 0.01 equiv.). Anhydrous sparged MeCN (2 mL), allyltrimethylsilane (48 µL, 0.30 mmol, 3.00 equiv.) and trifluoroacetic acid (12 µL, 0.15 mmol, 1.50 equiv.) were added. The reaction mixture was degassed by three freeze–pump–thaw cycles and the vessel placed into a transparent, water-cooled jacket. The mixture was stirred under constant irradiation with a Kessil PR160L 427 nm LED lamp for 18 h, after which the solvent was removed *in vacuo* and the residue purified by flash column chromatography [silica gel, see specific compounds for exact conditions].

General Procedure E: *para*-Halogenation

3-methyl-2-(methyl(phenyl)amino)cyclohex-2-en-1-one (**2.27**) (1.00 equiv.) and NBS or NIS (1.05 equiv., see specific compounds for exact conditions) were dissolved in MeCN (0.1 M) and stirred at room temperature for 2 h. The mixture was diluted with Et_2O and washed with sat. $NaHCO_{3\,(aq)}$, twice with water, and brine. The organic layer was concentrated *in vacuo* and the crude product purified with flash column chromatography [silica gel, see specific compounds for exact conditions].

General Procedure F: Amination of α-Bromocarbonyls

Prepared according to a modified literature method.[122]

N-methylaniline (0.17 mL, 1.60 mmol, 1.00 equiv.), the desired α-bromocarbonyl (2.00 mmol, 1.25 equiv.), and Na_2CO_3 (254 mg, 2.40 mmol, 1.20 equiv.) were added to flask and MeOH (2.4 mL) added. The mixture was stirred at 75 °C for 3.5 h, before being allowed to cool to room temperature. The solution was filtered, and the solid residue washed with EtOAc. The solution was washed three times with water and once with brine and the organic layer dried over Na_2SO_4, filtered, and concentrated *in vacuo*. The crude product purified with flash column chromatography [silica gel, see specific compounds for exact conditions].

General Procedure G: Enantiomeric Ratio Calculation

Purified samples of the compound of interest were analysed by HPLC (chiral stationary phase) [see specific compounds for exact details]. The retention times and UV absorption spectra were compared with those of a known racemic sample of the compound.

Synthesis of the racemates was achieved by **General Procedure B: Enantioselective Cross-Coupling** (as naphthoate substrates were unreactive in the symmetric **General Procedure A**). The PyBOX ligand chosen was the simplified symmetric 2,6-bis(4,5-dihydrooxazol-2-yl)pyridine (see in Table 3.3, Entry 1), where the pendant R group was a hydrogen atom.

General Procedure H: Quantitative NMR Progression Tracking

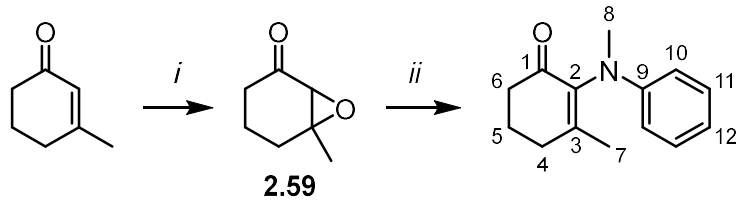
An oven-dried Youngs NMR was charged with $Ir(dFppy)_3$ (0.4 mg, 0.0005 mmol, 0.01 equiv.). To it was added dimethyl terephthalate (as a quantitative standard, 0.81 mg, 0.0042 mmol, 0.084 equiv.) in anhydrous d_3-MeCN (50 µL), allyltrimethylsilane (24 µL, 0.15 mmol, 3.00 equiv.), trifluoroacetic acid (6 µL, 0.075 mmol, 1.50 equiv.), and 4a,9-dimethyl-2,3,4,4a,9,9a-hexahydro-1H-carbazol-1-one (**2.31**) (11 mg, 0.05 mmol, 1.00 equiv.) in anhydrous d_3-MeCN (0.50 mL). The reaction mixture was degassed by three freeze–pump–thaw cycles and the vessel placed into a transparent, water-cooled jacket. The mixture was irradiated with a Kessil PR160L 427 nm LED lamp in intervals of 1 h, between which it was submitted to ^{1}H quantitative NMR. After three

hours total of irradiation, the vessel was again submitted to ^{1}H quantitative NMR, and irradiated for a further 15 h (18 h in total). A final ^{1}H quantitative NMR measurement was taken.

5.2 Characterisation of Compounds

5.2.1 Photochemistry (Section 2)

3-Methyl-2-(methyl(phenyl)amino)cyclohex-2-en-1-one (2.27)



2.59

Prepared according to a modified literature method and the data are in agreement with those previously reported.[53]

i. 3-methylcyclohex-2-en-1-one (1.94 mL, 18.18 mmol, 1.00 equiv.) was dissolved in MeOH at 0 °C. Hydrogen peroxide (30% w/w in water, 5.57 mL, 54.54 mmol, 3.00 equiv.) and NaOH (3 M in water, 1.2 mL, 3.64 mmol, 0.2 equiv.) were slowly added, and the mixture stirred at room temperature for 1 h. The mixture was poured into ice and brine, extracted three times with CH_2Cl_2, and the combined organic extracts were washed with water, dried over Na_2SO_4, filtered, and concentrated *in vacuo*. The crude product was used without further purification.

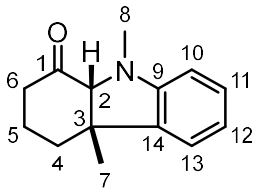
ii. The title compound was prepared according to the general procedure C using 6-methyl-7-oxabicyclo[4.1.0]heptan-2-one (**2.59**) (500 mg, 3.97 mmol) and N-methylaniline (0.51 mL, 4.76 mmol). The crude product was purified by flash column chromatography [silica gel, 33% Et_2O in pentane] to afford the product as an orange oil (467 mg, 2.17 mmol, 55%).

^{1}H NMR (400 MHz, $CDCl_3$) δ 7.22 – 7.12 (m, 2H, H11), 6.67 (tt, *J* = 7.0, 1.0 Hz, 1H, H12), 6.59 – 6.50 (m, 2H, H10), 3.02 (s, 3H, H8), 2.58 – 2.47 (m, 4H, H4 and H6), 2.06 (dq, *J* = 7.5, 6.0 Hz, 2H, H5), 1.88 (d, *J* = 1.0 Hz, 3H, H7).

^{13}C NMR (101 MHz, $CDCl_3$) δ 196.1 (C1), 158.6 (C9), 148.3 (C3), 139.7 (C2), 129.1 (C11), 116.7 (C12), 111.6 (C10), 38.8 (C6), 37.8 (C8), 32.2 (C4), 22.1 (C5), 20.13 (C7).

HRMS (ESI$^+$) *m/z* Calcd. for $C_{14}H_{18}NO$ $(M+H)^+$ 216.1383, found 216.1422

4a,9-Dimethyl-2,3,4,4a,9,9a-hexahydro-1H-carbazol-1-one (2.31)



Prepared according to a modified literature method and the data are in agreement with those previously reported.[53]

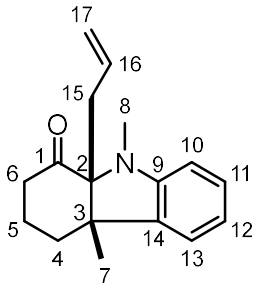
A flame dried Schlenk tube was charged with 3-methyl-2-(methyl(phenyl)amino)cyclohex-2-en-1-one (**2.27**) (108 mg, 0.50 mmol, 1.00 equiv.), $Ir(dFppy)_3$ (3.8 mg, 0.005 mmol, 0.01 equiv.), and potassium acetate (48 mg, 0.50 mmol, 1.00 equiv.). Anhydrous sparged MeCN (6 mL) was added, and the vessel placed into a transparent, water-cooled jacket. The reaction mixture was stirred under constant irradiation with a Kessil PR160L 427 nm LED lamp for 18 h, after which the solvent was removed *in vacuo* and the residue purified by flash column chromatography [silica gel, 5% Et_2O in pentane] to afford the product as a colourless oil (58 mg, 0.27 mmol, 54%)

^{1}H NMR (400 MHz, $CDCl_3$) δ 7.16 (td, *J* = 7.5, 1.5 Hz, 1H, H11), 7.02 (dd, *J* = 7.5, 1.5 Hz, 1H, H13), 6.80 (td, *J* = 7.5, 1.0 Hz, 1H, H12), 6.58 (d, *J* = 8.0 Hz, 1H, H10), 3.14 (d, *J* = 1.2 Hz, 1H, H2), 2.74 – 2.64 (m, 1H, H6'), 2.70 (s, 3H, H8), 2.39 – 2.25 (m, 1H, H6''), 1.96 – 1.56 (m, 4H, H4 and H5), 1.40 (s, 3H, H7).

^{13}C NMR (101 MHz, $CDCl_3$) δ 212.1 (C1), 151.6 (C9), 137.9 (C14), 128.2 (C11), 121.5 (C13), 119.3 (C12), 108.6 (C10), 82.0 (C2), 48.9 (C3), 38.1 (C6), 36.6 (C4), 35.1 (C8), 24.4 (C7), 21.3 (C5).

HRMS (ESI^+) *m/z* Calcd. for $C_{14}H_{17}NONa$ $(M+Na)^+$ 238.1202, found 238.1202

9a-Allyl-4a,9-dimethyl-2,3,4,4a,9,9a-hexahydro-1H-carbazol-1-one (2.40)



The data are in agreement with those previously reported this compound.[123]

The title compound was prepared according to the general procedure D using 4a,9-dimethyl-2,3,4,4a,9,9a-hexahydro-1H-carbazol-1-one (**2.31**) (21.5 mg). The crude product was purified by flash column chromatography [silica gel, 5% Et_2O in pentane] to afford the product as a colourless oil (15 mg, 0.039 mmol, 39%).

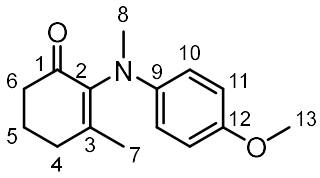
^{1}H NMR (600 MHz, $CDCl_3$) δ 7.10 (td, *J* = 7.5, 1.5 Hz, 1H, H11), 6.89 (dd, *J* = 7.5, 1.5 Hz, 1H, H13), 6.68 (td, *J* = 7.5, 1.0 Hz, 1H, H12), 6.36 (d, *J* = 7.5 Hz, 1H, H10), 5.59 (ddt, *J* = 17.0, 10.0, 7.0 Hz, 1H, H16), 5.09 (dq, *J* = 17.0, 1.5 Hz, 1H, H17'), 4.95 (dq, *J* = 10.0, 1.5 Hz, 1H, H17''), 2.82 (s, 3H, H8), 2.74 (ddt, *J* = 15.5, 7.0, 1.5 Hz, 1H, H15'), 2.59 (ddt, *J* = 15.5, 7.0, 1.5 Hz, 1H, H15''), 2.41 (dddd, *J* = 15.5, 6.0, 4.5, 1.5 Hz, 1H, H6'), 2.29 (ddd, *J* = 15.5, 9.5, 7.0 Hz, 1H, H6''), 1.93 (dddd, *J* = 14.0, 5.0, 3.5, 1.5 Hz, 1H, H4'), 1.80 – 1.70 (m, 2H, H5), 1.66 (ddd, *J* = 14.0, 12.0, 4.0 Hz, 1H, H4''), 1.32 (s, 3H, H7).

^{13}C NMR (151 MHz, $CDCl_3$) δ 214.3 (C1), 151.1 (C9), 135.1 (C14), 134.3 (C16), 128.3 (C11), 120.9 (C13), 118.2 (C17), 117.7 (C12), 105.3 (C10), 79.8 (C2), 52.2 (C3), 39.5 (C6), 36.8 (C4), 34.1 (C15), 30.6 (C8), 22.9 (C7), 20.7 (C5).

FTIR (neat) ν = 3078, 3048, 3024, 2958, 2932, 2853, 2817, 2359, 1706, 1638, 1605, 1487, 1457, 1446, 1423, 1369, 1305, 1247, 1214, 1159, 1120, 1081, 1042, 1021, 991, 926, 914, 872, 841, 739, 701, 659, 639, 618

HRMS (ESI$^+$) *m/z* Calcd. for $C_{17}H_{21}ONNa$ $(M+Na)^+$ 278.1515, found 278.1528

2-((4-Methoxyphenyl)(methyl)amino)-3-methylcyclohex-2-en-1-one (2.81)



The title compound was prepared according to the general procedure C using 6-methyl-7-oxabicyclo[4.1.0]heptan-2-one (**2.59**) (100 mg, 0.79 mmol) and 4-methoxy-N-methylaniline (0.130 mg, 0.95 mmol). The crude product was purified by flash column chromatography [silica gel, 40% Et_2O in pentane] to afford the product as an orange oil (103 mg, 0.42 mmol, 53%).

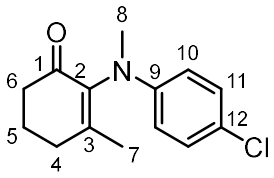
^{1}H NMR (400 MHz, $CDCl_3$) δ 6.84 – 6.72 (m, 2H, H11), 6.63 – 6.41 (m, 2H, H10), 3.73 (s, 3H, H13), 2.99 (s, 3H, H8), 2.60 – 2.42 (m, 4H, H4 and H6), 2.04 (dq, *J* = 8.0, 6.0 Hz, 2H, H5), 1.89 (d, *J* = 1.0 Hz, 3H, H7).

^{13}C NMR (101 MHz, $CDCl_3$) δ 185.1 (C1), 158.6 (C3), 151.6 (C9), 148.2 (12), 140.4 (C2), 115.0 (C11), 112.8 (C10), 56.0 (C13), 39.2 (C6), 38.4 (C8), 32.5 (C4), 22.4 (C5), 20.4 (C7).

FTIR (neat) v = 2915, 1707, 1676, 1632, 1510, 1471, 1421, 1378, 1353, 1323, 1284, 1240, 1222, 1180, 1134, 1115, 1064, 1034, 929, 847, 812, 790, 761, 711, 645, 618

HRMS (ESI$^+$) *m/z* Calcd. for $C_{15}H_{19}NO_2Na$ $(M+Na)^+$ 268.1308, found 268.1310

2-((4-Chlorophenyl)(methyl)amino)-3-methylcyclohex-2-en-1-one (2.82)



The title compound was prepared according to the general procedure C using 6-methyl-7-oxabicyclo[4.1.0]heptan-2-one (**2.59**) (100 mg, 0.79 mmol) and 4-chloro-N-methylaniline (116 µL, 0.95 mmol). The crude product was purified by flash column chromatography [silica gel, 33% Et_2O in pentane] to afford the product as an orange oil (20.6 mg, 0.082 mmol, 10%).

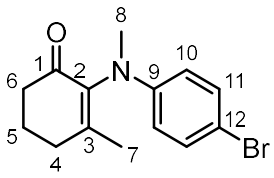
^{1}H NMR (400 MHz, $CDCl_3$) δ 7.10 (d, *J* = 9.1 Hz, 2H, H11), 6.45 (d, *J* = 9.0 Hz, 2H, H10), 2.99 (s, 3H, H8), 2.58 – 2.47 (m, 4H, H4 and H6), 2.11 – 2.00 (m, 2H, H5), 1.87 (s, 3H, H7).

^{13}C NMR (101 MHz, $CDCl_3$) δ 196.0 (C1), 159.0 (C3), 147.1 (C9), 139.6 (C2), 129.0 (C11), 121.7 (C12), 112.9 (C10), 38.8 (C6), 38.2 (C8), 32.3 (C4), 22.2 (C5), 20.2 (C7).

FTIR (neat) ν = 2971, 2871, 2380, 1717, 1678, 1630, 1595, 1495, 1427, 1378, 1358, 1343, 1324, 1291, 1225, 1182, 1119, 1064, 953, 926, 815, 730, 633

HRMS (ESI$^+$) *m/z* Calcd. for $C_{14}H_{16}{}^{35}ClNONa$ $(M+Na)^+$ 272.0813, found 272.0817

2-((4-Bromophenyl)(methyl)amino)-3-methylcyclohex-2-en-1-one (2.86)



The title compound was prepared according to the general procedure E using 3-methyl-2-(methyl(phenyl)amino)cyclohex-2-en-1-one (**2.27**) (215 mg, 1.00 mmol) and N-bromosuccinimide (181 mg, 1.05 mmol). The crude product was purified by flash column

chromatography [silica gel, 50% Et_2O in pentane] to afford the product as an orange oil (205 mg, 0.70 mmol, 70%).

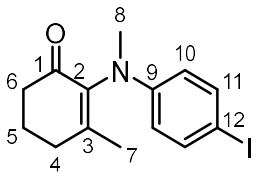
^{1}H NMR (400 MHz, $CDCl_3$) δ 7.23 (d, *J* = 9.0 Hz, 2H, H11), 6.40 (d, *J* = 9.0 Hz, 2H, H10), 2.98 (s, 3H, H8), 2.58 – 2.46 (m, 4H, H4 and H6), 2.10 – 2.01 (m, 2H, H5), 1.87 (d, *J* = 1.0 Hz, 3H, H7).

^{13}C NMR (101 MHz, $CDCl_3$) δ 195.8 (C1), 159.1 (C3), 147.5 (C9), 139.5 (C2), 131.9 (C11), 113.5 (C10), 108.8 (C12), 38.8 (C6), 38.1 (C8), 32.3 (C4), 22.1 (C5), 20.2 (C7).

FTIR (neat) ν = 2946, 2868, 2817, 1675, 1630, 1588, 1493, 1452, 1426, 1377, 1357, 1342, 1323, 1290, 1226, 1181, 1138, 1118, 1064, 995, 926, 812, 788, 733, 673, 649

HRMS (ESI^+) *m/z* Calcd. for $C_{14}H_{16}{}^{79}BrNONa$ $(M+Na)^+$ 316.0308, found 316.0311

2-((4-Iodophenyl)(methyl)amino)-3-methylcyclohex-2-en-1-one (2.87)



The title compound was prepared according to the general procedure E using 3-methyl-2-(methyl(phenyl)amino)cyclohex-2-en-1-one (**2.27**) (108 mg, 0.50 mmol) and N-iodosuccinimide (118 mg, 0.53 mmol). The crude product was purified by flash column chromatography [silica gel, 33% Et_2O in pentane] to afford the product as a green oil (110 mg, 0.32 mmol, 64%).

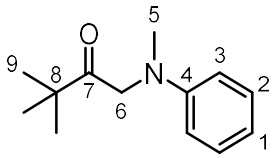
^{1}H NMR (400 MHz, $CDCl_3$) δ 7.39 (d, *J* = 9.0 Hz, 2H, H11), 6.31 (d, *J* = 9.0 Hz, 2H, H10), 2.97 (s, 3H, H8), 2.63 – 2.43 (m, 4H, H4 and H6), 2.05 (dq, *J* = 12.0, 6.0 Hz, 2H, H5), 1.86 (s, 3H, H7).

^{13}C NMR (101 MHz, $CDCl_3$) δ 195.8 (C1), 159.1 (C3), 148.1 (C9), 139.4 (C2), 137.7 (C11), 114.2 (C10), 77.9 (C12), 38.8 (C6), 38.0 (C8), 32.3 (C4), 22.1 (C5), 20.2 (C7).

FTIR (neat) ν = 2870, 2817, 2248, 1713, 1672, 1629, 1587, 1489, 1451, 1425, 1410, 1377, 1358, 1343, 1292, 1269, 1227, 1181, 1139, 1116, 1072, 1059, 1011, 991, 927, 910, 809, 733, 647

HRMS (ESI^+) *m/z* Calcd. for $C_{14}H_{16}INONa$ $(M+Na)^+$ 364.0169, found 364.0181

3,3-Dimethyl-1-(methyl(phenyl)amino)butan-2-one (2.97)



Prepared according to a modified literature method[124] and the data are in agreement with those previously reported.[125]

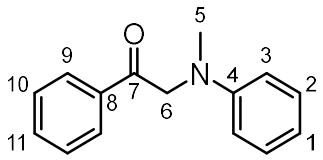
To NaI (180 mg, 1.20 mmol, 1.20 equiv.) was added anhydrous MeCN (2 mL). 1-Bromopinacolone (134 µL, 1.00 mmol, 1.00 equiv.), N-methylaniline (108 µL, 1.00 mmol, 1.00 equiv.), and DIPEA (17 µL, 0.1 mmol, 0.1 equiv.) were added, and the mixture stirred at 40 °C for 24 h. The mixture was diluted with EtOAc and washed three times with water and once with brine and the organic layer dried over Na_2SO_4, filtered, and concentrated *in vacuo*. The crude product purified with flash column chromatography (1% EtOAc in toluene) to give the brown oil (26 mg, 0.13 mmol, 13%)

^{1}H NMR (400 MHz, $CDCl_3$) δ 7.30 – 7.09 (m, 2H, H2), 6.71 (tt, *J* = 7.5, 1.0 Hz, 1H, H1), 6.64 – 6.56 (m, 2H, H3), 4.32 (s, 1H, 2H, H6), 2.99 (s, 3H, H5), 1.24 (s, 6H, H9).

^{13}C NMR (101 MHz, $CDCl_3$) δ 212.2 (C7), 149.4 (C4), 129.3 (C2), 117.0 (C1), 112.1 (C3), 57.0 (C6), 43.5 (C6), 39.5 (C5), 26.6 (C9).

HRMS (ESI^+) *m/z* Calcd. for $C_{13}H_{19}INONa$ $(M+Na)^+$ 228.1359, found 228.1373

2-(Methyl(phenyl)amino)-1-phenylethan-1-one (2.98)



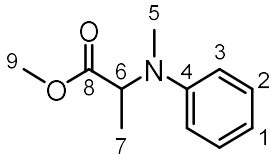
The data are in agreement with those previously reported.[126]

The title compound was prepared according to the general procedure F using 2-bromoacetophenone (398 mg). The crude product was purified by flash column chromatography [silica gel, 10% Et_2O in pentane] to afford the product as a brown oil (51 mg, 0.22 mmol, 14%).

^{1}H NMR (400 MHz, $CDCl_3$) δ 8.05 – 7.88 (m, 2H, H9), 7.70 – 7.39 (m, 3H, H10 and H11), 7.25 – 7.12 (m, 2H, H2), 6.86 – 6.60 (m, 3H, H1 and H3), 4.79 (s, 2H, H6), 3.11 (s, 3H, H5).

^{13}C NMR (101 MHz, $CDCl_3$) δ 196.6 (C7), 149.3 (C4), 135.6 (C8), 133.7 (C11), 129.4 (C2), 129.0 (C10), 128.0 (C9), 117.3 (C1), 112.5 (C3), 59.13 (C6), 39.7 (C5).

Methyl N-methyl-N-phenylalaninate (2.99)



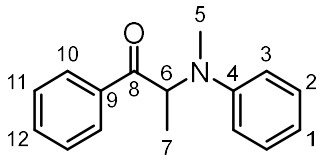
The data are in agreement with those previously reported.[127]

The title compound was prepared according to the general procedure F using methyl 2-bromopropanoate (223 µL). The crude product was purified by flash column chromatography [silica gel, 10% Et_2O in pentane] to afford the product as a brown oil (72 mg, 0.37 mmol, 23%).

^{1}H NMR (400 MHz, $CDCl_3$) δ 7.25 (dd, *J* = 9.0, 7.0 Hz, 2H, H2), 6.82 – 6.73 (m, 3H, H1 and H3), 4.53 (q, *J* = 7.0 Hz, 1H, H6), 3.70 (s, 3H, H9), 2.89 (s, 3H, H5), 1.48 (d, *J* = 7.0 Hz, 3H, H7).

^{13}C NMR (101 MHz, $CDCl_3$) δ 174.0 (C8), 149.7 (C4), 129.3 (C2), 117.8 (C1), 113.6 (C3), 57.2 (C6), 52.1 (C9), 33.1 (C5), 15.3 (C7).

2-(Methyl(phenyl)amino)-1-phenylpropan-1-one (2.100)



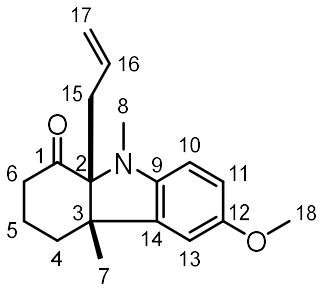
The data are in agreement with those previously reported.[124]

The title compound was prepared according to the general procedure F using 2-bromopropiophenone (304 µL). The crude product was purified by flash column chromatography [silica gel, 5% Et_2O in pentane] to afford the product as a brown oil (206 mg, 0.86 mmol, 53%).

^{1}H NMR (400 MHz, $CDCl_3$) δ 7.95 – 7.86 (m, 2H, H10), 7.55 – 7.48 (m, 1H, H12), 7.42 – 7.34 (m, 2H, H11), 7.34 – 7.27 (m, 2H, H2), 6.88 – 6.82 (m, 2H, H3), 6.83 – 6.78 (m, 1H, H1), 5.28 (q, *J* = 6.5 Hz, 1H, H6), 2.66 (s, 3H, H5), 1.41 (d, *J* = 6.5 Hz, 3H, H7).

^{13}C NMR (101 MHz, $CDCl_3$) δ 199.7 (C8), 148.5 (C4), 135.9 (C9), 133.3 (C12), 129.7 (C2), 128.7 (C11), 128.5 (C10), 117.6 (C1), 112.8 (C3), 58.6 (C6), 32.9 (C5), 11.9 (C7).

9a-Allyl-6-methoxy-4a,9-dimethyl-2,3,4,4a,9,9a-hexahydro-1H-carbazol-1-one (2.106)



The title compound was prepared according to the general procedure D using 2-((4-methoxyphenyl)(methyl)amino)-3-methylcyclohex-2-en-1-one (**2.81**) (24.5 mg). The crude product was purified by flash column chromatography [silica gel, 5% Et_2O in pentane] to afford the product as a colourless oil (10 mg, 0.034 mmol, 34%).

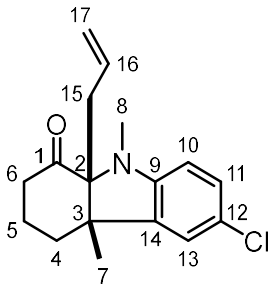
^{1}H NMR (400 MHz, $CDCl_3$) δ 6.70 – 6.60 (m, 1H, H11), 6.55 (d, *J* = 2.5 Hz, 1H, H13), 6.26 (d, *J* = 8.5 Hz, 1H, H10), 5.58 (ddt, *J* = 17.0, 10.0, 7.0 Hz, 1H, H16), 5.07 (dq, *J* = 17.0, 1.5 Hz, 1H, H17'), 4.94 (dd, *J* = 10.0, 2.0 Hz, 1H, H17''), 3.75 (s, 3H, H18), 2.78 (s, 3H, H8), 2.73 (ddt, *J* = 15.5, 7.0, 1.5 Hz, 1H, H15'), 2.57 (ddt, *J* = 15.5, 7.0, 1.5 Hz, 1H, H15''), 2.42 (dddd, *J* = 15.0, 6.5, 5.0, 1.5 Hz, 1H, H6'), 2.33 – 2.23 (m, 1H, H6''), 1.97 – 1.88 (m, 1H, H4'), 1.83 – 1.61 (m, 3H, H4'' and H5), 1.30 (s, 3H, H7).

^{13}C NMR (101 MHz, $CDCl_3$) δ 214.4 (C1), 152.9 (C9), 145.5 (C12), 136.8 (C14), 134.3 (C16), 118.1 (C17), 111.7 (C11), 109.2 (C13), 105.2 (C10), 80.0 (C2), 56.1 (C3), 52.2 (C3), 39.6 (C6), 36.6 (C4), 34.1 (C15), 31.0 (C8), 22.6 (C7), 20.8 (C5).

FTIR (neat) v = 2940, 2364, 1710, 1705, 1664, 1638, 1599, 1522, 1500, 1496, 1433, 1422, 1368, 1281, 1255, 1225, 1211, 1134, 1121, 1050, 1033, 993, 917, 865, 828, 799, 733, 694, 628

HRMS (ESI^+) *m/z* Calcd. for $C_{18}H_{23}NO_2Na$ $(M+Na)^+$ 308.1621, found 308.1616

9a-Allyl-6-chloro-4a,9-dimethyl-2,3,4,4a,9,9a-hexahydro-1H-carbazol-1-one (2.107)



The title compound was prepared according to the general procedure D using 2-((4-chlorophenyl)(methyl)amino)-3-methylcyclohex-2-en-1-one (**2.82**) (25.0 mg). The crude product was purified by flash column chromatography [silica gel, 5% Et_2O in pentane] to afford the product as a colourless oil (11 mg, 0.036 mmol, 36%).

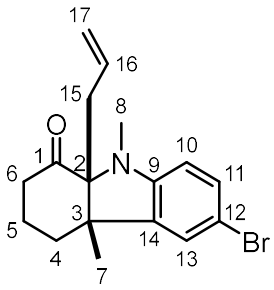
^{1}H NMR (400 MHz, $CDCl_3$) δ 7.04 (dd, *J* = 8.5, 2.0 Hz, 1H, H11), 6.83 (d, *J* = 2.0 Hz, 1H, H13), 6.26 (d, *J* = 8.5 Hz, 1H, H10), 5.57 (ddt, *J* = 17.0, 10.0, 7.0 Hz, 1H, H16), 5.10 (dq, *J* = 17.0, 1.5 Hz, 1H, H17'), 4.98 (dq, *J* = 10.0, 1.5 Hz, 1H, H17''), 2.81 (s, 3H, H8), 2.74 (ddt, *J* = 15.5, 7.0, 1.5 Hz, 1H, H15'), 2.57 (ddt, *J* = 15.5, 7.0, 1.5 Hz, 1H, H15''), 2.41 (dtd, *J* = 15.5, 5.0, 1.5 Hz, 1H, H6'), 2.30 (ddd, *J* = 15.5, 9.0, 8.0 Hz, 1H, H6''), 1.91 (dddd, *J* = 13.0, 5.0, 3.5, 1.5 Hz, 1H, H4'), 1.80 – 1.62 (m, 3H, H4'' and H5), 1.29 (s, 3H, H7).

^{13}C NMR (101 MHz, $CDCl_3$) δ 213.9 (C1), 149.7 (C9), 136.8 (C14), 133.8 (C16), 127.9 (C11), 122.2 (C12), 121.4 (C13), 118.6 (C17), 106.1 (C10), 80.1 (C2), 52.3 (C3), 39.5 (C6), 36.4 (C4), 34.1 (C15), 30.7 (C8), 22.8 (C7), 20.8 (C5).

FTIR (neat) v = 2936, 2869, 2815, 1712, 1639, 1603, 1486, 1459, 1447, 1420, 1362, 1314, 1273, 1214, 1125, 1089, 1063, 991, 916, 874, 806, 736, 661, 649, 634

HRMS (ESI^+) *m/z* Calcd. for $C_{17}H_{20}{}^{35}ClNONa$ $(M+Na)^+$ 312.1126, found 312.1120

9a-Allyl-6-bromo-4a,9-dimethyl-2,3,4,4a,9,9a-hexahydro-1H-carbazol-1-one (2.108)



The title compound was prepared according to the general procedure D using 2-((4-bromophenyl)(methyl)amino)-3-methylcyclohex-2-en-1-one (**2.86**) (29.4 mg). The crude product was purified by flash column chromatography [silica gel, 5% Et_2O in pentane] to afford the product as a colourless oil (20.3 mg, 0.061 mmol, 61%).

^{1}H NMR (400 MHz, $CDCl_3$) δ 7.17 (dd, *J* = 8.0, 2.0 Hz, 1H, H11), 6.95 (d, *J* = 2.0 Hz, 1H, H10), 6.22 (d, *J* = 8.0 Hz, 1H, H13), 5.57 (ddt, *J* = 17.0, 10.0, 7.0 Hz, 1H, H16), 5.10 (dq, *J* = 17.0, 1.5 Hz, 1H, H17'), 4.98 (dq, *J* = 10.0, 1.5 Hz, 1H, H17''), 2.80 (s, 3H, H8), 2.74 (ddt, *J* = 15.5, 7.0, 1.5 Hz, 1H, H15'), 2.63 – 2.50 (m, 1H, H15''), 2.40 (dtd, *J* = 15.5, 5.5, 1.5 Hz, 1H, H6'), 2.30 (dt, *J* = 15.5, 8.0 Hz, 1H, H6''), 1.95 – 1.85 (m, 1H, H4'), 1.82 – 1.60 (m, 3H, H4'' and H3), 1.29 (s, 3H, H7).

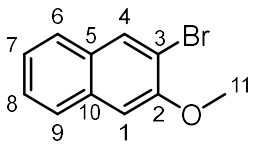
^{13}C NMR (101 MHz, $CDCl_3$) δ 213.7 (C1), 150.1 (C9), 137.3 (C14), 133.8 (C16), 130.9 (C11), 124.1 (C13), 118.6 (C17), 109.2 (C12), 106.8 (C10), 80.1 (C2), 52.3 (C3), 39.5 (C6), 36.5 (C4), 34.1 (C15), 30.7 (C8), 22.5 (C7), 20.8 (C5).

FTIR (neat) ν = 3076, 2937, 2816, 1710, 1637, 1598, 1484, 1458, 1414, 1362, 1312, 1272, 1215, 1127, 1084, 991, 917, 873, 802, 779, 733, 702, 648

HRMS (ESI$^+$) *m/z* Calcd. for $C_{17}H_{20}{}^{79}BrNONa$ $(M+Na)^+$ 356.0621, found 356.0597

5.2.2 Iron-Catalysed Oxidation (Section 3)

2-Bromo-3-methoxynaphthalene (3.40)



Prepared according to a modified literature method and the data are in agreement with those previously reported.[128]

A solution of 2-methoxynaphthalene (1.00 g, 6.32 mmol, 1.00 equiv.) in anhydrous THF (7.5 mL) was cooled to -78 °C and *n*-BuLi (1.6 M in hexanes, 4.08 mL, 6.53 mmol, 1.03 equiv.) added. The mixture was stirred at room temperature for 1 h, and cooled to -78 °C. 1,2-dibromoethane (1.27 g, 0.58 mL, 6.74 mmol, 1.07 equiv.) was added at -78 °C, and the mixture stirred for 20 h at room temperature. The mixture was poured into sat. $NH_4Cl_{(aq.)}$ (5 mL) and extracted three times with Et_2O. The combined organic extracts were washed with brine, dried over $MgSO_4$, filtered and concentrated *in vacuo*. The crude product was purified by recrystallization from hexane to afford the product as a colourless solid (24%, 1.52 mmol, 0.37 g).

M.P. = 64–65 °C, hexane (lit. 65–66 °C);

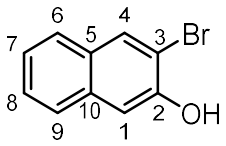
^{1}H NMR (400 MHz, $CDCl_3$) δ = 8.06 (s, 1H, H4), 7.75 – 7.66 (m, 2H, H6 and H9), 7.46 (ddd, *J* = 8.0, 7.0, 1.5, 1H, H7), 7.36 (ddd, *J* = 8.0, 7.0, 1.0, 1H, H8), 7.16 (s, 1H, H1), 4.01 (s, 3H, H11);

^{13}C NMR (101 MHz, $CDCl_3$) δ = 153.7 (C2), 133.7 (C10), 132.4 (C4), 129.6 (C5), 126.9 (2C, C7 and C9), 126.7 (C6), 124.6 (C8), 113.5 (C3), 106.8 (C1), 56.4 (C11);

FTIR (neat) ν = 1466, 1251, 1216, 1043, 865, 753, 711 cm^{-1};

HRMS (GS EI) *m/z* Calcd. for $C_{11}H_9{}^{79}BrO$ (M^+) 235.98313, found 235.98368

3-Bromonaphthalen-2-ol (3.41)



Prepared according to a modified literature method and the data are in agreement with those previously reported.[128]

A solution of 2-bromo-3-methoxynaphthalene (**3.40**) (0.30 g, 1.27 mmol, 1.00 equiv.) in anhydrous CH_2Cl_2 (1 mL) was cooled to -78 °C and BBr_3 (1 M in CH_2Cl_2, 2.03 mL, 2.03 mmol, 1.60 equiv.) added. After the mixture stirred for 20 h at room temperature, ice was added (1 g) at 0 °C. The resulting mixture was extracted three times with CH_2Cl_2, and the combined organic extracts were washed with brine, dried over $MgSO_4$, filtered, and concentrated *in vacuo*. The crude product was purified by recrystallization from hexane to afford the product as a colourless solid (0.23 g, 1.04 mmol, 82%).

M.P. = 74–75 °C, hexane (lit. 79–80 °C);

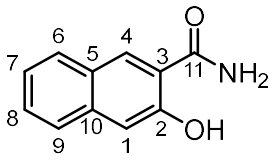
^{1}H NMR (400 MHz, $CDCl_3$) δ 8.03 (d, *J* = 0.5, 1H, H4), 7.78 – 7.62 (m, 2H, H6 and H9), 7.45 (ddd, *J* = 8.0, 7.0, 1.5, 1H, H7), 7.39 (d, *J* = 0.5, 1H, C1), 7.35 (ddd, *J* = 8.0, 7.0, 1.0, 1H, C8), 5.62 (s, 1H, OH);

^{13}C NMR (101 MHz, $CDCl_3$) δ 149.6 (C2), 134.2 (C10), 131.4 (C4), 129.6 (C5), 127.1 (C9), 126.9 (C7), 126.7 (C6), 124.6 (C8), 112.7 (C3), 110.9 (C1);

FTIR (neat) v = 3517, 3475, 3385, 1589, 1501, 1443, 1391, 1360, 1341, 1265, 1220, 1000, 870, 744 cm^{-1};

HRMS (ESI^-) *m/z* Calcd. for $C_{10}H_6O^{79}Br$ $(M-H)^-$ 220.9608, found 220.9605

3-Hydroxy-2-naphthamide (3.37)



Prepared according to a modified literature method and the data are in agreement with those previously reported.[129]

3-hydroxy-2-naphthoic acid (1.00 g, 5.31 mmol, 1.00 equiv.) was suspended in anhydrous CH_2Cl_2 (45 mL) and a drop of DMF, and $SOCl_2$ (1.26 g, 0.73 mL, 10.62 mmol, 2.00 equiv.) was added. The mixture was stirred for 1 h at 35 °C, and the solvent removed *in vacuo*. The residue was dissolved in CH_2Cl_2 (12 mL) and was added dropwise to a stirring mixture of concentrated NH_4OH (10 mL) and CH_2Cl_2 (6 mL). The mixture was stirred at room temperature for 24 h and acidified to pH 3 with 10% HCl. The precipitate was filtered off, washed with sat. $NaHCO_{3\ (aq.)}$ and purified by flash column chromatography [silica gel, 33% Et_2O in pentane] to afford the product as a yellow solid (0.36 g, 1.96 mmol, 37%).

M.P. = 203–207 °C, (lit. 216–218 °C);

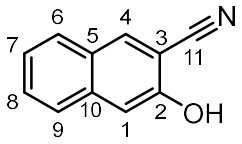
^{1}H NMR (400 MHz, DMSO-d_6) δ = 12.46 (s, 1H, OH), 8.60 (s, 1H, NH), 8.54 (s, 1H, H4), 8.03 (s, 1H, NH), 7.81 (dd, *J* = 8.5, 1.0, 1H, H9), 7.73 (dd, *J* = 8.5, 1.0, 1H, H6), 7.50 (ddd, *J* = 8.0, 7.0, 1.5, 1H, H7), 7.34 (ddd, *J* = 8.0, 7.0, 1.0, 1H, H8), 7.25 (s, 1H, H1).;

^{13}C NMR (101 MHz, DMSO-d_6) δ 171.3 (C11), 156.4 (C2), 136.4 (C10), 129.8 (C4), 128.7 (C9), 128.3 (C7), 126.4 (C5), 125.8 (C6), 123.6 (C8), 117.3 (C3), 110.7 (C1);

FTIR (neat) v = 3414, 3198, 1687, 1650, 1519, 1454, 1337, 1243, 1103, 804, 733 cm^{-1};

HRMS (ESI^+) *m/z* Calcd. for $C_{11}H_{10}O_2N$ $(M+H)^+$ 188.0706, found 188.0707

3-Hydroxy-2-naphthonitrile (3.38)



Prepared according to a modified literature method and the data are in agreement with those previously reported.[130]

To a solution of 3-hydroxy-2-naphthamide (**3.37**) (0.30 g, 1.60 mmol, 1.00 equiv.) in anhydrous DMF (8 mL) was added $POCl_3$ (0.19 mL, 2.08 mmol, 1.30 equiv.) at 0 °C. The mixture was allowed to stir for 0.5 h at 0 °C. The mixture was washed with sat. $NaHCO_{3\ (aq.)}$ and water, and the organic layer dried with $MgSO_4$. The solvent was removed *in vacuo* and no further purification was needed to afford the product as a yellow solid (0.21 g, 1.26 mmol, 79%).

M.P. = 170–173 °C (lit. 183–186°C);

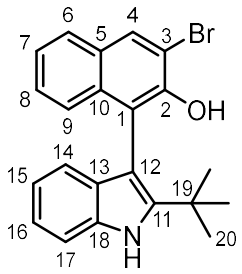
^{1}H NMR (400 MHz, DMSO) δ = 11.06 (s, 1H, OH), 8.42 (s, 1H, H4), 7.88 (dd, *J* = 8.5, 1.0, 1H, H9), 7.78 (dd, *J* = 8.5, 1.0, 1H, H6), 7.55 (ddd, *J* = 8.5, 7.0, 1.5, 1H, H7), 7.39 (ddd, *J* = 8.0, 7.0, 1.0, 1H, H8), 7.32 (s, 1H, H1);

^{13}C NMR (101 MHz, DMSO) δ 154.6 (C2), 136.2 (C10), 135.9 (C4), 129.3 (C7), 128.3 (C9), 126.6 (C5), 126.2 (C6), 124.3 (C8), 116.9 (C11), 109.7 (C1), 101.9 (C3);

FTIR (neat) ν = 3249, 2981, 2919, 2237, 1628, 1603, 1454, 1392, 1365, 1349, 1249, 1222, 1178, 1142, 1093, 875, 742, 664 cm^{-1};

HRMS (ESI^-) m/z Calcd. for $C_{11}H_6ON\ (M-H)^-$ 168.0445, found 168.0447.

3-Bromo-1-(2-(tert-Butyl)-1H-indol-3-yl)naphthalen-2-ol (3.46)



The title compound was prepared according to General Procedure B using 3-bromonaphthalen-2-ol (**3.41**) (22.3 mg, 0.10 mmol), 2-(*tert*-butyl)-1H-indole (26.0 mg, 0.15 mmol) and 2,6-bis((S)-4-(naphthalen-1-yl)-4,5-dihydrooxazol-2-yl)pyridine (**3.26**) (5.6 mg, 0.012 mmol). The crude product was purified by flash column chromatography [silica gel, 33% CH_2Cl_2 in pentane] to afford the product as a yellow foam (36.3 mg, 0.092 mmol, 92%).

^{1}H NMR (400 MHz, $CDCl_3$) δ = 8.39 (s, 1H, NH), 8.16 (s, 1H, H4), 7.78 – 7.73 (m, 1H, H9), 7.45 (dt, *J* = 8.0, 1.0, 1H, H17), 7.36 – 7.26 (m, 3H, H6, H7, and H8), 7.22 (ddd, *J* = 8.0, 7.0, 1.5, 1H, H16), 7.00 (ddd, *J* = 8.0, 7.0, 1.0, 1H, H15), 6.92 (dd, *J* = 8.0, 1.0, 1H, H14), 5.63 (s, 1H, OH), 1.25 (s, 9H, H20);

^{13}C NMR (101 MHz, $CDCl_3$) δ 148.8 (C2), 146.5 (C11), 135.0 (C18), 134.2 (C10), 132.0 (C4), 129.6 (2C, C13 and C5), 127.2 (C9), 126.7 (C7), 125.8 (C6), 124.2 (C8), 122.6 (C16), 120.5 (C15), 119.2 (C14), 116.9 (C3), 111.0 (C1), 110.6 (C17), 102.0 (C12), 33.5 (C19), 30.2 (C20);

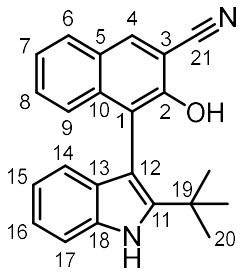
FTIR (neat) ν = 2961, 2852, 1459, 1378, 1263, 1204, 1149, 746 cm^{-1};

HRMS (ESI^+) m/z Calcd. for $C_{22}H_{21}ON^{79}Br$ $(M+H)^+$ 394.0801, found 394.0801;

HPLC ChiralPak IB (5% *i*-PrOH in hexane, 1.0 mL min^{-1}, T= 25 °C, 276 nm); τ_R (minor) = 10.4 min, τ_R (major) = 17.4 min;

e.r. = 85:15

4-(2-(tert-Butyl)-1H-indol-3-yl)-3-hydroxy-2-naphthonitrile (3.45)



The title compound was prepared according to the general procedure B using 3-hydroxy-2-naphthonitrile (**3.38**) (22.3 mg, 0.10 mmol), 2-(tert-butyl)-1H-indole (26.0 mg, 0.15 mmol) and 2,6-bis((S)-4-(naphthalen-1-yl)-4,5-dihydrooxazol-2-yl)pyridine (**3.45**) (5.6 mg, 0.012 mmol). The crude product was purified by flash column chromatography [silica gel, 33% CH_2Cl_2 in pentane] to afford the product as a yellow foam (1.4 mg, 0.004 mmol, 4%).

^{1}H NMR (400 MHz, DMSO) δ = 11.10 (s, 1H, OH), 9.29 (s, 1H, NH), 8.48 (s, 1H, H4), 8.01 – 7.89 (m, 1H, 9), 7.43 (dt, *J* = 8.0, 1.0, 1H, 17), 7.42 – 7.33 (m, 2H, H7 and H8), 7.12 – 7.09 (m, 1H, H6), 7.06 (ddd, *J* = 8.0, 7.0, 1.0, 1H, H16), 6.81 (ddd, *J* = 8.0, 7.0, 1.0, 1H, H15), 6.61 (d, *J* = 8.0, 1H, H14), 1.16 (s, 9H, H20);

^{13}C NMR (101 MHz, DMSO) δ 152.5 (C2), 146.1 (C11), 137.1 (C18), 135.6 (C10), 135.0 (C4), 129.4 (C5), 129.0 (C7), 128.6 (C9), 126.9 (C13), 125.1 (C6), 123.9 (C8), 120.7 (C16), 118.6 (C15), 117.9 (C14), 117.7 (C21), 117.3 (C3), 110.8 (C17), 101.8 (C1), 100.6 (C12), 33.2 (C19), 29.8 (C20);

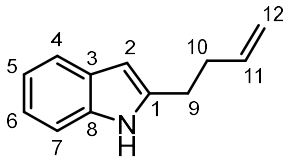
FTIR (neat) ν = 3372, 2917, 2229, 1622, 1598, 1458, 1380, 1323, 1218, 1202, 749, 720 cm^{-1};

HRMS (ESI^+) m/z Calcd. for $C_{23}H_{21}ON_2(M+H)^+$ 341.1648, found 341.1649;

HPLC ChiralPak IG (20% *i*-PrOH in hexane, 1.0 mL min^{-1}, T= 25 °C, 276 nm); τ_R (minor) = 4.8 min, τ_R (major) = 5.7 min;

e.r. = 66:34

2-(But-3-en-1-yl)-1H-indole (3.51)



Prepared according to a modified literature method and the data are in agreement with those previously reported.[131] A solution of 2-methylindole (1.00 g, 7.62 mmol, 1.00 equiv.) in anhydrous Et_2O (23 mL) was cooled to 0 °C and *n*-BuLi (1.6 M in hexanes, 14.3 mL, 22.86 mmol, 3.00 equiv.), potassium *tert*-butoxide (1.70 g, 15.24 mmol, 2.00 equiv.) and THF (15 mL) added sequentially. The mixture was stirred for 30 min at 20 °C, and cooled to -78 °C, and allyl bromide (1.83 g, 1.32 mL, 15.24 mmol, 2.00 equiv.) added dropwise over 5 min. After 2 h at -78 °C, the mixture was warmed to room temperature and MeOH (5 mL) was added and stirred for 1h. Additional MeOH (20 mL) was added, and the mixture left to stir for 18 h. The mixture was diluted with water and extracted three times with Et_2O. The combined organic extracts were washed with brine, dried over $MgSO_4$, filtered and concentrated *in vacuo*. The crude product was purified by flash column chromatography [silica gel, 5% EtOAc in pentane] to afford the product as a colourless low melting point solid (0.37 g, 2.13 mmol, 28%);

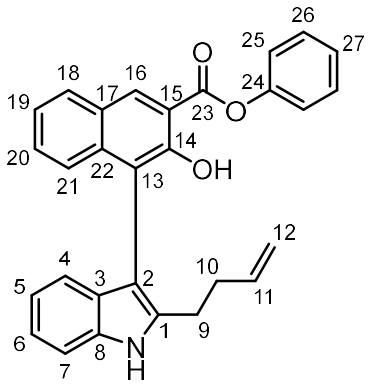
^{1}H NMR (400 MHz, $CDCl_3$) δ = 7.91 (s, 1H, NH), 7.53 (dt, *J* = 7.5, 1.0, 1H, H4), 7.30 (dq, *J* = 8.0, 1.0, 1H, H7), 7.17 – 7.03 (m, 2H, H5 and H6), 6.26 (dt, *J* = 2.0, 1.0, 1H, H2), 5.93 (ddt, *J* = 17.0, 10.0, 6.5, 1H, H11), 5.13 (dq, *J* = 17.0, 1.5, 1H, $H12_{trans}$), 5.06 (dq, *J* = 10.0, 1.5, 1H, $H12_{cis}$), 2.98 – 2.79 (m, 2H, H9), 2.55 – 2.43 (m, 2H, H10);

^{13}C NMR (101 MHz, $CDCl_3$) δ 139.3 (C8), 137.8 (C11), 136.0 (C1), 128.9 (C3), 121.2 (C6), 120.0 (C4), 119.8 (C5), 115.8 (C12), 110.5 (C7), 99.9 (C2), 33.4 (C10), 27.8 (C9);

FTIR (neat) ν = 3403, 1458, 1415, 1287, 997, 912, 783, 748 cm^{-1};

HRMS (ESI^+) m/z Calcd. for $C_{12}H_{14}N$ $(M+H)^+$ 172.1121, found 172.1120

Phenyl 4-(2-(but-3-en-1-yl)-1H-indol-3-yl)-3-hydroxy-2-naphthoate (3.55)



The title compound was prepared according to the general procedure B using phenyl 3-hydroxy-2-naphthoate (26.4 mg, 0.10 mmol), 2-(but-3-en-1-yl)-1H-indole (**3.51**) (25.7 mg, 0.15 mmol) and 2,6-bis((S)-4-(naphthalen-1-yl)-4,5-dihydrooxazol-2-yl)pyridine (**3.26**) (5.6 mg, 0.012 mmol). The crude product was purified by flash column chromatography [silica gel, 33% CH_2Cl_2 in pentane] to afford the product as a yellow foam (29.9mg, 0.069 mmol, 69%).

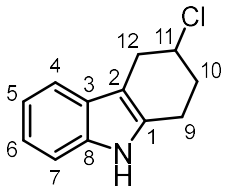
^{1}H NMR (400 MHz, $CDCl_3$) δ = 10.42 (d, *J* = 0.5, 1H, OH), 8.87 (s, 1H, H16), 8.27 (s, 1H, NH), 8.11 – 7.89 (m, 1H, H21), 7.61 – 7.53 (m, 1H, H18), 7.50 (m, 2H, H25), 7.45 – 7.29 (m, 6H, H7, H19, H20, H26, and H27), 7.17 (ddd, *J* = 8.0, 7.0, 1.5, 1H, H6), 7.08 (d, *J* = 8.0, 1H, H4), 7.02 (ddd, *J* = 8.0, 7.0, 1.0, 1H, H5), 5.82 (ddt, *J* = 17.0, 10.0, 6.5, 1H, H11), 5.15 – 4.90 (m, 2H, H12), 2.78 (td, *J* = 7.5, 1.5, 2H, H9), 2.38 (dtd, *J* = 9.0, 7.5, 7.0, 1.5, 2H, H10).

^{13}C NMR (101 MHz, $CDCl_3$) δ 169.3 (C23), 154.8 (C14), 150.4 (C24), 138.5 (C1), 138.1 (C11), 137.8 (C8), 135.7 (C22), 132.9 (C16), 129.9 (C25), 129.8 (C21), 129.5 (C27), 129.0 (C17), 127.3 (C3), 126.7 (C20), 126.1 (C18), 124.1 (C6), 121.9 (C26), 121.5 (C19), 119.9 (C5), 119.5 (C4), 117.1 (C15), 115.8 (C12), 113.6 (C13), 110.8 (C7), 106.6 (C2), 33.2 (C10), 26.6 (C9).

FTIR (neat) v = 3411, 2934, 1687, 1459, 1317, 1284, 1202, 1163, 792, 737, 689 cm^{-1};

HRMS (ESI^-) m/z Calcd. for $C_{29}H_{22}O_3N$ $(M-H)^-$ 432.1605, found 432.1597

3-Chloro-2,3,4,9-tetrahydro-1H-carbazole (3.52)



A screw-top vial was charged with $FeCl_3$ (anhydrous, 1.6 mg, 0.010 mmol, 0.067 equiv.) and indole **3.51** (25.7 mg, 0.15 mmol, 1.00 equiv.) under air. The solids were dissolved in [1:1] CH_2Cl_2/HFIP (1 mL) and tBuOOtBu (21.9 mg, 27 µL, 0.15 mmol, 1.00 equiv.) was added. The reaction was then stirred for 16 h at room temperature. After this time, the mixture filtered through a short plug of silica [eluting liberally with CH_2Cl_2]. The filtrate was concentrated in vacuo and the residue was purified by flash column chromatography [silica gel, 5% EtOAc in pentane] to afford the product as a white solid (10.6 mg, 0.051 mmol, 34%,).

M.P. = 107–108 °C;

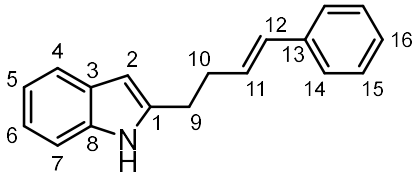
^{1}H NMR (400 MHz, $CDCl_3$) δ = 7.73 (s, 1H, NH), 7.51 – 7.38 (m, 1H, H4), 7.29 (dt, *J* = 8.0, 1.0, 1H, H7), 7.15 (ddd, *J* = 8.0, 7.0, 1.5, 1H, H6), 7.13 – 7.08 (m, 1H, H5), 4.52 (dddd, *J* = 8.0, 7.0, 5.0, 3.0, 1H, H11), 3.33 (ddq, *J* = 16.0, 5.0, 1.5, 1H, H12'), 3.09 – 3.03 (m, 1H, H12''), 3.03 – 2.93 (m, 1H, H9'), 2.85 (dddt, *J* = 16.5, 7.5, 6.0, 1.5, 1H, H9''), 2.41 – 2.22 (m, 2H, H10);

^{13}C NMR (101 MHz, $CDCl_3$) δ 136.2 (C8), 132.2 (C1), 127.4 (C3), 121.7 (C6), 119.6 (C5), 117.9 (C4), 110.7 (C7), 107.5 (C2), 56.7 (C11), 32.5 (C10), 32.0 (C12), 21.5 (C9);

FTIR (neat) v = 3403, 2919, 2849, 1466, 1432, 1260, 1328, 1280, 1258, 1237, 1200, 1143, 1009, 913, 861, 743, 667, 664 cm^{-1};

HRMS (ESI^+) m/z Calcd. for $C_{12}H_{13}N^{35}Cl$ $(M+H)^+$ 172.1121, found 172.1120

(E)-2-(4-Phenylbut-3-en-1-yl)-1H-indole (3.91)



Prepared according to a modified literature method.[132]

Into anhydrous CH_2Cl_2 (4.6 mL) degassed with argon was added 2-(but-3-en-1-yl)-1H-indole (**3.51**) (150 mg, 0.88 mmol, 1.00 equiv.), *trans*-stilbene (631 mg, 3.51 mmol, 4.00 equiv.), and second-generation Grubbs catalyst (29.8 mg, 0.035 mmol, 0.040 equiv.). The mixture was stirred for 18 h at 40 °C, after which the solvent was removed *in vacuo* and the residue purified by flash column chromatography [silica gel, 0–5% EtOAc in pentane] to afford the product as a brown solid (126 mg, 0.51 mmol, 58%).

M.P. = 110–113 °C;

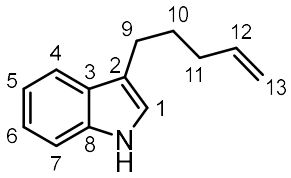
^{1}H NMR (400 MHz, $CDCl_3$) δ = 7.92 (s, 1H, NH), 7.54 (dd, *J* = 7.5, 1.5, 1H, H4), 7.40 – 7.27 (m, 5H, H7, H14, and H15), 7.26 – 7.19 (m, 1H, H16), 7.16 – 7.05 (m, 2H, H5 and H6), 6.49 (dt, *J* = 16.0, 1.5, 1H, H12), 6.37 – 6.27 (m, 2H, H2 and H11), 3.07 – 2.87 (m, 2H, H9), 2.74 – 2.57 (m, 2H, H10);

^{13}C NMR (101 MHz, $CDCl_3$) δ = 139.1 (C8), 137.6 (C13), 136.0 (C1), 131.2 (C12), 129.5 (C11), 128.9 (C3), 128.7 (C15), 127.3 (C16), 126.2 (C14), 121.3 (C6), 120.0 (C4), 119.8 (C5), 110.5 (C7), 100.0 (C2), 32.8 (C10), 28.4 (C9);

FTIR (neat) ν = 3407, 1457, 1419, 1288, 967, 784, 745, 709, 694, 649 cm^{-1};

HRMS (ESI^+) m/z Calcd. for $C_{18}H_{18}N$ $(M+H)^+$ 248.1434, found 248.1435

3-(Pent-4-en-1-yl)-1H-indole (3.107)



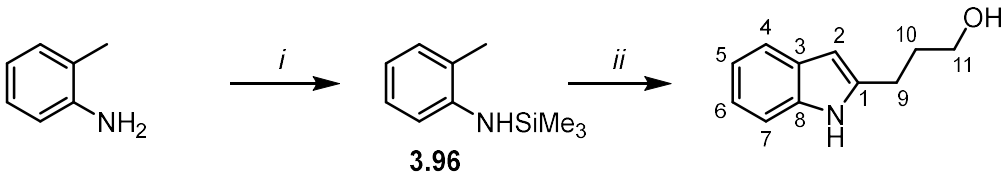
Prepared according to a modified literature method and the data are in agreement with those previously reported.[133] Indole (0.58 g, 4.91 mmol, 1.50 equiv.) was dissolved in benzene (5 mL) and MeMgI (3 M in anhydrous Et_2O, 1.7 mL, 5.24 mmol, 1.60 equiv.) was added dropwise. 5-Bromopentene (0.4 mL, 3.28 mmol, 1.00 equiv.) was added and the mixture stirred at 80 °C for 27 h. The reaction mixture was cooled and quenched with sat. $NH_4Cl_{(aq.)}$. The organic phase was separated, and the aqueous phase extracted with EtOAc twice. The organic layer was washed with water and brine, dried over $MgSO_4$, and concentrated *in vacuo*. The residue was purified by flash column chromatography [silica gel, 5% EtOAc in pentane] to afford the product as a pink oil (305 mg, 1.10 mmol, 34%)

^{1}H NMR (400 MHz, $CDCl_3$) δ = 7.89 (s, 1H, NH), 7.62 (dd, *J* = 8.0, 1.0 Hz, 1H, H4), 7.36 (dt, *J* = 8.0, 1.0 Hz, 1H, H7), 7.20 (ddd, *J* = 8.0, 7.0, 1.5 Hz, 1H, H6), 7.12 (ddd, *J* = 8.0, 7.0, 1.0 Hz, 1H, H5), 6.98 (dt, *J* = 2.0, 1.0 Hz, 1H, H1), 5.88 (ddt, *J* = 17.0, 10.0, 6.5 Hz, 1H, H12), 5.32 – 4.84 (m, 2H, H13), 2.83 – 2.75 (m, 2H, H9), 2.27 – 2.12 (m, 2H, H11), 1.83 (tt, *J* = 8.5, 7.0 Hz, 2H, H10).

^{13}C NMR (101 MHz, $CDCl_3$) δ = 139.0 (C12), 136.5 (C8), 127.7 (C3), 122.0 (C6), 121.3 (C1), 119.23 (C5), 119.13 (C4), 116.88 (C2), 114.70 (C13), 111.2 (C7), 33.8 (C11), 29.5 (C10), 24.7 (C9).

HRMS (ESI^+) m/z Calcd. for $C_{13}H_{16}N$ $(M+H)^+$ 186.1277, found 186.1271

3-(1H-Indol-2-yl)propan-1-ol (3.97)



3.96

Error! Bookmark not defined. Prepared according to a modified literature method and the data are in agreement with those previously reported.[134]

i. A stirred mixture of *o*-toluidine (1.07 g, 10 mmol, 1.00 equiv.), hexamethyldisilazane (6.48 mL, 31 mmol, 3.1 equiv.), and LiI (26.8 mg, 0.2 mmol, 0.02 equiv.) was treated with chlorotrimethylsilane (76 µL, 0.6 mmol, 0.06 equiv.) and heated to 126 °C. After 22 h, the excess HMDS was removed *in vacuo* to give a crude sample of **3.96** as a brown oil.

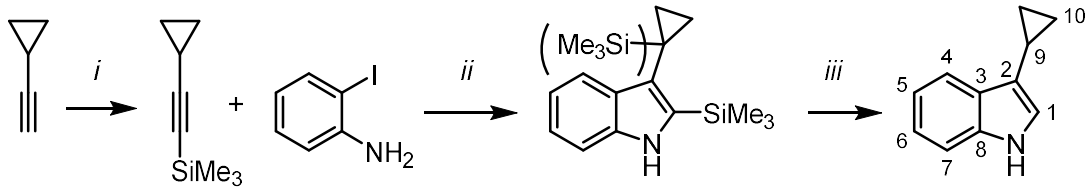
ii. The crude sample of **3.96** was dissolved in anhydrous hexane (65 mL) and *n*-BuLi solution (2.5 M in hexanes, 8 mL, 20 mmol, 2.00 equiv.) added dropwise. The solution was heated to 69 °C for 6 h and allowed to cool to room temperature. The solution was added *via* cannula to a stirred solution of γ-butyrolactone (0.84 mL, 11 mmol, 1.10 equiv.) in THF (40 mL) at -78 °C. The mixture was allowed to warm to room temperature and stirred for 30 min, before being diluted with Et_2O (100 mL) and quenched with ice water (100 mL). The organic phase was extracted three times with Et_2O. The combined organic extracts were washed with brine, dried over Na_2SO_4, and concentrated *in vacuo*. The residue was purified by flash column chromatography [silica gel, 20-40% EtOAc in pentane] to afford the product as a brown oil (324 mg, 1.80 mmol, 18%)

^{1}H NMR (400 MHz, $CDCl_3$) δ = 8.19 (s, 1H, NH), 7.53 (ddt, *J* = 7.5, 1.5, 1.0 Hz, 1H, H4), 7.30 (dq, *J* = 8.0, 1.0 Hz, 1H, H7), 7.17 – 7.03 (m, 2H, H5 and H6), 6.26 (dq, *J* = 2.0, 1.0 Hz, 1H, H2), 3.76 (t, *J* = 6.0 Hz, 2H, H11), 2.90 (td, *J* = 7.0, 1.0 Hz, 2H, H9), 1.98 (tt, *J* = 7.5, 6.9 Hz, 2H, H10).

^{13}C NMR (101 MHz, $CDCl_3$) δ 139.1 (C1), 136.0 (C8), 128.8 (C3), 121.1, (C6), 119.8 (C4), 119.6 (C5), 110.4 (C7), 99.7 (C2), 62.2 (C11), 31.7 (C10), 24.7 (C9).

HRMS (ESI^+) m/z Calcd. for $C_{11}H_{14}NO$ $(M+H)^+$ 176.1070, found 176.1075

3-Cyclopropyl-1H-indole (3.114)



3.110 3.112/3.113 3.114

Prepared according to a modified literature method and the data are in agreement with those previously reported.[135]

i. To a stirring solution of cyclopropylacetylene (1.27 mL, 15 mmol, 1.00 equiv.) in anhydrous THF (5 mL) at -78 °C was added *n*-BuLi (1.5 M in hexanes, 10.7 mL, 15.5 mmol, 1.03 equiv.) dropwise. The solution was allowed to stir for 30 min at this temperature, after which chlorotrimethylsilane (1.98 mL, 15.6 mmol, 1.04 equiv.) was added. The reaction mixture was then stirred at -78 °C for 1 h. The reaction mixture was then warmed to room temperature, diluted with and filtered through a pad of Na_2SO_4 layered on silica gel, eluting with pentane/Et_2O (4:1). The filtrate was concentrated under reduced pressure to afford **3.110**, which was used without further purification.

ii. $Pd(dppf)Cl_2$ (817 mg, 10 mmol, 0.10 equiv.), **3.110** (1.52 g, 11 mmol, 1.10 equiv.), 2-iodoaniline (2.19 g, 10 mmol, 1.00 equiv.), sodium carbonate (3.18 g, 30 mmol, 3.00 equiv.) and lithium chloride (445 mg, 10.5 mmol, 1.05 equiv.) in anhydrous sparged DMF (200 mL) were heated at 100 °C for 18 h. The reaction mixture was then cooled to room temperature, diluted with Et_2O (300 mL) and washed with sat. $NH_4Cl_{(aq)}$ (500 mL) and water (500mL). The organic layer was then dried over Na_2SO_4, filtered and concentrated to afford an inseparable mixture of **3.112** and **3.113** which was carried on to the next step as a mixture.

iii. To the inseparable mixture **3.112** and **3.113** was added tetra-*n*-butylammonium fluoride (464 mg, 4.98 mmol, 1.50 equiv.) in anhydrous THF (7 mL). This mixture was refluxed for 4 h before quenching with water and extracting into CH_2Cl_2. The combined organic extracts were washed

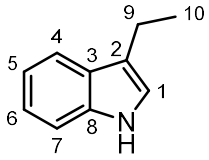
with brine, dried over Na_2SO_4, and concentrated *in vacuo*. The residue was resubjected to the procedure as the reaction had not reached completion. Upon repetition, the residue was purified by flash column chromatography [silica gel, 2-5% Et_2O in pentane] to afford the product as a yellow solid (375 mg, 2.39 mmol, 24%).

^{1}H NMR (400 MHz, $CDCl_3$) δ 7.82 (s, 1H, NH), 7.75 (d, *J* = 8.0 Hz, 1H, H4), 7.34 (d, *J* = 8.0 Hz, 1H, H7), 7.20 (ddd, *J* = 8.0, 7.0, 1.5 Hz, 1H, H6), 7.13 (td, *J* = 7.5, 1.0 Hz, 1H, H5), 6.92 – 6.87 (m, 1H, H1), 1.96 (tdd, *J* = 8.0, 5.5, 4.5 Hz, 1H, H9), 0.95 – 0.83 (m, 2H, H10'), 0.69 – 0.61 (m, 2H, H10'').

^{13}C NMR (101 MHz, $CDCl_3$) δ 136.5 (C8), 128.3 (C3), 122.2 (C6), 120.5 (C1), 119.3 (3C, C2, C4 and C5), 111.2 (C7), 6.3 (C9), 6.1 (C10).

HRMS (ESI$^+$) m/z Calcd. for $C_{11}H_{12}N$ $(M+H)^+$ 158.0964, found 158.0964

3-Ethyl-1*H*-indole (3.164)



The title compound was prepared according to a modified literature procedure. The data are consistent with those previously reported.[116]

Lithium aluminium hydride solution (2M in THF, 1.67 mL, 3.35 mmol, 2.70 equiv.) was diluted in anhydrous THF (1 mL) and cooled to 0 °C. 3-Acetylindole (200 mg, 1.26 mmol) was added. The mixture was allowed to warm to room temperature and stirred for 4 h. Additional lithium aluminium hydride solution (2M, 1.67 mL, 3.35 mmol, 2.70 equiv.) was added and left to stir for another 16 h, producing a white suspension. The reaction was cooled to 0 °C, then water (0.25 mL), aqueous NaOH solution (15%, 0.25 mL), and water (0.75 mL) were added dropwise sequentially. The slurry was stirred vigorously for 30 min, diluted with Et_2O and anhydrous $MgSO_4$ was added. The suspension was filtered over Celite and washed with Et_2O. The solvent was

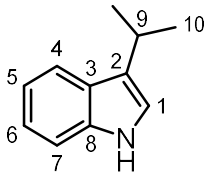
removed under reduced pressure and no further purification was necessary, producing the product (0.12 g, 0.80 mmol, 64%) as a brown solid.

^{1}H NMR (400 MHz, $CDCl_3$) δ 7.88 (s, 1H, NH), 7.63 (dq, *J* = 8.0, 1.0, 1H, H4), 7.36 (dt, *J* = 8.0, 1.0, 1H, H7), 7.20 (ddd, *J* = 8.0, 7.0, 1.0, 1H, H6), 7.12 (ddd, *J* = 8.0, 7.0, 1.0, 1H, H5), 6.98 (dt, *J* = 2.0, 1.0, 1H, H1), 2.81 (qd, *J* = 7.5, 1.0, 2H, H9), 1.35 (t, *J* = 7.5, 3H, H10).

^{13}C NMR (101 MHz, $CDCl_3$) δ = 136.6 (C8), 127.6 (C3), 122.0 (C6), 120.5 (C1), 119.2 (C5), 119.1 (C4), 119.0 (C2), 111.2 (C7), 18.5 (C9), 14.6 (C10).

LRMS (ESI^+) *m/z* Calcd. for $C_8H_{12}N$ $(M+H)^+$ 146.1, found 146.1

3-Isopropy-1*H*-indole (3.165)



The title compound was prepared according to a modified literature procedure. The data are consistent with those previously reported.[136]

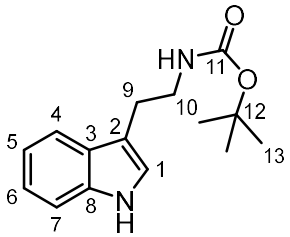
Triethylsilane (0.98 mL, 6.15 mmol, 2.40 equiv.) and trichloroacetic acid (628 mg, 3.85 mmol, 1.50 equiv.) were dissolved in toluene (1.3 mL) and warmed to 70 °C. Indole (300 mg, 2.56 mmol, 1.00 equiv.) was dissolved in acetone (208 µL, 2.82 mmol, 1.1 equiv.) and toluene (1.3 mL). The indole solution was added dropwise to the warmed mixture and stirred for 1 h at 70 °C. The reaction was quenched with an aqueous solution of Na_2CO_3 (10%, 10 mL). The organic layer was separated, washed twice with water, dried over anhydrous $MgSO_4$, and concentrated under reduced pressure. The crude material was purified by flash column chromatography (5% Et_2O in pentane) to afford the product (0.276 g, 1.74 mmol, 67%) as a brown solid.

^{1}H NMR (400 MHz, $CDCl_3$) δ = 7.88 (s, 1H, NH), 7.67 (ddt, *J* = 8.0, 1.5, 1.0, 1H, H4), 7.36 (dt, *J* = 8.0, 1.0, 1H, H7), 7.19 (ddd, *J* = 8.0, 7.0, 1.5, 1H, H6), 7.11 (ddd, *J* = 8.0, 7.0, 1.0, 1H, H5), 6.96 (dd, *J* = 2.0, 1.0, 1H, H1), 3.22 (pd, *J* = 7.0, 2.0, 1H, H9), 1.38 (d, *J* = 7.0, 6H, H10).

^{13}C NMR (101 MHz, $CDCl_3$) δ = 136.7 (C8), 128.4 (C3), 124.2 (C2), 122.0 (C6), 119.5 (C4), 119.3 (C1), 119.1 (C5), 111.2 (C7), 25.6 (C9), 23.5 (C10).

LRMS (ESI^+) *m/z* Calcd. for $C_7H_{14}N$ $(M+H)^+$ 160.1, found 160.1

tert-Butyl (2-(1H-indol-3-yl)ethyl)carbamate (S1)



The title compound was prepared according to a modified literature procedure. The data are consistent with those previously reported. [137]

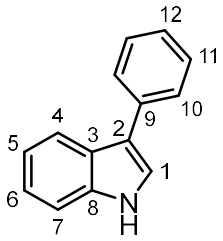
Tryptamine (0.50 g, 3.12 mmol, 1.00 equiv.) was dissolved in dioxane (2.5 mL). NEt_3 (0.9 mL, 6.45 mmol, 2.10 equiv.) and a solution of Boc_2O (0.75 g, 3.43 mmol, 1.10 equiv.) in dioxane (2.5 mL) were added. The mixture was stirred at room temperature for 1 h, and the resulting solution concentrated *in vacuo*. The crude residue was purified by flash column chromatography (1:2 pentane/Et_2O) to afford the product as white solid (0.801 g, 3.08 mmol, 99%).

^{1}H NMR (400 MHz, $CDCl_3$) δ = 8.09 (s, 1H, NH), 7.61 (dt, *J* = 8.0, 1.0, 1H, H4), 7.37 (dt, *J* = 8.0, 1.0, 1H, H7), 7.21 (ddd, *J* = 8.0, 7.0, 1.0, 1H, H6), 7.12 (ddd, *J* = 8.0, 7.0, 1.0, 1H, H5), 7.03 (s, 1H, H1), 4.60 (s, 1H, NH), 3.49 (q, *J* = 7.0, 1H, H10), 2.96 (td, *J* = 7.0, 1.0, 1H, H9), 1.44 (s, 9H, H13).

^{13}C NMR (101 MHz, $CDCl_3$) δ = 156.2 (C11), 136.5 (C8), 127.5 (C3), 122.3 (C6), 122.1 (C1), 119.6 (C5), 119.0 (C4), 113.3 (C2), 111.3 (C7), 66.0 (C12), 41.1 (C10), 28.6 (C13), 26.0 (C9)

HRMS (ESI^+) m/z Calcd. for $C_{15}H_{20}N_2O_2$ $(M+H)^+$ 261.1598, found 261.1597

3-Phenyl-1*H*-indole (3.168)



The title compound was prepared according to a modified literature procedure. The data are consistent with those previously reported.[138]

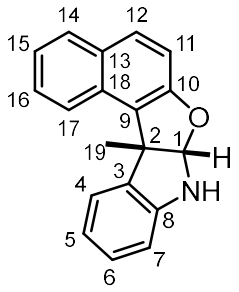
2.10 g of 70:30 dimethyl urea/L-tartaric acid was heated to 70 °C to obtain a clear melt. Phenyl hydrazine hydrochloride (200 mg, 1.39 mmol, 1.00 equiv.) and phenylacetaldehyde (162 µL, 1.39 mmol, 1.00 equiv.) were added and the mixture stirred at 70 °C for 0.25 h. The reaction was quenched by adding water (5 mL) while still hot and then being allowed to cool to room temperature. The crude product was extracted twice with CH_2Cl_2 (5 mL) and the combined organic layers washed with water. The organic layer was dried over Na_2SO_4, and the solvent removed under reduced pressure. The crude product was purified by flash column chromatography [silica gel, 5% EtOAc in pentane] to give the product as a brown solid (113 mg, 0.585 mmol, 42%).

^{1}H NMR (400 MHz, $CDCl_3$) δ = 8.23 (s, 1H, NH), 7.99 – 7.92 (m, 1H, H4), 7.73 – 7.62 (m, 2H, H10), 7.53 – 7.41 (m, 3H, H11 and H7), 7.38 (d, *J* = 2.5, 1H, H1), 7.32 – 7.17 (m, 3H, H5, H6, and H12).

^{13}C NMR (101 MHz, $CDCl_3$) δ 136.3 (C8), 135.5 (C3), 128.9 (C11), 127.7 (C10), 126.1 (C16), 126.1 (C2), 122.6 (C12), 121.9 (C1), 120.5 (C5), 120.0 (C4), 118.9 (C9), 111.5 (C7).

LRMS (ESI^+) *m/z* Calcd. for $C_{14}H_{12}N$ $(M+H)^+$ 194.1, found 194.1

12b-Methyl-7a,12b-dihydro-8H-naphtho[1',2':4,5]furo[2,3-b]indole (3.171)



Prepared according to General Procedure A with 2-naphthol (14.4 mg) and 3-methylindole (19.7 mg). Crude product was purified by flash column chromatography [silica gel, 5% EtOAc in toluene] to afford the product as a yellow oil (22 mg, 0.080 mmol, 80%).

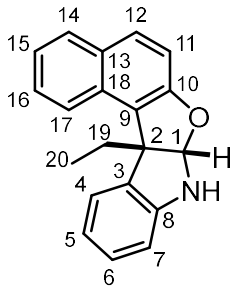
^{1}H NMR (400 MHz, $CDCl_3$) δ = 8.32 (dq, *J* = 8.5, 1.0, 1H, H17), 7.84 – 7.77 (m, 1H, H14), 7.67 – 7.64 (m, 1H, H12), 7.63 – 7.59 (m, 1H, H4), 7.57 (ddd, *J* = 8.5, 7.0, 1.5, 1H, H16), 7.33 (ddd, *J* = 8.0, 7.0, 1.0, 1H, H15), 7.11 (d, *J* = 8.5, 1H, H11), 7.06 (td, *J* = 7.5, 1.0, 1H, H6), 6.76 (td, *J* = 7.5, 1.0, 1H, H5), 6.70 (dt, *J* = 8.0, 1.0, 1H, H7), 6.14 (d, *J* = 2.5, 1H, H1), 5.03 (s, 1H, NH), 2.01 (s, 3H, H19);

^{13}C NMR (101 MHz, $CDCl_3$) δ 156.9 (C10), 147.5 (C8), 133.5 (C3), 130.6 (C18), 130.4 (C13), 129.9 (C12), 129.7 (C14), 128.3 (C6), 126.9 (C16), 124.2 (C4), 122.9 (C9), 122.8 (C15), 122.6 (C17), 119.8 (C5), 112.6 (C11), 109.5 (C7), 105.5 (C1), 58.2 (C2), 25.0 (C19);

FTIR (neat) ν = 3402, 3053, 2924, 2852, 1718, 1627, 1610, 1520, 1483, 1371, 1352, 1314, 1259, 1241, 1202, 1155, 1106, 1018, 977, 928, 899, 867, 813, 751, 667, 653, 621 cm^{-1};

HRMS (ESI^+) *m/z* Calcd. For $C_{19}H_{16}ON$ $(M+H)^+$ 274.1226, found 274.1224.

12b-Ethyl-7a,12b-dihydro-8H-naphtho[1',2':4,5]furo[2,3-b]indole (3.172)



Prepared according to General Procedure A with 2-naphthol (14.4 mg) and 3-ethylindole **3.164** (21.7 mg). The crude product was purified by flash column chromatography [silica gel, 5% EtOAc in toluene] to the product as a yellow oil (20 mg, 0.070 mmol, 70%).

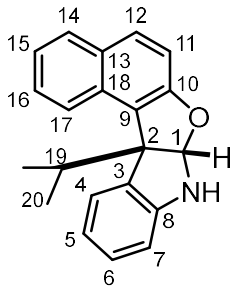
^{1}H NMR (400 MHz, $CDCl_3$) δ = 8.28 (d, *J* = 8.5, 1H, H17), 7.80 (dd, *J* = 8.0, 1.5, 1H, H14), 7.64 (d, *J* = 8.5, 1H, H12), 7.61 – 7.55 (m, 1H, H4), 7.59 – 7.50 (m, 1H, H16), 7.36 – 7.27 (m, 1H, H15), 7.10 (d, *J* = 9.0, 1H, H11), 7.05 (td, *J* = 7.5, 1.0, 1H, H6), 6.75 (td, *J* = 7.5, 1.0, 1H, H5), 6.69 (d, *J* = 7.5, 1H, H7), 6.27 (s, 1H, H1), 5.03 (s, 1H, NH), 2.62 (dq, *J* = 14.5, 7.5, 1H, H19'), 2.27 (dq, *J* = 14.5, 7.5, 1H, H19''), 0.89 (t, *J* = 7.5, 3H, H20).

^{13}C NMR (101 MHz, $CDCl_3$) δ 157.6 (C10), 147.8 (C8), 132.7 (C3), 130.9 (C18), 130.3 (C13), 129.9 (C12), 129.7 (C14), 128.2 (C6), 126.9 (C16), 124.3 (C4), 122.8 (C15), 122.4 (C17), 120.8 (C9), 119.7 (C5), 112.6 (C11), 109.4 (C7), 102.3 (C1), 63.5 (C2), 30.1 (C19), 9.2 (C20).

FTIR (neat) v = 3412, 3056, 2926, 2855, 1627, 1610, 1519, 1483, 1461, 1372, 1345, 1314, 1261, 1239, 1192, 1154, 1137, 1082, 1036, 992, 959, 897, 813, 744, 646

HRMS (ESI^+) *m/z* Calcd. For $C_{20}H_{18}ON$ $(M+H)^+$ 288.1383, found 288.1380

12b-Isopropyl-7a,12b-dihydro-8H-naphtho[1',2':4,5]furo[2,3-b]indole (3.173)



Prepared according to General Procedure A with 2-naphthol (14.4 mg) and 3-isopropylindole **3.165** (23.9 mg). The crude product was purified by flash column chromatography [silica gel, 2.5% EtOAc in toluene] to afford the product as a yellow oil (8.2 mg, 0.027 mmol, 27%).

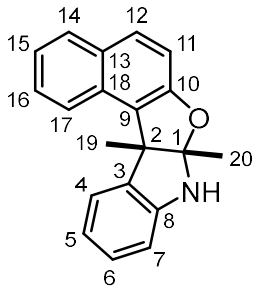
^{1}H NMR (400 MHz, $CDCl_3$) δ = 8.30 (dd, *J* = 8.5, 1.0, 1H, H17), 7.82 – 7.75 (m, 1H, H14), 7.62 (d, *J* = 8.5, 1H, H12), 7.59 (dd, *J* = 7.5, 1.0, 1H, H4), 7.57 – 7.49 (m, 1H, H16), 7.30 (ddd, *J* = 8.0, 7.0, 1.0, 1H, H15), 7.08 (d, *J* = 8.5, 1H, H11), 7.02 (td, *J* = 7.5, 1.0, 1H, H6), 6.73 (td, *J* = 7.5, 1.0, 1H, H5), 6.65 (dt, *J* = 8.0, 1.0, 1H, H7), 6.35 (s, 1H, H1), 3.30 (p, *J* = 7.0, 1H, H19), 0.90 – 0.86 (m, 6H, H20' and H20'')

^{13}C NMR (101 MHz, $CDCl_3$) δ 129.9 (C12), 129.7 (C14), 128.1 (C6), 126.9 (C16), 124.0 (C4), 122.8 (C15), 122.5 (C17), 119.6 (C5), 112.5 (C11), 109.2 (C7), 98.4 (C1), 33.1 (C19), 18.1 (C20). Quaternary carbons could not be observed.

FTIR (neat) ν = 3415, 3056, 2963, 2872, 1621, 1597, 1518, 1464, 1385, 1344, 1263, 1212, 1145, 1098, 1028, 817, 747, 630

HRMS (ESI^+) *m/z* Calcd. For $C_{21}H_{20}ON$ $(M+H)^+$ 302.1539, found 302.1536

7a,12b-Dimethyl-7a,12b-dihydro-8H-naphtho[1',2':4,5]furo[2,3-b]indole (3.174)



Prepared according to General Procedure A with 2-naphthol (14.4 mg) and 2,3-dimethylindole (21.7 mg). The crude product was purified by flash column chromatography [silica gel, 5% EtOAc in toluene] to afford the product as yellow oil (15 mg, 0.052 mmol, 52%).

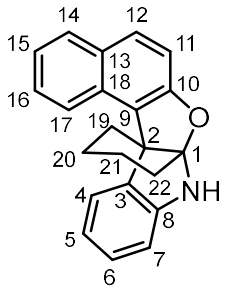
^{1}H NMR (400 MHz, $CDCl_3$) δ = 8.31 (dd, *J* = 8.5, 1.0, 1H, H17), 7.83 – 7.71 (m, 1H, H14), 7.69 – 7.61 (m, 1H, H12), 7.61 – 7.45 (m, 2H, H4 and H16), 7.30 (ddd, *J* = 8.0, 7.0, 1.0, 1H, H15), 7.08 (d, *J* = 8.5, 1H, H11), 7.03 (td, *J* = 7.5, 1.5, 1H, H6), 6.76 (td, *J* = 7.5, 1.0, 1H, H5), 6.64 (dt, *J* = 8.0, 1.0, 1H, H7), 1.92 (s, 3H, H19), 1.73 (s, 3H, H20).

^{13}C NMR (101 MHz, $CDCl_3$) δ 155.7 (C10), 146.8 (C8), 133.4 (C3), 130.7 (C18), 130.3 (C13), 129.7 (C12), 129.5 (C14), 128.0 (C6), 126.7 (C16), 124.3 (C4), 122.9 (C9), 122.6 (C15), 122.0 (C17), 119.5 (C5), 112.5 (C11), 110.9 (C1), 109.0 (C7), 58.6 (C2), 21.2 (C19), 20.9 (C20).

FTIR (neat) ν = 3381, 3054, 2927, 2854, 1626, 1610, 1519, 1484, 1471, 1439, 1383, 1350, 1322, 1278, 1240, 1208, 1175, 1154, 1121, 1071, 1016, 978, 862, 810, 745, 703

HRMS (ESI^+) *m/z* Calcd. For $C_{20}H_{18}ON$ $(M+H)^+$ 288.1383, found 288.1380.

8H-7a,12b-Butanonaphtho[1',2':4,5]furo[2,3-b]indole (3.175)



Prepared according to General Procedure A with 2-naphthol (14.4 mg) and 1,2,3,4-tetrahydrocarbazole (25.7 mg). The crude product was purified by flash column chromatography [silica gel, 5% EtOAc in toluene] to afford the product as a yellow oil (28 mg, 0.088 mmol, 88%).

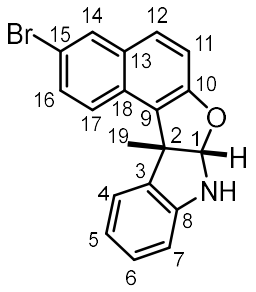
^{1}H NMR (400 MHz, $CDCl_3$) δ = 8.27 (dd, *J* = 8.5, 1.0, 1H, H17), 7.80 (dt, *J* = 8.0, 1.0, 1H, H14), 7.64 (d, *J* = 8.7, 1H, H12), 7.56 – 7.48 (m, 2H, H4 and H16), 7.31 (ddd, *J* = 8.0, 7.0, 1.0, 1H, H15), 7.08 (d, *J* = 8.5, 1H, H11), 7.05 (td, *J* = 7.5, 1.0, 1H, H6), 6.76 (td, *J* = 7.5, 1.0, 1H, H5), 6.72 – 6.66 (m, 1H, H7), 2.61 (ddd, *J* = 14.0, 7.0, 5.5, 1H, H19'), 2.44 – 2.32 (m, 1H, H19''), 2.25 – 2.06 (m, 2H, H22), 1.61 (ddt, *J* = 12.5, 8.0, 6.0, 2H, H21), 1.51 – 1.39 (m, 2H, H20).

^{13}C NMR (101 MHz, $CDCl_3$) δ 156.7 (C10), 147.5 (C8), 133.3 (C3), 131.1 (C18), 130.4 (C13), 129.7 (C12), 129.6 (C14), 128.1 (C6), 126.7 (C16), 124.3 (C4), 122.7 (C15), 122.7 (C9), 122.3 (C17), 119.8 (C5), 112.7 (C11), 109.6 (C7), 109.4 (C1), 59.0 (C2), 31.9 (C19), 30.8 (C22), 19.1 (C21), 18.8 (C20).

FTIR (neat) ν = 3381, 3054, 2942, 2862, 1626, 1610, 1520, 1469, 1371, 1351, 1320, 1268, 1205, 1073, 982, 903, 810, 743, 703, 629

HRMS (ESI$^+$) *m/z* Calcd. For $C_{22}H_{20}ON$ $(M+H)^+$ 314.1539, found 314.1534

3-Bromo-12b-methyl-7a,12b-dihydro-8H-naphtho[1',2':4,5]furo[2,3-b]indole (3.186)



Prepared according to General Procedure A with 6-bromo-2-naphthol (22.3 mg) and 3-methylindole (19.7 mg). Crude product was purified by flash column chromatography [silica gel, 5% EtOAc in toluene] to afford the product as a yellow oil (15.8 mg, 0.056 mmol, 56%).

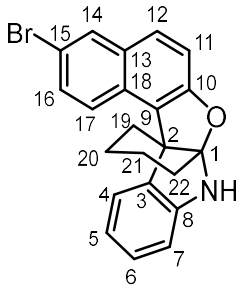
^{1}H NMR (400 MHz, $CDCl_3$) δ 8.18 (d, *J* = 9.0 Hz, 1H, H17), 7.95 (d, *J* = 2.0 Hz, 1H, H14), 7.62 (dd, *J* = 8.0, 2.0 Hz, 1H, H16), 7.57 – 7.50 (m, 2H, H4 and H12), 7.10 (d, *J* = 9.0 Hz, 1H, H11), 7.06 (td, *J* = 7.5, 1.0 Hz, 1H, H6), 6.76 (td, *J* = 7.5, 1.0 Hz, 1H, H5), 6.70 (dt, *J* = 8.0, 1.0 Hz, 1H, H7), 6.14 (s, 1H, H1), 1.97 (s, 3H, H19).

^{13}C NMR (101 MHz, $CDCl_3$) δ 157.3 (C10), 147.4 (C8), 133.1 (C3), 131.5 (C14), 130.1 (C16), 129.9 (C18), 129.0 (2C, C12 and C13), 128.4 (C6), 124.2 (C17), 124.0 (C4), 119.9 (C5), 119.0 (C15), 116.3 (C9), 113.7 (C11), 109.5 (C7), 105.5 (C1), 58.1 (C2), 24.9 (C19).

FTIR (neat) ν = 3410, 2960, 2928, 2361, 2340, 1683, 1623, 1608, 1589, 1576, 1506, 1484, 1469, 1449, 1415, 1376, 1353, 1314, 1261, 1241, 1203, 1191, 1154, 1132, 1106, 1068, 1023, 975, 908, 878, 816, 803, 745, 734, 680, 651, 631

HRMS (ESI^+) *m/z* Calcd. For $C_{19}H_{15}{}^{79}BrNO$ $(M+H)^+$ 352.0332, found 352.0322

3-Bromo-8H-7a,12b-butanonaphtho[1',2':4,5]furo[2,3-b]indole (3.191)



Prepared according to General Procedure A with 6-bromo-2-naphthol (22.3 mg) and 1,2,3,4-tetrahydrocarbazole (25.7 mg). Crude product was purified by flash column chromatography [silica gel, 5% EtOAc in toluene] to afford the product as a yellow oil (30mg, 0.076 mmol, 76%).

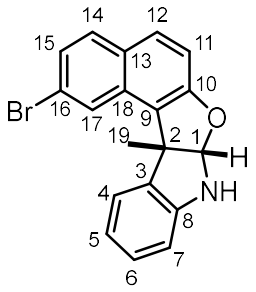
^{1}H NMR (400 MHz, $CDCl_3$) δ 8.13 (d, *J* = 9.0 Hz, 1H, H17), 7.95 (d, *J* = 2.0 Hz, 1H, H14), 7.58 (dd, *J* = 9.0, 2.0 Hz, 1H, H16), 7.54 (d, *J* = 9.0 Hz, 1H, H12), 7.44 (dd, *J* = 7.5, 1.0 Hz, 1H, H4), 7.10 (d, *J* = 8.5 Hz, 1H, H11), 7.05 (td, *J* = 7.5, 1.0 Hz, 1H, H6), 6.76 (td, *J* = 7.5, 1.0 Hz, 1H, H5), 6.68 (dt, *J* = 8.0, 1.0 Hz, 1H, H7), 2.54 (ddd, *J* = 14.0, 7.5, 5.0 Hz, 1H, H19'), 2.36 (ddd, *J* = 14.0, 7.5, 4.5 Hz, 1H, H19''), 2.21 – 2.10 (m, 2H, H22), 1.69 – 1.55 (m, 2H, H21), 1.50 – 1.39 (m, 2H, H20).

^{13}C NMR (101 MHz, $CDCl_3$) δ 157.0 (C10), 147.5 (C8), 132.7 (C3), 131.4 (C18), 131.3 (C14), 129.9 (C16), 129.4 (C13), 128.6 (C12), 128.1 (C6), 124.0 (C17), 123.8 (C4), 123.0 (C15), 119.7 (C5), 116.7 (C9), 113.7 (C11), 109.5 (C1), 109.4 (C7), 58.69 (C2), 31.8 (C19), 30.6 (C22), 19.0 (C21), 18.6 (C20).

FTIR (neat) ν = 3388, 2940, 2866, 2246, 1622, 1609, 1584, 1504, 1483, 1468, 1402, 1374, 1348, 1319, 1276, 1256, 1223, 1204, 1156, 1118, 1072, 1024, 1003, 983, 952, 909, 878, 814, 801, 733, 649

HRMS (ESI^+) *m/z* Calcd. For $C_{22}H_{19}{}^{79}BrNO$ $(M+H)^+$ 392.0645, found 392.0651

2-Bromo-12b-methyl-7a,12b-dihydro-8H-naphtho[1',2':4,5]furo[2,3-b]indole (3.187)



Prepared according to General Procedure A with 7-bromo-2-naphthol (22.3 mg) and 3-methylindole (19.7 mg). Crude product was purified by flash column chromatography [silica gel, 10% EtOAc in toluene] to afford the product as a yellow oil (6 mg, 0.017 mmol, 17%).

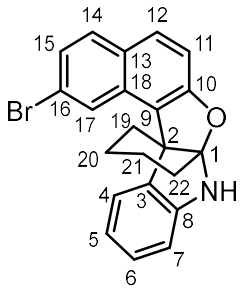
^{1}H NMR (400 MHz, $CDCl_3$) δ 8.42 (d, *J* = 2.0 Hz, 1H, H17), 7.66 (d, *J* = 8.5 Hz, 1H, H14), 7.63 – 7.58 (m, 1H, H12), 7.56 – 7.51 (m, 1H, H4), 7.38 (dd, *J* = 8.5, 2.0 Hz, 1H, H15), 7.14 – 7.04 (m, 2H, H6 and H11), 6.80 (td, *J* = 7.5, 1.0 Hz, 1H, H5), 6.71 (dt, *J* = 7.5, 1.0 Hz, 1H, H7), 6.15 (s, 1H, H1), 1.98 (s, 3H, H19).

^{13}C NMR (101 MHz, $CDCl_3$) δ 157.6 (C10), 147.2 (C8), 132.8 (C18), 131.7 (C13), 131.1 (C14), 129.8 (C12), 128.6 (C16), 128.3 (C6), 126.1 (C15), 124.7 (C17), 123.9 (C4), 122.1 (C3), 121.3 (C9), 119.9 (C5), 112.9 (C11), 109.4 (C7), 105.5 (C1), 57.9 (C2), 24.75 (C19).

FTIR (neat) ν = 3400, 2962, 2926, 2851, 1722, 1621, 1578, 1505, 1484, 1469, 1448, 1376, 1353, 1312, 1266, 1239, 1205, 1111, 1069, 1023, 992, 909, 868, 832, 750, 734, 647, 626

HRMS (ESI^+) *m/z* Calcd. For $C_{19}H_{15}{}^{79}BrNO$ $(M+H)^+$ 352.0332, found 352.0336

2-Bromo-8H-7a,12b-butanonaphtho[1',2':4,5]furo[2,3-b]indole (3.192)



Prepared according to General Procedure A with 7-bromo-2-naphthol (22.3 mg) and 1,2,3,4-tetrahydrocarbazole (25.7 mg). Crude product was purified by flash column chromatography [silica gel, 5% EtOAc in toluene] to afford the product as a yellow oil (24mg, 0.061 mmol, 61%).

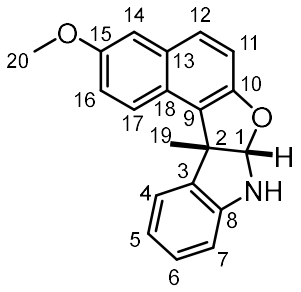
^{1}H NMR (400 MHz, $CDCl_3$) δ 8.38 (d, *J* = 2.0 Hz, 1H, H17), 7.65 (d, *J* = 9.0 Hz, 1H, H14), 7.60 (d, *J* = 9.0 Hz, 1H, H12), 7.53 – 7.42 (m, 1H, H4), 7.37 (dd, *J* = 9.0, 2.0 Hz, 1H, H15), 7.13 – 6.99 (m, 2H, H6 and H11), 6.79 (td, *J* = 7.5, 1.0 Hz, 1H, H5), 6.68 (dt, *J* = 7.5, 9.0 Hz, 1H, H7), 2.55 (ddd, *J* = 14.0, 7.0, 5.0 Hz, 1H, H19'), 2.36 (ddd, *J* = 14.0, 7.5, 5.0 Hz, 1H, H19''), 2.20 – 2.10 (m, 2H, H22), 1.60 (ddt, *J* = 12.5, 7.5, 6.0 Hz, 2H, H21), 1.51 – 1.38 (m, 2H, H20).

^{13}C NMR (101 MHz, $CDCl_3$) δ 157.5 (C10), 147.4 (C8), 132.6 (C18), 132.0 (C13), 131.0 (C14), 129.6 (C12), 128.5 (C16), 128.1 (C6), 126.0 (C15), 124.4 (C17), 124.0 (C4), 122.0 (C3), 121.2 (C9), 119.8 (C5), 113.0 (C11), 109.6 (C1), 109.4 (C7), 58.6 (C2), 31.7 (C19), 30.6 (C22), 18.9 (C21), 18.6 (C20).

FTIR (neat) ν = 3396, 2955, 2938, 2362, 1726, 1620, 1576, 1504, 1483, 1468, 1445, 1435, 1409, 1374, 1351, 1319, 1272, 1254, 1205, 1151, 1117, 1065, 984, 909, 860, 832, 804, 770, 758, 734, 650

HRMS (ESI^+) *m/z* Calcd. For $C_{22}H_{19}{}^{79}BrNO$ $(M+H)^+$ 392.0645, found 392.0649

3-Methoxy-12b-methyl-7a,12b-dihydro-8H-naphtho[1',2':4,5]furo[2,3-b]indole (3.188)



Prepared according to General Procedure A with 6-methoxy-2-naphthol (17.4 mg) and 3-methylindole (19.7 mg). Crude product was purified by flash column chromatography [silica gel, 10% EtOAc in toluene] to afford the product as a yellow oil (6 mg, 0.020 mmol, 20%).

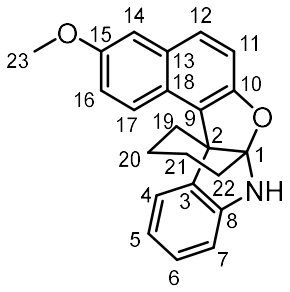
^{1}H NMR (400 MHz, $CDCl_3$) δ 8.22 (d, *J* = 9.0 Hz, 1H, H17), 7.59 – 7.50 (m, 2H, H4 and H12), 7.26 – 7.21 (m, 1H, H16), 7.14 (d, *J* = 2.5 Hz, 1H, H14), 7.09 – 7.01 (m, 2H, H6 and H11), 6.75 (td, *J* = 7.5, 1.0 Hz, 1H, H5), 6.69 (dt, *J* = 8.0, 1.0 Hz, 1H, H7), 6.11 (s, 1H, H1), 3.90 (s, 3H, H20), 1.98 (s, 3H, H19).

^{13}C NMR (101 MHz, $CDCl_3$) δ 155.4 (C10), 155.3 (C15), 147.5 (C8), 133.4 (C18), 132.5 (C13), 128 (2C, C6 and C12), 125.9 (C3), 124.1 (2C, C4 and C17), 123.2 (C9), 119.8 (C5), 119.6 (C16), 112.9 (C11), 109.5 (C7), 107.9 (C14), 105.2 (C1), 58.3 (C2), 55.5 (C20), 25.0 (C19).

FTIR (neat) ν = 2959, 2925, 2853, 2360, 2340, 2251, 1610, 1583, 1521, 1485, 1468, 1451, 1425, 1372, 1314, 1271, 1234, 1201, 1169, 1109, 1086, 1038, 1022, 975, 932, 909, 853, 821, 801, 737, 700, 638

HRMS (ESI^+) *m/z* Calcd. For $C_{20}H_{18}NO_2$ $(M+H)^+$ 304.1332, found 304.1325

3-Methoxy-8H-7a,12b-butanonaphtho[1',2':4,5]furo[2,3-b]indole (3.193)



Prepared according to General Procedure A with 6-methoxy-2-naphthol (17.4 mg) and 1,2,3,4-tetrahydrocarbazole (25.7 mg). Crude product was purified by flash column chromatography [silica gel, 10% EtOAc in toluene] to afford the product as a yellow oil (10mg, 0.030 mmol, 30%).

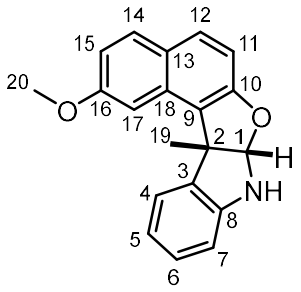
^{1}H NMR (400 MHz, $CDCl_3$) δ 8.17 (d, *J* = 9.0 Hz, 1H, H17), 7.61 – 7.50 (m, 1H, H12), 7.49 – 7.41 (m, 1H, H4), 7.21 (dd, *J* = 9.0, 2.5 Hz, 1H, H16), 7.14 (d, *J* = 2.5 Hz, 1H, H14), 7.07 – 7.00 (m, 2H, H6 and H11), 6.75 (td, *J* = 7.5, 1.0 Hz, 1H, H5), 6.67 (dt, *J* = 7.5, 1.0 Hz, 1H, H7), 3.89 (s, 3H, H23), 2.61 – 2.48 (m, 1H, H19), 2.43 – 2.30 (m, 1H, H19), 2.23 – 2.06 (m, 2H, H22), 1.66 – 1.51 (m, 2H, H21), 1.49 – 1.38 (m, 2H, H20).

^{13}C NMR (101 MHz, $CDCl_3$) δ 155.3 (C10), 155.1 (C15), 147.7 (C8), 133.2 (C18), 131.3 (C13), 128.1 (2C, C6 and C12), 126.3 (C3), 124.2 (C4), 123.8 (C17), 123.1 (C9), 119.7 (C5), 119.4 (C16), 113.0 (C11), 109.5 (C7), 109.1 (C1), 107.8 (C14), 59.0 (C2), 55.4 (C23), 32.1 (C19), 30.9 (C22), 19.3 (C21), 18.9 (C20).

FTIR (neat) ν = 3393, 2958, 2922, 2852, 2359, 1723, 1611, 1601, 1519, 1484, 1466, 1425, 1371, 1354, 1320, 1268, 1238, 1204, 1168, 1113, 1087, 1038, 1002, 984, 909, 851, 821, 800, 735, 650

HRMS (ESI^+) *m/z* Calcd. For $C_{23}H_{21}NO_2Na$ $(M+Na)^+$ 366.1465, found 366.1450

2-Methoxy-12b-methyl-7a,12b-dihydro-8H-naphtho[1',2':4,5]furo[2,3-b]indole (3.189)



Prepared according to General Procedure A with 7-methoxy-2-naphthol (17.4 mg) and 3-methylindole (19.7 mg). Crude product was purified by flash column chromatography [silica gel, 10% EtOAc in toluene] to afford the product as a yellow oil (6 mg, 0.020 mmol, 20%)

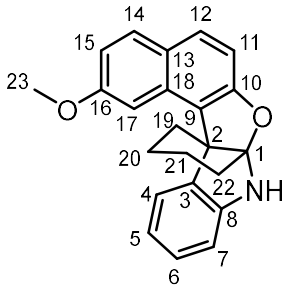
^{1}H NMR (400 MHz, $CDCl_3$) δ 7.70 (d, *J* = 9.0 Hz, 1H, H14), 7.65 – 7.52 (m, 3H, H4, H12, and H17), 7.06 (td, *J* = 7.5, 1.0 Hz, 1H, H6), 6.99 (dd, *J* = 9.0, 2.5 Hz, 1H, H15), 6.95 (d, *J* = 8.5 Hz, 1H, H11), 6.76 (td, *J* = 7.5, 1.0 Hz, 1H, H5), 6.70 (dt, *J* = 7.5, 1.0 Hz, 1H, H7), 6.13 (s, 1H, H1), 4.03 (s, 3H, H20), 1.99 (s, 3H, H19).

^{13}C NMR (101 MHz, $CDCl_3$) δ 158.4 (C10), 157.4 (C16), 147.6 (C8), 133.4 (C18), 131.7 (C13), 131.1 (C14), 129.7 (C12), 128.3 (C6), 125.8 (C3), 123.9 (C4), 121.9 (C9), 119.7 (C5), 114.9 (C15), 110.1 (C11), 109.5 (C7), 105.5 (C1), 102.0 (C17), 58.0 (C2), 55.5 (C20), 24.4 (C19).

FTIR (neat) ν = 3406, 2943, 2867, 2842, 1776, 1712, 1631, 1585, 1518, 1484, 1470, 1451, 1429, 1380, 1314, 1260, 1243, 1227, 1208, 1180, 1133, 1107, 1039, 1020, 998, 909, 832, 736, 668, 644, 620

HRMS (ESI^+) *m/z* Calcd. For $C_{20}H_{18}NO_2$ $(M+H)^+$ 304.1332, found 304.1325

2-Methoxy-8H-7a,12b-butanonaphtho[1',2':4,5]furo[2,3-b]indole (3.194)



Prepared according to General Procedure A with 6-methoxy-2-naphthol (17.4 mg) and 1,2,3,4-tetrahydrocarbazole (25.7 mg). Crude product was purified by flash column chromatography [silica gel, 10% EtOAc in toluene] to afford the product as a yellow oil (19 mg, 0.056 mmol, 56%)

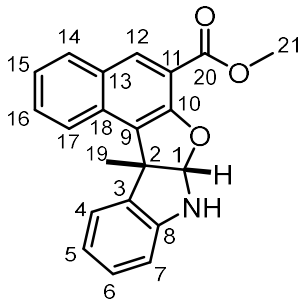
^{1}H NMR (400 MHz, $CDCl_3$) δ 7.69 (d, *J* = 9.0 Hz, 1H, H14), 7.61 – 7.51 (m, 3H, H4, H12, and H17), 7.05 (td, *J* = 7.5, 1.0 Hz, 1H, H6), 7.01 – 6.93 (m, 2H, H11 and H15), 6.77 (td, *J* = 7.5, 1.0 Hz, 1H, H5), 6.68 (dd, *J* = 8.0, 1.0 Hz, 1H, H7), 4.01 (s, 3H, H23), 2.61 – 2.35 (m, 2H, H19), 2.25 – 2.04 (m, 2H, H22), 1.61 (tt, *J* = 8.0, 6.0 Hz, 2H, H21), 1.46 (ddt, *J* = 9.5, 7.0, 4.0 Hz, 2H, H20).

^{13}C NMR (101 MHz, $CDCl_3$) δ 158.3 (C10), 157.1 (C16), 147.8 (C8), 132.9 (C18), 132.1 (C13), 131.0 (C14), 129.4 (C12), 128.1 (C6), 125.8 (C3), 124.1 (C4), 121.9 (C9), 119.5 (C5), 114.8 (C15), 110.2 (C11), 109.6 (C7), 109.3 (C1), 101.6 (C17), 58.6 (C2), 55.5 (C23), 31.5 (C19), 30.8 (C22), 19.2 (C21), 18.8 (C20).

FTIR (neat) ν = 3396, 2937, 2865, 2248, 1630, 1584, 1518, 1484, 1468, 1430, 1405, 1381, 1365, 1319, 1272, 1233, 1219, 1206, 1174, 1149, 1133, 1036, 1022, 984, 909, 857, 828, 733, 650, 629

HRMS (ESI^+) *m/z* Calcd. For $C_{23}H_{22}NO_2$ $(M+H)^+$ 344.1645, found 344.1636

Methyl 12b-methyl-7a,12b-dihydro-8H-naphtho[1',2':4,5]furo[2,3-b]indole-6-carboxylate (3.224)



Prepared according to General Procedure B with methyl 3-hydroxy-2-naphthoate (20 mg), 3-methylindole (20 mg), and 2,6-bis((S)-4-(naphthalen-1-yl)-4,5-dihydrooxazol-2-yl)pyridine (**3.26**) (5.6 mg, 0.012 mmol). The crude product was purified by flash column chromatography [silica gel, 5% EtOAc in toluene] to afford the product as a yellow oil (18 mg, 0.054 mmol, 54%).

^{1}H NMR (400 MHz, $CDCl_3$) δ = 8.36 (s, 1H, H12), 8.34 (dd, *J* = 8.5, 1.0, 1H, H17), 7.92 – 7.83 (m, 1H, H14), 7.64 (ddd, *J* = 8.5, 7.0, 1.5, 1H, H16), 7.60 – 7.54 (m, 1H, H4), 7.36 (ddd, *J* = 8.0, 7.0, 1.0, 1H, H15), 7.05 (td, *J* = 7.5, 1.0, 1H, H6), 6.74 (td, *J* = 7.5, 1.0, 1H, H5), 6.69 (dt, *J* = 7.5, 1.0, 1H, H7), 6.26 (dd, *J* = 2.5, 1.0, 1H, H1), 5.22 (s, 1H, NH), 3.95 (s, 3H, H21), 2.01 (s, 3H, H19).

^{13}C NMR (101 MHz, $CDCl_3$) δ 165.6 (C20), 155.7 (C10), 147.5 (C8), 133.4 (C12), 132.9 (C3), 132.8 (C13), 131.0 (C14), 129.3 (C18), 129.2 (C16), 128.5 (C6), 125.4 (C11), 124.1 (C4), 123.7 (C15), 122.6 (C17), 119.7 (C5), 115.3 (C9), 109.5 (C7), 106.2 (C1), 57.3 (C2), 52.3 (C21), 24.8 (C19).

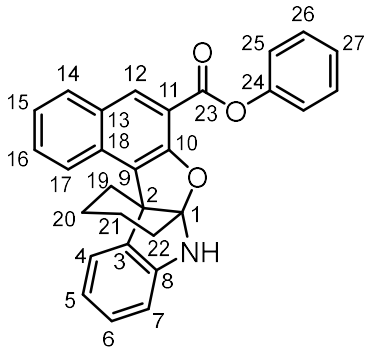
FTIR (neat) ν = 3381, 3055, 2358, 1718, 1629, 1610, 1516, 1483, 1456, 1363, 1343, 1304, 1232, 1207, 1168, 1134, 1072, 989, 971, 896, 793, 743, 703, 617

HRMS (ESI^+) m/z Calcd. For $C_{21}H_{18}O_3N$ $(M+H)^+$ 332.1281, found 332.1278

HPLC ChiralPak IB (20% *i*-PrOH in hexane, 1.0 mL min^{-1}, T= 25 °C, 276 nm); τ_R (minor) = 10.7 min, τ_R (major) = 18.4 min;

e.r. = 73:27

Phenyl 8H-7a,12b-butanonaphtho[1',2':4,5]furo[2,3-b]indole-6-carboxylate (3.225)



Prepared according to General Procedure B with phenyl 3-hydroxy-2-naphthoate (26.4 mg), 1,2,3,4-tetrahydrocarbazole (25.7 mg), and 2,6-bis((S)-4-(naphthalen-1-yl)-4,5-dihydrooxazol-2-yl)pyridine (**3.26**) (5.6 mg, 0.012 mmol). The crude product was purified by flash column chromatography [silica gel, 5% EtOAc in toluene] to afford the product as a yellow oil (13.3 mg, 0.031 mmol, 31%).

^{1}H NMR (400 MHz, $CDCl_3$) δ 8.54 (s, 1H, H12), 8.33 (dd, *J* = 8.5, 1.0 Hz, 1H, H17), 7.92 (dd, *J* = 8.5, 1.5 Hz, 1H, H14), 7.63 (ddd, *J* = 8.5, 7.0, 1.5 Hz, 1H, H16), 7.50 – 7.39 (m, 3H, H4 and H26), 7.37 (ddd, *J* = 8.0, 7.0, 1.0 Hz, 1H, H15), 7.29 – 7.23 (m, 3H, H25 and H27), 7.05 (td, *J* = 7.5, 1.0 Hz, 1H, H6), 6.74 (td, *J* = 7.5, 1.0 Hz, 1H, H5), 6.68 (d, *J* = 7.5 Hz, 1H, H7), 2.65 (ddd, *J* = 14.0, 8.0, 4.5 Hz, 1H, H19'), 2.44 – 2.37 (m, 1H, H19''), 2.28 – 2.20 (m, 2H, H22), 1.69 – 1.55 (m, 2H, H21), 1.53 – 1.41 (m, 2H, H20).

^{13}C NMR (101 MHz, $CDCl_3$) δ 163.4 (C23), 156.3 (C10), 151.1 (C24), 147.7 (C8), 133.6 (C13), 133.5 (C12), 132.8 (C18), 131.1 (C14), 129.5 (C26), 129.3 (C16), 129.2 (C11), 128.3 (C6), 125.9 (C27), 125.6 (C3), 124.1 (C4), 123.6 (C15), 122.3 (C17), 122.0 (C25), 119.7 (C5), 114.7 (C9), 110.4 (C1), 109.6 (C7), 58.3 (C2), 32.1 (C19), 30.8 (C22), 19.3 (C21), 18.9 (C20).

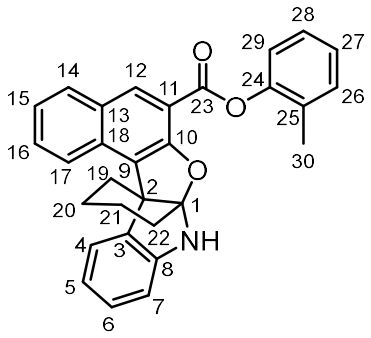
FTIR (neat) ν = 3057, 2948, 2869, 2359, 2336, 2252, 1734, 1628, 1610, 1592, 1514, 1492, 1471, 1454, 1409, 1345, 1303, 1277, 1219, 1192, 1163, 1120, 1093, 1073, 1043, 1018, 982, 910, 875, 799, 782, 735, 689, 646, 630

HRMS (ESI^+) *m/z* Calcd. For $C_{29}H_{24}NO_3$ $(M+H)^+$ 434.1751, found 434.1744

HPLC ChiralPak IB (20% *i*-PrOH in hexane, 1.0 mL min^{-1}, T= 25 °C, 276 nm); τ_R (minor) = 10.9 min, τ_R (major) = 12.4 min;

e.r. = 74:26

o-Tolyl 8H-7a,12b-butanonaphtho[1',2':4,5]furo[2,3-b]indole-6-carboxylate (3.237)



Prepared according to General Procedure B with o-tolyl 3-hydroxy-2-naphthoate (27.8 mg), 1,2,3,4-tetrahydrocarbazole (25.7 mg) and 2,6-bis((S)-4-(4-methoxyphenyl)-4,5-dihydrooxazol-2-yl)pyridine (**3.233**) (5.2 mg, 0.012 mmol). Crude product was purified by flash column chromatography [silica gel, 10% EtOAc in toluene] to afford the product as a yellow oil (18 mg, 0.039 mmol, 39%)

^{1}H NMR (400 MHz, $CDCl_3$) δ 8.56 (s, 1H, H12), 8.34 (dd, *J* = 8.5, 1.0 Hz, 1H, H17), 7.93 (dd, *J* = 8.5, 1.5 Hz, 1H, H14), 7.64 (ddd, *J* = 8.5, 7.0, 1.5 Hz, 1H, H16), 7.48 (dd, *J* = 7.5, 1.0 Hz, 1H, H4), 7.37 (ddd, *J* = 8.0, 7.0, 1.0 Hz, 1H, H15), 7.30 – 7.15 (m, 4H, H26, H27, H28, H29), 7.06 (td, *J* = 7.5, 1.0 Hz, 1H, H6), 6.75 (td, *J* = 7.5, 1.0 Hz, 1H, H5), 6.68 (dd, *J* = 7.5, 1.0 Hz, 1H, H7), 2.66 (ddd, *J* = 14.0,

8.0, 4.5 Hz, 1H, H19'), 2.44 – 2.37 (m, 1H, H19''), 2.29 (s, 3H, H30), 2.26 – 2.17 (m, 2H, H22), 1.62 (tdd, *J* = 15.0, 12.0, 7.0 Hz, 2H, H21), 1.48 (dqd, *J* = 13.5, 6.5, 4.5 Hz, 2H, H20).

^{13}C NMR (101 MHz, $CDCl_3$) δ 163.3 (C23), 156.3 (C10), 149.7 (C24), 147.7 (C8), 133.6 (C13), 133.5 (C12), 132.9 (C18), 131.2 (C26), 131.1 (C14), 130.5 (C25), 129.3 (C16), 129.2 (C11), 128.3 (C6), 126.9 (C28), 126.0 (C27), 125.6 (C3), 124.1 (C4), 123.6 (C15), 122.4 (C17), 122.3 (C29), 119.6 (C5), 114.7 (C9), 110.33 (C1), 109.6 (C7), 58.3 (C2), 32.1 (C19), 30.8 (C22), 19.3 (C21), 18.9 (C20), 16.6 (C30).

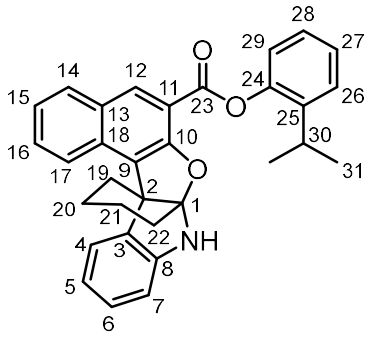
FTIR (neat) ν = 3389, 2962, 2926, 2855, 2364, 1737, 1629, 1611, 1512, 1490, 1469, 1452, 1362, 1345, 1304, 1262, 1222, 1199, 1175, 1159, 1111, 1046, 1016, 983, 911, 845, 820, 804, 784, 738, 705, 650, 628

HRMS (ESI^+) *m/z* Calcd. For $C_{30}H_{26}NO_3$ $(M+H)^+$ 488.1907, found 448.1906

HPLC ChiralPak IB (20% *i*-PrOH in hexane, 1.0 mL min^{-1}, T= 25 °C, 276 nm); τ_R (minor) = 8.8 min, τ_R (major) = 13.8 min;

e.r. = 83:17

2-Isopropylphenyl 8H-7a,12b-butanonaphtho[1',2':4,5]furo[2,3-b]indole-6-carboxylate (3.238)



Prepared according to General Procedure B with 2-isopropylphenyl 3-hydroxy-2-naphthoate (30.6 mg), 1,2,3,4-tetrahydrocarbazole (25.7 mg), and 2,6-bis((S)-4-(4-methoxyphenyl)-4,5-dihydrooxazol-2-yl)pyridine (**3.233**) (5.2 mg, 0.012 mmol). Crude product was purified by flash column chromatography [silica gel, 10% EtOAc in toluene] to afford the product as a yellow oil (25 mg, 0.053 mmol, 53%)

^{1}H NMR (400 MHz, $CDCl_3$) δ 8.47 (s, 1H, H12), 8.25 (dd, *J* = 8.5, 1.0 Hz, 1H, H17), 7.84 (dd, *J* = 8.5, 1.5 Hz, 1H, H14), 7.55 (ddd, *J* = 8.5, 7.0, 1.5 Hz, 1H, H16), 7.40 (dd, *J* = 7.5, 1.0 Hz, 1H, H4), 7.33 – 7.25 (m, 2H, H15 and H26), 7.20 – 7.13 (m, 2H, H27 and H28), 7.13 – 7.06 (m, 1H, H29), 6.97 (td, *J* = 7.5, 1.0 Hz, 1H, H6), 6.67 (td, *J* = 7.5, 1.0 Hz, 1H, H5), 6.60 (dd, *J* = 8.0, 1.0 Hz, 1H, H7), 3.15 (p, *J* = 7.0 Hz, 1H, H30), 2.57 (ddd, *J* = 14.0, 8.0, 4.5 Hz, 1H, H19'), 2.38 – 2.26 (m, 1H, H19''), 2.19 – 2.07 (m, 2H, H22), 1.62 – 1.47 (m, 2H. H21), 1.47 – 1.32 (m, 2H, H20), 1.22 – 1.14 (m, 6H, H31)

^{13}C NMR (101 MHz, $CDCl_3$) δ 163.6 (C23), 156.1 (C10), 148.4 (C24), 147.6 (C8), 140.3 (C25), 133.5 (C12), 133.4 (C13), 132.7 (C18), 131.0 (C14), 129.2 (C16), 129.1 (C11), 128.2 (C6), 126.6 (2C, C26 and C28), 126.1 (C27), 125.5 (C3), 124.0 (C4), 123.5 (C15), 122.7 (C29), 122.2 (C17), 119.5 (C5), 114.7 (C9), 110.26 (C1), 109.5 (C7), 58.2 (C2), 32.0 (C19), 30.6 (C22), 27.5 (C30), 23.1 (C31'), 23.0 (C31''), 19.1 (C21), 18.8 (C20).

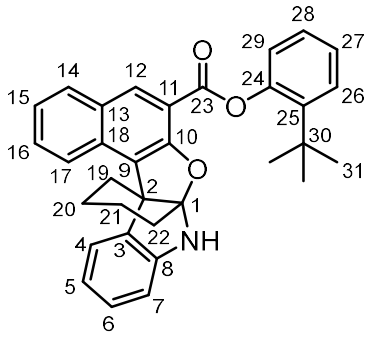
FTIR (neat) ν = 3394, 2962, 2920, 2851, 2252, 1735, 1689, 1629, 1594, 1514, 1487, 1469, 1450, 1363, 1344, 1303, 1276, 1236, 1219, 1197, 1178, 1160, 1119, 1083, 1044, 1015, 984, 909, 859, 809, 783, 752, 733, 646

HRMS (ESI^+) *m/z* Calcd. For $C_{32}H_{30}NO_3$ $(M+H)^+$ 476.2220, found 476.2220

HPLC ChiralPak IB (10% *i*-PrOH in hexane, 1.0 mL min^{-1}, T= 25 °C, 276 nm); τ_R (minor) = 9.1 min, τ_R (major) = 9.9 min;

e.r. = 78:22

2-(tert-Butyl)phenyl 8H-7a,12b-butanonaphtho[1',2':4,5]furo[2,3-b]indole-6-carboxylate (3.239)



Prepared according to General Procedure B with 2-(*tert*-butyl)phenyl 3-hydroxy-2-naphthoate (32.0 mg), 1,2,3,4-tetrahydrocarbazole (25.7 mg), and 2,6-bis((S)-4-(4-methoxyphenyl)-4,5-dihydrooxazol-2-yl)pyridine (**3.233**) (5.2 mg, 0.012 mmol). Crude product was purified by flash column chromatography [silica gel, 10% EtOAc in toluene] to afford the product as a yellow oil (14 mg, 0.029 mmol, 29%)

^{1}H NMR (400 MHz, $CDCl_3$) δ 8.57 (s, 1H, H12), 8.34 (dd, *J* = 8.5, 1.0 Hz, 1H, H17), 7.97 – 7.89 (m, 1H, H14), 7.63 (ddd, *J* = 8.4, 6.8, 1.3 Hz, 1H, H16), 7.49 (dd, *J* = 7.5, 1.0 Hz, 1H, H4), 7.45 (dd, *J* = 8.0, 2.0 Hz, 1H, H26), 7.37 (ddd, *J* = 8.0, 7.0, 1.0 Hz, 1H, H15), 7.29 – 7.18 (m, 2H, H27 and H28),

7.14 (dd, *J* = 8.0, 1.5 Hz, 1H, H29), 7.06 (td, *J* = 7.5, 1.0 Hz, 1H, H6), 6.75 (td, *J* = 7.5, 1.0 Hz, 1H, H15), 6.68 (d, *J* = 8.0 Hz, 1H, H7), 2.64 (ddd, *J* = 14.0, 7.5, 5.5 Hz, 1H, H19'), 2.43 (ddd, *J* = 14.0, 7.0, 5.0 Hz, 1H, H19''), 2.21 (dd, *J* = 7.0, 6.0 Hz, 2H, H22), 1.71 – 1.54 (m, 2H, H21), 1.53 – 1.46 (m, 2H, H20), 1.42 (s, 9H, H31).

^{13}C NMR (101 MHz, $CDCl_3$) δ 164.0 (C23), 156.0 (C10), 149.4 (C24), 147.7 (C8), 141.3 (C25), 133.9 (C12), 133.5 (C13), 132.7 (C18), 131.0 (C14), 129.2 (C16), 129.2 (C11), 128.2 (C6), 127.1 (C26), 126.8 (C28), 125.6 (C27), 125.6 (C3), 124.5 (C29), 124.1 (C4), 123.5 (C15), 122.2 (C17), 119.5 (C5), 114.8 (C9), 110.27 (C1), 109.4 (C7), 58.2 (C2), 52.5 (C30), 34.6 (C19), 31.9 (C22), 30.4 (C31), 19.1 (C21), 18.7 (C20).

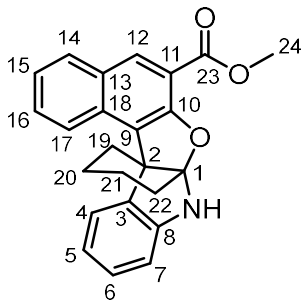
FTIR (neat) ν = 3391, 2951, 2869, 1733, 1723, 1629, 1610, 1594, 1513, 1486, 1469, 1441, 1363, 1344, 1304, 1277, 1235, 1220, 1185, 1160, 1119, 1088, 1056, 1038, 1016, 984, 910, 783, 752, 733, 687, 665, 647, 625

HRMS (ESI^+) *m/z* Calcd. For $C_{33}H_{32}NO_3$ $(M+H)^+$ 490.2377, found 490.2384

HPLC ChiralPak IB (10% *i*-PrOH in hexane, 1.0 mL min^{-1}, T= 25 °C, 276 nm); τ_R (minor) = 6.3 min, τ_R (major) = 7.3 min;

e.r. = 76:24

Methyl 8H-7a,12b-butanonaphtho[1',2':4,5]furo[2,3-b]indole-6-carboxylate (3.234)



Prepared according to General Procedure B with methyl 3-hydroxy-2-naphthoate (20 mg), 1,2,3,4-tetrahydrocarbazole (25.7 mg) and 2,6-bis((S)-4-(4-methoxyphenyl)-4,5-dihydrooxazol-2-yl)pyridine (**3.233**) (5.2 mg, 0.012 mmol)). Crude product was purified by flash column chromatography [silica gel, 5% EtOAc in toluene] to afford the product as a yellow oil (29 mg, 0.079 mmol, 79%).

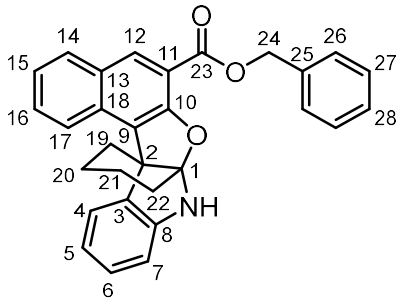
^{1}H NMR (400 MHz, $CDCl_3$) δ = 8.34 (s, 1H, H12), 8.30 (dd, *J* = 8.5, 1.0, 1H, H17), 7.86 (ddt, *J* = 8.0, 1.0, 0.5, 1H, H14), 7.59 (ddd, *J* = 8.5, 7.0, 1.5, 1H, H16), 7.45 (dd, *J* = 7.5, 1.2, 1H, H4), 7.38 – 7.29 (m, 1H, H15), 7.04 (td, *J* = 7.5, 1.0, 1H, H6), 6.72 (td, *J* = 7.5, 1.0, 1H, H5), 6.67 (dt, *J* = 7.5, 1.0, 1H, H7), 4.88, (s, 1H, NH), 3.93 (s, 3H, H24), 2.62 (ddd, *J* = 14.0, 8.0, 4.5, 1H, H19'), 2.43 – 2.31 (m, 1H, H19''), 2.31 – 2.10 (m, 2H, H22), 1.72 – 1.53 (m, 2H, H21), 1.45 (ddt, *J* = 10.0, 7.0, 4.5, 2H, H20).

^{13}C NMR (101 MHz, $CDCl_3$) δ 165.5 (C23), 155.8 (C10), 147.6 (C8), 133.1 (C13), 132.8 (C12), 132.8 (C18), 130.8 (C14), 129.1 (C3), 128.8 (C16), 128.1 (C6), 125.1 (C11), 124.0 (C4), 123.3 (C15), 122.2 (C17), 119.5 (C5), 115.3 (C9), 110.1 (C1), 109.5 (C7), 58.1 (C2), 52.1 (C24), 31.9 (C19), 30.6 (C22), 19.1 (C21), 18.7 (C20).

FTIR (neat) ν = 3731, 3380, 2926, 2855, 2363, 2341, 1719, 1627, 1457, 1344, 1308, 1252, 1205, 1165, 1074, 956, 910, 862, 821, 785, 741, 654, 634, 617

HRMS (ESI^+) *m/z* Calcd. For $C_{24}H_{22}O_3N$ $(M+H)^+$ 372.1594, found 372.1588

Benzyl 8H-7a,12b-butanonaphtho[1',2':4,5]furo[2,3-b]indole-6-carboxylate (3.236)



Prepared according to General Procedure B with benzyl 3-hydroxy-2-naphthoate (26.4 mg), 1,2,3,4-tetrahydrocarbazole (25.7 mg) and 2,6-bis((S)-4-(4-methoxyphenyl)-4,5-dihydrooxazol-2-yl)pyridine (**3.233**) (5.2 mg, 0.012 mmol). Crude product was purified by flash column chromatography [silica gel, 10% EtOAc in toluene] to afford the product as a yellow oil (32 mg, 0.071 mmol, 71%)

^{1}H NMR (400 MHz, $CDCl_3$) δ 8.37 (s, 1H. H12), 8.30 (d, *J* = 8.5 Hz, 1H, H17), 7.87 – 7.82 (m, 1H, H14), 7.59 (ddd, *J* = 8.5, 7.0, 1.5 Hz, 1H, H16), 7.54 – 7.48 (m, 2H, H26), 7.45 (dd, *J* = 7.5, 1.0 Hz, 1H, H4), 7.39 (tt, *J* = 6.5, 1.0 Hz, 2H, H27), 7.36 – 7.29 (m, 2H, H15 and H28), 7.04 (td, *J* = 7.5, 1.0 Hz, 1H, H6), 6.73 (td, *J* = 7.5, 1.0 Hz, 1H, H5), 6.66 (dt, *J* = 7.5, 1.0 Hz, 1H, H7), 5.59 – 5.27 (m, 2H, H24), 2.62 (ddd, *J* = 14.0, 8.0, 4.5 Hz, 1H, H19'), 2.43 – 2.34 (m, 1H, H19''), 2.23 (td, *J* = 7.0, 5.5 Hz, 2H, H22), 1.68 – 1.56 (m, 2H, H21), 1.50 – 1.39 (m, 2H, H20).

^{13}C NMR (101 MHz, $CDCl_3$) δ 164.8 (C23), 156.1 (C10), 147.7 (C8), 136.4 (C25), 133.2 (C18), 132.9 (C12), 132.8 (C13), 130.9 (C14), 129.2 (C11), 129.0 (C16), 128.6 (2C, C27), 128.2 (4C, C6, C26, and C28), 125.3 (C3), 124.1 (C4), 123.5 (C15), 122.3 (C17), 119.6 (C5), 115.3 (C9), 110.2 (C1), 109.5 (C7), 66.6 (C24), 58.2 (C2), 32.0 (C19), 30.7 (C22), 19.2 (C21), 18.9 (C20).

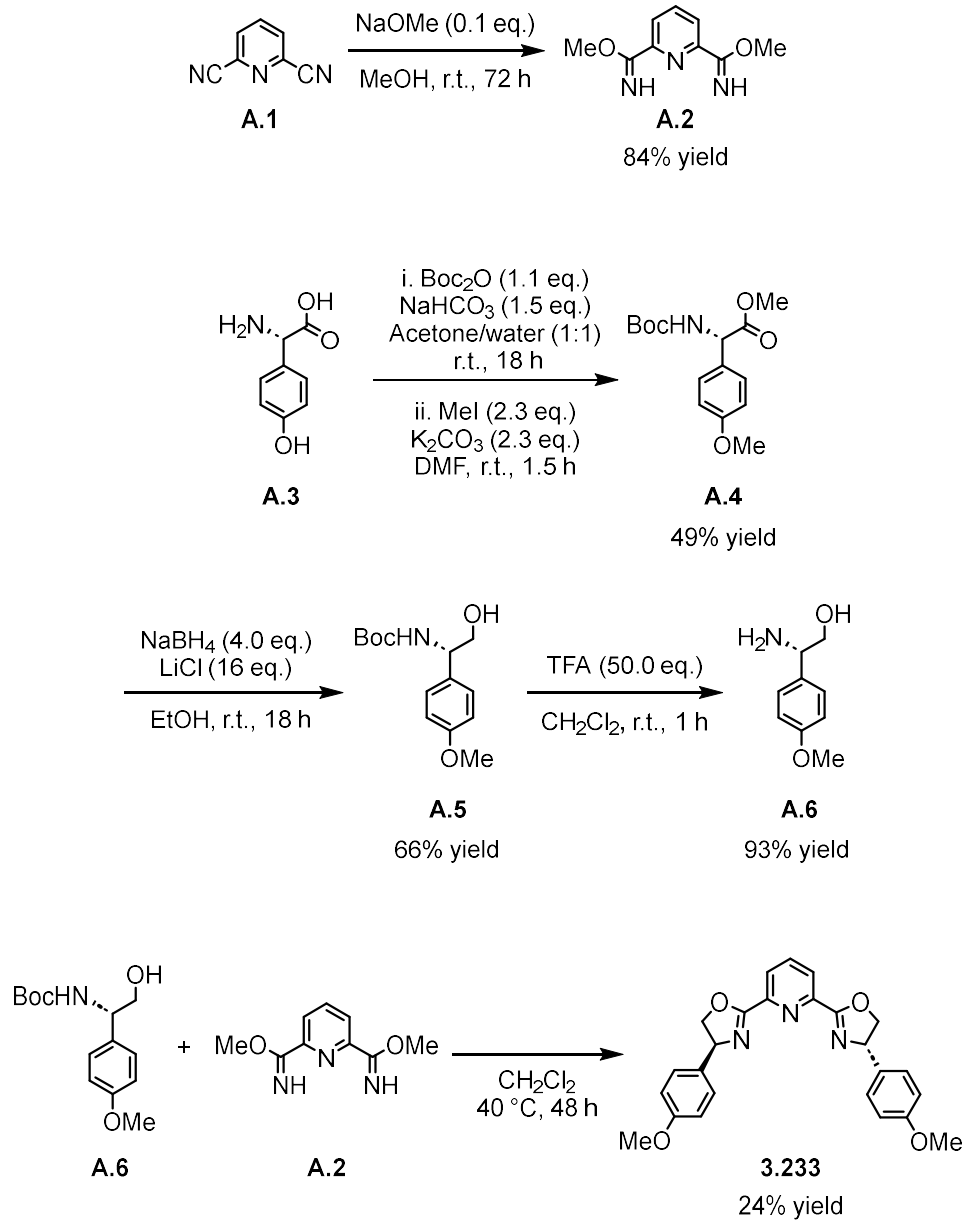
FTIR (neat) ν = 3364, 3032, 2947, 2863, 2244, 1713, 1629, 1609, 1514, 1478, 1453, 1374, 1347, 1302, 1257, 1201, 1163, 1129, 1096, 1061, 1043, 1023, 975, 953, 908, 866, 785, 751, 734, 699, 673, 648

HRMS (ESI$^+$) *m/z* Calcd. For $C_{30}H_{26}NO_3$ $(M+H)^+$ 448.1907, found 448.1912

HPLC ChiralPak IB (20% *i*-PrOH in hexane, 1.0 mL min^{-1}, T= 25 °C, 276 nm); τ_R (minor) = 8.3 min, τ_R (major) = 8.7 min;

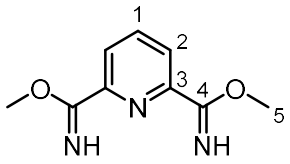
e.r. = 87:13

Appendix A



Scheme A.1 Synthesis of **3.233**

Dimethyl pyridine-2,6-bis(carbimidate) (A.2)



Prepared according to a modified literature method and the data are in agreement with those previously reported.[91]

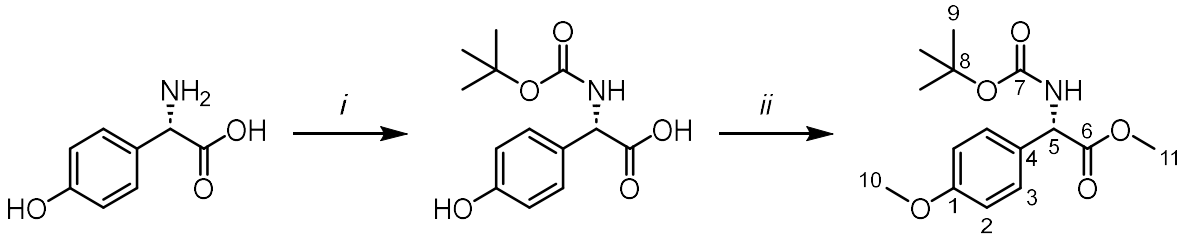
To a round bottom flask containing 2,6-pyridinedicarbonitrile (0.90 g, 6.98 mmol, 1.00 equiv.), MeOH (18 mL) and NaOMe (47 mg, 0.87 mmol, 0.125 equiv.) were added. The mixture was then stirred at room temperature for 72 h and after this time, neutralised by the addition of AcOH (50 µL, 0.87 mmol, 0.125 equiv.). After stirring for 5 min, the solvent was removed by rotary evaporation. The residue was then taken up in CH_2Cl_2 (20 mL), washed with water (20 mL), dried over Na_2SO_4, filtered and concentrated in vacuo to afford pure product as a white solid (76%, 1.50 g, 5.30 mmol).

^{1}H NMR (400 MHz, $CDCl_3$) δ 9.24 (s, 1H, NH), 7.95 – 7.91 (m, 3H, H1 and H2), 4.04 (s, 6H, H5).

^{13}C NMR (101 MHz, $CDCl_3$) δ 166.2 (C4), 147.2 (C3), 139.1 (C1), 122.7 (C2), 54.2 (C5).

HRMS (ESI^+) *m/z* Calcd. For $C_9H_{12}N_3O_2$ $(M+H)^+$ 194.0924, found 194.0920

Methyl (S)-2-((tert-butoxycarbonyl)amino)-2-(4-methoxyphenyl)acetate (A.4)



Prepared according to a modified literature method and the data are in agreement with those previously reported.[139]

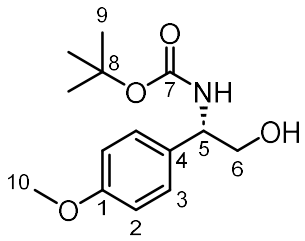
i. (S)-2-amino-2-(4-hydroxyphenyl)acetic acid (2.00 g, 11.98 mmol, 1.00 equiv.) was dissolved in [1:1] acetone/water (120 mL) and di-*tert*-butyl dicarbonate (2.87 g, 13.17 mmol, 1.10 equiv.) and $NaHCO_3$ (1.51 g, 17.96 mmol, 1.50 equiv.) were added. The mixture was stirred at room temperature for 18 h, after which the acetone was removed *in vacuo* and the aqueous solution acidified to pH 2. The resulting suspension was extracted three times with EtOAc and the combined organic extracts were washed with brine, dried over Na_2SO_4, filtered, and concentrated *in vacuo* to afford the product as white solid that was used without further purification.

ii. The (S)-2-((tert-butoxycarbonyl)amino)-2-(4-hydroxyphenyl)acetic acid (11.98 mmol, 1.00 equiv.) was dissolved in DMF (170 mL) and to this solution, K_2CO_3 (3.72 g, 26.96 mmol, 2.25 equiv) followed by CH_3I (1.67 mL, 29.95 mmol, 2.5 equiv) were added. The obtained reaction mixture was stirred for 1.5 h at room temperature after which it was poured into water (300 mL) under vigorous stirring. The aqueous solution was extracted three times with EtOAc and the combined organic extracts were washed with brine, dried over Na_2SO_4, filtered, and concentrated *in vacuo* to afford the product as white solid (1.72 g, 5.82 mmol, 49% over two steps)

^{1}H NMR (200 MHz, $CDCl_3$) δ 7.32 – 7.22 (m, 2H, H2), 6.87 (d, *J* = 9.0 Hz, 2H, H3), 5.25 (d, *J* = 7.5 Hz, 1H, H5), 3.79 (s, 3H, H10), 3.71 (s, 3H, H11), 1.42 (s, 9H, H9).

LRMS (ESI$^+$) *m/z* Calcd. For $C_{15}H_{24}NO_4$ $(M+H)^+$ 282.2, found 282.2

tert-Butyl (S)-(2-hydroxy-1-(4-methoxyphenyl)ethyl)carbamate (A.5)



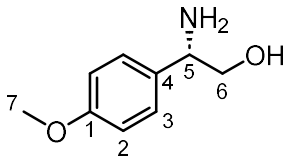
Prepared according to a modified literature method and the data are in agreement with those previously reported.[140]

Methyl (S)-2-((tert-butoxycarbonyl)amino)-2-(4-methoxyphenyl)acetate (**A.4**) (4.65 g, 15.76 mmol) was dissolved in anhydrous ethanol (318 ml), and $NaBH_4$ (2.87 g, 75.93 mmol, 4.80 equiv.) and LiCl (2.67 g, 0.25 mol, 15.50 equiv.) were added. The mixture was kept stirred at room temperature for 18 h, after which HCl (1 M in water, 250 ml) and water (170 ml) were added, and the mixture extracted with Et_2O (330 ml). The organic phase was washed with sat. $NaHCO_{3\,(aq.)}$ and brine, dried over Na_2SO_4, and concentrated under reduced pressure. Recrystallization of the crude residue in ethanol gave the product as a white solid (2.80 g, 10.4 mmol, 66%)

^{1}H NMR (400 MHz, $CDCl_3$) δ 7.22 (d, *J* = 8.5 Hz, 2H, H2), 6.89 (d, *J* = 8.5 Hz, 1H, H3), 5.10 (s, 1H, H6'), 4.73 (s, 1H, H6''), 3.80 (s, 3H, H10), 1.43 (s, 9H, H9).

HRMS (ESI$^+$) *m/z* Calcd. For $C_{14}H_{21}NO_4$ $(M+H)^+$ 290.1363, found 290.1362

(S)-2-Amino-2-(4-methoxyphenyl)ethan-1-ol (A.6)



Prepared according to a modified literature method and the data are in agreement with those previously reported.[141]

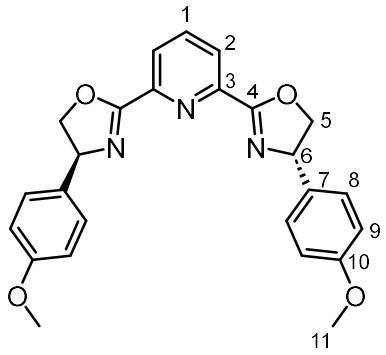
tert-butyl (S)-(2-hydroxy-1-(4-methoxyphenyl)ethyl)carbamate (**A.5**) (752 mg, 2.82 mmol, 1.00 equiv.) was dissolved in CH_2Cl_2 (42 mL) and trifluoroacetic acid (10.6 mL, 0.14 mol, 50.00 equiv.) was added dropwise. The mixture was allowed to stir for 1 h at room temperature before the solvent was removed *in vacuo*. The residue was dissolved in aqueous NaOH (20% w/w) and extracted with CH_2Cl_2 three times. The combined organic extracts were washed with water, dried over Na_2SO_4, filtered, and concentrated *in vacuo* to afford the product as yellow solid (440 mg, 2.63 mmol, 93%).

^{1}H NMR (400 MHz, $CDCl_3$) δ 7.25 (d, *J* = 8.5 Hz, 2H, H2), 6.89 (d, *J* = 8.5 Hz, 2H, H3), 4.00 (dd, *J* = 8.5, 4.5 Hz, 1H, H5), 3.80 (s, 3H, H7), 3.70 (dd, *J* = 10.5, 4.5 Hz, 1H, H6'), 3.53 (dd, *J* = 10.5, 8.5 Hz, 1H, H6'').

^{13}C NMR (101 MHz, $CDCl_3$) δ 159.1 (C1), 135.0 (C4), 127.7 (C2), 114.2 (C3), 68.3 (C6), 56.8 (C5), 55.5 (C7).

HRMS (ESI^+) *m/z* Calcd. For $C_9H_{14}NO_2$ $(M+H)^+$ 168.1019, found 168.1009

2,6-Bis((*S*)-4-(4-methoxyphenyl)-4,5-dihydrooxazol-2-yl)pyridine (3.233)



Prepared according to a modified literature method and the data are in agreement with those previously reported.[91]

A screw-top 2-dram vial was charged with dimethyl pyridine-2,6-bis(carbimidate) (**A.2**) (50 mg, 0.26 mmol, 1.00 equiv.), (S)-2-amino-2-(4-methoxyphenyl)ethan-1-ol (**A.6**) (87 mg, 0.52 mmol, 2.00 equiv.) and CH_2Cl_2 (2 mL). The vial was then sealed and heated to 69 °C. After 48 h, the reaction was cooled to room temperature and the solvent removed *in vacuo*. The crude product was purified by flash column chromatography [silica gel, [50–80% + 1% NEt_3] EtOAc in pentane] followed by recrystallisation from hot EtOAc to give the product as a white solid (20 mg, 0.045 mmol, 18%).

^{1}H NMR (400 MHz, $CDCl_3$) δ 8.33 (d, *J* = 8.0 Hz, 2H, H2), 7.90 (t, *J* = 8.0 Hz, 1H, H1), 7.28 – 7.21 (m, 4H, H9), 6.94 – 6.85 (m, 4H, H8), 5.41 (dd, *J* = 10.5, 8.5 Hz, 2H, H6), 4.90 (dd, *J* = 10.5, 8.5 Hz, 2H, H5'), 4.40 (t, *J* = 8.5 Hz, 2H, H5''), 3.80 (s, 6H, H11).

^{13}C NMR (101 MHz, $CDCl_3$) δ 163.4 (C10), 159.4 (C4), 147.0 (C3), 137.5 (C1), 134.0 (C7), 128.2 (C8), 126.4 (C2), 114.4 (C9), 75.7 (C5), 70.0 (C6), 55.5 (C11).

HRMS (ESI^+) *m/z* Calcd. For $C_{25}H_{24}N_3O_4$ $(M+H)^+$ 430.1761, found 430.1756

References

1. Stewart, R. Atom transfer mechanisms in oxidation processes. *Experientia* **15**, 401–406 (1959).

2. Marcus, R. A. Chemical and Electrochemical Electron-Transfer Theory. *Annu Rev Phys Chem* **15**, 155–196 (1964).

3. Lu, L., Shi, R. & Lei, A. Single-electron transfer oxidation-induced C-H bond functionalization via photo-/ electrochemistry. *Trends Chem* **4**, 179–190 (2022).

4. Horn, E. J., Rosen, B. R. & Baran, P. S. Synthetic organic electrochemistry: An enabling and innately sustainable method. *ACS Cent Sci* **2**, 302–308 (2016).

5. Nair, V. & Deepthi, A. Cerium(IV) ammonium nitrate - A versatile single-electron oxidant. *Chem Rev* **107**, 1862–1891 (2007).

6. Shaw, M. H., Twilton, J. & MacMillan, D. W. C. Photoredox Catalysis in Organic Chemistry. *J Org Chem* **81**, 6898–6926 (2016).

7. Sawyer, D. T. & Williams, R. J. P. "Reactivity of Hydrogen Peroxide, Alkyl Hydroperoxides, and Peracids", *Oxygen Chemistry* (New York, 1992; online edn, Oxford Academic, 12 Nov. 2020).

8. Harding, K. E., May, L. M. & Dick, K. F. Selective Oxidation of Allylic Alcohols with Chromic Acid. *J Org Chem* **40**, 1664–1665 (1975).

9. Dash, S., Patel, S. & Mishra, B. K. Oxidation by permanganate: synthetic and mechanistic aspects. *Tetrahedron* **65**, 707–739 (2009).

10. Shetgaonkar, S. E., Jothish, S., Dohi, T. & Singh, F. V. Iodine(V)-Based Oxidants in Oxidation Reactions. *Molecules* **28**, 5250 (2023).

11. Castellan, A., Bart, J. C. J. & Cavallaro, S. Synthesis of adipic acid via the nitric acid oxidation of cyclohexanol in a two-step batch process. *Catal Today* **9**, 285–299 (1991).

12. Saikia, I., Borah, A. J. & Phukan, P. Use of Bromine and Bromo-Organic Compounds in Organic Synthesis. *Chem Rev* **116**, 6837–7042 (2016).

13. Williamson, K. S., Michaelis, D. J. & Yoon, T. P. Advances in the chemistry of oxaziridines. *Chem Rev* **114**, 8016–8036 (2014).

14. Miller, J. L., Lawrence, J. M. I. A., Rodriguez del Rey, F. O. & Floreancig, P. E. Synthetic applications of hydride abstraction reactions by organic oxidants. *Chem Soc Rev* **51**, 5660–5690 (2022).

15. Capaldo, L. & Ravelli, D. Hydrogen Atom Transfer (HAT): A Versatile Strategy for Substrate Activation in Photocatalyzed Organic Synthesis. *European J Org Chem* **2017**, 2056–2071 (2017).

16. van Leeuwen, P. W. N. M. Catalysis, Homogeneous. *Encyclopedia of Physical Science and Technology (Third Edition)* 457–490 (Academic Press, 2003).

17. Narayan, R., Matcha, K. & Antonchick, A. P. Metal-Free Oxidative C-C Bond Formation through C-H Bond Functionalization. *Chemistry - A European Journal* **21**, 14678–14693 (2015).

18. Lei, A. *et al.* Oxidative Cross-Coupling Reactions. *Oxidative Cross-Coupling Reactions* 1–229 (Wiley-VCH, 2016)

19. Guo, S. R., Kumar, P. S. & Yang, M. Recent Advances of Oxidative Radical Cross-Coupling Reactions: Direct α-C(sp3)–H Bond Functionalization of Ethers and Alcohols. *Adv Synth Catal* **359**, 2–25 (2017).

20. Jana, R., Pathak, T. P. & Sigman, M. S. Advances in transition metal (Pd,Ni,Fe)-catalyzed cross-coupling reactions using alkyl-organometallics as reaction partners. *Chem Rev* **111**, 1417–1492 (2011).

21. Mayr, H., Kempf, B. & Ofial, A. R. π-nucleophilicity in carbon-carbon bond-forming reactions. *Acc Chem Res* **36**, 66–77 (2003).

22. Brown, D. G. & Boström, J. Analysis of Past and Present Synthetic Methodologies on Medicinal Chemistry: Where Have All the New Reactions Gone? *J Med Chem* **59**, 4443–4458 (2016).

23. Sato, K., Isoda, M., Tarui, A. & Omote, M. Reductive Carbon–Carbon Bond Forming Reactions with Carbonyls Mediated by Rh–H Complexes. *European J Org Chem* **2020**, 6503–6511 (2020).

24. Moragas, T., Correa, A. & Martin, R. Metal-Catalyzed Reductive Coupling Reactions of Organic Halides with Carbonyl-Type Compounds. *Chemistry – A European Journal* **20**, 8242–8258 (2014).

25. Matsuo, J., Kawai, H. & Ishibashi, H. One-pot carbon–carbon bond formation at the β-position of cyclic ketones: oxidative Michael addition with alkyl malonates. *Tetrahedron Lett* **48**, 3155–3158 (2007).

26. Matsuo, J., Tanaki, Y. & Ishibashi, H. One-pot oxidative Mannich-type reaction of lactams with alkyl malonates. *Tetrahedron Lett* **48**, 3233–3236 (2007).

27. Chu, X. Q., Meng, H., Zi, Y., Xu, X. P. & Ji, S. J. Metal-free oxidative direct C(sp3)–H bond functionalization of ethers with α,α-diaryl allylic alcohols. *Chemical Communications* **50**, 9718–9721 (2014).

28. Liu, C., Zhang, H., Shi, W. & Lei, A. Bond formations between two nucleophiles: Transition metal catalyzed oxidative cross-coupling reactions. *Chem Rev* **111**, 1780–1824 (2011).

29. Liu, C., Zhang, H., Shi, W. & Lei, A. Bond Formations between Two Nucleophiles: Transition Metal Catalyzed Oxidative Cross-Coupling Reactions. *Chem. Rev* **111**, 1780–1824 (2011).

30. Jin, L., Zhao, Y., Zhu, L., Zhang, H. & Lei, A. Highly Selective Palladium-Catalyzed Oxidative C(sp2)–C(sp3) Cross-Coupling of Arylzinc and Alkylindium Reagents through Double Transmetallation. *Adv Synth Catal* **351**, 630–634 (2009).

31. Docherty, J. H. *et al.* Transition-Metal-Catalyzed C–H Bond Activation for the Formation of C–C Bonds in Complex Molecules. *Chem Rev* **123**, 7692–7760 (2023).

32. Dalton, T., Faber, T. & Glorius, F. C−H Activation: Toward Sustainability and Applications. *ACS Cent. Sci* **7**, 245–261 (2021).

33. Yang, Y., Lan, J. & You, J. Oxidative C-H/C-H Coupling Reactions between Two (Hetero)arenes. *Chem Rev* **117**, 8787–8863 (2017).

34. Funes-Ardoiz, I. & Maseras, F. Oxidative Coupling Mechanisms: Current State of Understanding. *ACS Catal* **8**, 1161–1172 (2018).

35. Shi, Z. *et al.* Suzuki–Miyaura Coupling Reaction by Pd(II)-Catalyzed Aromatic C–H Bond Activation Directed by an N-Alkyl Acetamino Group. *Angewandte Chemie International Edition* **46**, 5554–5558 (2007).

36. Wen, Z. K. *et al.* Palladium-Catalyzed Controllable Reductive/Oxidative Heck Coupling between Cyclic Enones and Thiophenes via C-H Activation. *Org Lett* **21**, 9545–9549 (2019).

37. Bian, M., Li, L. & Ding, H. Recent Advances on the Application of Electrocyclic Reactions in Complex Natural Product Synthesis. *Synthesis (Stuttg)* **49**, 4383–4413 (2017).

38. Woodward, R. B. & Hoffmann, R. The Conservation of Orbital Symmetry. *Angew. Chem. Int. Ed.* **8**, 781–853 (1969).

39. Huisgen, R. 1,5,-Electrocyclizations—An Important Principle of Heterocyclic Chemistry. *Angew. Chem. Int. Ed.* **19**, 947–973 (1980).

40. Karplus, M. *et al.* Photochemical Six-Electron Heterocyclization Reactions. *Acc Chem Res* **16**, 210–218 (1983).

41. Kos, M. *et al.* Oxidative Photocyclization of Aromatic Schiff Bases in Synthesis of Phenanthridines and Other Aza-PAHs. *International Journal of Molecular Sciences* **21**, 5868 (2020).

42. Lenz, G. R. Enamide Photochemistry. Formation of Oxyprotoberberines by the Elimination of Ortho Substituents in 2-aroyl-1-methylene-1,2,3,4-tetrahydroisoquinolines. *J Org Chem* **39**, 2839–2845 (1974).

43. Ferris, J. P. *et al.* Photochemistry of Ortho-Substituted Benzene Derivatives and Related Heterocycles. *J Am Chem Soc* **96**, 2010–2014 (1974).

44. Hernandez-Perez, A. C., Vlassova, A. & Collins, S. K. Toward a visible light mediated photocyclization: Cu-based sensitizers for the synthesis of [5]helicene. *Org Lett* **14**, 2988–2991 (2012).

45. Strieth-Kalthoff, F. & Glorius, F. Triplet Energy Transfer Photocatalysis: Unlocking the Next Level. *Chem* **6**, 1888–1903 (2020).

46. Lockhart, Z. *et al.* A radical-polar crossover approach to complex nitrogen heterocycles via the triplet state. *ChemRxiv.* (2023) doi:10.26434/CHEMRXIV-2023-PCV6M.

47. Schultz, A. G. *et al.* Heteroatom Directed Photoarylation. Synthetic Potential of the Heteroatom Oxygen. *J Am Chem Soc* **100**, 2150–2162 (1978).

48. Schultz, A. G. & Motyka, L. Photochemical Heterocyclizations of Systems Isoelectronic with the Pentadienyl Anion. in *Organic Photochemistry*. (Marcel Dekker, Inc., 1983).

49. Sharma, S., Singh, J. & Sharma, A. Visible Light Assisted Radical-Polar/Polar-Radical Crossover Reactions in Organic Synthesis. *Adv Synth Catal* **363**, 3146–3169 (2021).

50. Wiles, R. J. & Molander, G. A. Photoredox-Mediated Net-Neutral Radical/Polar Crossover Reactions. *Isr J Chem* **60**, 281–293 (2020).

51. Pitzer, L., Schwarz, J. L. & Glorius, F. Reductive radical-polar crossover: traditional electrophiles in modern radical reactions. *Chem Sci* **10**, 8285–8291 (2019).

52. Kashima, C. & Harada, K. Synthesis and reaction of optically active morpholinones. *J Chem Soc Perkin 1* 1521–1526 (1988).

53. Münster, N., Parker, N. A., van Dijk, L., Paton, R. S. & Smith, M. D. Visible Light Photocatalysis of 6π Heterocyclization. *Angew. Chem. Int. Ed.* **56**, 9468–9472 (2017).

54. Singh, A. *et al.* Facile synthesis and complete characterization of homoleptic and heteroleptic cyclometalated Iridium(III) complexes for photocatalysis. *J Organomet Chem* **776**, 51–59 (2015).

55. Castagnola, M. B., Illuminati, G. & Ortaggi, G. The electron donor properties of ferrocene. The oxidation of ferrocene by carboxylic acids. *J Organomet Chem* **60**, c17 (1973).

56. Shine, H. J. & Piette, L. Ion-radicals. The Reaction of Thioaromatic Compounds with Acids. II. Diphenyl Disulfide, Thianthrene and Thianthrene Oxides. *J Am Chem Soc* **84**, 4798–4806 (1962).

57. Eberson, L. *et al.* Thermal and Photochemical Reactions of Aromatic Compounds in Trifluoroacetic Acid, Involving Carbocations and Radical Cations. *Acta Chem Scand* **46**, 630–643 (1992).

58. Eberson, L. & Radner, F. Formation of the Radical Cation of 1,2,3,4,5,6,7,8-0ctamethylanthracene from Bis(pentamethylpheny1)methane in Trifluoroacetic Acid . *J Chem Soc Chem Commun* **18**, 1233 (1991).

59. Eberson, L. & Radner, F. Why is Trifluoroacetic acid such an effective one-electron oxidant? *Acta Chem Scand* **45**, 1093–1095 (1991).

60. Hu, J., Wang, J., Nguyen, T. H. & Zheng, N. The chemistry of amine radical cations produced by visible light photoredox catalysis. *Beilstein Journal of Organic Chemistry* **9**, 1977–2001 (2013).

61. Freeman, D. B., Furst, L., Condie, A. G. & Stephenson, C. R. J. Functionally diverse nucleophilic trapping of iminium intermediates generated utilizing visible light. *Org Lett* **14**, 94–97 (2012).

62. Parker, V. D. & Tilset, M. Facile Proton Transfer Reactions of N,N-Dimethylaniline Cation Radicals. *J Am Chem Soc* **113**, 8778–8781 (1991).

63. Guindon, Y., Guérin, B., Chabot, C. & Ogilvie, W. Stereoselective radical carbon-carbon bond forming reactions of β-alkoxy esters: Atom and group transfer allylations under bidentate chelation controlled conditions. *J Am Chem Soc* **118**, 12528–12535 (1996).

64. Porter, N. A., Wu, J. H., Zhang, G. & Reed, A. D. Enantioselective Free Radical Allyl Transfers from Allylsilanes Promoted by Chiral Lewis Acids. *J Org Chem* **62**, 6702–6703 (1997).

65. Eckert, F. *et al.* Prediction of acidity in acetonitrile solution with COSMO-RS. *J Comput Chem* **30**, 799–810 (2009).

66. Kütt, A. *et al.* Strengths of Acids in Acetonitrile. *European J Org Chem* **2021**, 1407–1419 (2021).

67. Tshepelevitsh, S. *et al.* On the Basicity of Organic Bases in Different Media. *European J Org Chem* **2019**, 6735–6748 (2019).

68. Ōki, M. *Recent Advances in Atropisomerism*. *Top. Stereochem*. 1–81 (John Wiley & Sons, Ltd, 1983).

69. Laplante, S. R. *et al.* Assessing atropisomer axial chirality in drug discovery and development. *J Med Chem* **54**, 7005–7022 (2011).

70. Chen, Y., Yekta, S. & Yudin, A. K. Modified BINOL ligands in asymmetric catalysis. *Chem Rev* **103**, 3155–3211 (2003).

71. del Corte, X., Martínez de Marigorta, E., Palacios, F., Vicario, J. & Maestro, A. An overview of the applications of chiral phosphoric acid organocatalysts in enantioselective additions to C—O and C—N bonds. *Organic Chemistry Frontiers* **9**, 6331–6399 (2022).

72. Clayden, J., Moran, W. J., Edwards, P. J. & Laplante, S. R. The Challenge of Atropisomerism in Drug Discovery. *Angew. Chem. Int. Ed.* **48**, 6398–6401 (2009).

73. Basilaia, M., Chen, M. H., Secka, J. & Gustafson, J. L. Atropisomerism in the Pharmaceutically Relevant Realm. *Acc Chem Res* **55**, 2904–2919 (2022).

74. Lanman, B. A. *et al.* Discovery of a Covalent Inhibitor of KRASG12C (AMG 510) for the Treatment of Solid Tumors. *J Med Chem* **63**, 52–65 (2020).

75. Szlávik, Z. *et al.* Structure-guided discovery of a selective mcl-1 inhibitor with cellular activity. *J Med Chem* **62**, 6913–6924 (2019).

76. Lovering, F., Bikker, J. & Humblet, C. Escape from flatland: Increasing saturation as an approach to improving clinical success. *J Med Chem* **52**, 6752–6756 (2009).

77. Saal, C., Becker, A., Krier, M. & Fuchß, T. Atropisomerism – A Neglected Way to Escape Out of Solubility Flatlands. *J Pharm Sci* **111**, 206–213 (2022).

78. Luz, J. G. *et al.* Indole Glucocorticoid Receptor Antagonists Active in a Model of Dyslipidemia Act via a Unique Association with an Agonist Binding Site. *J Med Chem* **58**, 6607–6618 (2015).

79. Anilkumar, G. N. *et al.* I. Novel HCV NS5B polymerase inhibitors: Discovery of indole 2-carboxylic acids with C3-heterocycles. *Bioorg Med Chem Lett* **21**, 5336–5341 (2011).

80. Sharma, K. *et al.* 3-Naphthylindoles as new promising candidate antioxidant, antibacterial, and antibiofilm agents. *Research on Chemical Intermediates* **43**, 2387–2399 (2017).

81. Sun, H. R., Sharif, A., Chen, J. & Zhou, L. Atroposelective Synthesis of Heterobiaryls through Ring Formation. *Chemistry – A European Journal* **29**, e202300183 (2023).

82. Wei, J., Zhu, M., Zhang, B., Li, K. & Zhang, X. Recent advances in atroposelective synthesis of axially chiral heterobiaryl featuring indole frameworks. *Tetrahedron* **149**, 133716 (2023).

83. He, C., Hou, M., Zhu, Z. & Gu, Z. Enantioselective Synthesis of Indole-Based Biaryl Atropisomers via Palladium-Catalyzed Dynamic Kinetic Intramolecular C-H Cyclization. *ACS Catal* **7**, 5316–5320 (2017).

84. Bisag, G. D. *et al.* Central-to-Axial Chirality Conversion Approach Designed on Organocatalytic Enantioselective Povarov Cycloadditions: First Access to Configurationally Stable Indole–Quinoline Atropisomers. *Chemistry - A European Journal* **25**, 15694–15701 (2019).

85. Aslam, S. *et al.* Heterocyclic Electrochemistry: Renewable Electricity in the Construction of Heterocycles. *ACS Omega* **8**, 6175–6217 (2023).

86. Gulevich, A. V., Dudnik, A. S., Chernyak, N. & Gevorgyan, V. Transition metal-mediated synthesis of monocyclic aromatic heterocycles. *Chem Rev* **113**, 3084–3213 (2013).

87. Xu, W. L., Zhao, W. M., Zhang, R. X., Chen, J. & Zhou, L. Organocatalytic cycloaddition–elimination cascade for atroposelective construction of heterobiaryls. *Chem Sci* **12**, 14920–14926 (2021).

88. Cheng, D. J. & Shao, Y. D. Advances in the Catalytic Asymmetric Synthesis of Atropisomeric Hexatomic N-Heterobiaryls. *Adv Synth Catal* **362**, 3081–3099 (2020).

89. Lu, D. L. *et al.* Atroposelective Construction of Arylindoles by Chiral Phosphoric Acid-Catalyzed Cross-Coupling of Indoles and Quinones. *Org Lett* **21**, 6000–6004 (2019).

90. Qi, L. W., Mao, J. H., Zhang, J. & Tan, B. Organocatalytic asymmetric arylation of indoles enabled by azo groups. *Nature Chemistry* **10**, 58–64 (2017).

91. Surgenor, R. Catalytic Enantioselective Synthesis of Heterobiaryl Atropisomers [PhD Thesis]. University of Oxford, 2021.

92. Surgenor, R. R., Liu, X., Keenlyside, M. J. H., Myers, W. & Smith, M. D. Enantioselective synthesis of atropisomeric indoles via iron-catalysed oxidative cross-coupling. *Nature Chemistry* **15**, 357–365 (2022).

93. Hansch, C., Leo, A. & Taft, R. W. A Survey of Hammett Substituent Constants and Resonance and Field Parameters. *Chem Rev* **91**, 165–195 (1991).

94. Shalit, H., Dyadyuk, A. & Pappo, D. Selective Oxidative Phenol Coupling by Iron Catalysis. *J Org Chem* 1677–1686 (2019)

95. Zhou, W. *et al.* Recent advances in electrocatalytic generation of indole-derived radical cations and their applications in organic synthesis. *Chinese Chemical Letters* **35**, 108902 (2024).

96. Per-Formed Research; Z, D. Z. L. Determining complete electron flow in the cofactor photoreduction of oxidized photolyase. *PNAS* **110**, 12966–12971 (2013).

97. Solar, S., Getoff, N., Surdhar, P. S., Armstrong, D. A. & Singh, A. Oxidation of tryptophan and N-methylindole by N3•, Br2•-, and (SCN)2•- radicals in light-and heavy-water solutions: A pulse radiolysis study. *Journal of Physical Chemistry* **95**, 3639–3643 (1991).

98. Sun, H., Sun, K. & Sun, J. Recent Advances of Marine Natural Indole Products in Chemical and Biological Aspects. *Molecules 2023, Vol. 28, Page 2204* **28**, 2204 (2023).

99. Kochanowska-Karamyan, A. J. & Hamann, M. T. Marine indole alkaloids: Potential new drug leads for the control of depression and anxiety. *Chem Rev* **110**, 4489–4497 (2010).

100. Gentry, E. C., Rono, L. J., Hale, M. E., Matsuura, R. & Knowles, R. R. Enantioselective Synthesis of Pyrroloindolines via Noncovalent Stabilization of Indole Radical Cations and Applications to the Synthesis of Alkaloid Natural Products. *J Am Chem Soc* **140**, 3394–3402 (2018).

101. Rathore, V. & Kumar, S. Visible-light-induced metal and reagent-free oxidative coupling of sp2 C–H bonds with organo-dichalcogenides: synthesis of 3-organochalcogenyl indoles. *Green Chemistry* **21**, 2670–2676 (2019).

102. Zhao, P. *et al.* Copper-Catalyzed Aerobic Oxidative Amination of Indole Derivatives via Single-Electron Transfer. *ChemCatChem* **12**, 3207–3211 (2020).

103. Liu, X. *et al.* Unraveling the Structure and Reactivity Patterns of the Indole Radical Cation in Regioselective Electrochemical Oxidative Annulations. *J Am Chem Soc* **145**, 3175–3186 (2023).

104. Yoshlda, K. Regiospecific Anodic Cyanation of Pyrroles and Indoles. *J Am Chem Soc* **99**, 6111–6113 (1977).

105. Qin, J. H., Luo, M. J., An, D. L. & Li, J. H. Electrochemical 1,2-Diarylation of Alkenes Enabled by Direct Dual C–H Functionalizations of Electron-Rich Aromatic Hydrocarbons. *Angew. Chem. Int. Ed.* **60**, 1861–1868 (2021).

106. Gilmore, K., Mohamed, R. K. & Alabugin, I. V. The Baldwin rules: revised and extended. *Wiley Interdiscip Rev Comput Mol Sci* **6**, 487–514 (2016).

107. Encinas, M. V., Lissi, E. A., Majmud, C. & Olea, A. F. Reactivity of tert-butoxyl radicals towards substituted indole derivatives. *Int J Chem Kinet* **23**, 761–766 (1991).

108. Vasilopoulos, A., Krska, S. W. & Stahl, S. S. C(sp3)-H methylation enabled by peroxide photosensitization and Ni-mediated radical coupling. *Science* **372**, 398–403 (2021).

109. Burgett, A. W. G., Li, Q., Wei, Q. & Harran, P. G. A Concise and Flexible Total Synthesis of (-)-Diazonamide A. *Angewandte Chemie - International Edition* **42**, 4961–4966 (2003).

110. Wu, Q. X. *et al.* Azonazine, a novel dipeptide from a Hawaiian marine sediment-derived fungus, Aspergillus insulicola. *Org Lett* **12**, 4458–4461 (2010).

111. Denizot, N. *et al.* Bioinspired direct access to benzofuroindolines by oxidative [3 + 2] annulation of phenols and indoles. *Org Lett* **16**, 5752–5755 (2014).

112. Li, L., Yuan, K., Jia, Q. & Jia, Y. Eight-Step Total Synthesis of Phalarine by Bioinspired Oxidative Coupling of Indole and Phenol. *Angewandte Chemie - International Edition* **58**, 6074–6078 (2019).

113. Shu, C. *et al.* Lewis Acid Catalyzed [3+2] Coupling of Indoles with Quinone Monoacetals or Quinone Imine Ketal. *European J Org Chem* **2014**, 4467–4471 (2014).

114. Beaud, R., Guillot, R., Kouklovsky, C. & Vincent, G. FeCl 3 -Mediated Friedel–Crafts Hydroarylation with Electrophilic N -Acetyl Indoles for the Synthesis of Benzofuroindolines. *Angew. Chem. Int. Ed.* **124**, 12714–12718 (2012).

115. Chan, C., Li, C., Zhang, F. & Danishefsky, S. J. Studies toward the total synthesis of phalarine: a survey of some biomimetic possibilities. *Tetrahedron Lett* **47**, 4839–4841 (2006).

116. Tomakinian, T., Guillot, R., Kouklovsky, C. & Vincent, G. Direct Oxidative Coupling of N-Acetyl Indoles and Phenols for the Synthesis of Benzofuroindolines Related to Phalarine. *Angew. Chem. Int. Ed.* **53**, 11881–11885 (2014).

117. Liu, K., Tang, S., Huang, P. & Lei, A. External oxidant-free electrooxidative [3 + 2] annulation between phenol and indole derivatives. *Nat Commun* **8**, (2017).

118. Guo, L., Chen, G., Li, H., Tung, C.-H. & Wang, Y. Visible-light-driven [3 + 2] cyclization of phenols with indoles and olefins using recyclable Ag_3 PO_4 nanoparticles. *Green Chemistry* **25**, 7102–7108 (2023).

119. Yu, Q. *et al.* Enantioselective oxidative phenol-indole [3 + 2] Coupling enabled by biomimetic mn(iii)/brønsted acid relay catalysis. *ACS Catal* **9**, 7285–7291 (2019).

120. Lu, Z. yu *et al.* Enantioselective synthesis of C3 substituted benzofuroindolines via catalytic asymmetric [3 + 2] cyclization of 3-substituted indoles with p-benzoquinones. *Tetrahedron Lett* **76**, 153233 (2021).

121. You, Y. *et al.* Enantioselective [3 + 2] annulation of tryptanthrin-derived ketimines and 2-naphthols: access to polycyclic indolo[2,1-b]quinazoline derivatives Org. Chem. Front., **11**, 2002–2007 (2024)

122. Liu, Y., Lee, Y. H., Zhang, Q., Cui, Y. & Ling, X. Y. Plasmonic nanopillar arrays encoded with multiplex molecular information for anti-counterfeiting applications. *J Mater Chem C Mater* **4**, 4312–4319 (2016).

123. Lockhart, Z. A radical–polar crossover approach to complex nitrogen heterocycles via the triplet state. [PhD Thesis]. University of Oxford, (2021).

124. Mulvihill, M. J., Cesario, C., Smith, V., Beck, P. & Nigro, A. Regio- and Stereospecific Syntheses of *syn*- and *anti*- 1,2-Imidazolylpropylamines from the Reaction of 1,1‘-Carbonyldiimidazole with *syn*- and *anti*- 1,2-Amino Alcohols. *J Org Chem* **69**, 5124–5127 (2004).

125. Tayama, E., Ishikawa, M., Iwamoto, H. & Hasegawa, E. Copper(II)–acid co-catalyzed intermolecular substitution of electron-rich aromatics with diazoesters. *Tetrahedron Lett* **53**, 5159–5161 (2012).

126. Li, W., Duan, Y., Zhang, M., Cheng, J. & Zhu, C. A photoredox catalyzed radical–radical coupling reaction: facile access to multi-substituted nitrogen heterocycles. *Chem. Comm.* **52**, 7596–7599 (2016).

127. Zhang, J., Jiang, J., Li, Y., Zhao, Y. & Wan, X. A new strategy for the construction of α-amino acid esters via decarboxylation. *Org Lett* **15**, 3222–3225 (2013).

128. Niimi, K. *et al.* [2,2']Bi[naphtho[2,3-b]furanyl]: A versatile organic semiconductor with a furan-furan junction. *Chem. Comm.* **48**, 5892–5894 (2012).

129. Farat, O. K., Ananyev, I. V., Varenichenko, S. A., Tatarets, A. L. & Markov, V. I. Vilsmeier-Haack reagent: An efficient reagent for the transformation of substituted 1,3-naphthoxazines into xanthene-type dyes. *Tetrahedron* **75**, 2832–2842 (2019).

130. Kim, Y. E. *et al.* Bi-aryl analogues of salicylic acids: Design, synthesis and sar study to ameliorate endoplasmic reticulum stress. *Drug Des Devel Ther* **15**, 3593–3604 (2021).

131. Coldham, I., Dobson, B. C., Fletcher, S. R. & Franklin, A. I. Intramolecular Dipolar Cycloaddition Reactions to Give Substituted Indoles – A Formal Synthesis of Deethylibophyllidine. *European J Org Chem* **2007**, 2676–2686 (2007).

132. Palmer, A. M. *et al.* Synthesis and Evaluation of 7H-8,9-Dihydropyrano[2,3-c]imidazo[1,2-a]pyridines as Potassium-Competitive Acid Blockers. *J. Med. Chem.* **50**, 6240–6264 (2007).

133. Youn, S. W., Pastine, S. J. & Sames, D. Ru(III)-Catalyzed Cyclization of Arene-Alkene Substrates via Intramolecular Electrophilic Hydroarylation. *Org Lett* **6**, 581–584 (2004).

134. Smith, A. B., Visnick, M., Haseltine, J. N. & Sprengeler, P. A. Organometallic reagents in synthesis : A new protocol for construction of the indole nucleus. *Tetrahedron* **42**, 2957–2969 (1986).

135. Smith, A. J. *et al.* New reductive rearrangement of N-arylindoles triggered by the Grubbs–Stoltz reagent Et3SiH/KOtBu. *Chem Sci* **11**, 3719–3726 (2020).

136. Zhang, Y., Stephens, D., Hernandez, G., Mendoza, R. & Larionov, O. V. Catalytic Diastereo- and Enantioselective Annulations between Transient Nitrosoalkenes and Indoles. *Chemistry - A European Journal* **18**, 16612–16615 (2012).

137. Feldman, K. S. & Ngernmeesri, P. Dragmacidin e synthesis studies. Preparation of a model heptacyclic core structure. *Org Lett* **12**, 4502–4505 (2010).

138. Gore, S., Baskaran, S. & König, B. Fischer indole synthesis in low melting mixtures. *Org Lett* **14**, 4568–4571 (2012).

139. Yang, X., Beroske, L. P., Kemmink, J., Rijkers, D. T. S. & Liskamp, R. M. J. Synthesis of bicyclic tripeptides inspired by the ABC-ring system of vancomycin through ruthenium-based cyclization chemistries. *Tetrahedron Lett* **58**, 4542–4546 (2017).

140. Miranda, I. L. *et al.* Stereoselective synthesis of (−)-cytoxazone and its unnatural congener (+)-5-epi-cytoxazone. *Chirality* **33**, 479–489 (2021).

141. O'brien, P., Osborne, S. A. & Parker, D. D. Asymmetric aminohydroxylation of substituted styrenes: applications in the synthesis of enantiomerically enriched arylglycinols and a diamine. *J. Chem. Soc., Perkin Trans. 1*, 2519, (1998).